ISSN 0021-9673

VOL. 637 NO. 1 MAY 7, 1993

JOURNAL OF CHROMATOGRAPHY

INCLUDING ELECTROPHORESIS AND OTHER SEPARATION METHODS

ELSEVIER

JOURNAL OF CHROMATOGRAPHY

INCLUDING ELECTROPHORESIS AND OTHER SEPARATION METHODS

Scope. The *Journal of Chromatography* publishes papers on all aspects of **chromatography, electrophoresis** and related methods. Contributions consist mainly of research papers dealing with chromatographic theory, instrumental developments and their applications. The section *Biomedical Applications*, which is under separate editorship, deals with the following aspects: developments in and applications of chromatographic and electrophoretic techniques related to clinical diagnosis or alterations during medical treatment; screening and profiling of body fluids or tissues related to the analysis of active substances and to metabolic disorders; drug level monitoring and pharmacokinetic studies; clinical toxicology; forensic medicine; veterinary medicine; occupational medicine; results from basic medical research with direct consequences in clinical practice. In *Symposium volumes*, which are under separate editorship, proceedings of symposia on chromatography, electrophoresis and related methods are published.

Submission of Papers. The preferred medium of submission is on disk with accompanying manuscript (see *Electronic manuscripts* in the Instructions to Authors, which can be obtained from the publisher, Elsevier Science Publishers B.V., P.O. Box 330, 1000 AH Amsterdam, Netherlands). Manuscripts (in English; *four* copies are required) should be submitted to: Editorial Office of *Journal of Chromatography*, P.O. Box 681, 1000 AR Amsterdam, Netherlands, Telefax (+31-20) 5862 304, or to: The Editor of *Journal of Chromatography*, *Biomedical Applications*, P.O. Box 681, 1000 AR Amsterdam, Netherlands. Review articles are invited or proposed in writing to the Editors who welcome suggestions for subjects. An outline of the proposed review should first be forwarded to the Editors for preliminary discussion prior to preparation. Submission of an article is understood to imply that the article is original and unpublished and is not being considered for publication elsewhere. For copyright regulations, see below.

Publication. The *Journal of Chromatography* (incl. *Biomedical Applications*) has 40 volumes in 1993. The subscription prices for 1993 are:

J. Chromatogr. (incl. *Cum. Indexes*, *Vols. 601–650*) + *Biomed. Appl.* (Vols. 612–651):
Dfl. 8520.00 plus Dfl. 1320.00 (p.p.h.) (total *ca.* US$ 5622.75)

J. Chromatogr. (incl. *Cum Indexes*, *Vols. 601–650*) only (Vols. 623–651):
Dfl. 7047.00 plus Dfl. 957.00 (p.p.h.) (total *ca.* US$ 4573.75)

Biomed. Appl. only (Vols. 612–622):
Dfl. 2783.00 plus Dfl. 363.00 (p.p.h.) (total *ca.* US$ 1797.75).

Subscription Orders. The Dutch guilder price is definitive. The US$ price is subject to exchange-rate fluctuations and is given as a guide. Subscriptions are accepted on a prepaid basis only, unless different terms have been previously agreed upon. Subscriptions orders can be entered only by calender year (Jan.–Dec.) and should be sent to Elsevier Science Publishers, Journal Department, P.O. Box 211, 1000 AE Amsterdam, Netherlands, Tel. (+31-20) 5803 642, Telefax (+31-20) 5803 598, or to your usual subscription agent. Postage and handling charges include surface delivery except to the following countries where air delivery via SAL (Surface Air Lift) mail is ensured: Argentina, Australia, Brazil, Canada, China, Hong Kong, India, Israel, Japan*, Malaysia, Mexico, New Zealand, Pakistan, Singapore, South Africa, South Korea, Taiwan, Thailand, USA. *For Japan air delivery (SAL) requires 25% additional charge of the normal postage and handling charge. For all other countries airmail rates are available upon request. Claims for missing issues must be made within six months of our publication (mailing) date, otherwise such claims cannot be honoured free of charge. Back volumes of the *Journal of Chromatography* (Vols. 1–611) are available at Dfl. 230.00 (plus postage). Customers in the USA and Canada wishing information on this and other Elsevier journals, please contact Journal Information Center, Elsevier Science Publishing Co. Inc., 655 Avenue of the Americas, New York, NY 10010, USA, Tel. (+1-212) 633 3750, Telefax (+1-212) 633 3764.

Abstracts/Contents Lists published in Analytical Abstracts, Biochemical Abstracts, Biological Abstracts, Chemical Abstracts, Chemical Titles, Chromatography Abstracts, Current Awareness in Biological Sciences (CABS), Current Contents/Life Sciences, Current Contents/Physical, Chemical & Earth Sciences, Deep-Sea Research/Part B: Oceanographic Literature Review, Excerpta Medica, Index Medicus, Mass Spectrometry Bulletin, PASCAL-CNRS, Referativnyi Zhurnal, Research Alert and Science Citation Index.

US Mailing Notice. *Journal of Chromatography* (ISSN 0021-9673) is published weekly (total 52 issues) by Elsevier Science Publishers (Sara Burgerhartstraat 25, P.O. Box 211, 1000 AE Amsterdam, Netherlands). Annual subscription price in the USA US$ 4573.75 (subject to change), including air speed delivery. Application to mail at second class postage rate is pending at Jamaica, NY 11431. **USA POSTMASTERS**: Send address changes to *Journal of Chromatography*, Publications Expediting, Inc., 200 Meacham Avenue, Elmont, NY 11003. Airfreight and mailing in the USA by Publications Expediting.

See inside back cover for Publication Schedule, Information for Authors and information on Advertisements.

0021-9673/93/$06.00

Printed in the Netherlands

VOL. 637, NO. 1 JOURNAL OF CHROMATOGRAPHY MAY 7, 1993

CONTENTS

(Abstracts/Contents Lists published in Analytical Abstracts, Biochemical Abstracts, Biological Abstracts, Chemical Abstracts, Chemical Titles, Chromatography Abstracts, Current Awareness in Biological Sciences (CABS), Current Contents/Life Sciences, Current Contents/Physical, Chemical & Earth Sciences, Deep-Sea Research/Part B: Oceanographic Literature Review, Excerpta Medica, Index Medicus, Mass Spectrometry Bulletin, PASCAL-CNRS, Referativnyi Zhurnal, Research Alert and Science Citation Index)

REVIEW

REGULAR PAPERS

Column Liquid Chromatography

Gas Chromatography

Electrophoresis

(Continued overleaf)

Contents (continued)

SHORT COMMUNICATIONS

Column Liquid Chromatography

BOOK REVIEWS

JOURNAL OF CHROMATOGRAPHY

VOL. 637 (1993)

JOURNAL of CHROMATOGRAPHY

INCLUDING ELECTROPHORESIS AND OTHER SEPARATION METHODS

ELSEVIER

AMSTERDAM — LONDON — NEW YORK — TOKYO

0021-9673/93/$06.00

Printed in the Netherlands.

Reversed Phase CHIRAL HPLC Column

NEW CHIRALCEL® OD-R

Indapamide

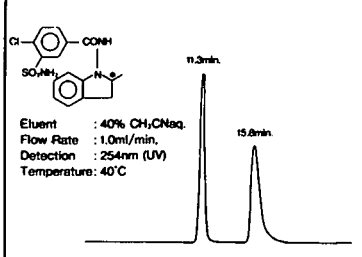

Eluent : 40% CH_3CNaq.
Flow Rate : 1.0ml/min.
Detection : 254nm (UV)
Temperature: 40°C

Verapamil

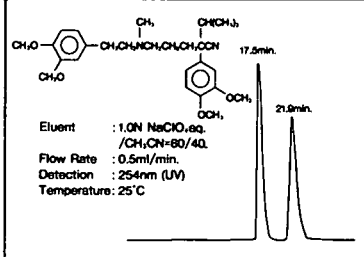

Eluent : 1.0N $NaClO_4$aq. /CH_3CN=60/40.
Flow Rate : 0.5ml/min.
Detection : 254nm (UV)
Temperature: 25°C

Hydroxyzine

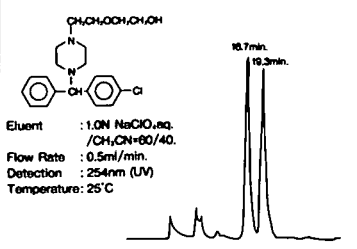

Eluent : 1.0N $NaClO_4$aq. /CH_3CN=60/40.
Flow Rate : 0.5ml/min.
Detection : 254nm (UV)
Temperature: 25°C

Propranolol

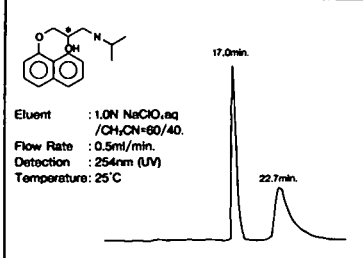

Eluent : 1.0N $NaClO_4$aq /CH_3CN=60/40.
Flow Rate : 0.5ml/min.
Detection : 254nm (UV)
Temperature: 25°C

Pindolol

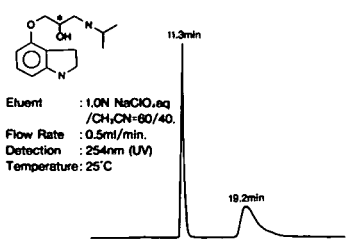

Eluent : 1.0N $NaClO_4$aq /CH_3CN=60/40.
Flow Rate : 0.5ml/min.
Detection : 254nm (UV)
Temperature: 25°C

1-Phenoxy-2-Propanol

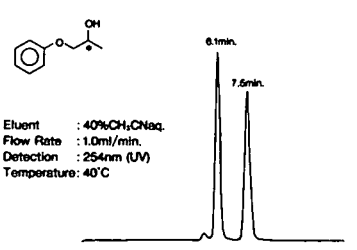

Eluent : 40%CH_3CNaq.
Flow Rate : 1.0ml/min.
Detection : 254nm (UV)
Temperature: 40°C

Alimemazine

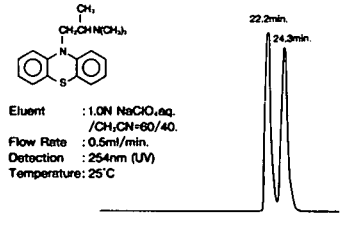

Eluent : 1.0N $NaClO_4$aq. /CH_3CN=60/40.
Flow Rate : 0.5ml/min.
Detection : 254nm (UV)
Temperature: 25°C

Trimepramine

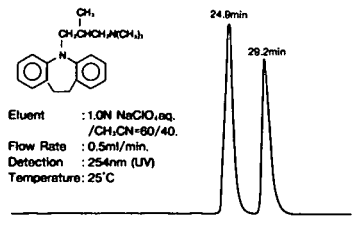

Eluent : 1.0N $NaClO_4$aq. /CH_3CN=60/40.
Flow Rate : 0.5ml/min.
Detection : 254nm (UV)
Temperature: 25°C

4-Pheny-2-butanol

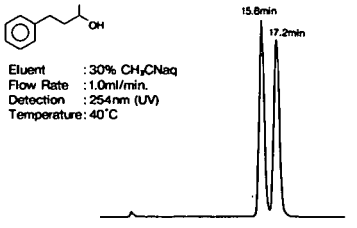

Eluent : 30% CH_3CNaq
Flow Rate : 1.0ml/min.
Detection : 254nm (UV)
Temperature: 40°C

CBZ-Val.

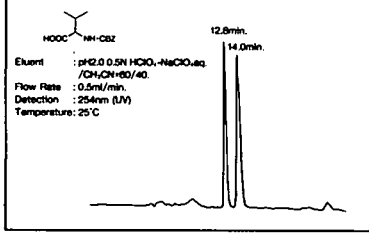

Eluent : pH2.0 0.5N $HClO_4$-$NaClO_4$aq. /CH_3CN=60/40.
Flow Rate : 0.5ml/min.
Detection : 254nm (UV)
Temperature: 25°C

3-Phenylbutyric acid

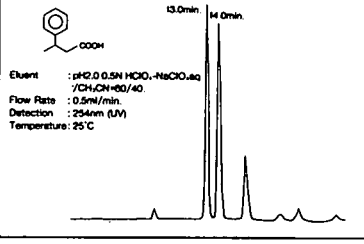

Eluent : pH2.0 0.5N $HClO_4$-$NaClO_4$aq /CH_3CN=60/40.
Flow Rate : 0.5ml/min.
Detection : 254nm (UV)
Temperature: 25°C

2-Phenylbutyric acid

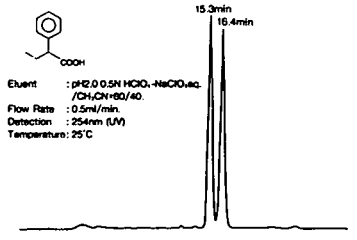

Eluent : pH2.0 0.5N $HClO_4$-$NaClO_4$aq. /CH_3CN=60/40.
Flow Rate : 0.5ml/min.
Detection : 254nm (UV)
Temperature: 25°C

For more information about CHIRALCEL OD-R column, please give us a call.

DAICEL CHEMICAL INDUSTRIES, LTD.
CHIRAL CHEMICALS DIVISION 8-1, Kasumigaseki 3-chome, Chiyoda-ku, Tokyo 100, JAPAN
Phone: +81-3-3507-3151 Facsimile: +81-3-3507-3193

AMERICA
CHIRAL TECHNOLOGIES, INC.
730 SPRINGDALE DRIVE
DRAWER I EXTON, PA 19341
Phone: 215-594-2100
Facsimile: 215-594-2325

EUROPE
DAICEL (EUROPA) GmbH
Ost Street 22
4000 Düsseldorf 1, Germany
Phone: +49-211-369848
Facsimile: +49-211-364429

ASIA/OCEANIA
DAICEL CHEMICAL (ASIA) PTE. LTD.
65 Chulia Street #40-07
OCBC Centre, Singapore 0104.
Phone: +65-5332511
Facsimile: +65-5326454

Journal of Chromatography, 637 (1993) 1–11
Elsevier Science Publishers B.V., Amsterdam

CHROM. 24 968

Review

Gas chromatographic separation of perfluorocarbons

T.K.P. O'Mahony, A.P. Cox* and D.J. Roberts

School of Chemistry, University of Bristol, Cantock's Close, Bristol BS8 1TS (UK)

(First received September 15th, 1992; revised manuscript received February 9th, 1993)

ABSTRACT

This paper presents an overview of the gas chromatographic separation of perfluorocarbons. A summary is given of relevant information on the separation and identification of individual molecules, isomeric mixtures and multi-component mixtures of perfluorocarbons. Different types of columns (packed and capillary), fluorinated stationary phases, and detectors are described. Future work towards quantitative analysis with the possible use of fluorinated capillary columns is indicated.

CONTENTS

1. INTRODUCTION

The term "perfluoro" denotes fluorine substitution of all hydrogen atoms attached to carbon atoms except those whose substitution would affect the nature of the functional group. Perfluorocarbons vary in their physical state depending on their molecular formula, in general, C_1–C_4 are gases, C_5–C_{19} are liquids and C_{20}–C_{24} are solids [1]. They have structures analogous to the familiar hydrocarbons but possess very different chemical and physical properties. They are generally chemically inert but have varying degrees of toxicity, ranging from the "non-toxic" fluids such as *n*-perfluorohexane, perfluorodecalin and perfluoro(1-methyldecalin) [2] to the most toxic of all perfluorinated molecules, perfluoroisobutylene (iso-C_4F_8). The latter is ten times more toxic than phosgene and has a T.W.A. (time weighted average, v/v) of 10 ppb [3].

A preliminary investigation by our research group [4], into the gas-phase pyrolysis of perfluorocarbons, mainly perfluoroalkanes, -alkenes

* Corresponding author.

0021-9673/93/$24.00

and -cycloalkanes suggested that gas chromatography (GC) would be the preferred analytical technique for the identification and quantitative analysis of their decomposition products. Since the advent of GC in 1952 [5], perfluorocarbons have been studied mainly in tandem with chloro and hydrofluorocarbons. Perfluorocarbons have also been studied as a specialist class of compounds for use both as atmospheric tracers [6–9] and in tagging applications [10,11]. The present article has been compiled to give an overview of the GC separation of perfluorocarbons. The perfluorocarbon compounds reviewed are those containing carbon and fluorine only, with no functional group. The GC of perfluorocarbons will be discussed under three main headings: separation (packed and capillary column), detector response and fluorinated stationary phases.

2. SEPARATION OF PERFLUOROCARBONS

Early GC studies involved a search for suitable columns to separate and identify individual or small specific groups of perfluorocarbons. Perfluorocarbons often have very low polarity, hence a non-polar column is expected to be more suitable. However, the separation and identification of multi-component perfluorocarbon mixtures has proved difficult due to their varying degrees of polarity and differences in their physical properties, especially their wide range of boiling points.

2.1. Packed columns

As early as 1955, Tatlow and co-workers separated perfluorohexabenzene [12] and numerous perfluorocyclohexadienes [13,14] on a 6-ft. (1 ft. = 30.48 cm) glass column containing a 1:2 ratio of dinonylphthalate liquid substrate with kieselguhr (Celite 545) as the solid support. These authors made the suggestion that "other high boiling liquids such as the chlorofluoro oils and silicones . . ." would be useful stationary phases for perfluorocarbon analyses. This led Reed [15] to investigate the chromatographic behaviour of *n*-perfluoropentane, *n*-perfluoroheptane and *n*-perfluorononane on several fluorocarbon and hydrocarbon stationary phases. Results showed that these fluorocarbon phases —the ethyl ester of Kel F acid 8114 [$Cl(CF_2CFCl)_3CF_2CO_2C_2H_5$], Kel F No. 90 grease [$Cl(CF_2CFCl)_3CF_3$], perfluorokerosine and perfluorotributylamine— gave better separation of perfluorocarbon mixtures than the hydrocarbon stationary phases —di-(2-ethylhexyl) sebacate [$X-(CH_2)_8-X$, where $X = CO_2CH_2-CH(C_2H_5)(CH_2)_3CH_3$] and *n*-hexadecane. However, these fluorinated phases were not suitable for the separation of perfluorocarbon isomers with similar boiling points. Fluorinated stationary phases will be discussed further in section 4.

Pyrolytic studies of chlorodifluoromethane [16] yielded several C_3–C_5 perfluorocarbons. However, these products eluted too rapidly when separated on a 9-ft. column containing firebrick impregnated with dibutylphthalate. Campbell and Gudzinowicz [17] studied the separation of CF_4, C_2F_4, C_3F_6, cyclo- and iso-C_4F_8, obtained from the pyrolytic degradation of PTFE; four different liquid substrates on a Chromosorb W (diatomite–amorphous silica [18]) solid support were used. They found that the three non-fluorinated stationary phases, Apiezon L (hydrocarbon grease), a polymeric phenyl ether with a molecular mass $\approx$ 15 000 and diisodecylphthalate gave poor performance and suggested that the Kel F No. 3 oil [$Cl(CF_2CFCl)_7CF_3$] was superior for the separation of perfluorocarbons. Reed and co-workers then reported the separation of both the C_6F_{14} [19,20] and C_7F_{16} isomers [21] by use of *n*-hexadecane on Chromosorb P held at 30°C. A very long column (17 m) was used which is limited to the separation of perfluorocarbon isomers with less than 8 carbon atoms by the narrow operating temperature range 20–50°C of *n*-hexadecane. However, MacKenzie and Wilson [22], using *n*-hexadecane did identify perfluoro-1,1-dimethylcyclopentane (C_7F_{14}) from the pyrolysis of perfluorobicyclohexyl.

Greene and Wachi [23] concluded that the Kel F oils were not completely satisfactory for separating low-molecular-mass perfluorocarbons (C_1–C_4) and they reported the separation of C_1–C_4 perfluorocarbons on a GSC column of silica gel and on a GLC column of 1H,7H-dodecafluoroheptyl acrylate (DFHA) [CH_2=

$CHCO_2CH_2(CF_2CF_2)_3H$] on Chromosorb W. The silica gel column was programmed from room temperature to 180°C, with a total elution time of 60 min for the eleven C_1–C_4 compounds. However, the *cis* and *trans* isomers of perfluoro-2-butene were not separated. With the GLC column, the eleven C_1–C_4 perfluorocarbons were separated in about 18 min at 0°C including the *cis* and *trans* isomers of perfluoro-2-butene. Cyclo-C_3F_6 and perfluoro-1-propene were not resolved. Davenport and Miller [24] and Rogers *et al.* [25] using the same type of columns as Greene and Wachi [23], silica gel and DFHA on Chromosorb W, studied the breakdown products of the photolysis of perfluorocyclobutane [24] and pyrolysis–GC of *n*-perfluoropentane [25]. Davenport and Miller reported up to 47 chromatographic peaks with an elution time of 15 h, most of which were unidentified. However, they did identify C_2F_4, C_2F_6, C_3F_8 and cyclo-C_4F_8. Rogers *et al.* identified five pyrolysis products in all, C_2F_4, C_2F_6, C_3F_6, C_3F_8 and *n*-C_4F_{10} with a total elution time of 10 minutes. Meanwhile Tatlow and co-workers [26–30] again using a column containing dinonylphthalate on kieselguhr separated and identified several perfluoroaromatic compounds. These had been obtained from the defluorination of cyclic aliphatic fluorocarbons [26,27] and highly fluorinated cyclohexanes [27–30], and from pyrolytic reactions of perfluoroisopropylcyclohexane [30].

In 1968, Drennan and Matula [31], using a composite Porapak column (2 ft. 50–80 mesh Poropak T in series with 4 ft. of 50–80 mesh Poropak N), separated a carbonyl fluoride–carbon dioxide mixture. Bright and Matula [32] using various Porapak supports of differing polarity (N, Q, R, S and T) separated fourteen low-molecular-mass perfluorocarbons ranging from CF_4 to iso-C_4F_8. The advantage of this type of column was the elimination of liquid substrate bleed onto the detector, enabling operation up to 200°C with minimum retention times. The aim was to use Porapak columns for the analysis of combustion products of low-molecular-mass perfluorocarbons. One point to note is that Fig. 1 of reference 32 contains several errors, for example, two individual peaks in the chromatogram of their Fig. 1 are assigned retention times of 10.4 min for iso-C_4F_8 and 15.4 min for $(CF_3)_2C{=}CF_2$, respectively. Unfortunately, $(CF_3)_2C{=}CF_2$ and iso-C_4F_8 represent the same compound under different nomenclature. The peak at 10.4 min could be perfluoro-1-butene, with iso-C_4F_8 having the retention time of 15.4 min. Nevertheless the Porapak column proved to be the most suitable for separating low-molecular-mass perfluorocarbon mixtures. Wright and Askew [33] extended the use of the silica gel column [23–25] by separating the C_1–C_8 *n*-perfluoroalkanes into their respective molecular mass classes. A dual-column system was used to eliminate the base line drift observed in earlier studies [33]. The authors listed no overlapping peaks, no tailing and a satisfactory separation of air and CF_4, as advantages for the dual column method. However, the separation of isomers was not realized.

In 1978, Shields and Nieman [34] reported the separation of selected hydrocarbons and perfluorocarbons (isomers of C_5F_{12}, C_6F_{14} and C_7F_{16}) on a graphitized carbon black column to which a moderately polar stationary phase 0.1% (w/w) SP-1000 (prepared from polyethylene glycol and tetraphthalic acid) had been added. Various investigators [35–39] had reported the use of graphitized carbon black as an efficient material for separating hydrocarbon isomers. Results showed that this new column allowed the separation of isomeric perfluorocarbons as effectively as the *n*-hexadecane column. In addition, it operates over a larger molecular mass range and with improved analysis times. Its only disadvantage is the rather low sample capacity, not a problem for analytical applications.

In the early 1980s GC of perfluorocarbons centred around the detection of the highly toxic perfluoroisobutylene (iso-C_4F_8) because of its formation in the work place in processes such as condensation reflow soldering [40]. Markevka *et al.* [41] generated a reference sample of iso-C_4F_8 and quantitatively determined it in air mixtures using a Carbowax 400 (polyethylene glycol) on a Porasil C (pure silica) column. However, no attempt was made to separate other perfluorocarbons. Meanwhile, Buravtsev *et al.* [42] using a Porapak column, identified iso-C_4F_8 in the dimerization of tetrafluoroethylene in an adiabatic compression device.

More recently, Ainagos [43] used a silica gel column to study the pyrolysis products of *n*-perfluorohexane. A similar study of the pyrolysis of *n*-perfluorooctyl-1-sulphonyl fluoride [44] identified products such as *n*-C_8F_{18}, *n*-$C_{12}F_{26}$ and *n*-$C_{16}F_{34}$. These were separated using a GLC column containing 5% SE-30 (dimethylsiloxane) on Chromosorb P. The GC separation and determination of impurities in sulphur hexafluoride [45] was performed using a silica gel column containing 25% diisooctyl sebacate. Impurities discovered included CF_4, C_2F_6, C_3F_8 and *n*-C_4F_{10}. Table 1 (GLC) and Table 2 (GSC) list the most useful packed columns reported.

2.2. Capillary columns

A recent advance in chromatography is to distribute the stationary phase as a film of liquid on the internal wall of columns with capillary dimensions (capillary or open tubular columns). However capillary columns have not been fully exploited for the analysis of perfluorocarbons. Only a few examples have been found and are given in Table 3. Ghaoui *et al.* [46] used an alumina open tubular column to separate C_5 and C_6 perfluoroalkanes. DeBortoli and Peechio [47] used a fused-silica capillary column for determining *n*-perfluoroheptane and *n*-perfluorooctane in air after trapping on a graphitized carbon black bed. The use of perfluorocarbons as tracers in the atmosphere [48] led Begley *et al.* [49] to study high-molecular-mass perfluorocarbons ($M_r > 250$) such as perfluorodecalin. They employed a fused-silica capillary column coated with SE-54 (5% diphenyl/94% dimethyl/1% vinyl polysiloxane). Femtogram level detection was achieved by using electron-capture negative ion chemical ionization mass spectrometry (ECNICI-MS).

TABLE 2

GSC PACKED COLUMNS

Column	Perfluorocarbons separated	Refs.
Silica gel	CF_4, C_2F_4, C_2F_6, C_3F_8, cyclo-C_4F_8, iso-C_4F_8	23–25, 43
	n-(C_2F_6, C_3F_8, C_4F_{10}, C_5F_{12}, C_6F_{14}, C_7F_{16}, C_8F_{18})	33
	C_2F_4, C_2F_6, C_3F_6, C_3F_8, *n*-C_4F_{10}	43
Porapak	CF_4, C_2F_4, C_2F_6, C_3F_6, C_3F_8, 1-C_4F_8, 2-C_4F_8, iso-C_4F_8	32
	Iso-C_4F_8	42

TABLE 3

CAPILLARY COLUMNS

Column	Perfluorocarbons separated	Ref.
Alumina plot	*n*-C_5F_{12}, *n*-C_6F_{14}	46
Fused silica	$C_6F_{13}CF_3$, $C_6F_{12}(CF_3)_2$	47
Fused silica/SE-54	$M_r > 250$	49

TABLE 1

GLC PACKED COLUMNS

Column	Perfluorocarbons separated	Refs.
Dinonylphthalate on kieselguhr	C_6F_6, cyclo-C_6F_{10}	12–14, 26–30
Kel F acid 8114 on Celite	Isomers of C_5F_{12}, C_7F_{16} and C_9F_{20}	15
Kel F No. 3 on Chromosorb W	CF_4, C_2F_4, C_3F_6, cyclo-C_4F_8, iso-C_4F_8	17
Hexadecane on Chromosorb P	C_6F_{14} isomers	19, 20
	C_7F_{16} isomers, C_7F_{14} isomers	21, 22
DFHA on Chromosorb W	CF_4, C_2F_4, C_2F_6, C_3F_6, C_3F_8, cyclo-C_4F_8, iso-C_4F_8	23–25
SP-1000 on graphitized carbon black	Isomers of C_5F_{12}, C_6F_{14} and C_7F_{16}	34
Carbowax 400 on Porasil C	Iso-C_4F_8	3, 40, 41
SE-30 on Chromosorb P	*n*-C_8F_{18}, *n*-$C_{12}F_{26}$, *n*-$C_{16}F_{34}$	44
Diisooctylsebacate on silica gel	CF_4, C_2F_6, C_3F_8 and *n*-C_4F_{10}	45

3. DETECTOR RESPONSE TO PERFLUOROCARBONS

Various detectors have been used for the detection of perfluorocarbons. The electron-capture detector, first introduced by Lovelock and Lipsky [50], can be the most sensitive for halogenated compounds and is also highly selective. In 1966 Clemons and Altshuller [51] measured the response of an electron-capture detector to numerous halogenated substances. They found that responses for perfluorocarbons varied from extremely low for CF_4 to high for C_6F_6. Christophorou *et al.* [52] reported on the general tendency of perfluorocarbons to undergo non-dissociative electron capture. As early as 1971 Lovelock [53] reported the presence of fluorinated hydrocarbons in the atmosphere which were detectable by electron-capture detection (ECD). Saltzman *et al.* [54] conducted successful tracer experiments with cyclo-C_4F_8. Other compounds detected with ECD such as perfluoromethylcyclohexane, perfluorodimethylcyclohexane and perfluorodecalin are tracers which can be separated from most atmosphere halocarbons on conventional silicone columns [55,56]. Dietz *et al.* [56] used perfluorinated taggants in blasting caps and explosives for later detection by electron-capture monitors. A useful general reference on the electron-capture detector is the book by Poole and Zlatkis [57]. Simmonds [58] successfully used the electron-capture detector as a monitor of halocarbons in the atmosphere. The large rate constant for electron attachment for C_7F_{14} has been reported by Chen and Wentworth [59].

The response of flame ionization detectors has been similarly investigated. In the 1970s the response of a flame ionization detector was investigated for CF_4–C_8F_{18} perfluoroalkanes using silica gel [60] and Porapak [61] columns. CF_4 showed essentially no response in comparison to a response approaching unity as the number of carbon atoms increases towards eight atoms. This is a result of the C–F bond being more difficult to break compared with the C–C bond in the perfluorocarbons and explains the high response of the flame ionization detector to larger molecular masses. A group of Japanese workers have determined the retention indexes of 221 halogenated organic compounds although only four perfluorocarbons were determined [62]. The use of a hydrogen-rich flame in connection with a flame ionization detector [63] showed that low carbon numbers, CF_4 and C_2F_6, increased their detector response compared with a normal flame ionization detector [60,61]. In addition, for high carbon number perfluorocarbons such as cyclo-C_6F_{12} and cyclo-C_7F_{14} [64], it was proved that they have a response similar to that of the corresponding hydrocarbon and independent of the conditions of the flame. The use of a helium ionization detector [65], (operating on the basis of ionization by metastable helium with sufficient energy (19 eV) to ionize CF_4 as well as the higher-M_r perfluorocarbons) showed a greater response for C_2–C_5 perfluorocarbons than that reported for both the flame ionization [60,61,63–65] and electron-capture detectors [51]. Table 4 shows the response to CF_4 for the various detectors.

TABLE 4

DETECTOR RESPONSE FOR CF_4

Detector	Response (Coulomb mol^{-1})	Column	Ref.
Electron-capture	$7.2 \cdot 10^{-7}$	Alumina	51
Flame ionization	$1.1 \cdot 10^{-6}$	Silica gel	60
Flame ionization	$7.6 \cdot 10^{-5}$	Porapak	61
Flame ionization, H_2 rich	$2.3 \cdot 10^{-5}$	Porapak	63
Flame ionization, H_2 rich	$2.7 \cdot 10^{-4}$	Silica gel	64
Helium ionization	$4.4 \cdot 10^{-3}$	Porasil	65

4. FLUORINATED STATIONARY PHASES

A further development, in perfluorocarbon chromatography, has been the use of perfluorinated stationary phases. The intention was to extend the range of organic compounds that could be analysed by GC and also permit the analysis of thermally labile compounds. Intermolecular forces in fluorinated hydrocarbons are significantly weaker than in the equivalent hydrocarbon, thus making the separation of high-

molecular-mass or thermally labile samples possible at lower temperatures than on conventional non-fluorinated phases [61,66–68]. A more recent paper tested six phases one of which was perfluorodecalin [69].

Reed [15] initiated the use of perfluorocarbon stationary phases with his investigation into the chromatographic behavior of n-C_5F_{12}, n-C_7F_{16} and n-C_9F_{20} on perfluorokerosine and perfluorotributylamine. Results showed that these perfluorinated stationary phases gave better separation of perfluorocarbons than hydrocarbon phases. Campbell and Gudzinowicz [17] compared fluorinated and non-fluorinated stationary phases, during an investigation into the pyrolysis of commercial PTFE. They found that the non-fluorinated stationary phases gave poor performance and suggested that the Kel F oil-fluorinated phase was superior for the separation of high-boiling perfluorocarbons. Brown *et al.* [68] favoured the use of fluorinated stationary phases for the separation of perfluorocarbons and perfluoroalcohols. The pyrolytic reactions of perfluoroisopropylcyclohexane and various perfluorodicyclohexyl alkanes were investigated by Letchford *et al.* [30]. They used perfluoro-1,2-dicyclohexylethane as the stationary phase to separate and identify newly prepared perfluorocyclopentenes. However, column efficiencies were generally poor.

In 1975, Vernon and Edwards [70,71] studied four fluorinated stationary phases. Three of the phases, Kel F No. 90 grease, Fluorolube 2000 (chlorofluorocarbon) and silicone QF-1 [poly(methyl-3,3,3-trifluoropropyl siloxane)] had been available for some time, while the fourth phase Krytox 240 AC (perfluoroalkyl ether) was a new stationary phase. A range of aromatic perfluorocarbons, perfluoroparaffins and perfluorolefins were studied chromatographically on these four stationary phases. The authors compared these phases using column efficiencies, retention indices (I) and McReynolds constants (ΔI) as defined in refs. 72–75.

Table 5 gives the McReynolds constants for the stationary phases investigated by Vernon and Edwards [70]. All are of low polarity, with Krytox the least polar and silicone QF-1 having the highest polarity. The authors found that the film stability and column efficiency of fluorinated phases could be dramatically enhanced by incorporating polar anchor groups into its structure. Krytox was the first of this stationary phase type and was found to give the highest retention indices.

In 1983, Dhanesar and Poole [76,77] described the properties of a new perfluorocarbon stationary phase, Fomblin YR [$(OCFCF_3CF_2)_n$–$(OCF_2)_m$] similar to Krytox. This new phase provided thermally stable column packings with acceptable column efficiency for general chromatographic use, especially for low-polarity organic compounds. Fomblin YR, with a molecular mass of 6000–7000, provides columns of high efficiency that can be used at temperatures up to 250°C. Above this temperature the stationary phase film is no longer homogenous and the column efficiency declines. Fomblin YR provides some of the weakest non-polar interactions exhibited by any thermally stable phase. The authors suggested that this perfluoroalkyl ether phase might prove useful for separating perfluorocarbons.

Fluorocarbon surfactants containing polar

TABLE 5

McREYNOLDS CONSTANTS FOR VARIOUS STATIONARY PHASES AND SOLUTES [70]

Phase	McReynolds constant				
	Benzene	n-Butanol	2-Pentanone	Nitropropane	Pyridine
Krytox	4	148	86	147	93
Kel F No. 90	41	135	134	153	111
Fluorolube 2000	75	192	148	200	158
Silicone QF-1	130	225	336	432	281

functional groups, for example Fluorad FC-430, an aliphatic perfluoroalkyl polymeric ester, were shown to function effectively as a stationary phase for GC [78,79]. Potential applications included separation of thermally sensitive brominated compounds, low level hydrocarbons and the separation of oxygenated hydrocarbons in aqueous systems. Likewise, the tetraalkylammonium perfluoroalkane sulphonate liquid organic salts proved to have acceptable chromatographic properties towards a wide range of polar solutes [66,67].

A chromatographic investigation [80,81] into several perfluorinated {PTFE, fluortensid $[CF_3(CF_2)_nCF{=}CF{-}CF_2(OCH_2CH_2)_mOCH_3]$ where $n = 6–8$ and $m = 2–5$ and a Kel F oil $Cl(CF_2{-}CFCl)_nCl$} and non-fluorinated (squalane, polyethylene glycol) stationary liquid phases coated on a Chromosorb P support was carried out. Retention indices and McReynolds constants were reported for each individual stationary phase, using the following perfluorocarbon solutes: perfluoro(C_6–C_{10}) carboxylic methyl esters [80], normal C_6–C_{10} perfluoroalkanes and perfluorocyclobenzene [81]. These results showed that the fluorinated stationary phases were more selective for perfluorocarbons than the non-fluorinated phases. However, no results were given for low-molecular-mass (C_1–C_4) perfluorocarbons. Glajch and Schindel [82] used Krytox to separate numerous chlorofluorocarbons (Freons) and their isomers in the presence of reactive gases, such as HF and HCl. The columns employed were a 5% Krytox 143 AC on Carbopack (graphitized carbon black) and a 2.5% krytox/2.5% benzophenone on Carbopack. Both these columns were found to be inert to reactive gases and therefore could be used for on-line analysis of fluorocarbons in processes in which acid gases might be present. The columns gave excellent selectivity for the chlorofluorocarbons and fast analysis times at reasonable temperatures [82].

Pomaville and Poole [83] studied the chromatographic properties of eight fluorinated phases: perfluoroalkane ($C_{22}F_{46}$), Kel F oil [17,71], Fluortensid [81], Krytox [70,71,82], Fomblin YR [76,77]. Zonyl E-91 (fluoroalkyl ester of camphoric acid) [78], Fluorads FC 430 and FC 431 (fluorocarbon surfactants) [78,79] and PPF-20 (a polyperfluorophenylene ether). The McReynolds constants and column efficiencies were given for each phase; the retention mechanism of organic solutes and the strength of dispersion interactions with each phase was established. Reduced peak tailing and faster elution times were observed for compounds containing hydrogen-bonding functional groups. Preparation of efficient column packings with these phases was also reported. However, the authors were mainly concerned with the chromatographic properties of their phases and not

TABLE 6

FLUORINATED STATIONARY PHASES

Name	Structure	Refs.
Fluorad FC 430, 431	Fluorocarbon surfactant	78, 79
Fluorolube	$Cl(CF_2CFCl)CF_2COOR$	71, 83
Fluortensid	$CF_3(CF_2)_nCFCFCF_2(OCH_2CH_2)_3OCH_3$	80, 81, 83
Fomblin	$-(OCFCF_3CF_2)_n-(OCF_2)_m$	76, 77, 83
Kel F	$Cl(CF_2CFCl)_nCF_3$	17, 70, 71, 83
Krytox	$F-(CFCF_3-CF_2O)_n-CF_2CF_3$	70, 71, 82, 83
PTFE	$-(CF_2)_n-$	80, 81
PPF-20	Poly(perfluorophenylene) ether	83
Perfluorodicyclohexylethane	$(C_6F_{11})_2CFCF_3$	30
Perfluorokerosine	$C_{14}F_{30}$	15
Perfluorotributylamine	$[CF_3(CF_2)_3]_3N$	15
Silicone QF	Poly(methyl-3,3,3,trifluoropropylsiloxane)	70, 71
Zonyl E-91	Fluoroalkyl ester of camphoric acid	83

the separating of any particular solutes except those for the calculation of the McReynolds constant. They suggested that new perfluorinated phases should be synthesized and investigated exclusively for chromatographic purposes. Table 6 gives a list of the highly fluorinated stationary phases used in GC.

5. DISCUSSION

As outlined above numerous researchers have investigated the GC of perfluorocarbons, each one employing columns and detectors for their own area of interest. A variety of columns have been employed to separate and identify various perfluorocarbons (Tables 1, 2, 3 and 6). Some columns have been used to analyze for one individual perfluorocarbon, others have been designed to separate isomeric and multicomponent mixtures. The different physical properties associated with perfluorocarbons —gases (C_1–C_4), liquids (C_5–C_{19}) and solids (C_{20}–C_{24})— present a difficulty in making the simultaneous separation of low- to high-molecular-mass perfluorocarbons on a single column. The majority of the chromatographic analyses have been performed on the separation and identification of the gases and C_5–C_9 liquids. The present survey has revealed little information regarding the analysis of the C_{10}–C_{19} liquids and C_{20}–C_{24} solids. A difficulty is that thick film GC columns are required to separate the low-boiling-point compounds as well as starting from a subambient temperature. When temperature programming this type of column the upper temperature limit of the phase is reached quite quickly and the detector is affected by column bleed. It is therefore usual to use columns that cover the boiling point range for each compound. Sometimes the capillary columns are coupled together to extend the range of compounds that can be separated.

The silica gel column [23–25,33,43,45,60] proved to be the most successful column for the separation of gas and liquid mixtures of perfluorocarbons. However, elution times are often impractical. The Porapak column [32] proved to be more efficient with reasonable elution times for C_1–C_4 gas analysis. Note, that this column renders an electron-capture detector inoperative, due to a high level of polymeric bleeding [4]. Isomeric mixtures were first separated by Reed [15,20] and Askew and Reed [21] using a *n*-hexadecane on Chromosorb P column. Shields and Nieman [34] continued with this work, using the column, SP1000 on graphitized carbon black, which allowed the separation of (C_5–C_7) isomers. They found their column to be more efficient than the *n*-hexadecane column, with shorter analysis times and the ability to separate over a larger molecular mass range.

Research into new perfluorinated stationary phases, as suggested by Pomaville and Poole [83], has not been reported. Table 6 lists the fluorinated stationary phases which are used in GC. These phases have been used mainly for the separation of chemically reactive compounds such as metal halides, interhalogen compounds, and the halides of hydrogen, sulphur, phosphorus, freons and other high fluorinated organic molecules [66–68,70,71,76,77,79–84]. Little work has been done with these columns for the analysis of perfluorocarbons. Nevertheless, they have extended the molecular mass range of samples that can be analyzed by GC and permit the analysis of thermally labile substances. However, with the introduction of Krytox [70,71,82,83] and Fomblin [76,77,83] and the investigation into other fluorinated stationary phases, it has been observed that the new fluorinated stationary phases may be selective for perfluorocarbons. Although film stability deteriorates markedly at about 100°C for the early fluorinated phases, due to their weak interactions with the support. The temperature tolerance of the new fluorinated phases is in the range 200–250°C [83]. The relative simplicity in the preparation of these chemically inert, low polarity functionalized fluorinated phases makes them favourable for the separation of low polarity perfluorocarbons. Conventional packed columns have been used extensively to separate perfluorocarbons. Capillary columns with their greater resolution and efficiency, have yet to be fully exploited for perfluorocarbons although they are now widely used for other halocarbons. For the gases usually subambient temperatures are required as well as 5-μm thick films or

porous-layer open tubular columns to obtain longer retention times for these more volatile compounds.

The flame ionization and electron-capture detectors are the two most popular detectors for perfluorocarbons. The bulk of the work has been done with conventional flame ionization detection. However, for low-molecular-mass perfluorocarbons a hydrogen-rich flame or metastable helium ionization is necessary to provide reasonable response factors. The electron-capture detector is generally more sensitive but can become unworkable due to polymeric bleeding from some columns. Mass spectrometer detectors, again very sensitive, will become increasingly important when capillary columns become more widely used for perfluorocarbon analysis.

6. CONCLUSIONS

GC has been effective in separating C_1–C_9 perfluorocarbons. The majority of the analyses have been performed on packed columns. This is due to their simplicity in preparation compared to the difficulty in preparation and cost of a capillary column. Future work needs to be directed towards capillary GC especially for the separation of low-molecular-mass perfluorocarbons. In addition, the separation of high-molecular-mass C_{18}–C_{24} perfluorocarbon molecules needs to be studied more extensively. No chromatography column, as yet mentioned in the literature will separate all perfluorocarbons. The possible use of perfluorinated stationary phases for capillary GC may be one way forward.

In the past most authors carried out qualitative GC analysis of perfluorocarbons with only a few reporting quantitative results. In China some workers have carried out a quantitative analysis on fluorocarbons in artificial blood preparations using perfluorobenzene as an internal standard. One of the blood substituents was relatively "non-toxic" perfluorodecalin [85]. There is also a demand now for quantitative results particularly when handling toxic compounds such as perfluoroisobutylene. Therefore limits of detection and sensitivity of the detector will need to be determined, in order to measure the very low levels of perfluorocarbons and their breakdown products in complex mixtures, for example air samples.

7. ACKNOWLEDGEMENTS

T.K.P. O'M. thanks SERC for a CASE Studentship. The authors thank Rhône-Poulenc (I.S.C. Division) Avonmouth, Bristol for their interest in this work and for financial support. The authors also wish to thank the referees for their constructive criticism.

REFERENCES

1 R.E. Banks, *Fluorocarbons and their Derivatives*, Oldbourne, London, 1964.
2 S.W. Green, *Chem. Ind.*, January (1969) 63.
3 L.J. Turbini and F.M. Zado, *Elec. Pck. Prod.*, 20 (1980) 49.
4 T.K.P. O'Mahon, A.P. Cox and D.J. Roberts, *Analyst*, 118 (1993).
5 A.J.P. Martin and A.T. James, *Biochem. J.*, 50 (1952) 679.
6 J.E. Lovelock and G.J. Ferber, *Atmos. Environ.*, 16 (1982) 1467.
7 J.G. Ferber, K. Telegadas, J.L. Heffter, C.R. Ray and R.N. Dietz, *Report 1981, EPA-600/7-81-006 Order No. PB 81-188138*; available from NTIS, Springfield, VA. From *Gov. Rep. Announce. Index (U.S.)*, 81 (1981) 3645.
8 R.J. Lagomarsino, J. Raymond and N. Latner, *J. Chromatogr.*, 595 (1992) 359.
9 R.R. Draxler, R. Dietz, R.J. Lagomarsino and G. Start, *Atmos. Environ., Part A*, 25A (1991) 2815.
10 R.N. Dietz, R.W. Goodrich and E.A. Cote, *Proc. New Concepts Symposium and Workshop on Detection and Identification of Explosives*, US Departments of Treasury, Energy, Justice and Transportation, NTIS, Springfield, VA, 1978, p. 281.
11 R.N. Dietz and G. Senum, *Perfluorocarbon vapor tagging of blasting cap detonators, US Pat. Appl.* 9623, 24 Oct. 1980.
12 D.E.M. Evans and J.C. Tatlow, *J. Chem. Soc. (London)*, (1955) 1184.
13 J.A. Godsell, M. Stacey and J.C. Tatlow, *Nature (London)*, 178 (1956) 199.
14 R.P. Smith and J.C. Tatlow, *J. Chem. Soc. (London)*, (1957) 2505.
15 T.M. Reed, *Anal. Chem.*, 30 (1958) 221.
16 J. Serpenit, *Chim. Anal. (Paris)*, 41 (1959) 146.
17 R.H. Campbell and B.J. Gudzinowicz, *Anal. Chem.*, 33 (1961) 845.
18 L.S. Ettre and A. Zlatkis, *The Practice of Gas Chromatography*, Interscience, 1967, pp. 184–195.

19 T.M. Reed, J.F. Walter, R.R. Cecil and R.D. Dresdner, *Ind. Eng. Chem.*, 51 (1959) 271.
20 T.M. Reed, *J. Chromatogr.*, 9 (1962) 419.
21 W.C. Askew and T.M. Reed, *J. Chromatogr.*, 69 (1972) 359.
22 D.R. MacKenzie and V.H. Wilson, *J. Chem. Soc. (B)*, (1968) 762.
23 S.A. Greene and F.M. Wachi, *Anal. Chem.*, 35 (1963) 928.
24 J.E. Davenport and G.H. Miller, *J. Phys. Chem.*, 73 (1969) 809.
25 R.R. Rogers, G.S. Born, W.V. Kessler and J.E. Christian, *Anal. Chem.*, 45 (1973) 567.
26 B. Gething, C.R. Patrick, J.C. Tatlow, R.E. Banks, A.K. Barbour and A.E. Tipping, *Nature (London)*, 183 (1959) 586.
27 B. Gething, C.R. Patrick, M. Stacey and J.C. Tatlow, *Nature (London)*, 183 (1959) 588.
28 P.L. Coe, C.R. Patrick and J.C. Tatlow, *Tetrahedron*, 9 (1960) 240.
29 J. Burdon, D.J. Gilman, C.R. Patrick, M. Stacey and J.C. Tatlow, *Nature (London)*, 186 (1960) 231.
30 B.R. Letchford, C.R. Patrick and J.C. Tatlow, *Tetrahedron*, 20 (1964) 1381.
31 G.A. Dreenan and R.A. Matula, *J. Chromatogr.*, 34 (1968) 77.
32 R.N. Bright and R.A. Matula, *J. Chromatogr.*, 35 (1968) 217.
33 J.R. Wright and W.C. Askew, *J. Chromatogr. Sci.*, 9 (1971) 651.
34 R.R. Shields and J.A. Nieman, *Anal. Chem.*, 50 (1978) 661.
35 F.T. Eggersten, H.S. Knight and S. Groennings, *Anal. Chem.*, 28 (1956) 302.
36 I. Halász and Cs. Horváth, *Nature (London)*, 197 (1963) 71.
37 W. Schneider, H. Bruddereck and I. Halász, *Anal. Chem.*, 36 (1964) 153.
38 A. Di Corcia and R. Samperi, *J. Chromatogr.*, 107 (1975) 99.
39 A. Di Corcia and R. Samperi, *Anal. Chem.*, 47 (1975) 1853.
40 R.P. Menichelli, *Am. Ind. Hyg. Assoc. J.*, 43 (1982) 286.
41 J.S. Markevka, G.D. Johnson, D.F. Hagen and R.D. Danielson, *Anal. Chem.*, 54 (1982) 2607.
42 N.N. Buravtsev, A.S. Grigor'ev and Y.A. Kolbanoskii, *Kinet. Katal.*, 26 (1985) 7.
43 A.F. Ainagos, *Kinet. Katal.*, 32 (1991) 802.
44 M. Napoli, C. Fraccaro, A. Scipioni and R. Armelli, *J. Fluor. Chem.*, 24 (1984) 377.
45 Z.T. Wang, F.P. Yus and S.K. Hsia, *Zh. Anal. Khim.*, 41 (1986) 649.
46 L. Ghaoui, E. Dessai, W.E. Wentworth, S. Weisner, A. Zlatkis and E. Chen, *Chromatographia*, 20 (1985) 422.
47 M. DeBortoli and E. Peechio, *J. High. Resolut. Chromatogr. Chromatogr. Commun.*, 8 (1985) 422.
48 T.W. D'Ottavio, R.W. Goodrich and R.N. Dietz, *Environ. Sci. Technol.*, 20 (1986) 100.
49 P. Begley, B. Foulger and P. Simmonds, *J. Chromatogr.*, 445 (1988) 119.
50 J.E. Lovelock and S.R. Lipsky, *J. Am. Chem. Soc.*, 82 (1960) 431.
51 C.A. Clemons and A.P. Altshuller, *Anal. Chem.*, 38 (1966) 133.
52 L.G. Christophorou, D.L. McCorkle and A.A. Christodoutides, in L.G. Christophorou (Editor), *Electron Molecule Interactions and their Applications*, Vol. 1, Academic Press, New York, 1984, p. 548.
53 J.E. Lovelock, *Nature (London)*, 230 (1971) 379.
54 B.E. Saltzman, A.I. Coleman and C.A. Clemons, *Anal. Chem.*, 38 (1966) 753.
55 F.W. Williams and H.G. Eaton, *Anal. Chem.*, 46 (1974) 179.
56 R.N. Dietz, R.W. Goodrich and E.A. Cote, *Report 1978 BNL-25050, CONF-78 10115-2*; available from NTIS, Springfield, VA. From *Energy Res. Abstr.*, 4(9) (1979), Abstr. No. 24375.
57 A. Zlatkis and C.F. Poole (Editors), *Electron Capture —Theory and Practice in Chromatography* (*Journal of Chromatography Library*, Vol. 20), Elsevier, Amsterdam, Oxford, 1981.
58 P.G. Simmonds, in A. Zlatkis and C.F. Poole (Editors), *Electron Capture —Theory and Practice in Chromatograpy* (*Journal of Chromatography Library*, Vol. 20), Elsevier, Amsterdam, Oxford, 1981, Ch. 12, p. 256.
59 W.E. Wentworth and E.C.M. Chen, in A. Zlatkis and C.F. Poole (Editors), *Electron Capture —Theory and Practice in Chromatography* (*Journal of Chromatography Library*, Vol. 20), Elsevier, Amsterdam, Oxford, Ch. 3.
60 W.C. Askew and K.D. Maduskar, *J. Chromatogr. Sci.*, 9 (1971) 703.
61 A.T. Blades, *J. Chromatogr. Sci.*, 11 (1973) 267.
62 A. Yasuhara, M. Morita and K. Fuwa, *J. Chromatogr.*, 328 (1985) 35.
63 M.A. Pringuer, J. Porter, T.A. Gough and C.F. Simpson, *J. Chromatogr. Sci.*, 17 (1979) 387.
64 E.M. Proksch, P. Gehringer and W. Gzinovatz, *J. Chromatogr. Sci.*, 17 (1979) 568.
65 F.F. Andrawes, E.K. Gibson, Jr. and D.A. Bafus, *Anal. Chem.*, 52 (1980) 1377.
66 R.M. Pomaville and C.F. Poole, *J. Chromatogr.*, 468 (1989) 261.
67 R.M. Pomaville and C.F. Poole, *J. Chromatogr.*, 499 (1990) 749.
68 I. Brown, I.L. Chapman and G.J. Nicholson, *Aust. J. Chem.*, 21 (1968) 1125.
69 K.V. Egorova, V.I. Pakhomova, E.I. Petrova and M.S. Vigdergauz, *Izv. Vyssh. Uchebn. Zaved., Khim. Khim. Tekhnol.*, 34, No. 8 (1991) 63.
70 F. Vernon and G.T. Edwards, *J. Chromatogr. Sci.*, 110 (1975) 73.
71 F. Vernon and G.T. Edwards, *J. Chromatogr. Sci.*, 114 (1975) 87.
72 W.O. McReynolds, *J. Chromatogr. Sci.*, 8 (1970) 685.
73 L.S. Ettre, *Chromatographia*, 6 (1973) 489.
74 L.S. Ettre, *Chromatographia*, 7 (1974) 39.

75 L.S. Ettre, *Chromatographia*, 7 (1974) 261.
76 S.C. Dhanesar and C.F. Poole, *Anal. Chem.*, 55 (1983) 1462.
77 S.C. Dhanesar and C.F. Poole, *J. Chromatogr.*, 267 (1983) 388.
78 S.C. Dhanesar and C.F. Poole, *Anal. Chem.*, 55 (1983) 2148.
79 W.W. Blaser and W.R. Kracht, *J. Chromatogr. Sci.*, 16 (1978) 111.
80 U. Müller, P. Dietrich and D. Prescher, *J. Chromatogr.*, 147 (1978) 31.
81 U. Müller, P. Dietrich and D. Prescher, *J. Chromatogr.*, 259 (1983) 243.
82 J.L. Glajch and W.G. Schindel, *L.C.-G.C. Mag.*, 4 (1986) 574.
83 R.M. Pomaville and C.F. Poole, *Anal. Chim. Acta.*, 200 (1987) 151.
84 P. Varughese, M.E. Gangoda and R.K. Gilpin, *J. Chromatogr. Sci.*, 26 (1988) 401.
85 W.J. Cao, W.Y. Huang, Y.Q. He, X.M. Du, H.S. Huang and C.P. Luo, *Yu Chi Hua Hsueh*, 4 (1981) 267–272.

Journal of Chromatography, 637 (1993) 13–18
Elsevier Science Publishers B.V., Amsterdam

CHROM. 24 912

Study of band broadening in enantioselective separations using microcrystalline cellulose triacetate

I. The linear case

Stephen C. Jacobson

Division of Analytical Chemistry, Oak Ridge National Laboratory, Oak Ridge, TN 37831-6142 (USA)

Andreas Seidel-Morgenstern

Institute of Technical Chemistry, Technical University, W-1000 Berlin (Germany)

Georges Guiochon*

Division of Analytical Chemistry, Oak Ridge National Laboratory, Oak Ridge, TN 37831-6142 (USA) and Department of Chemistry, University of Tennessee, Knoxville, TN 37996-1501 (USA)

(First received September 9th, 1992; revised manuscript received January 25th, 1993)

ABSTRACT

Linear chromatographic data were obtained for the enantiomers of Tröger's base separated on microcrystalline cellulose triacetate with pure ethanol as the mobile phase. The efficiency was determined for flow-rates between 0 1 and 1.0 ml/min at temperatures of 303, 318, 333 and 348 K. The efficiency is poor (below 100 plates) at 303 K, but increases rapidly with increasing temperature. From studies of the effects of these two parameters, the band profile dispersion is attributed to flow anisotropy and adsorption–desorption kinetics. The experimental elution profiles are compared with calculated profiles as a check on the quality of the efficiency measurements.

INTRODUCTION

The utility of microcrystalline cellulose triacetate (CTA) as a chiral discriminator for liquid chromatography has been exploited for 20 years [1–7]. Because it is readily available and inexpensive for a stationary phase, it has become popular for enantioselective separations [8]. Although it exhibits good mechanical stability, it provides for many separations an efficiency that is far below what is desirable for HPLC. The mobile phase flow-rate [4,6] and the column temperature [5–7] can have marked effects on the resolution for a given separation, and in this respect their contributions to the efficiency of the phase system have been studied as separate entities. The reason why the efficiency of well packed columns is so low still eludes our understanding [8].

The separation of the enantiomers of Tröger's base on CTA has already been studied [1,6–8]

* Corresponding author. Address for correspondence: Department of Chemistry, University of Tennessee, Knoxville, TN 37996-1501, USA.

0021-9673/93/$06.00

and constitutes a convenient benchmark of enantioselective separations. This separation is attractive to study because the modest resolution achieved results from the combination of an excellent separation factor and a relatively poor column efficiency at moderate temperatures. Consequently, we can expect a substantial enhancement of the resolution by manipulating properly the mobile phase linear velocity and the column temperature. In this work, we analyzed the contributions of the mass transfer resistances to the band profile dispersion, and especially the contribution of the adsorption–desorption kinetics, as functions of these operating parameters.

EXPERIMENTAL

Equipment

The chromatographic experiments were performed on an HP 1090 liquid chromatograph (Hewlett-Packard, Palo Alto, CA, USA) equipped with a temperature-controlled column oven, a multi-solvent delivery system, a diode-array UV detector and a computer data acquisition system.

Materials

The microcrystalline cellulose triacetate (CTA) was packed into the column (25 cm × 0.46 cm I.D.) using a slurry technique with ethanol as the push solvent. Prior to packing, the CTA was swollen by boiling in ethanol for *ca.* 30 min [1].

Tröger's base (TB) and 1,3,5-tri-*tert.*-butylbenzene (TTBB) were purchased from Fluka (Buchs, Switzerland) and ethanol (100% pure) from Midwest Grain Products (Weston, MO, USA).

Procedures

All chromatograms were obtained under isocratic conditions with ethanol as the mobile phase. Each injection contained 150 ng of each enantiomer of TB and 160 ng of TTBB. The UV detector was set at 220 nm. Chromatograms were obtained at 303, 318, 333 and 348 K for flow-rates of 0.1, 0.2, 0.3, 0.4, 0.5, 0.6, 0.8 and 1.0 ml/min. The efficiency data were extracted from the peak widths at half-height.

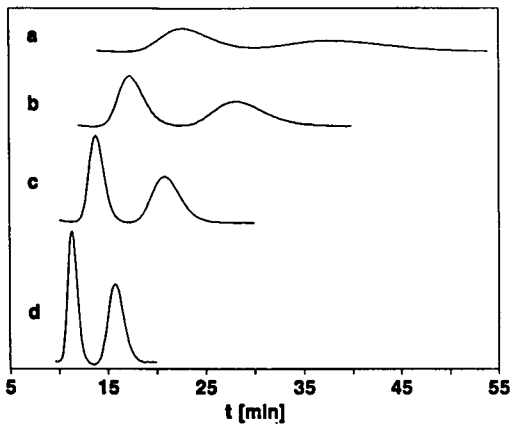

Fig. 1. Chromatograms of Tröger's base (TB) at (a) 303, (b) 318, (c) 333 and (d) 348 K. Experimental conditions: stationary phase, microcrystalline cellulose triacetate; mobile phase, pure ethanol; flow-rate, 0.4 ml/min.

RESULTS AND DISCUSSION

Retention and efficiency data

In Fig. 1 the elution profiles of Tröger's base (TB) are shown for the four temperatures studied. Simply by raising the temperature from 303 to 348 K, a dramatic improvement in the band profiles is observed. These results are in agreement with previously published results [5–7]. Both enantiomer band widths decrease sharply with increasing temperature, because of a combination of a decrease in their retention times and an increase in the column efficiency.

In Fig. 2 and Table I, the temperature dependence of the retention factors and the separation factor are reported. The adsorption enthalpies of TTBB, (−)-TB and (+)-TB are −4.60, −20.1 and −22.3 kJ/mol, respectively. To demonstrate the increase in column efficiency at a flow-rate of 0.4 ml/min, the plate numbers (Table II) increase from 798, 91 and 67 at 303 K to 1207, 652 and 459 at 348 K for (TTBB), (−)-TB and (+)-TB, respectively. This is a sevenfold increase for the TB enantiomers and a 50% increase for the least retained TTBB.

Previously, TTBB was used as an unretained marker [2], but on this column the compound showed a slight retention compared with an impurity in the TTBB sample. The choice to track the impurity as the void marker was made because at the different temperatures the void

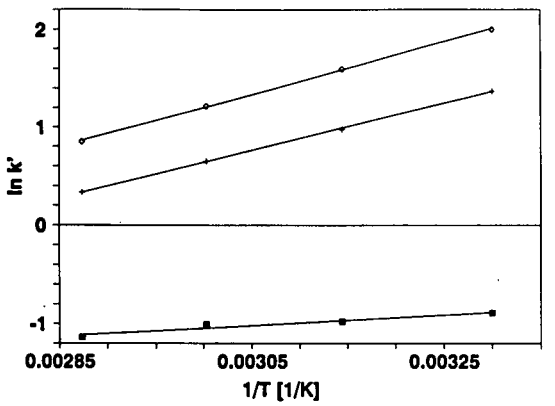

Fig. 2. Variation of the logarithm of the retention factors with the inverse of the absolute temperature. ■ = TTBB; + = (−)-TB; ◇ = (+)-TB.

TABLE I

CAPACITY FACTORS, k', AND SELECTIVITIES, α

T (K)	k'_{TTBB}	$k'_{(-)\text{-TB}}$	$k'_{(+)\text{-TB}}$	$\alpha_{(-,+)}$
303	0.41	3.95	7.38	1.87
318	0.38	2.66	4.94	1.86
333	0.37	1.92	3.39	1.76
348	0.32	1.40	2.34	1.67
ΔH_{ads} (kJ/mol)	−4.60	−20.1	−22.3	

TABLE II

PLATE NUMBERS AT A FLOW-RATE OF 0.4 ml/min

T (K)	TTBB	(−)-TB	(+)-TB
303	798	91	67
318	894	181	131
333	1024	336	213
348	1207	652	459

volume for this unknown remained constant at 1.88 ml, whereas for TTBB a significant decrease in retention occurred with an increase in temperature (Table I). The fact that TTBB is slightly retained although similar in mass to the TB enantiomers (the molecular masses of TTBB and TB are 246 and 250, respectively) makes it likely that no size-exclusion phenomena enter into a comparison between the compounds.

In Figs. 3–6, the height equivalent to a theoretical plate, H (cm), is plotted *versus* the mobile

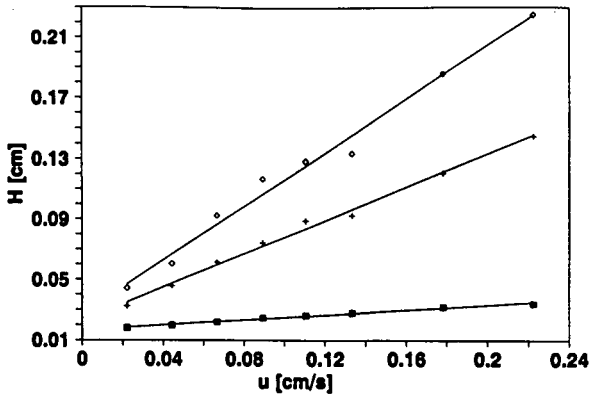

Fig. 3. Van Deemter plot at 333 K. ■ = TTBB; + = (−)-TB; ◇ = (+)-TB.

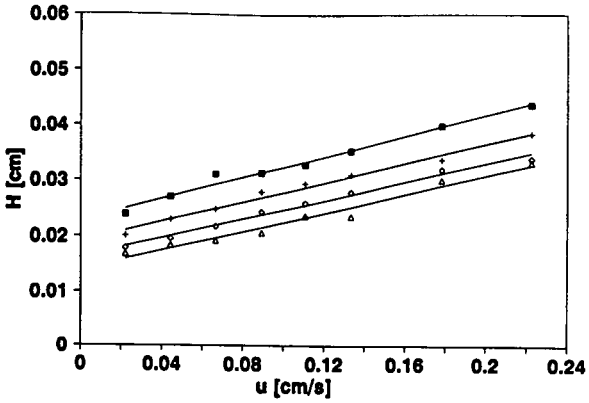

Fig. 4. Van Deemter plot of TTBB at (■) 303, (+) 318; (◇) 333 and (△) 348 K.

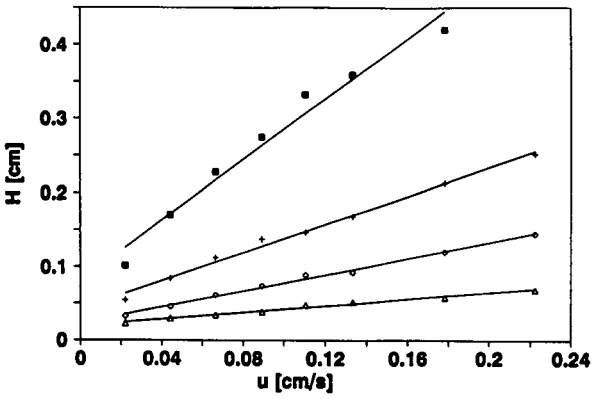

Fig. 5. Van Deemter plot of (−)-TB at (■) 303, (+) 318, (◇) 333 and (△) 348 K.

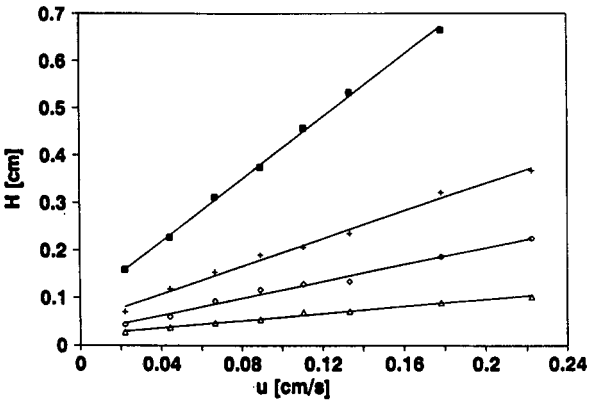

Fig. 6. Van Deemter plot of (+)-TB at (■) 303, (+) 318, (◇) 333 and (△) 348 K.

phase linear velocity, u (cm/s), in Van Deemter plots. Fig. 3 shows the efficiency for the temperature 333 K. For all temperatures, the tendency is identical with that for the more retained (+)-TB, having the lowest efficiency, followed by the (−)-TB, having an intermediate efficiency, and finally TTBB, having the highest efficiency.

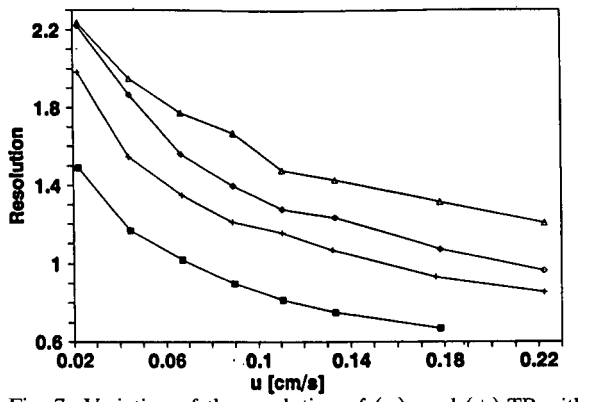

Fig. 7. Variation of the resolution of (−)- and (+)-TB with the mobile phase linear velocity at (■) 303, (+) 318, (◇) 333 and (△) 348 K.

For Figs. 4–6, the variation of the column efficiency for each compound is plotted for the four temperatures. A pattern again develops in that as the temperature increases, the efficiency increases. As a result, the resolution (Fig. 7) is strongly influenced by both the mobile phase velocity and the column temperature. In order to achieve a comparable resolution, *e.g.*, 1.5, a linear flow velocity of *ca.* 0.02 cm/s needs to be used at 303 K whereas 0.14 cm/s, a seven times higher velocity, can be used for 348 K.

Temperature dependence of the mass transfer resistances

In order to describe the change in the efficiency with both the flow velocity and temperature, a modified Van Deemter equation is chosen [9]:

$$H = A + C_s u \tag{1}$$

where

$$C_s = \frac{2k'}{(1+k')^2 k_f} \tag{2}$$

k' is the retention factor and k_f the rate constant of the adsorption–desorption kinetics. The second term of the classical Van Deemter equation, which accounts for axial molecular diffusion, is eliminated because this term is very small under

TABLE III

FLOW ANISOTROPY TERM, A, AND KINETICS TERM, C_s

	A (cm)			C_s(s)		
T (K)	TTBB	(−)-TB	(+)-TB	TTBB	(−)-TB	(+)-TB
303	0.0229	0.0815	0.0858	0.0946	2.04	3.29
318	0.0191	0.0429	0.0487	0.0874	0.955	1.46
333	0.0164	0.0228	0.0273	0.0835	0.553	0.888
348	0.0141	0.0191	0.0218	0.0839	0.230	0.374
ΔH_{act} (kJ/mol)[a]				0.271	49.3	54.5

[a] Activation energy for k_f (eqn. 2).

the present experimental conditions. In the measured range (0.1–1.0 ml/min), the experimental data failed to show a minimum (Figs. 3–6), in agreement with previous findings [4,6]. The inability to observe a measurable minimum for the van Deemter plots indicates the column efficiency is controlled by the contributions of the flow anisotropy and the mass transfer resistances (*i.e.*, the adsorption–desorption kinetics and the kinetics of diffusion across the particles). It was not possible to extend the range of our investigation. At flow-rates below 0.1 ml/min the pumps of the chromatograph failed to maintain a constant flow-rate, and above 1.0 ml/min the stability of the packing at the higher temperatures was in question.

The eddy diffusion term, A, in eqn. 1 should be constant. However, we observe that it varies with increasing temperature (Table III). This can be attributed to the particle size distribution of the packing material (15–25 μm), and to its irregularity. We find also that, for a given temperature, the two enantiomers have nearly the same A value, but that the value corresponding to TTBB falls slightly below in each instance. These differences may arise from the inaccuracy of eqn. 1. The flow anisotropy is diffusion dependent as the molecule must diffuse into and out of adjacent streams of fluid traveling at different velocities [10]. Further, neglecting the classical B/u term in the Van Deemter equation enhances the flow-rate dependence of A. However, fitting the data to more elaborate constructions for this term failed to yield worthwhile parameters.

From Tables I and III and eqn. 2, values of the apparent adsorption–desorption coefficients, k_f, were calculated. As the measurements were made at high velocity, this coefficient is more accurate than A. In Fig. 8, the data are plotted as ln k_f *versus* $1/T$. The experimental data lie along reasonably straight lines, and from the slopes of these lines the activation energies are calculated to be 0.271, 49.3 and 54.5 kJ/mol for TTBB, (−)-TB and (+)-TB, respectively. With energies this large the contribution from the adsorption–desorption kinetics cannot be overlooked in the case of the two enantiomers.

It is striking that whereas the activation energy

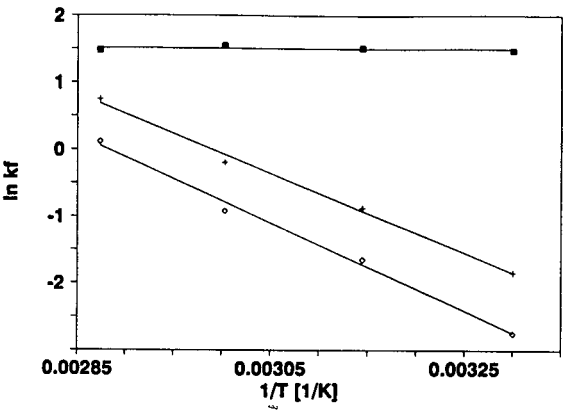

Fig. 8. Variation of ln k_f (eqn. 2) with $1/T$. ■ = TTBB; + = (−)-TB; (◇) = (+)-TB.

for TTBB (Table III) is eighteen times smaller than its adsorption enthalpy (Table I), the activation energies are 2.5 times larger than the adsorption enthalpies for the two TB enantiomers. The unusually large values of these activation energies suggest that the contribution to the mass transfer resistance which controls band broadening in the present instance is the kinetics of adsorption–desorption or of the formation of the chiral discrimination complex.

The band profiles obtained are very close to Gaussian. The retention times and standard deviations measured on these profiles are in excellent agreement with the values calculated using the transport-dispersive model [11], the values of k_f determined in this work and the experimental adsorption isotherm [7] in its linear range, or those derived from the model of Van Deemter *et al.* [9].

CONCLUSIONS

The structure of microcrystalline cellulose is extremely complex [6], which has so far prevented an understanding of the mechanisms of retention and enantioselective separations on this stationary phase. No satisfactory suggestions have yet been made. The study of the kinetics of phase equilibrium during the chromatographic separation shows that band broadening is due to a small contribution of flow anisotropy, similar for the two enantiomers under isothermal conditions, and a major contribution due to mass

transfer resistances. The activation energy of this latter contribution suggests that it involves more of the kinetics of the retention mechanism, presumably a form of adsorption–desorption, than of mass transfer kinetics by intraparticle diffusion.

By better segregation of the contributions to dispersion, more accurate simulations of the band profiles can be ascertained, especially when the kinetics vary greatly for the components of the system. Also, by being able to predict accurately the elution profiles, optimization of the operating parameters for a minimum analysis time with a given degree of resolution becomes that much more valuable. It is certainly satisfactory to observe that, as predicted by theory, the band profiles are still nearly symmetrical at very low column efficiencies.

SYMBOLS

A	flow anisotropy term (cm)
B	axial diffusion coefficient (cm^2/s)
C	mobile phase concentration of the solute (mol/l)
C_s	kinetics term (s)
H	height equivalent to a theoretical plate (cm)
k'	retention factor
k_f	apparent adsorption–desorption coefficient (s^{-1})
T	temperature (K)
u	mobile phase linear velocity (cm/s)
α	selectivity
ΔH_{act}	activation energy (kJ/mol)
ΔH_{ads}	adsorption enthalpy (kJ/mol)

ACKNOWLEDGEMENTS

We gratefully acknowledge the gift of the HP 1090 by Hewlett-Packard (Palo Alto, CA, USA). The microcrystalline cellulose triacetate was graciously supplied by Dr. J.N. Kinkel (E. Merck, Darmstadt, Germany). This work was supported in part by grant CHE-9201662 from the National Science Foundation and by the cooperative agreement between the University of Tennessee and the Oak Ridge National Laboratory. We acknowledge the continuous support of our computational effort by the University of Tennessee Computing Center.

REFERENCES

1 G. Hesse and R. Hagel, *Chromatographia*, 6 (1973) 277.
2 H. Koller, K.-H. Rimböck and A. Mannschreck, *J. Chromatogr.*, 282 (1983) 89.
3 E. Francotte, R.M. Wolf, D. Lohmann and R. Mueller, *J. Chromatogr.*, 347 (1985) 25.
4 A.M. Rizzi, *J. Chromatogr.*, 478 (1989) 71.
5 A.M. Rizzi, *J. Chromatogr.*, 478 (1989) 87.
6 R. Isaaksson, P. Erlandsson, L. Hansson, A. Holmberg and S. Berner, *J. Chromatogr.*, 498 (1990) 257.
7 A. Seidel-Morgenstern and G. Guiochon, *J. Chromatogr.*, 631 (1993) 37.
8 E. Francotte and A. Junker-Buchheit, *J. Chromatogr.*, 576, (1992) 1.
9 J.J. van Deemter, F.J. Zuiderweg and A. Klinkenberg, *Chem. Eng. Sci.*, 5 (1956) 271.
10 L. Lapidus and N.L. Amundson, *J. Phys. Chem.*, 56 (1952) 984.
11 S. Golshan-Shirazi and G. Guiochon, *J. Chromatogr.*, 603 (1992) 1.

Journal of Chromatography, 637 (1993) 19–28
Elsevier Science Publishers B.V., Amsterdam

CHROM. 24 913

Study of band broadening in enantioselective separations using microcrystalline cellulose triacetate

II. Frontal analysis

Andreas Seidel-Morgenstern

Institute of Technical Chemistry, Technical University, W-1000 Berlin (Germany)

Stephen C. Jacobson

Division of Analytical Chemistry, Oak Ridge National Laboratory, Oak Ridge, TN 37831-6142 (USA)

Georges Guiochon*

Division of Analytical Chemistry, Oak Ridge National Laboratory, Oak Ridge, TN 37831-6142 (USA) and Department of Chemistry, University of Tennessee, Knoxville, TN 37996-1501 (USA)

(First received September 9th, 1992; revised manuscript received January 25th, 1993)

ABSTRACT

Frontal analysis is classically used to measure adsorption isotherms, and in this work the isotherms of Tröger's base were determined on microcrystalline cellulose triacetate with ethanol as solvent at 30, 40 and 50°C for the (−)-enantiomer and at 30°C for the (+)-enantiomer. The isotherms of the first eluted (−)-enantiomer are described satisfactorily by the Langmuir equation at all temperatures. In contrast, the isotherm of the longer retained (+)-enantiomer possesses a pronounced inflection point and can be described by a quadratic isotherm equation. However, besides supplying information about the adsorption equilibrium, frontal analysis data can be used to determine kinetic parameters. Using the equilibrium-dispersive model of chromatography, the apparent axial dispersion coefficient was derived by fitting the breakthrough curve for each concentration step. The values are in general agreement with those obtained from the classical determination of the efficiency of elution profiles under linear conditions. However, the apparent dispersion coefficient determined from frontal analysis depends on the concentration.

INTRODUCTION

The equilibrium isotherm is the most important prerequisite for modeling separation processes in liquid chromatography. In the present state of our understanding of phase equilibria, this information can be obtained only on the basis of experimental investigations. The different methods of adsorption isotherm measurements have been reviewed recently by Katti and Guiochon [1]. For chromatographic systems that have low efficiency, frontal analysis (FA) is the most suitable method.

* Corresponding author. Address for correspondence: Department of Chemistry, University of Tennessee, Knoxville, TN 37996-1501, USA.

0021-9673/93/$06.00

Besides isotherms, kinetic parameters must also be known, because of their effect on band broadening. To study mass transfer and adsorption kinetics, different approaches are available. Most often, small injections are made at different flow rates, and their profiles are analyzed on the basis of the Van Deemter plot or of the theory of statistical moments. These measurements are carried out in the linear range of the adsorption isotherms. This permits the study of the contributions of the different kinetic phenomena.

It has been demonstrated for all chromatographic systems that we have studied that the different possible kinetic effects, *e.g.*, axial dispersion in the bulk phase, diffusion through a laminar boundary layer around the solid particles, different types of intraparticle mass transfer resistances and adsorption–desorption kinetics, can be satisfactorily combined into an apparent dispersion coefficient [1–5]. This coefficient can be conveniently determined from the retention time and band width of injections of small sample sizes. However, when applying this method one is not assured that the apparent dispersion coefficient remains independent of the concentration.

The purpose of this work was a further analysis of experimental frontal analysis data that were collected to determine adsorption isotherms. A value of the apparent dispersion coefficient was determined for each of the breakthrough curves measured, thus covering a wide concentration range. The results are compared with those of the analysis of elution band profiles, and the dependence of this kinetic parameter on the average concentration can be studied.

Recently we reported an experimental investigation of the adsorption isotherms of Tröger's base enantiomers (TB) on swollen microcrystalline cellulose triacetate (CTA) from ethanol solutions [6]. CTA is an important stationary phase, widely used for enantioselective separations by preparative chromatography. Many racemates have been successfully separated with this material [7]. CTA has good mechanical properties and is relatively inexpensive compared with other chiral phases. TB is a classical racemate [8]. In our recent studies its unusual retention behavior on CTA observed by several workers was explained as the consequence of different isotherm shapes for the two TB enantiomers [5,6]. Whereas the isotherm of the less retained (−)-enantiomer could be described by a Langmuir isotherm equation, the isotherm of the longer retained (+)-enantiomer exhibited an inflection point and a quadratic isotherm equation was needed for its description.

THEORY

Frontal analysis

In FA, successive step changes in the eluent composition at the column inlet are performed. Solving the integral mass balance equation at each breakthrough curve gives one point of the isotherm. The amount adsorbed during each step of an FA run is obtained from

$$t_R = t_0\left[1 + F \cdot \frac{q(C_E) - q_0}{C_E - C_0}\right] \quad (1)$$

where $q_0 = q_0(C_0)$ is the amount adsorbed at equilibrium before the step change from concentration C_0 to concentration C_E at column inlet, $q(C_E)$ is the amount adsorbed at equilibrium after the step change, t_0 is the retention time of a non-retained component and F is the phase ratio. Eqn. 1 allows the determination of the point of the isotherm, $q(C_E)$, from the retention time of the breakthrough front, t_R.

Owing to the self-sharpening of the breakthrough fronts, the concentration steps ought to be positive for the determination of isotherms of the Langmuir type. If the curvature of the isotherm is opposite, decreasing concentration steps should be used.

Adsorption isotherms

Simple considerations of statistical thermodynamics result in the following general adsorption isotherm equation [9,10]:

$$q = q_s \cdot \frac{C(b_1 + 2b_2C + 3b_3C^2 + \cdots + nb_nC^{n-1})}{1 + b_1C + b_2C^2 + b_3C^3 + \cdots + b_nC^n} \quad (2)$$

where the product nq_s is the saturation capacity of the adsorbent and the temperature dependent coefficients b_i are related to the partition functions for an individual molecule adsorbed on the ith monomolecular layer [9].

The first- ($b_{2+} = 0$) and second-order ($b_{3+} = 0$) equations of the general type proposed in eqn. 2 are the Langmuir and the quadratic isotherm equations, respectively [10]. The adsorption of only one molecule on each adsorption site of the saturated monolayer is assumed in the former model, but that of two molecules in the latter.

In a recent study, the applicability of the Langmuir and the quadratic isotherm equations for describing the adsorption isotherms of the (−)- and (+)-enantiomers of TB on CTA was shown [5,6].

Equilibrium dispersive model of chromatography

In the mass balance of the simplified equilibrium-dispersive model of chromatography [1], the effects of back-mixing and possible mass transfer limitations are combined into the apparent dispersion coefficient D_{ap}:

$$\frac{\partial C}{\partial t} + F \cdot \frac{\partial q}{\partial t} + u \cdot \frac{\partial C}{\partial x} = D_{ap_i} \cdot \frac{\partial^2 C}{\partial x^2} \tag{3}$$

In this equation the concentrations in the stationary and mobile phases, q and C, respectively, are related through the adsorption isotherm:

$$q = f(C) \tag{4}$$

As both phases are assumed to be in equilibrium, the phase ratio $F = (1 - \epsilon_T)/\epsilon_T$ is based on the total porosity, ϵ_T, representing the liquid fraction in the interstitial space of the column and in the pores of the stationary phase. This porosity is usually determined by measuring the retention time of a non-retained component. The parameter u is the average linear velocity.

Under linear conditions, the apparent dispersion coefficient is related to the number of theoretical plates, N_P, by the equation

$$D_{ap} = \frac{uL}{2N_P} \tag{5}$$

where L is the column length.

In several investigations, this simple model was found to be suitable to describe separations by liquid chromatography [4,11]. Preparative chromatographic columns are packed with particles that are much smaller than those used in large-scale adsorption processes. Hence the more detailed considerations of mass transfer processes in the bed particles which are needed to model these methods and require the inclusion of additional kinetic equations [10] are not necessary in chromatography.

As a consequence of the efficiency of HPLC columns, the boundary conditions (BC) required to solve eqn. 3 can be simplified. Instead of Danckwert's BC for the column inlet, the simple condition

$$C(t, x = 0) = C_E(t) \tag{6}$$

can be used. If a pulse injection is to be simulated, $C_E(t)$ is usually assumed to be a rectangular function. When simulating the FA experiments, consecutive step functions have to be implemented in eqn. 6.

The second boundary condition and the initial condition required to solve eqn. 3 are

$$\left.\frac{\partial C}{\partial x}\right|_{x=L} = 0 \tag{7}$$

The algorithms available for calculating numerical solutions of this problem have been recently reviewed by Katti and Guiochon [1]. For many applications, the very efficient finite difference method proposed by Rouchon *et al.* [11] can be considered as adequate. In this algorithm, the term in eqn. 3 describing the dispersion of the profile is not calculated, but it is simulated by the numerical dispersion of the calculation. This requires selecting the optimum size for the mesh of the (x, t)-grid used in the numerical integration [12].

EXPERIMENTAL

Equipment

The determination of isotherms by FA and the measurement of elution profiles were performed using an HP1090 liquid chromatograph (Hewlett-Packard, Palo Alto, CA, USA), equipped with a temperature-controlled column chamber, a sol-

vent-delivery system, an automatic sample injector, a rapid-scan UV photodiode-array detector and a data station. The detector was calibrated using the plateaux in the FA runs. For a wavelength of 300 nm the slightly non-linear response was fitted with a third-order polynomial for TB concentrations up to 0.005 mol/l.

Materials

Stationary phase. A sample of microcrystalline CTA (15–25 μm) was kindly supplied by Dr. J.N. Kinkel (E. Merck, Darmstadt, Germany). A 10×0.46 cm I.D. stainless-steel column was packed using a slurry technique. Prior to packing, CTA was boiled in ethanol for 30 min to allow its swelling. After cooling and decanting, the suspension was treated in an ultrasonic bath for 5 min at ambient temperature and poured into the packing chamber. An 80-ml volume of ethanol was applied as pushing solvent at a pressure of 275 bar. The work reported in the Part I [13] was carried out with a 25-cm column, which explains some minor differences in the retention factor and adsorption enthalpy.

Following Koller *et al.* [14], the total column porosity was measured by injecting 1,3,5-tri-*tert.*-butylbenzene (TTBB). The retention volume of TTBB varies by less than 2% in the temperature range studied. As it is nearly independent of the temperature within the experimental errors, TTBB can be considered as non-retained on CTA. The results discussed in the Part I [13] show that this is a good approximation. The column efficiency for TTBB was about 400 theoretical plates. The total void volume of the column was 1.0 ml, leading to a total porosity $\epsilon_T = 0.602$. This corresponds to a phase ratio $F = (1 - \epsilon_T)/\epsilon_T = 0.661$.

An additional volume of tubing (0.78 ml) caused a time delay for step injections which were made with the solvent-delivery system, compared with small sample injections made with the automatic sample injector.

Mobile phase and chemicals. All experiments were performed under isocratic conditions, using pure ethanol (100%) from Midwest Grain Products (Weston, MO, USA). Enantiomers of Tröger's base (TB), $C_{17}H_{18}N_2$ ($M = 250.35$ g/mol), with a purity >99.5%, and 1,3,5-tri-*tert.*-butylbenzene were purchased from Fluka (Buchs, Switzerland). All compounds were used as received.

Procedure

The concentration of the solutions used for the FA experiments was chosen to be *ca.* 0.0048 mol/l. The experiments were carried out using the automatic solvent-delivery system to generate the concentration steps. Only steps of increasing concentration were performed for the (−)-enantiomer of TB. Owing to the inflection point observed on the (+)-TB isotherm, several steps with decreasing concentration were also recorded for this enantiomer. The combined analysis of adsorption and desorption steps permits a more accurate determination of isotherms with an inflection point [5,6]. The primary chromatographic data were transferred to the VAX 8700 of the University of Tennessee Computing Center for further processing. The retention time of each concentration front could be determined with a precision better than 1.5%.

Ten concentration steps were performed to determine ten points for each isotherm. The flow-rate in all FA experiments was kept at 0.5 ml/min. Measurements were made at a column temperature of 30, 40 and 50°C for the (−)-enantiomer and at 30°C for the (+)-enantiomer. In addition, elution profiles of small size samples of both TB enantiomers were measured at the same temperatures, to determine the number of theoretical plates according to standard methods, from the retention times and the peak widths [13].

RESULTS AND DISCUSSION

Adsorption isotherms

Fig. 1 shows the FA chromatograms obtained at the three temperatures investigated for the (−)-enantiomer. In Fig. 2 the FA chromatogram of the (+)-enantiomer at 30°C is given.

The equilibrium isotherms obtained for the adsorption of the TB-enantiomers on CTA are shown in Fig. 3. The lines were calculated by fitting the data points to the Langmuir isotherm $[q = q_s b_1 C/(1 + b_1 C)]$ for the (−)-enantiomer and to the quadratic isotherm $[q = q_s C(b_1 +$

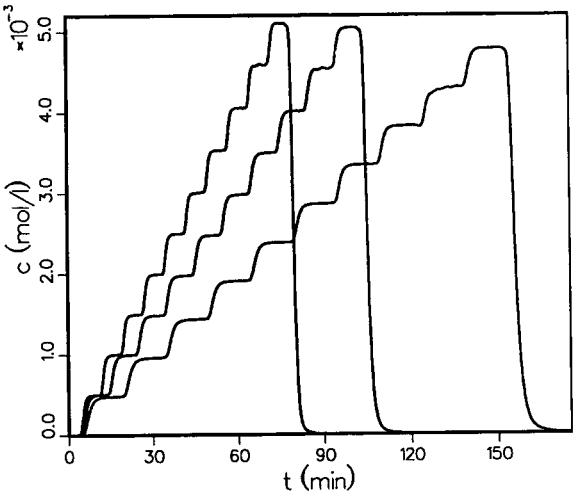

Fig. 1. Frontal analysis to determine the isotherms of the (−)-enantiomer of TB at 30, 40 and 50°C (right to left).

$2b_2C)/(1 + b_1C + b_2C^2)]$ for the (+)-enantiomer. In each case, the selected model describes the experimental isotherm very well. The Langmuir model was not able to account for the (+)-enantiomer isotherm. Although the inflection point is not conspicuous in Fig. 3, its existence has been demonstrated by a series of conclusive results published previously [5,6]. The values obtained for the parameters of the equations and the corresponding standard deviations are given in Table I. These values were calcu-

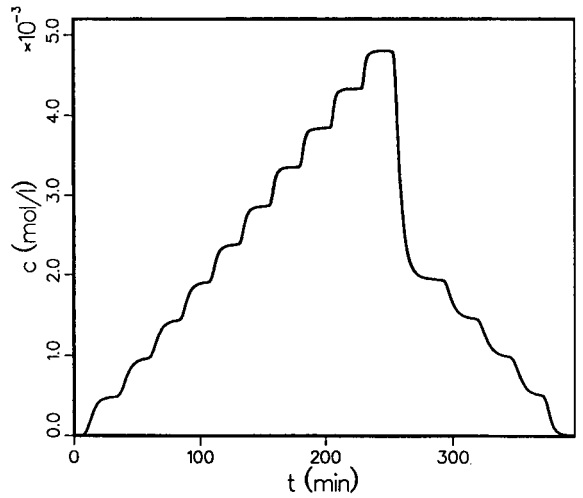

Fig. 2. Frontal analysis to determine the isotherm of the (+)-enantiomer at 30°C.

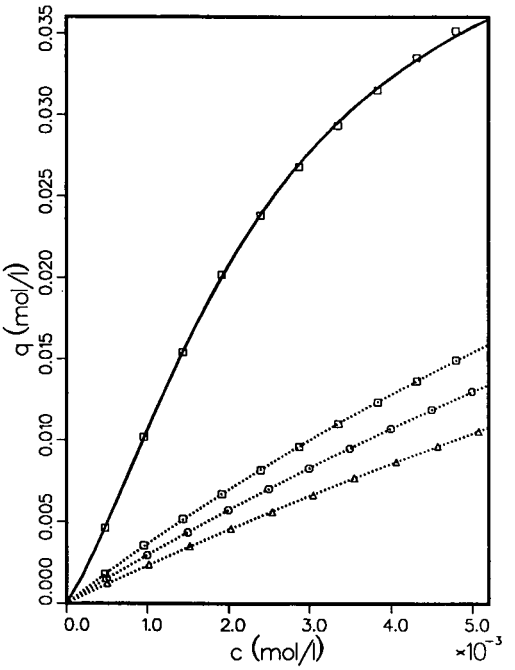

Fig. 3. Isotherms of the (−)-enantiomer of TB on CTA at 30, 40 and 50°C (dotted lines, top to bottom) and of the (+)-enantiomer at 30°C (solid line). The lines were calculated with the Langmuir isotherm for (−)-TB and with the quadratic isotherm equation for (+)-TB, parameters in Table I. The symbols designate the experimental data.

lated by minimizing the following objective function, using Marquard's method [15]:

$$\sigma\,(\%) = 100\sqrt{\frac{1}{N_D - P}\sum_{i=1}^{N_D}\left(\frac{q_i^{ex} - q_i^{th}}{q_i^{ex}}\right)^2} \qquad (9)$$

where N_D and P are the numbers of data points and model parameters, respectively.

A thermodynamic analysis of these and addi-

TABLE I

PARAMETERS OF THE ISOTHERM EQUATION (EQN. 2)

Enantiomer	T (K)	q_s (mol/l)	b_1 (l/mol)	b_2 (l²/mol²)	σ (%)
(−)-	303	0.0800	47.6	0	0.50
	313	0.0850	36.0	0	0.28
	323	0.0818	29.2	0	0.79
(+)-	303	0.0239	316.4	173 000	0.65

tional equilibrium parameters for the system TB–CTA–ethanol is given elsewhere [6].

Determination of efficiencies

The unusually broad peaks observed with CTA seriously limit its uses in analytical and preparative chromatography. A detailed study on the influence of solvent composition, temperature and pressure on the efficiency of CTA columns has been performed by Rizzi [16]. The results prove that intraparticle mass transfer processes are the rate-limiting step for separations on CTA. As the apparent dispersion coefficient takes this effect into account, the equilibrium-dispersive model is able to simulate elution band profiles for TB [5].

For preparative purposes, longer CTA columns are necessary to achieve the efficiency required for the separation, and both the temperature and the solvent composition must be optimized carefully. However, as FA requires complete saturation of the stationary phase with the sample, shorter columns are advantageous for the determination of model parameters, as they allow important savings in time and chemicals.

The determination of the apparent dispersion coefficient, or the column efficiency, both linked by eqn. 5, was performed by comparing the theoretical curves generated by numerical solution of eqn. 3 with the experimental fronts. This comparison was done in the range of relevant values of the plate numbers, and gave the best estimate of the plate number. The objective function to be minimized was $OF = \Sigma(c_i^{ex} - c_i^{th})^2$

Owing to experimental problems, the last two step responses, corresponding to the two highest concentrations studied, were not included in the mathematical analysis. In this range, oscillations of the detector signal were observed (see the second to last or ninth plateau in Fig. 1), and the back-pressure was not stable.

The optimization procedure described above was applied first separately to each of the first eight breakthrough curves, then to the data of all eight fronts together. As grid sizes in the time domain had to be superimposed to minimize *OF*, a linear interpolation of the theoretical values had to be performed to match the times of the experimental data. Another problem was connected with the fact that the algorithm to solve eqn. 3 uses a time grid that is dependent on the theoretical plate number [11]. Since the step functions at the column inlet can be implemented in the numerical scheme only at the grid points, discontinuities appear in the objective function, depending on the plate number. This problem could be circumvented by shifting all experimental step responses in the time scale origin prior to data analysis.

We illustrate the effect of the optimization in Fig. 4 with results obtained in FA of the (−)-enantiomer at 30°C. Shown are the normalized deviations between experimental and theoretical data as a function of time for the first eight fronts. The curves given correspond to 10 (dotted line) and 90 (dashed line) theoretical plates. The plateaux can be recognized as the regions where the deviations between curves almost vanish. The residual errors at these plateaux are mainly due to small calibration errors and to concentration changes in the feed solution due to degassing with helium. Between the plateaux the differences are evident. The value of $N_P = 10$ is obviously too small, as at the beginning of the fronts the concentrations are smaller and at the end of the fronts they are higher than the

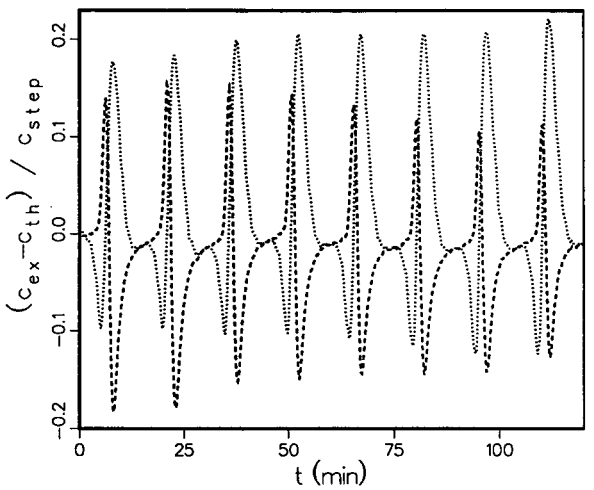

Fig. 4. Differences between experimental and theoretical FA experiment for the first eight steps of the FA experiment with the (−)-enantiomer of TB at 30°C. The dotted line was calculated with 10 and the dashed line with 90 theoretical plates.

theoretical values. The opposite holds for N_P = 90, and this value is too large.

In Fig. 5 we show the results obtained by making the best estimate of the column efficiency as explained above, for four individual fronts and for the data obtained with all eight fronts together. These plots of *OF versus* N_P show a best estimate of the plate number, which increases with increasing solute concentration in the case of the individual fronts.

Fig. 6 summarizes the results obtained as plots, for each four series of FA analysis, of the best estimate of the theoretical plate number *versus* the step rank. The trend observed at 30°C with the (−)-enantiomer, a slow increase in this estimate with increasing concentration, is found also at 40 and 50°C. The plot obtained for the (+)-enantiomer at 30°C is different. It exhibits a sharp minimum at the third step. These differences in mass transfer characteristics between the two TB enantiomers parallel the differences between their adsorption isotherms [5]. The minimum of the number of theoretical plates for the (+)-enantiomer is found at approximately the same concentration as the inflection point of the adsorption isotherm (0.001 mol/l). In agreement with Rizzi [16], the column efficiency for the (+)-enantiomer is only about two thirds of the value for the (−)-enantiomer.

At this point it should be emphasized that in the mathematical analysis performed, the correct isotherms are applied. Therefore, the improved efficiency observed at higher concentrations is not caused by the self-sharpening effect due to a favorably curved adsorption isotherm, but by an actual decrease in the apparent dispersion coeffi-

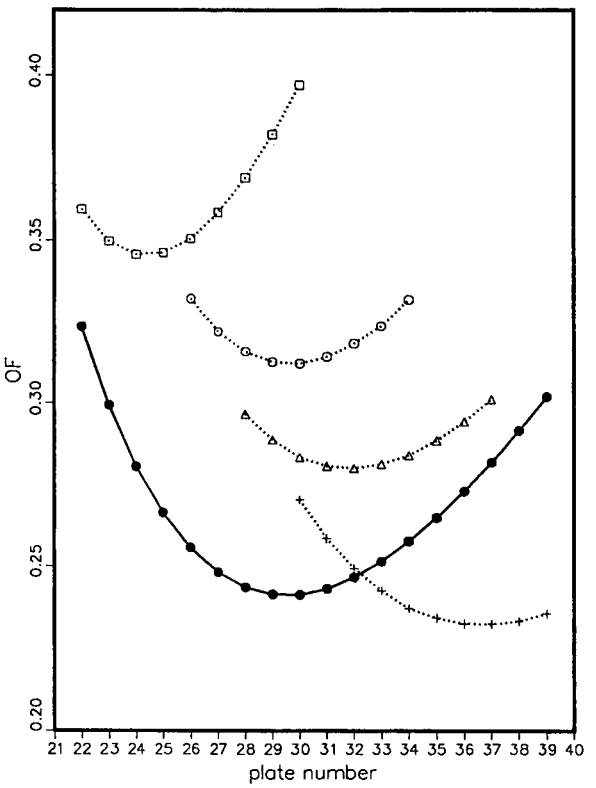

Fig. 5. Results of optimizing the number of theoretical plates for the FA run with the (−)-enantiomer at 30°C. □ = Second front in Fig. 1; ○ = fourth front; △ = sixth front; + = eighth front [in all four cases, *OF* in 10^{-7} (mol/L)^2]; ● = all data of the first eight fronts [*OF* in 10^{-6} (mol/L)^2].

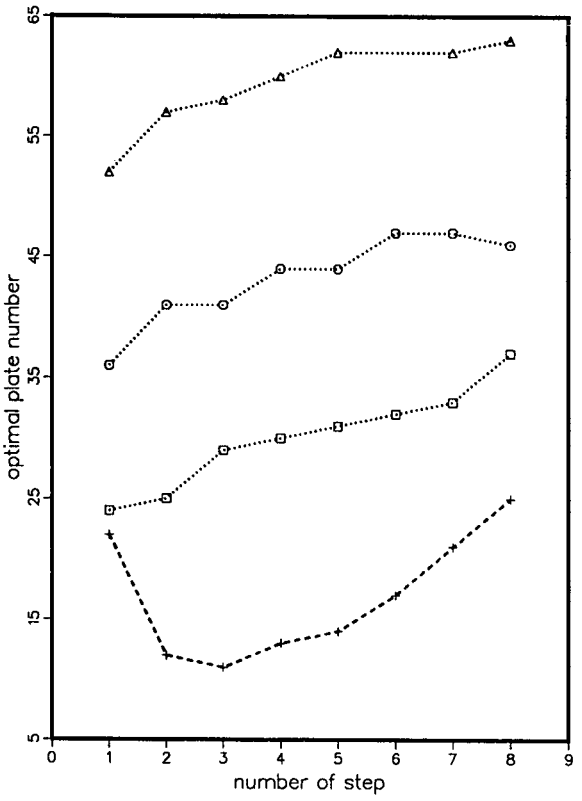

Fig. 6. Dependence of the best estimate of the number of theoretical plates on the rank of the step in the series of FA runs. The step size for each front was 0.00048 mol/l. □ = (−)-enantiomer, 30°C; ○ = (−)-enantiomer, 40°C; △ = (−)-enantiomer, 50°C; + = (+)-enantiomer, 30°C.

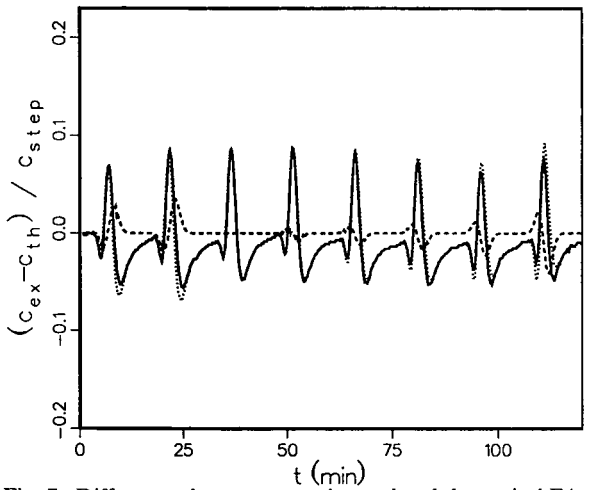

Fig. 7. Differences between experimental and theoretical FA experiments for the first eight steps of the FA experiment with the (−)-enantiomer of TB at 30°C. The solid line was calculated with the best estimate of the number of theoretical plates (see Fig. 5). The dotted line was calculated with the average number of 30 theoretical plates. The dashed line is the difference between the solid and the dotted lines.

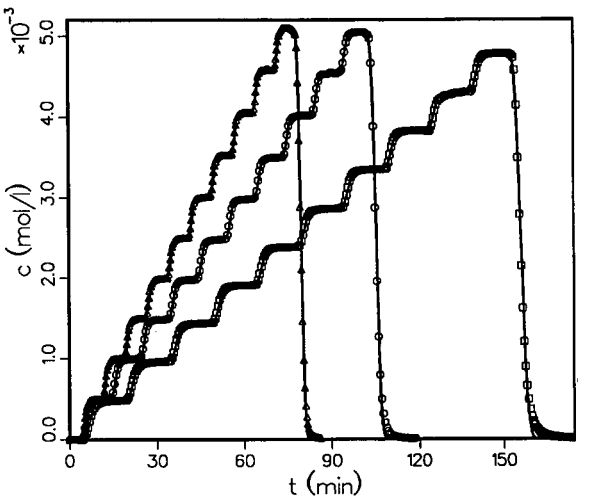

Fig. 8. Comparison between experimental and theoretical FA for the (−)-enantiomer of TB at 30, 40 and 50°C (right to left). The numbers of theoretical plates were 30, 43 and 60, respectively (see Table II).

cient. Whether this corresponds to an increase in the rate of mass transfer is another question.

Fig. 7 shows the deviations between the model and the same experimental data as used in Fig. 4. This time, the solid line was calculated with the best estimate of the theoretical plate number derived for each front, and the dotted line with the average value obtained from optimizing all eight fronts together. The dashed line gives the differences between these two lines. In Fig. 5 it was already clear that the minima are not very pronounced. From Fig. 7, we can conclude that the model used is suitable to describe the adsorption process considered. However, some deviations remain, that could not be eliminated, even when using the optimum values for each individual front. As intraparticle mass transfer is dominant, probably a two-phase model that would take into account the slow transfer in the stationary phase would be able to achieve improved simulations.

Figs. 8 and 9 compare the calculated and experimental FA chromatograms. In the calculations the theoretical plate numbers obtained from optimizing all eight fronts were used. The agreement is excellent. The small deviations in the tail of the desorption fronts of the (−)-enantiomer (Fig. 8) are mainly caused by the presence of a small amount of the longer retained (+)-enantiomer. The agreement appears to be much better in Figs. 8 and 9 than in Fig. 7, because of the smaller concentration scale used.

Thus, in the system studied, the use of a

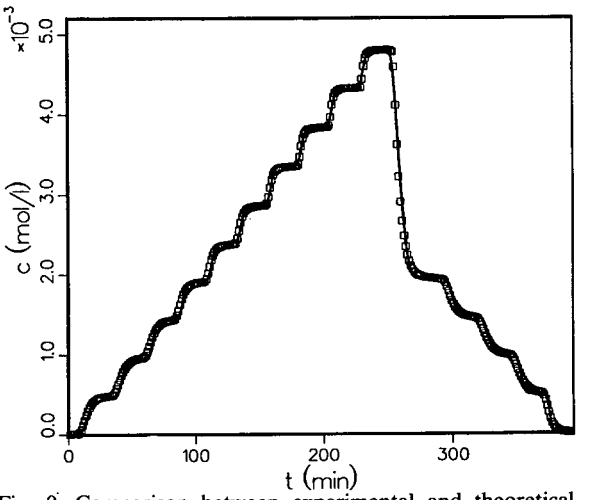

Fig. 9. Comparison between experimental and theoretical FA for the (+)-enantiomer of TB at 30°C. The number of theoretical plates was 16 (see Table II).

constant average mass transfer coefficient seems justified for the calculation of band profiles. However, it should be emphasized again that the increase in the plate number with increasing concentration that we have observed is a real effect. Similar observations were made in analyzing the kinetics of the adsorption of organic components on activated carbon. For the systems studied, a strong increase of the surface diffusion coefficient with increasing loading was reported [17].

In Table II, we compare the numbers of theoretical plates determined as described above by considering together the FA data for all eight fronts, and the values obtained by applying the classical method of evaluating the efficiency of the elution profiles obtained with small size samples. The agreement can be considered as satisfactory.

Finally, from the number of theoretical plates obtained from the elution profiles for the (−)-enantiomer at three different temperatures, it is possible to estimate the activation energy for the apparent dispersion coefficient. We obtain *ca.* 31.5 kJ/mol. This relatively large value is in general agreement with the activation energy of the kinetic parameter k_f discussed in Part I [13]. Axial dispersion, eddy diffusion and intraparticle diffusion processes are known to possess much lower activation energies. As a consequence, it can be concluded that, besides mass transfer resistances, the effect of the kinetics of adsorption–desorption is one of the main contributions to the apparent dispersion coefficient D_{ap}. The latter effect seems to have a dominant influence on the separation of the TB enantiomers on CTA.

TABLE II

NUMBERS OF THEORETICAL PLATES DETERMINED FROM INJECTIONS OF SMALL SIZE SAMPLES (SI) AND FRONTAL ANALYSIS (FA)

Enantiomer	T (K)	N_p(SI)	N_p(FA)
(−)-	303	29	30
	313	44	43
	323	63	60
(+)-	303	20	16

CONCLUSIONS

Our results demonstrate again the importance and usefulness of systematic studies of mass transfer in chromatography under linear conditions and by frontal analysis. These measurements provide an easy access to kinetic data which are useful to understand better the mechanism of the chromatographic process. This is especially useful for separations such as that of the (+)- and (−)-enantiomers of TB on CTA, where poor values of the production rate can be achieved because the positive effect of a high relative retention is offset by slow mass transfer inside the stationary phase.

The concentration dependence of D_{ap} observed during our measurements agrees with previous results [17]. General inclusion of this effect could make the mathematical model much more complicated. However, the concentration dependence seems to be rather inconsequential in the present instance. The use of an average apparent dispersion coefficient, determined from the simultaneous optimization of the data of several fronts, gave results in agreement with the direct determination of the efficiency under linear conditions [13], and calculated profiles in agreement with experimental values. This result validates the use of the equilibrium-dispersive model with a constant apparent diffusion coefficient.

SYMBOLS

b_i	parameter in isotherm equation (eqn. 1) $(l/mol)^i$
C	liquid (mobile) phase concentration (mol/l)
C_0	mobile phase concentration before the step (eqn. 1)
C_E	mobile phase concentration after the step
C_{step}	concentration step for one front in an FA experiment (mol/l)
D_{ap}	apparent dispersion coefficient (m^2/s)
F	phase ratio

L	column length (m)
N_P	number of theoretical plates
N_D	number of data
OF	objective function
P	number of parameters
q	stationary phase concentration (loading) (mol/l)
$q(C_E)$	stationary phase concentration at equilibrium with mobile phase concentration C_E (mol/l)
$q_0 = q(C_0)$	stationary phase concentration at equilibrium with mobile phase composition C_0 (mol/l)
q_S	saturation loading (mol/l)
t	time (s)
t_R	retention time (s)
t_0	retention time of a non-retained component (s)
T	temperature (K)
u	linear velocity, $u = L/t_0$ (m/s)
x	axial coordinate of column (m)

Greek letters

ϵ_T	total porosity
ρ	standard deviation, defined in eqn. 9

Superscripts

ex	experimental value
th	theoretical value

Subscript

E	at column inlet

ACKNOWLEDGEMENTS

We acknowledge the gift of microcrystalline cellulose triacetate and Tröger's base samples by Dr. J.N. Kinkel (E. Merck, Darmstadt, Germany). A.S.-M. is grateful for the support of his stay in Knoxville by the NATO Science Fellowship Program and by the German Academic Exchange Service (DAAD). The HP 1090 liquid chromatograph was a gift from Hewlett-Packard (Palo Alto, CA, USA). This work was supported in part by grant CHE-9201663 from the National Science Foundation and by the cooperative agreement between the University of Tennessee and the Oak Ridge National Laboratory. We acknowledge continuous support of our computational efforts by the University of Tennessee Computing Center.

REFERENCES

1 A. Katti and G. Guiochon, *Adv. Chromatogr.*, 32 (1991) 1.
2 M. Diack and G. Guiochon, *Anal. Chem.*, 63 (1991) 2608.
3 S. Golshan-Shirazi and G. Guiochon, in F. Dondi and G. Guiochon (Editors), *Proceedings of the NATO ASI on Advances in Chromatography and Related Techniques*, Kluwer, Delft, Netherlands, 1992, p. 35.
4 S.C. Jacobson, S. Golshan-Shirazi and G. Guiochon, *AIChE J.*, 36 (1991) 836.
5 A. Seidel-Morgenstern and G. Guiochon, *Chem. Eng. Sci.*, in press.
6 A. Seidel-Morgenstern and G. Guiochon, *J. Chromatogr.*, 631 (1993) 37.
7 E. Francotte and A. Junker-Buchheit, *J. Chromatogr.* 576 (1992) 1.
8 G. Hesse and R. Hagel, *Chromatographia*, 6 (1973) 277.
9 T.L. Hill, *An Introduction to Statistical Thermodynamics*, Addison-Wesley, Reading, MA, 1960.
10 D.M. Ruthven, *Principles of Adsorption and Adsorption Processes*, Wiley, New York, 1984.
11 P. Rouchon, M. Schonauer, P. Valentin and G. Guiochon, *Sep. Sci. Technol.*, 22 (1987) 1793.
12 M. Czok and G. Guiochon, *Comput. Chem. Eng.*, 14 (1990) 1435.
13 S.C. Jacobson, A. Seidel-Morgenstern and G. Guiochon, *J. Chromatogr.*, 637 (1993) 13.
14 H. Koller, K.-H. Rimbock and A. Mannschreck, *J. Chromatogr.*, 89 (1983) 282.
15 D.W. Marquardt, *J. Soc. Appl. Math*, 11 (1963) 431.
16 A.M. Rizzi, *J. Chromatogr.*, 478 (1989) 87.
17 M. Friedrich, A. Seidel and D. Gelbin, *Chem. Eng. Process.*, 24 (1988) 33.

Journal of Chromatography, 637 (1993) 29–34
Elsevier Science Publishers B.V., Amsterdam

CHROM. 24 882

Liquid chromatographic determination of chiral epoxides by derivatization with sodium sulphide, *o*-phthalaldehyde and an amino acid

A.L.L. Duchateau* and N.M.J. Jacquemin

Department FA, DSM Research BV, P.O. Box 18, 6160 MD Geleen (Netherlands)

H. Straatman and A.J. Noorduin

DSM Andeno BV, P.O. Box 81, 5900 AB Venlo (Netherlands)

(First received October 27th, 1992; revised manuscript received January 12th, 1993)

ABSTRACT

A high-performance liquid chromatographic method for the enantiomeric determination of chiral epoxides is described. By derivatization with sodium sulphide, *o*-phthalaldehyde and an optically pure amino acid, chiral mono- and 2,2-disubstituted epoxides were converted into diastereomeric isoindole derivatives. Separation of the diastereomers was carried out by reversed-phase chromatography and the derivatives were detected fluorimetrically. For a series of nine monosubstituted epoxides, good enantioselectivity was obtained ($\alpha = 1.3–1.7$). To study the effect on the chromatographic behaviour of the isoindole adducts, derivatization was carried out using four different amino acids. The derivatization procedure was optimized using glycidyl butyrate as test compound. Both the precision and accuracy of the method were investigated. The method was applied to monitor the enantiomeric purity of glycidyl butyrate obtained by lipase-catalysed hydrolysis of the racemate.

INTRODUCTION

Optically pure epoxides (oxiranes) are important chiral building blocks for a wide variety of chiral pharmaceuticals [1]. In conjunction with the synthesis, analytical methods are required for the control of the enantiomeric purity of the epoxides. Both gas and liquid chromatographic methods have been described for determining epoxide enantiomers. Complexation gas chromatography has been used to determine the enantiomeric composition of epoxyalkanes [2–4]. More recently, cyclodextrin chiral stationary phases for capillary gas chromatography have been described for the determination of chiral epoxides [5,6].

By applying a two-reaction derivatization sequence, followed by high-performance liquid chromatographic (HPLC) analysis of the derivatives, the enantiomeric determination of several chiral epoxides could be achieved [7]. Recently, a direct HPLC method has been described for the resolution of glycidyl tosylate and glycidyl-3-nitrobenzenesulphonate enantiomers [8]. Because of the presence of salts and enzyme in reaction mixtures from bio-organic syntheses of chiral epoxides, HPLC will generally be preferred to gas chromatography for the determination of the enantiomers. The existing HPLC methods for chiral epoxides show some drawbacks, however. In the method of Gal [7], long

* Corresponding author.

0021-9673/93/$06.00

reaction times are required to perform the aminolysis step. Moreover, the complete derivatization sequence cannot be automated. On the other hand, the direct method of Shaw and Barton [8] is unsuitable for the analysis of aqueous mixtures of chiral epoxides.

In order to extend the scope of HPLC methods for enantiomeric epoxides, a new approach was evaluated. Epoxides are known to give the corresponding thioglycol derivatives when treated with hydrogen sulphide in the presence of sodium [9]. Based on this reaction, a spectrofluorimetric method has been developed for the assay of epoxides [10]. In this method, epoxides are converted into thioglycol derivatives and subsequently treated with *o*-phthalaldehyde (OPA) and taurine to form fluorescent isoindole adducts. The HPLC determination of isoindole derivatives of several thiols and amines has been extensively reported. By using an optically active thiol compound, *e.g.*, N-acetyl-L-cysteine in the OPA reaction, it was shown that this reaction was also applicable to the enantiomeric determination of amino compounds [11].

The aim of this work was to develop a sensitive and specific HPLC method for the enantiomeric determination of monosubstituted epoxides. To that end, the chiral epoxides were first converted into the corresponding chiral thioglycol derivatives by reaction with sodium sulphide, whereafter OPA and an optically pure amino acid were used as reagents to form diastereomeric isoindole compounds. The retention, enantioselectivity and resolution of the fluorescent diastereomers were examined by reversed-phase chromatography. The method was found to be suitable for monitoring the enantiomeric excess of glycidyl butyrate obtained by lipase-catalysed hydrolysis of the racemate.

EXPERIMENTAL

Materials

(±)-Epichlorohydrin, (±)- and (*R*)-styrene oxide, (±)- and (*S*)-propylene oxide, (*R*)- and (*S*)-glycidyl tosylate, (*R*)- and (*S*)-2-methylglycidyl 4-nitrobenzoate, (±)- and (*S*)-glycidol, (±)-glycidyl phenyl ether, L-valine, L-leucine, L-alanine and L-phenylalanine were obtained from Aldrich (Milwaukee, WI, USA). The optical purity of the L-amino acids, as determined by HPLC on a Crownpak CR(+) column, was 99.9% for all four compounds. (±)-And (*R*)-glycidyl butyrate and (±)-benzyl-3,4-epoxybutyrate were supplied by Andeno (Venlo, Netherlands). OPA, sodium sulphide hydrate and HPLC-grade methanol were obtained from Merck (Darmstadt, Germany). Water was purified with a Milli-Q system (Millipore). All other chemicals were of analytical-reagent grade.

Instrumentation

The chromatographic system consisted of a Hewlett-Packard (Palo Alto, CA, USA) Model 1081 B liquid chromatograph and a Gilson Model 231-401 autosampling injector for derivatization and injection. The injection loop had a 20-μl capacity. The columns used were Nucleosil-120-C_{18} (250 × 4.0 mm I.D., 5 μm) from Macherey–Nagel (Düren, Germany) and LiChrosorb RP-18 (250 × 4.0 mm I.D., 7 μm) from Merck. The flow-rate was 1 ml/min and the column temperature was kept at 40°C.

The derivatives were monitored with a Hitachi (Tokyo, Japan) Model F-1000 fluorescence detector using an excitation wavelength of 330 nm and an emission wavelength of 440 nm. Quantification was performed with a Hewlett-Packard Model 3350 laboratory automation system.

Eluent, reagent and derivatization procedure

The eluent consisted of 50 m*M* sodium acetate buffer (titrated to pH 6.0 with acetic acid)–methanol (45:55, v/v).

For sodium sulphide, a 100 m*M* solution was prepared and titrated to pH 10.0 with acetic acid. The buffer solution was prepared by titrating 12.5 m*M* sodium tetraborate solution with potassium dihydrogenphosphate to pH 8.3. OPA reagent was prepared by dissolving OPA in water–methanol (1:1, v/v) to a concentration of 150 m*M*. The final reagent concentration (30 m*M*) was obtained by dilution with buffer (pH 8.3). A 30 m*M* amino acid solution (L-Val, L-Phe, L-Leu or L-Ala) was prepared by dissolving the compound in buffer (pH 8.3). The

epoxide standards and samples were dissolved in methanol.

Derivatization and injection were performed automatically with a Gilson Model 231-401 system. Into a vial the following were successively dispensed: 100 μl of sample solution and 100 μl of sodium sulphide solution. The contents of the vial were mixed and allowed to stand for 15 minutes at room temperature, then 100 μl of OPA reagent and 100 μl of the amino acid solution were added. The 400-μl volume was mixed and allowed to stand for 15 min at room temperature. Finally, an aliquot of the reaction mixture was injected into the chromatographic system.

RESULTS AND DISCUSSION

Investigation of the enantioselectivity of the derivatives

A series of monosubstituted chiral epoxides, together with a 2,2-disubstituted epoxide, were converted into the corresponding thioglycol derivatives using the sodium sulphide procedure described by Sano and Takitani [10]. The reaction of OPA and L-Val with the thioglycol compounds yielded highly fluorescent derivatives, which are assumed to be isoindole fluorophores. Maximum fluorescence response for the derivatives was obtained at an excitation wavelength of 330 nm and an emission wavelength of 440 nm. The enantioselectivity of the isoindole derivatives was examined using reversed-phase chromatography.

In Table I, the capacity factor (k'), selectivity (α) and resolution (R_s) of the diastereomers are shown. It can be seen that for a broad range of monosubstituted epoxides good enantioselectivity was obtained ($\alpha = 1.3–1.7$). For 2-methylglycidyl 4-nitrobenzoate only partial separation of the enantiomers could be obtained. As this compound is the only 2,2-disubstituted epoxide in the series, the low α-value obtained may possibly be associated with the occurrence of an extra substituent at the chiral carbon. In the case of racemic glycidyl butyrate, two minor peaks (R′ and S′) occurred in the chromatogram which were partly separated from the main peaks (Fig. 1a). By changing the pH of the mobile phase

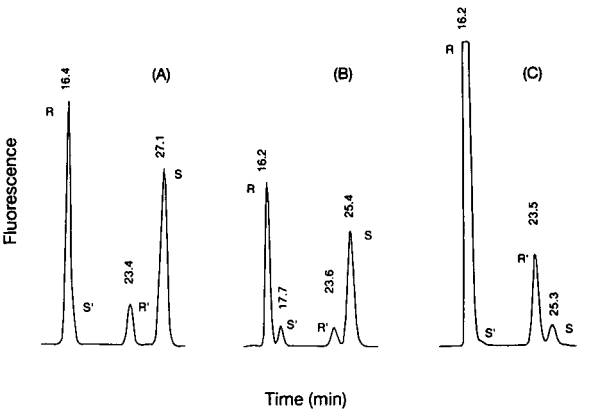

Fig. 1. Separation of the diastereomeric OPA–L-Val derivatives of (A, B) racemic and (C) non-racemic glycidyl butyrate. Conditions: column, LiChrosorb RP-18; mobile phase, 50 m*M* sodium acetate solution [(A) pH 6.0, (B, C) pH 4.6]–methanol (45:55, v/v); flow-rate, (A) 1 ml/min and (B, C) 1.5 ml/min.

from 6.0 to 4.6, the four peaks could be baseline separated (Fig. 1b). Analysis of non-racemic glycidyl butyrate showed that each of the two pairs of peaks gave the same enantiomeric excess (Fig. 1c). The occurrence of the two side-products may be explained by the fact that ring opening by treatment with Na_2S occurs at both carbons of the epoxide ring of glycidyl butyrate. Consequently, four diastereomeric reaction products will be formed after reaction with OPA–L-Val.

The proposed structures for these isoindole derivatives are shown in Fig. 2. As in neutral and basic solution nucleophilic attack occurs predominantly at the sterically less hindered site of the epoxide [12], the main products formed will be those involving C-3 ring opening, whereas the minor products result from C-2 ring opening.

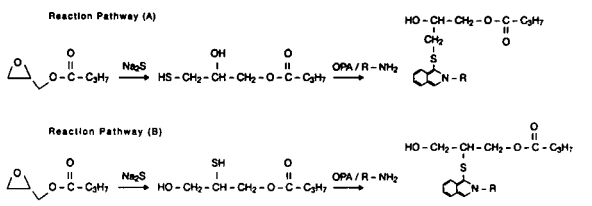

Fig. 2. Expected reaction pathway of glycidyl butyrate. (A) Pathway involving C-3 ring opening; (B) pathway involving C-2 ring opening.

TABLE I

CAPACITY FACTORS (k'), SELECTIVITIES (α) AND RESOLUTION (R_s) OF OPA–L-VAL DERIVATIVES OF RACEMIC EPOXIDES

Column: Nucleosil-120-C_{18}. For other conditions, see Experimental.

Structure	Compound	k'^a	α	R_s	MeOH(%)[b]
	Glycidol	0.81	1.28	1.99	55
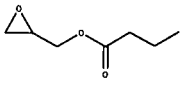	Glycidyl butyrate	3.25	1.60	9.24	55
	Epichlorohydrin	1.90	1.66	7.57	55
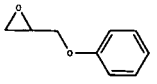	Glycidyl phenyl ether	6.10	1.62	11.70	55
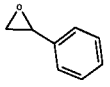	Styrene oxide	3.28	1.60	8.95	55
	Propylene oxide	1.39	1.50	2.91	55
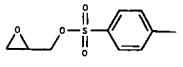	Glycidyl tosylate	4.24	1.53	7.59	55
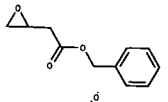	Benzyl 3,4-epoxybutyrate	1.50	1.57	3.25	65
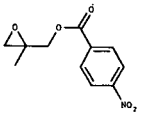	2-Methylglycidyl 4-nitrobenzoate	9.71	1.02	<0.5	35

[a] Capacity factor of first-eluted diastereomer.
[b] Percentage of methanol in the mobile phase.

With respect to the other epoxides studied, the formation of side-products was always less than 1% of the main products. In instances where an optically pure form of the epoxides studied was available, the elution order was determined. Using OPA–L-Val reagent, an elution order of *S*, *R* was found for glycidol, styrene oxide and propylene oxide, whereas for glycidyl butyrate and glycidyl tosylate the *R*-form eluted before the *S*-form.

However, the actual configuration around the chiral centre for the first- (or second-) eluting stereoisomer was the same for all five compounds mentioned. In the determination of chiral amino compounds by means of OPA in combination with a chiral thiol, the enantioselectivity of the diastereomeric adducts is influenced by the chemical structure of the amino compound [13]. We investigated the effects of four amino acids, L-Ala, L-Val, L-Phe and L-Leu, on the retention characteristics of the corresponding diastereomeric isoindoles obtained from glycidyl butyrate. The results are given in Fig. 3. Under the chromatographic conditions employed, baseline resolution could be obtained for all four diastereomers of glycidyl butyrate with either

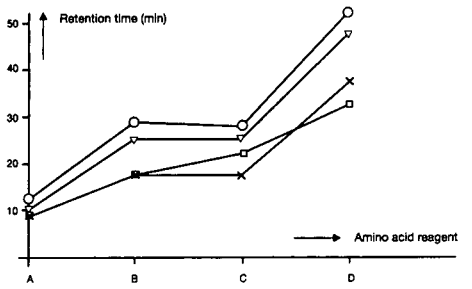

Fig. 3. Retention times of OPA–amino acid adducts of glycidyl butyrate using (A) L-Ala, (B) L-Val, (C) L-Phe and (D) L-Leu as chiral selectors. □ = (*R*)-glycidyl butyrate; ○ = (*S*)-glycidyl butyrate; ▽ = (*R*)-glycidyl butyrate (C-2 ring opening); × = (*S*)-glycidyl butyrate (C-2 ring opening). Column, LiChrosorb RP-18. For other conditions, see Experimental.

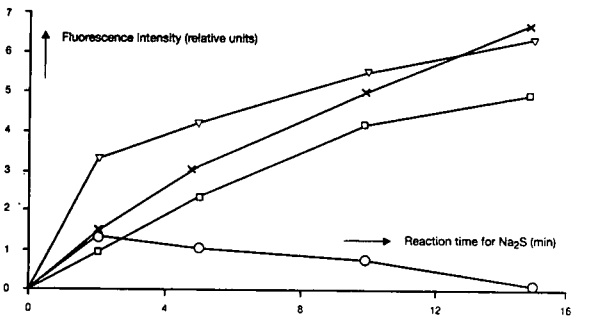

Fig. 4. Fluorescence response of the OPA–L-Phe adduct of (*R*)-glycidyl butyrate as a function of reaction time with sodium sulphide at different pH values: □ = pH 8; × = pH 10; ▽ = pH 12; ○ = pH 13.

L-Phe or L-Leu as chiral selectors. However, L-Phe offered the shortest analysis time.

The commercial availability of both D- and L-forms of amino acids is another important aspect in their use as chiral reagents for the determination of the enantiomeric excess of epoxides, because a proper selection between the D- and the L-forms of the amino acid gives the possibility of eluting an enantiomeric impurity before the corresponding enantiomer which is in excess, thus facilitating the accurate determination of the diastereomeric peak-area ratio.

Optimization of the derivatization procedure

Initially, the conversion of the epoxides into the corresponding thioglycol derivatives was carried out as described earlier [10]. Using this procedure, derivatives of glycidyl esters were formed in low yields.

In order to optimize the formation of thioglycol derivatives of glycidyl esters, derivative formation was studied using sodium sulphide solutions of different pH. The conversion of (*R*)-glycidyl butyrate with OPA–L-Phe reagent into the corresponding isoindole adduct at different pH as a function of reaction time is shown in Fig. 4. For sodium sulphide solutions with pH between 8 and 12, an increase in derivative formation with time was noted. At pH 13, derivative formation declined with time and an increase in the isoindole adduct of glycidol was measured (not shown), indicating hydrolysis of glycidyl butyrate. A sodium sulphide solution at pH 10 was chosen for further experiments. Using a 250-fold molar excess of OPA–L-Phe reagent, maximum fluorescence of glycidyl butyrate was obtained within 15 min. The detection limit for the first-eluting derivative of glycidyl butyrate, based on a signal-to-noise ratio of 3, was 2 pmol.

Accuracy of determination of enantiomeric excess

For several epoxides studied, the diastereomeric isoindole derivatives showed different specific fluorescence intensities. Differences of

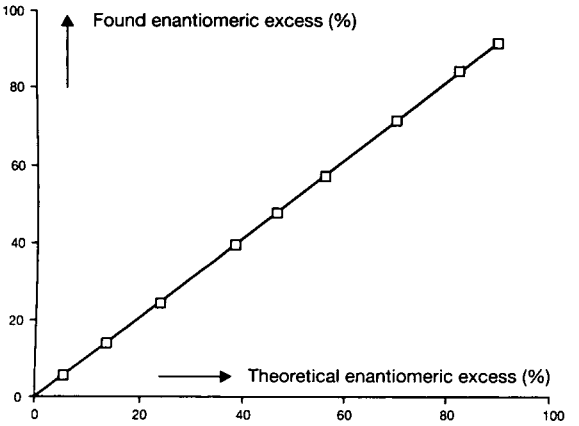

Fig. 5. Plot of theoretical enantiomeric excess *versus* found enantiomeric excess for glycidyl butyrate. Reagent: OPA–L-Phe.

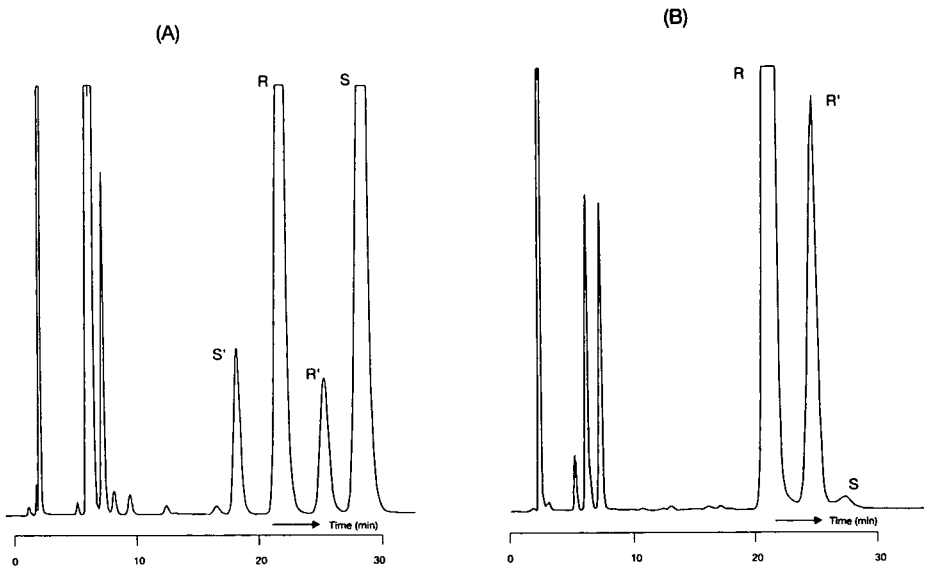

Fig. 6. Chromatograms of (A) racemic glycidyl butyrate and (B) (*R*)-glycidyl butyrate from enantioselective hydrolysis. S', R' = side-products from C-2 ring-opening. Column, LiChrosorb RP-18; reagent, OPA–L-Phe. For other conditions, see Experimental.

up to 20% were obtained for some epoxides. Therefore, quantitative measurements were made by comparing the peak areas of compounds of the same enantiomeric form.

The accuracy of the method, using the OPA–L-Phe reagent, was checked by determining the enantiomeric excess of enantiomeric mixtures of glycidyl butyrate, made up by weighing amounts of both the *R* and the racemic forms. The results are given in Fig. 5. Linear regression analysis indicated that the correlation coefficient was 0.99997. To illustrate the applicability of the method, representative chromatograms of glycidyl butyrate are shown in Fig. 6. That of the racemic substrate is given in Fig. 6a, and that of (*R*)-glycidyl butyrate obtained from an enantioselective hydrolysis experiment on the laboratory scale in Fig. 6b. The calculated enantiomeric excess of the product shown in Fig. 6b was 98.5%, with a relative standard deviation of 0.2% ($n = 4$).

REFERENCES

1 M. Klunder, S.Y. Ko and K.B. Sharpless, *J. Org. Chem.*, 51 (1986) 3710.
2 B.T. Golding, *Enzymes in Organic Synthesis*, Pitman, London, 1982, pp. 165–169.
3 A.Q.H. Habets-Crützen, S.J.N. Carlier, J.A.M. de Bont, D. Wistuba, V. Schurig, S. Hartmans and J. Tramper, *Enzyme Microb. Technol.*, 10 (1985) 17.
4 C.A.G.M. Weijers, C.G. van Ginkel and J.A.M. de Bont, *Enzyme Microb. Technol.*, 10 (1988) 214.
5 W.-Y. Li, H.L. Jin and D.W. Armstrong, *J. Chromatogr.*, 509 (1990) 303.
6 W. Dougherty, F. Liotta, D. Mondimore and W. Shun, *Tetrahedron Lett.*, 31 (1990) 4389.
7 J. Gal, *J. Chromatogr.*, 331 (1985) 349.
8 C.J. Shaw and D.L. Barton, *J. Pharm. Biomed. Anal.*, 9 (1991) 793.
9 F.N. Woodward, *J. Chem. Soc.*, (1948) 1892.
10 A. Sano and S. Takitani, *Anal. Chem.*, 57 (1985) 1687.
11 D.W. Aswad, *Anal. Biochem.*, 137 (1984) 405.
12 J. Gorzynski Smith, *Synthesis*, (1984) 629.
13 R.H. Buck and K. Krummen, *J. Chromatogr.*, 315 (1984) 279.

Journal of Chromatography, 637 (1993) 35–41
Elsevier Science Publishers B.V., Amsterdam

CHROM. 24 892

Selective on-line enrichment and separation of peptides having aromatic amino acids at their C-termini by column-switching high-performance liquid chromatography using an anhydrochymotrypsin-immobilized precolumn

Takafumi Ohta*, Kimihiro Ishimura and Shoji Takitani

Faculty of Pharmaceutical Sciences, Science University of Tokyo, 12 Ichigaya-Funagawara-Machi, Shinjuku-Ku, Tokyo 162 (Japan)

(First received October 19th, 1992; revised manuscript received December 29th, 1992)

ABSTRACT

A column switching high-performance liquid chromatographic system in which peptides retained on an anhydrochymotrypsin (AHC)-immobilized diol-silica precolumn were selectively transferred to and separated on a reversed-phase analytical column was developed. An investigation of the affinity characteristics of 40 peptides to the AHC precolumn showed that among eleven peptides having Tyr or Phe at their C-termini and more than five amino acid residues, ten were retained almost quantitatively on the precolumn, and two peptides having Trp at their C-termini were less retained. Two peptides having C-terminal $PheNH_2$ were also retained, but the peptide having C-terminal D-$PheNH_2$ was not retained. Among eighteen peptides having no aromatic amino acids at their C-termini, two were retained, one slightly and the other moderately. Calibration graphs for rat atrial natriuretic peptide constructed at various sample sizes were nearly identical, indicating that the peptide could be enriched by this system. The AHC precolumn showed no loss of analytical performance over 1 year, during which about 450 samples were analysed.

INTRODUCTION

High-performance liquid chromatography (HPLC) is now widely used for the determination of peptides. HPLC analysis of biological fluids for peptides, however, is restricted despite its high resolving power, and sample pretreatment is necessary in most instances to reduce the amount of interfering components and to enrich the analytes of interest. For this purpose, column switching (CS) is a powerful technique. Reversed-phase and immunoaffinity precolumns have so far been used [1–7]. The method using a reversed-phase precolumn is applicable to various peptides, but lacks selectivity. The immunoaffinity method offers high selectivity, but the preparation of antibody for each analyte is time consuming. Methods based on other bioaffinities such as enzyme–inhibitor or –substrate seem rational, but have not been used in the CS-HPLC analysis of peptides.

Anhydrotrypsin (AHT) and anhydrochymotrypsin (AHC) prepared by chemical modification of trypsin and chymotrypsin are known to be catalytically inert, but exhibit affinity toward peptides having Arg or Lys at their C-termini and those having aromatic amino acids at their C-termini, respectively [8–13]. Recently, we

* Corresponding author.

0021-9673/93/$06.00

have developed AHT- or AHC-immobilized diol-silica columns for the high-performance affinity chromatographic separation of peptides [14,15]. The excellent characteristics of these columns with regard to separation speed and stability indicated the possibility that they might be used as precolumns in the CS-HPLC analysis of peptides. A CS-HPLC system equipped with the AHT precolumn was developed, and it was found that the AHT precolumn selectively retained peptides having Arg or Lys at their C-termini although there were exceptions, and showed no decrease in retention after exposure for about 800 cycles to acidic eluents containing acetonitrile during 1 year [16].

In this study, we developed a CS-HPLC system equipped with an AHC-immobilized diol-silica precolumn for the selective enrichment and separation of peptides having aromatic amino acids at their C-termini. The performance of the system was ascertained by examining the affinity characteristics of various peptides with respect to the AHC precolumn.

EXPERIMENTAL

Materials

Peptides were purchased from the Peptide Institute (Osaka, Japan), Sigma (St. Louis, MO, USA), Peninsula (Belmont, CA, USA), Aldrich (Milwaukee, WI, USA) and Tokyo Kasei Kogyo (Tokyo, Japan). Diol-silica was prepared from Matrex silica beads (30–50 μm, 50 nm)(Amicon, Lexington, MA, USA) as described previously [16]. Other chemicals were of analytical-reagent grade. Deionized water (obtained with a Millipore RO-Q system) was used throughout.

Preparation of an AHC-immobilized precolumn

An AHC-immobilized precolumn (10 × 4.6 mm I.D.) was prepared as described previously [15]. In brief, diol-silica, prepared by silanization of Matrex silica beads with 3-glycidoxypropyltrimethoxysilane under anhydrous conditions followed by hydrolysis of the epoxy groups with 0.01 *M* perchloric acid, was activated with 2,2,2-trifluoroethanesulphonyl chloride (tresyl chloride), and AHC was immobilized on the diol silica by shaking the activated gel in phosphate buffer (pH 8.0) containing AHC. The amount of AHC immobilized on the diol silica was 43 mg/g. The column was stored in water at 4°C when not in use.

CS-HPLC

The set-up of the CS-HPLC system used is shown schematically in Fig. 1. A Model KHD-26 pump (P1) (Kyowa Seimitsu, Tokyo, Japan) was used for sample loading at a flow-rate of 0.5 ml/min with ice-cold water (S1) as the eluent. Peptide solution was injected on to the AHC precolumn (C1) through a Model 7125 injector (Rheodyne, Cotati, CA, USA) equipped with a 0.5-ml loop. After the injection, the precolumn was washed with S1 for 5 min, and then 0.5 ml of 20 m*M* acetate buffer (pH 5.0) was injected twice at an interval of 2 min to eliminate non-specific adsorption of peptides. The precolumn was further washed with S1 for 5 min. The switching valve, a Model E1E 002 (Senshu Kagaku, Tokyo, Japan), was then changed from "load" to "inject". A Model LC-6A pump (P2) (Shimadzu, Kyoto, Japan) was used for flushing the retained peptide from C1 on to the analytical column (C2) (Capcell Pak C_{18}; 150 × 4.6 mm I.D.) at a flow-rate of 1 ml/min with acetonitrile–10 m*M* H_3PO_4 (2–30:98–70, v/v) containing 0.1 *M* $NaClO_4$ and 0.5 *M* NaCl (S2) as eluents. This is the so-called straight-flushing mode [17]. The CS-HPLC system in which the retained peptide was flushed from C1 by interchanging the outlets of the switching valve connected to the injector and to waste and reversing the flow direction was also examined in certain cases (back-flushing mode [17]). The column

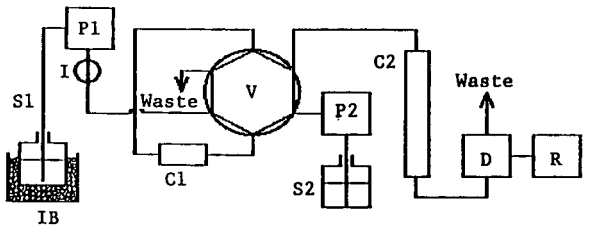

Fig. 1. Schematic diagram of the CS-HPLC system. P1 and P2 = pumps; C1 = precolumn; C2 = analytical column; I = injector; S1 and S2 = eluents; IB = ice-bath; V = switching valve; D = detector; R = integrator.

eluent was monitored at 214 nm with an SPD-6A detector (Shimadzu) connected to a Chromatopac C-R6A integrator (Shimadzu).

The percentage retention of each peptide on the AHC precolumn was calculated by dividing the peak area obtained with the precolumn by that obtained by injecting 50 μl of solution containing the corresponding amount of the peptide directly on to the analytical column.

RESULTS AND DISCUSSION

CS-HPLC conditions

The same HPLC conditions as those in the previous study for the AHT precolumn [16] were initially employed to examine the affinity characteristics of peptides with respect to the AHC precolumn. However, a preliminary study using several peptides showed that No. 15 gave a broad peak. No. 16 gave a sharper peak although eluted at a similar position. The peak broadening of No. 15 can therefore probably be attributed to the higher affinity of the peptide for the AHC precolumn. The eluents that enabled No. 15 to be eluted sharply were investigated, and addition of sodium chloride was found to be effective. Although the addition of sodium chloride was not necessarily required for all other peptides, eluents containing 0.5 *M* sodium chloride were used throughout this study for convenience.

Fig. 2 shows the effect of the flushing mode. A higher peak height was obtained by straight-flushing for No. 15, but by back-flushing for No. 22. However, no significant difference in peak area was observed between these flushing modes. Although the preferred flushing mode was expected to differ depending on the kinds of peptides involved, straight-flushing was employed exclusively in this study.

The CS-HPLC conditions other than those described above, such as the flow-rate of S1 and the kinds of washing solvents, were almost the same as those in the previous study with the AHT precolumn [16].

Affinity characteristics of various peptides

Table I shows the retentions of various peptides on the AHC precolumn after washing with

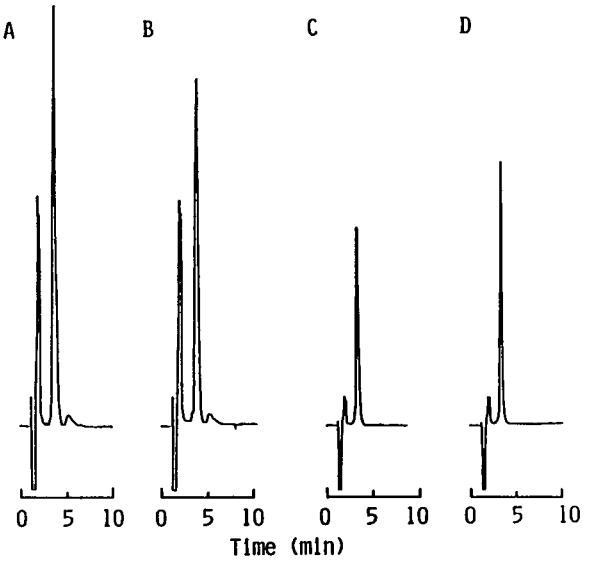

Fig. 2. Effect of flushing mode on peak shapes of (A, B) No. 15 and (C, D) No. 22. A and C, straight-flushing; B and D, back-flushing. Eluent S2, CH_3CN–10 m*M* H_3PO_4 (30:70, v/v) containing 0.1 *M* $NaClO_4$ and 0.1 *M* NaCl.

20 or 60 m*M* acetate buffer (pH 5.0). The peptides that had Tyr at their C-termini and more than five amino acid residues, except No. 9, were retained almost quantitatively on the precolumn after washing with 20 m*M* acetate buffer. These peptides, except Nos. 11 and 21, were also retained in good yield after washing with 60 m*M* acetate buffer. The peptides that had Phe at their C-termini and more than five amino acid residues were retained almost quantitatively after washing with 20 m*M* acetate buffer, and also in good yield, except Nos. 13 and 15, after washing with 60 m*M* acetate buffer. Nos. 7 and 17, having C-terminal $PheNH_2$, were retained, whereas No. 8, that had the same sequence as No. 7 but C-terminal D-$PheNH_2$ was not retained at all. The peptides having Trp at their C-termini, except No. 1, showed less affinity for the AHC precolumn. Among eighteen peptides that had no aromatic amino acids at their C-termini, three were retained slightly (Nos. 38 and 40) or moderately (No. 34).

On the other hand, almost all the peptides examined showed no or only a slight retention to the diol-silica precolumn, indicating that the retained peptides were recognized with the im-

TABLE I

AFFINITY CHARACTERISTICS OF PEPTIDES FOR THE AHC PRECOLUMN

No.	Peptide[a]	Retention (%)[b]			
		AHC precolumn		Diol-silica precolumn	
		20 m*M*[c]	60 m*M*[c]	20 m*M*[c]	60 m*M*[c]
1	Gly–Trp	0	–[d]	0	–[d]
2	Gly–D–$PheNH_2$	0	–	0	–
3	Gly–Leu–Tyr	0	–	0	–
4	Met–Leu–Phe	0	–	0	–
5	Phe–Gly–Gly–Phe	0	–	0	–
6	Asp–Arg–Val–Tyr	0	–	0	–
7	Phe–Met–Arg–$PheNH_2$	103	102	4	3
8	Phe–Met–Arg–D–$PheNH_2$	0	–	0	–
9	Arg–Lys–Glu–Val–Tyr	60	39	0	–
10	Arg–Ser–Arg–His–Phe	88	90	5	1
11	Arg–Lys–Asp–Val–Tyr	84	57	1	0
12	Ser–Met–Glu–Val–Arg–Gly–Trp (δ-melanocyte-stimulating hormone)	68	68	0	–
13	Arg–Val–Tyr–Ile–His–Pro–Phe (angiotensin III)	91	62	6	0
14	Tyr–Gly–Gly–Phe–Met–Arg–Phe	82	73	1	–
15	Asp–Arg–Val–Tyr–Ile–His–Pro–Phe (angiotensin II)	93	47	2	1
16	Arg–Pro–Pro–Gly–Phe–Ser–Pro–Phe	96	82	4	1
17	Asp–Tyr–Met–Gly–Trp–Met–Asp–$PheNH_2$ (cholecystokinin octapeptide 26–33)]	52	34	9	8
18	Trp–His–Trp–Leu–Gln–Leu–Lys–Pro–Gly–Gln–Pro–Met–Tyr (α-mating factor)	94	95	7	5
19	Trp–His–Trp–Leu–Ser–Phe–Ser–Lys–Gly–Glu–Pro–Met–Tyr (α-SK2 mating factor)	104	100	4	7
20	Cys–Ser–Cys–Ser–Ser–Leu–Met–Asp–Lys–Glu–Cys–Val–Tyr–Phe–Cys–His–Leu–Asp–Ile–Ile–Trp (endothelin 1)	43	15	0	–
21	Ser–Leu–Arg–Arg–Ser–Ser–Cys–Phe–Gly–Gly–Arg–Met–Asp–Arg–Ile–Gly–Ala–Gln–Ser–Gly–Leu–Gly–Cys–Asn–Ser–Phe–Arg–Tyr [atrial natriuretic peptide (human)]	89	67	16	18
22	Ser–Leu–Arg–Arg–Ser–Ser–Cys–Phe–Gly–Gly–Arg–Ile–Asp–Arg–Ile–Gly–Ala–Gln–Ser–Gly–Leu–Gly–Cys–Asn–Ser–Phe–Arg–Tyr (atrial natriuretic peptide (rat)]	96	96	15	12
23	Ala–Ala–Ala–Ala	0	–	0	–
24	Pro–Phe–Gly–Lys	0	–	0	–
25	Arg–Gly–Asp–Ser	0	–	0	–
26	Gly–Arg–Gly–Asp	0	–	0	–
27	Arg–Pro–Lys–Pro	6	2	4	3
28	Tyr–Gly–Gly–Phe–Met (Met-enkephalin)	0	–	0	–
29	Tyr–Gly–Gly–Phe–Leu (Leu-enkephalin)	0	–	0	–
30	Tyr–Pro–Phe–Pro–Gly (β-casomorphin 5)	0	–	0	–
31	Phe–Leu–Glu–Glu–Val	0	–	0	–
32	Tyr–Gly–Gly–Phe–Leu–Arg	4	4	4	5
33	Tyr–Pro–Phe–Pro–Gly–Pro–Ile	0	–	2	–
34	Arg–Val–Tyr–Ile–His–Pro–Ile	61	5	10	8
35	Ala–Ser–Thr–Thr–Thr–Asn–Tyr–Thr (peptide T)	0	–	0	–
36	Arg–Pro–Pro–Gly–Phe–Ser–Pro–Leu	2	1	1	1
37	Trp–Ala–Gly–Gly–Asp–Ala–Ser–Gly–Glu	0	–	0	–
38	Arg–Pro–Pro–Gly–Phe–Ser–Pro–Phe–Arg (bradykinin)	18	15	5	2
39	Tyr–Gly–Gly–Phe–Leu–Arg–Lys–Tyr–Pro (β-neoendorphin)	0	–	2	0
40	Ser–Gly–Ser–Ala–Lys–Val–Ala–Phe–Ser–Ala–Ile–Arg–Ser–Thr–Asn–His	16	13	16	14

[a] 1 nmol per 50-μl injection.
[b] Calculated on the basis of peak area.
[c] Concentration of acetate buffer (pH 5.0).
[d] Not determined.

mobilized AHC. The results with the diol-silica precolumn seem to indicate that the non-selective retention of No. 40 observed with the AHC precolumn is attributable to the support.

Ishii and co-workers [11–13] investigated the chromatographic behaviour of seventeen peptides (six C-terminal Tyr peptides, three C-terminal Phe peptides, four C-terminal Trp peptides and four other peptides) on an AHC-agarose column, and reported that peptides having aromatic amino acids at their C-termini, except two C-terminal Tyr dipeptides, were retained on the column. These characteristics generally coincide with our results, but there are several discrepancies. No. 6, which showed an affinity for the AHC-agarose column, was not retained on the precolumn in this study. This, however, is probably attributable to the difference in the evaluation method used for the affinity. In this study, the affinity was expressed as the percentage of peptides retained on the precolumn after elution with a definite volume of S1 and the washing buffer, whereas that for the AHC-agarose column as the pH values of eluents that enabled peptides to be eluted from the column. Therefore, it is possible that peptides showing weak affinity are washed out from the precolumn. In fact, the collection and analysis of the eluate from the precolumn showed that 99% of No. 6 was recovered in the eluate within 5 min after injection.

Another problem is the retention of Nos. 34 and 38, which have no aromatic amino acids at their C-termini. Although these two were not examined, it was reported previously that peptides having no aromatic amino acids at their C-termini showed no affinity for the AHC-agarose column [11,13]. We recently encountered a similar discrepancy: twelve out of thirty peptides having no Arg or Lys at their C-termini were retained on the AHT precolumn [16]. It is interesting that the non-selective adsorption of No. 34 was observed with both precolumns. As these precolumns were prepared by using diol-silica as a support and tresyl chloride as an activating reagent for immobilization of ligands, these common factors may be responsible for the non-selective adsorption.

In a previous study using the AHT precolumn [16], the use of 20 m*M* calcium chloride instead of acetate buffer as the washing solvent increased the selectivity of the precolumn, although decreasing concurrently the retention of some of the C-terminal Arg peptides and most of the C-terminal Lys peptides. The effect of the addition of calcium chloride to 20 m*M* acetate buffer (pH 5.0) was therefore examined in this study. As shown in Fig. 3, the retention of No. 34, a non-selectively adsorbed peptide, was depressed with increasing concentration of calcium chloride, and disappeared almost completely on addition of 5 m*M* calcium chloride. However, the retention of No. 13, a C-terminal Phe peptide, was also decreased. On the other hand, the retention of No. 22, a C-terminal Tyr peptide, was hardly affected by the addition of calcium chloride at least up to 5 m*M*. The retention of these peptides, Nos. 34, 13 and 22, were 23, 57 and 91%, respectively, when 15 m*M* sodium chloride, which had the same ionic strength as 5 m*M* calcium chloride, was added to the buffer. The retentions of other peptides having aromatic amino acids at their C-termini, Nos. 14, 16, 18, 19, 20 and 21, were 13, 19, 106, 95, 4 and 90%, respectively, when 20 m*M* acetate buffer containing 5 m*M* calcium chloride was used as the washing solvent. These results indicate that the addition of calcium chloride enhances the selectivity of the AHC precolumn, although decreasing concurrently the retention of some of the

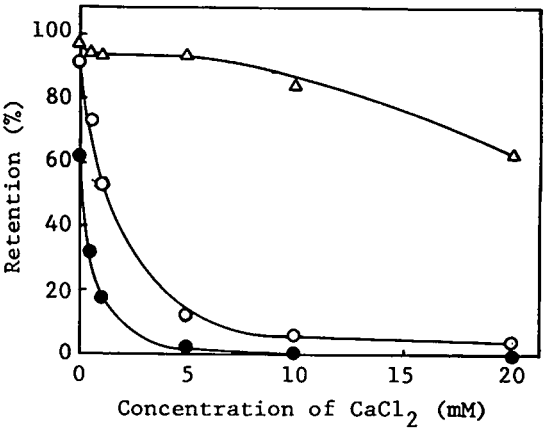

Fig. 3. Effect of addition of calcium chloride on the retention of peptides. ○, No. 13; △, No. 22; ●, No. 34.

peptides having aromatic amino acids at their C-termini. The reason why calcium chloride effectively suppresses the non-selective adsorption of peptides on AHC and AHT precolumns is obscure, but is under investigation in connection with the common factors for the preparation of both precolumns as described above.

Separation of a model peptide mixture

Fig. 4 shows the separation of a model peptide mixture by CS-HPLC. Peptides having aromatic amino acids at their C-termini were retained almost quantitatively, and other peptides were completely removed. Therefore, the CS-HPLC system equipped with theAHC precolumn is useful for the selective separation of peptides having aromatic amino acids at their C-termini.

Enrichment

As No. 22 showed a fairly high affinity for the AHC precolumn, as demonstrated in Fig. 3, an enrichment experiment was carried out using this peptide. Prior to the enrichment experiment, the optimum retention conditions for No. 22 were investigated. Back-flushing was employed because it gave a higher peak height for No. 22, as already shown in Fig. 2.

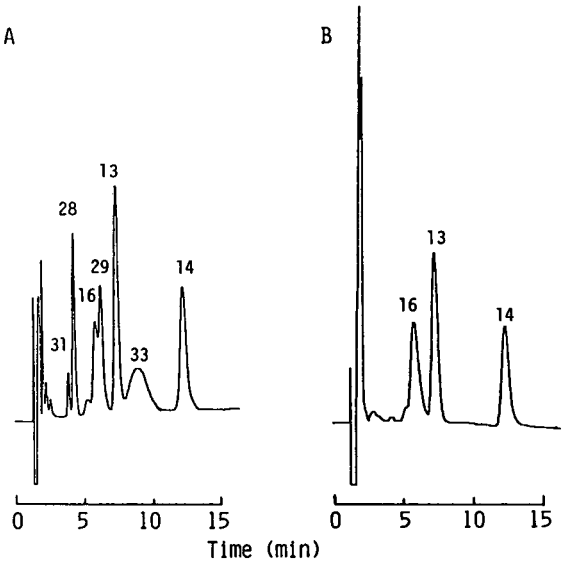

Fig. 4. HPLC separation of a model peptide mixture. A, without precolumn; B, with the AHC precolumn. Eluent S2, CH_3CN–10 m*M* H_3PO_4 (26:74, v/v) containing 0.1 *M* $NaClO_4$ and 0.5 *M* NaCl.

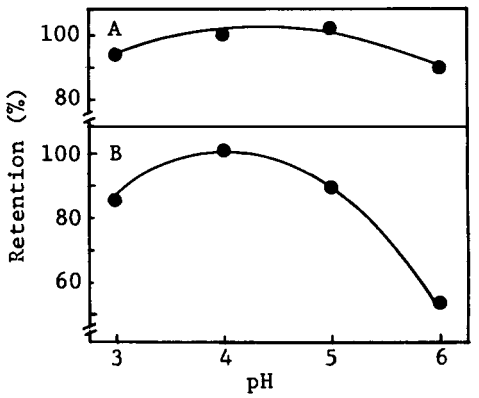

Fig. 5. Effect of pH of 60 m*M* acetate buffer on retention of No. 22. The retention was calculated on the basis of (A) peak area and (B) peak height.

Fig. 5 shows the effect of the pH of the washing buffer. The highest and quantitative retention was obtained at pH 4.0 when evaluated on the basis of peak height. The marked decrease in retention at pH 6.0 can probably be attributed to broadening of the sample zone in the precolumn, because the retention was not decreased so much when evaluated on the basis of peak area. Fig. 6 shows the effect of the concentration of washing buffers. The retention was not influenced with acetate buffer at least up to 0.3 *M*, but decreased gradually with increasing

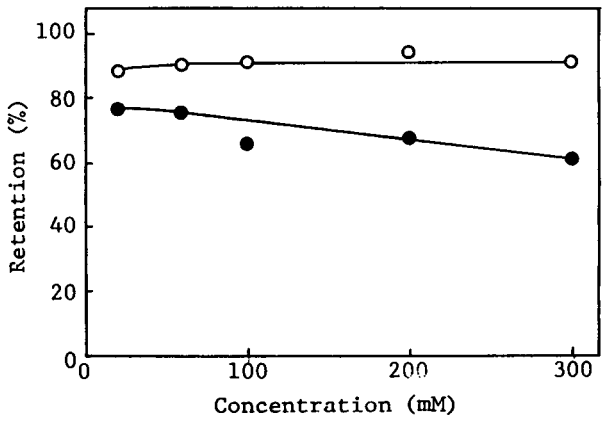

Fig. 6. Effect of concentration of washing buffers on retention of No. 22. The retention was calculated on the basis of peak height. ○ = Acetate buffer (pH 4.0); ● = phosphate buffer (pH 4.0).

concentration of phosphate buffer. Acetate buffer (pH 4.0, 60 m*M*) was therefore employed as the washing solvent.

The efficiency of enrichment was evaluated on the basis of the linearity and slope of calibration graphs constructed at three sample sizes (0.0625–1 nmol per 50-, 250- and 500-μl injection). The linear relationships ($r = 0.9975–0.9991$) between the peak height and the injected amount and the good reproducibility [relative standard deviations ($n = 4$) for 0.25 nmol = 2.5–5.4%] were observed at any sample size. The slope of the graph decreased with increase in sample size, but the slope obtained with 500-μl injections was still about 73% of that with 50-μl injections, indicating that the peptide could be enriched by this system.

Stability of the AHC precolumn

The stability of the AHC precolumn was evaluated by measuring the retentions of several peptides having aromatic amino acids at their C-termini after various periods of operation. The precolumn showed no decrease in retention after exposure for about 450 cycles to acidic eluents containing up to 30% acetonitrile during 1 year; the retentions of Nos. 13, 18 and 22 1 year after the preparation of the precolumn were 92, 100 and 94%, respectively.

CONCLUSIONS

The results demonstrate that in the CS-HPLC separation of peptides the AHC precolumn offers improved selectivity different from that obtained with the reversed-phase and immunoaffinity precolumns used previously. The AHC precolumn may be useful for on-line pretreatment in the HPLC determination of peptides having aromatic amino acids at their C-termini in biological fluids because of its high stability. In addition, this CS-HPLC system would be applicable for the rapid isolation and on-line identification of C-terminal peptide fragments from tryptic digests of proteins having aromatic amino acids at their C-termini. It would similarly be applicable for C-terminal peptide fragments from chymotryptic digests of proteins having no aromatic amino acids at their C-termini if the system were to be changed so that the non-retained fraction from the AHC precolumn is introduced into the analytical column.

REFERENCES

1 T. Hayashi, S. Sakamoto, T. Fuwa, I. Morita and H. Yoshida, *Anal. Sci.*, 3 (1987) 445.
2 T. Hayashi, S. Sakamoto, T. Fuwa, I. Wada and H. Yoshida, *Anal. Sci.*, 4 (1988) 313.
3 T. Hayashi, S. Sakamoto,I. Wada and H. Yoshida, *Chromatographia*, 27 (1989) 574.
4 T.T. Nguyen, A.D. Lean and H. Ong, *Anal. Biochem.*, 179 (1989) 24.
5 A. Foucault, H. Pinochet, R. Rosset and D. Tome, *Chromatographia*, 25 (1988) 822.
6 D.S. Stegehuis, U.R. Tjaden and J. Van Der Greef, *J. Chromatogr.*, 511 (1990) 137.
7 E. Reh, M. Kratzer, D. Zdunek and F. Lang, *Anal. Biochem.*, 196 (1991) 104.
8 H. Yokosawa and S. Ishii, *Biochem. Biophys. Res. Commun.*, 72 (1976) 1443.
9 T. Kumazaki, T. Nakano, F. Arisaka and S. Ishii, *Proteins Struct. Funct. Genet.*, 1 (1986) 100.
10 T. Kumazaki, K. Terasawa and S. Ishii, *J. Biochem.*, 102 (1987) 1539.
11 S. Ishii, H. Yokosawa, S. Shiba and K. Kasai, *Adv. Exp. Med. Biol.*, 120A (1989) 15.
12 K. Shimura, K. Kasai and S. Ishii, *J. Chromatogr.*, 350 (1985) 265.
13 T. Kumazaki, A. Fujitani, K. Terasawa, K. Shimura, K. Kasai and S. Ishii, *J. Biochem.*, 103 (1988) 297.
14 T. Ohta, T. Inoue, Y. Fukumoto and S. Takitani, *Chromatographia*, 30 (1990) 410.
15 T. Ohta, K. Ishimura and S. Takitani, *Chromatographia*, 33 (1992) 113.
16 T. Ohta, T. Inoue and S. Takitani, *J. Chromatogr.*, 543 (1991) 59.
17 R. Huber and K. Zech, in R.W. Frei and K. Zech (Editors), *Selective Sample Handling and Detection in High-Performance Liquid Chromatography: Part A*, Elsevier, Amsterdam, 1988, p. 109.

Journal of Chromatography, 637 (1993) 43–53
Elsevier Science Publishers B.V., Amsterdam

CHROM. 24 886

Determination of amino sugars in synthetic glycopeptides during the conditions of amino acid analysis utilizing precolumn derivatization and high-performance liquid chromatographic analysis

Livia Gorbics and Laszlo Urge

Wistar Institute of Anatomy and Biology, 3601 Spruce Street, Philadelphia, PA 19104 (USA)

Elisabeth Otvos-Papp

Department of Biology, University of Pennsylvania, Philadelphia, PA 19104 (USA)

Laszlo Otvos, Jr.*

Wistar Institute of Anatomy and Biology, 3601 Spruce Street, Philadelphia, PA 19104 (USA)

(First received September 24th, 1992; revised manuscript received December 14th, 1992)

ABSTRACT

The growing number of synthetic glycopeptides required an in-house method for the analysis of the final products. A reversed-phase high-performance liquid chromatographic protocol was developed to verify the presence of N-acetylglucosamine and N-acetylgalactosamine in synthetic glycopeptides after hydrolysis and derivatization with 4-dimethylaminoazobenzene-4′-sulphonyl chloride. Different sugar and glycoamino acid standards were used to separate the two carbohydrate moieties, and the location of the derivatized 2-aminoglucose was established by the use of radiolabeled sugar. The utility of the approach is demonstrated by the amino acid analysis of N- and O-glycosylated synthetic peptides and the method could provide an alternative for sugar analysis of glycoproteins.

INTRODUCTION

Many proteins contain modified amino acids for which no codons exist in the genome. To understand the biological function of post-translationally modified proteins and protein fragments, the chemical synthesis of glycosylated and phosphorylated peptides has become the central interest of biotechnology sector. In contrast to the single phosphate group on the phosphoproteins, both the N- and O-glycoslyated proteins carry complex oligosaccharide antennae [1]. The carbohydrate chain often carries a highly specific biological recognition structure [2], and extensive studies have been performed on the chromatographic analysis of these oligosaccharide systems [3–5]. As far as the peptide part is concerned, the removal of the first one or two monosaccharide units of the complex carbohydrate antennae seems to result in a much more dramatic conformational [6] and immunological [7] change than the removal of the remainder of the carbohydrate residues. In fact, we used

* Corresponding author.

0021-9673/93/$06.00

synthetic non-glycosylated and glycosylated peptides to demonstrate that incorporation of single N-acetylglucosamine (2-acetamido-2-deoxy-D-glucopyranose) (GlcNAc) moieties (at natural glycosylation sites) into T-cell epitopic peptides resulted in a break in the characteristic α-helical structures; the formation of β-turns was also observed [8]. Elongation of the carbohydrate only slightly enhanced this effect [8].

N-Acetylglucosamine and N-acetylgalactosamine (2-acetamido-2-deoxy-D-galactopyranose) (GalNAc) are the first sugar moieties attached to asparagines and serines/threonines for almost all N- and O-glycoproteins [9]. The elution time of the glycopeptides compared with their non-glycosylated analogs in reversed-phase high-performance liquid chromatography (RP-HPLC) is usually reduced owing to the incorporation of the hydrophilic carbohydrate [10]. Increased retention times compared with the predicted values (owing to induced conformational orientation on the surface of the bonded phase) were observed when synthetic glycopeptides exhibited more ordered secondary structures [11]. As an extreme, glycosylated analogs of peptide T, a pharmaceutically promising candidate against human immunodeficiency virus type-1 infection [12], assumed a β-turn conformation so stabilized that some of the glycopeptides could not be distinguished from their parent, non-glycosylated analog by RP-HPLC [13].

Amino acid analysis of synthetic peptides is historically accomplished by post- or precolumn derivatization after acidic hydrolysis [14–17]. Precolumn derivatization offers a sensitivity range at the low-picomole level [18], and a combination of the two more common precolumn techniques, using 4-dimethylaminoazobenzene-4′-sulphonyl chloride (DABS-Cl) and phenyl isothiocyanate, has been reported [19,20]. In addition to high sensitivity, the popularity of the DABS-Cl method also arises from use of a visible wavelength detection range and the stability of the derivatized amino acids [21,22]. As mono- and oligosaccharides are more sensitive than amino acids to acid hydrolysis [23,24], they are expected to be recovered in a lesser amount than regular amino acids. In contrast to the existing techniques based on analysis of the intact sugar moiety, we decided to derivatize the intermediate product of the hydrolysis featuring a free amino group. The procedure is similar to the derivatization of regular amino acids. Most synthetic peptide laboratories are equipped for amino acid analysis as the first screening of peptide integrity, offering a useful addition to the currently used mass spectrometry [25] for the verification of the integrity of the rapidly growing number of synthetic glycopeptides carrying a limited number of sugar residues. A rapid, in-house analysis of synthetic glycopeptides is further justified by the appearance of techniques to prepare them on automated peptide synthesizers [26]. Most recent reports from several laboratories have been aimed at the development of glycopeptide analytical strategies closer to the practice in biochemistry laboratories [27,28], but uncommon handling of the sugar derivatives could not be fully eliminated. We report here the application of DABS-Cl amino acid analysis in synthetic glycopeptides, N- and O-glycosylated analogs of peptide T5 and RGD analogs, conformationally and pharmacologically interesting fragments of the glycoprotein of the human immunodeficiency virus 1 and fibronectin.

EXPERIMENTAL

Chemicals

Unmodified and glycosylated T5 peptides were synthesized and purified as described previously [13]. The following peptides were investigated:

T5: H-TTNYT-NH_2;
NGlcNAcT5: H-N(GlcNAc)-TTNYT-NH_2;
T5GlcNAc: H-TTN (GlcNAc)-YT-NH_2;
TGalNAcT5: H-T(GalNAc)-TTNYT-NH_2;
RGD: Ac-GRGDSPK-NH_2;
N(GlcNAc)RGD: Ac-N(GlcNAc)GRGDSPK-NH_2;
N(GlcNAc)RGDN(GlcNAc): Ac-N(GlcNAc)-GRGDSPKN(GlcNAc)-NH_2;
RGD-O-glycoside: Ac-GRGDS(GlcNAc)PK-NH_2;
N(GlcNAc)PV: H-N(GlcNAc)PV-NH_2.

Sugar standards, glucosamine hydrochloride (2-amino-2-deoxy-D-glucopyranose hydrochloride), galactosamine hydrochloride (2-amino-

2-deoxy-D-galactopyranose hydrochloride), GlcNAc, GalNAc and 1-amino-glucose (1-amino-1-deoxy-β-D-glucose) were purchased from Sigma (St. Louis, MO, USA), H-Asn(GlcNAc)-OH from Oxford Glycosystems (Rosedale, NY, USA) and radiolabeled GlcNAc ([6-^{3}H]-2-acetamido-2-deoxy-β-D-glucopyranose) from American Radiolabeled Chemicals (St. Louis, MO, USA). Hydrolysis and dabsylating reagents and amino acid standards were purchased from Beckman (San Ramon, CA, USA); HPLC solvents and all other chemicals were obtained from Aldrich (Milwaukee, WI, USA).

Gas-phase hydrolysis

Lyophilized samples (twelve in 600-μl vials) and 700 μl of 6 *M* HCl were placed in a hydrolysis vessel (provided by Beckman; volume 113 cm^3), followed by flushing with argon and evacuation at 0.1 mbar (0.00145 p.s.i.; 1 p.s.i. = 6894.76 Pa) for 1–2 min. The vessel was placed in an oven 110°C for 1 or 10 h.

Dabsylation

$NaHCO_3$ buffer (20 μl) (pH 8.3) provided by Beckman was added to 1.5–3 μg of hydrolyzed peptide or 0.3–2 μg of hydrolyzed sugar standard, followed by the addition of 40 μg of DABS-Cl in 40 μl of acetonitrile. The vials were closed and placed in a drying oven at 70°C for 12–15 min. Ethanol–water (1:1, v/v) (440 μl) was added to the samples and 6–12% of the resulting solution was injected into the HPLC column.

HPLC

The Beckman System Gold HPLC apparatus consisted of a Model 126 programmable solvent-delivery module, a Model 167 scanning ultraviolet–visible detector module operating at 436 nm, an Altex 210A injector and a C_{18} Ultrasphere-DABS column (250 × 4.6 mm I.D.). The system was controlled by an IBM System-2 Model 55 SX using the Beckman System Gold Personal Chromatography software, version 6.0. The chromatographic conditions were as follows: solvent A (final pH 6.50–6.52) contained 115 ml of 0.11 *M* sodium citrate (pH 6.51), 845 ml of water and 40 ml of N,N-dimethylformamide; solvent B contained 300 ml of solvent A, 672 ml of acetonitrile and 28 ml of N,N-dimethylformamide; and the flow-rate was 1.4 ml/min. Table I shows the two different gradients used. The solvent vessels were continuously flushed with argon to keep the pH constant. All runs were carried out at room temperature.

TABLE I

SOLVENT COMPOSITION DURING RP-HPLC

	Time (min)	Solvent		Duration (min)
		A (%)	B (%)	
Gradient 1	Start	71	29	
	0	49	51	24
	24	14	86	10
	40	0	100	1
	47	71	29	0.25
	55			End of run
Gradient 2	Start	71	29	
	0	49	51	12
	12	14	86	5
	20	0	100	1
	27	71	29	0.25
	35			End of run

RESULTS AND DISCUSSION

Hydrolysis products and their identification

Fig. 1 outlines the possible cleavage products after acidic hydrolysis of a GlcNAc-coupled asparagine residue. The only final product that can be dabsylated is glucosamine (or similarly galactosamine for the O-glycopeptides). To test the possibility of incomplete hydrolysis, H-Asn-(GlcNAc)-OH and 1-amino-GlcNAc standards were subjected to derivatization and to the chromatographic conditions of amino acid analysis. DABS-Asn(GlcNAc)-OH was eluted just before the broad DABS-ONa peak, and was entirely absent after hydrolysis. Based on this, we disregarded the possibility of obtaining glucosamine-coupled asparagine. No new peak was found for unhydrolyzed 1-amino-GlcNAc (compared with the blank chromatogram), and after hydrolysis (1 h) only one peak, identical with the dabsylated glucosamine standard, was detected. Moreover, our standard procedure [29] to acylate 1-amino

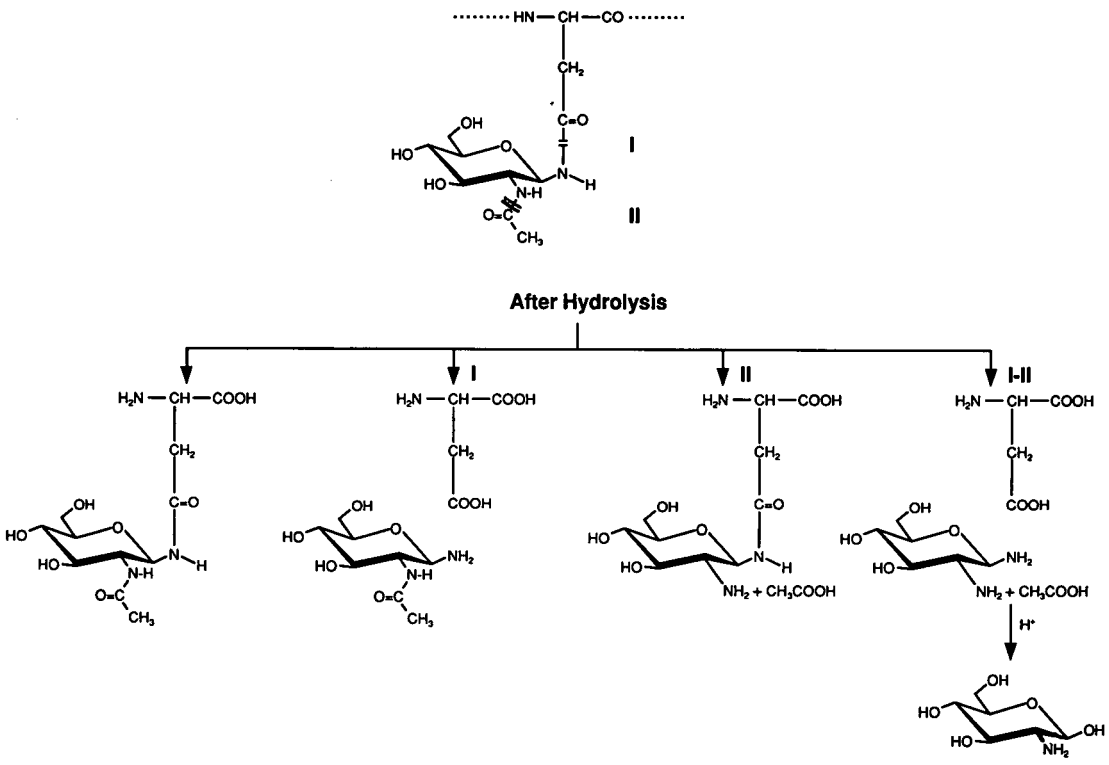

Fig. 1. The possible pathways of acidic hydrolysis of a GlcNAc-conjugated asparagine residue.

sugar derivatives with N-α-fluorenylmethoxycarbonyl-aspartic acid-α-*tert.*-butyl-β-pentafluoro-phenyl ester [Fmoc-Asp(OPfp)-O^{t}Bu] was unsuccessful after hydrolysis of the 1-amino-glucose for 1 h. In contrast, almost quantitative acylation of the same compound was achieved without hydrolysis, indicating the acid lability of the 1-amino sugar. This result is in good agreement with the previously reported lability of 1-amino sugars in an acidic environment [30]. Intact GlcNAc and GalNAc were not considered, as these compounds cannot be derivatized with DABS-Cl at the pH we used [17].

Amounts of 10 nmol of glucosamine hydrochloride and galactosamine hydrochloride standards were dabsylated, and 10% of them (10% of 10 nmol) were subjected to HPLC using gradient 1 (see Experimental). Gradient 1 is our method of choice for the determination of amino acids in peptides, because the mixture of dabsylated amino acid standards is baseline separated. New peaks were detected at 18.50 min for DABS-galactosamine and 19.05 min for DABS-glucosamine. These peaks fall between the DABS-proline (18.27 min) and DABS-valine (19.36 min) peaks. Whereas co-injection of the glucosamine and valine derivatives revealed two separate peaks, the galactosamine and proline derivatives could not be separated by this gradient. Fig. 2 shows the chromatograms obtained after injecting 8% of 5 nmol GlcNAc and GalNAc after hydrolysis for 1 h and dabsylation. The new peaks were detected at the position of the amino sugar standards. (The 1.2-min shift in the retention times of the dabsylated amino sugar peaks compared with the amino sugar standards reflects a column change and also a general shift of the peaks in RP-HPLC.) Moreover, co-injection of hydrolyzed GlcNAc and glucosamine or hydrolyzed GalNAc and galactosamine revealed single peaks. As Fig. 2 shows, the two different sugar derivatives are baseline separated. When the same procedure was applied to H-Asn(GlcNAc)-OH, peaks were detected at both Asx and glucosamine, as expected.

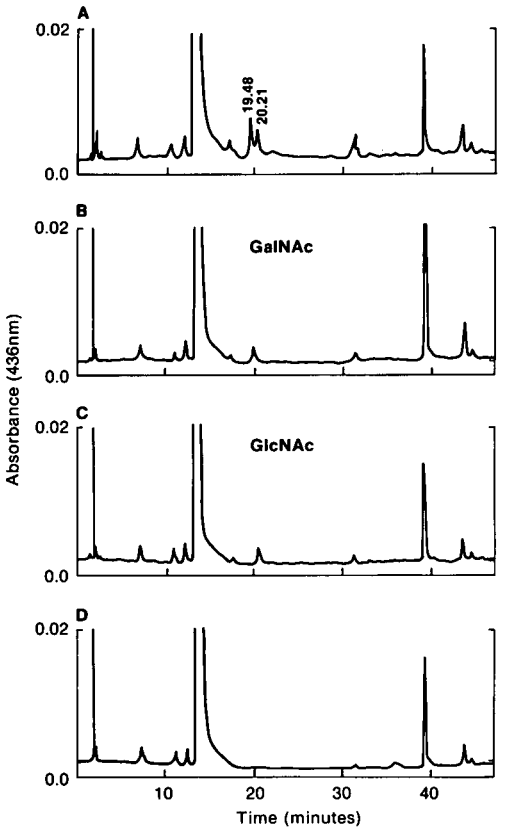

Fig. 2. Reversed-phase chromatography of hydrolyzed and dabsylated (C) GlcNAc, (B) GalNAc and (A) their mixture using gradient 1. Hydrolysis was carried out at 110°C for 1 h; 8% of 5 nmol sugar moieties were injected for the individual runs and 12% of 10 nmol GalNAc and 5 nmol GlcNAc were injected in (A). The detected ratio of the carbohydrates in (A) is 1.77:1 and 1.61:1, calculated on peak areas and peak heights, respectively. (D) blank.

Repeated attempts at fast atom bombardment mass spectrometry on several instruments failed to reveal any molecular ions from DABS-valine or DABS-glucosamine, even in the 100-μg range. Similar unsuccessful attempts were made to obtain molecular ions of phenylthiohydantoin-derivatized Asn(GlcNAc) and Asn(chitobiose) during peptide sequencing. Therefore, we used radioactively labeled GlcNAc (mixed with unlabeled GlcNAc) to verify the origin of the new peak found at 19–20 min. Fig. 3 shows the distribution of the counts after hydrolysis, dabsylation and HPLC separation. The major peak of the radioactivity was detected at the expected time. It should be noted that most of

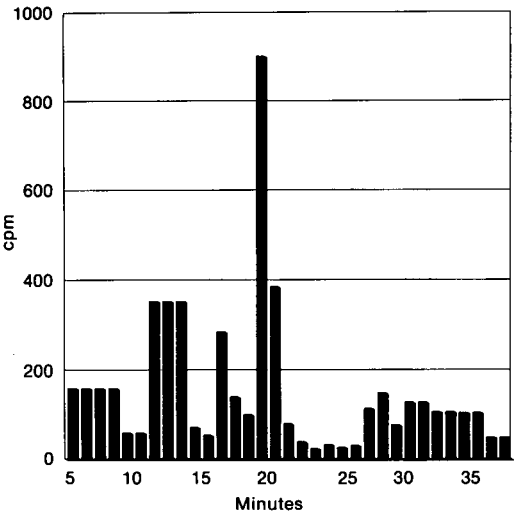

Fig. 3. Recovered radioactivity distribution of hydrolyzed and dabsylated ^{3}H-labeled GlcNAc in the amino acid region of the chromatogram. The total recovered radioactivity in the dabsylated amino acid range of the chromatogram was 3440 cpm, of which 1192 cpm corresponded to the dabsylated sugar at 19–20 min. The recovered radioactivity in the flow-through (corresponding to the underivatized sugar) was 8001 cpm.

the counts were found in the flow-through, indicating a low yield (14–19%) of dabsylation. When the same radiolabeled GlcNAc preparation in a 10 molar excess was hydrolyzed, derivatized and chromatographed together with the amino acid standards, DABS-glucosamine was repeatedly eluted between DABS-proline and DABS-valine, as Fig. 4 shows. As DABS-galac-

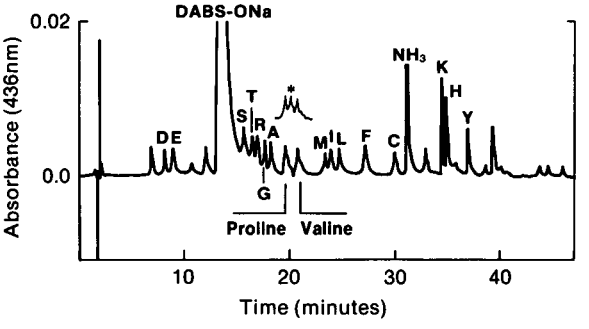

Fig. 4. DABS-glucosamine elutes between DABS-proline and DABS-valine using gradient 1. The full chromatogram corresponds to the dabsylated amino acid standard. The inset corresponds to the sugar region of a mixture of dabsylated amino acid standard, and an excess of hydrolyzed and dabsylated GlcNAc (marked with an asterisk).

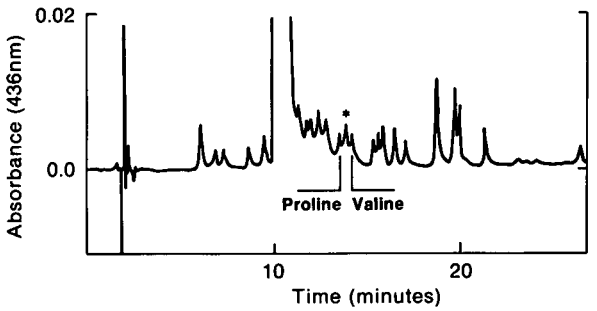

Fig. 5. DABS-galactosamine can be separated from DABS-proline and DABS-valine using gradient 2. The chromatogram was obtained by co-injection of a dabsylated amino acid standard, and an excess of hydrolyzed and dabsylated GalNAc (marked with an asterisk).

tosamine co-elutes with DABS-proline using gradient 1, this gradient (optimum for full amino acid analysis of glycopeptides containing the GlcNAc moiety) needs to be changed when GalNAc-containing peptides are to be analyzed. DABS-galactosamine can be resolved from DABS-proline using gradient 2 (the peak of the sugar derivative falls between the peaks of proline and valine derivatives), as Fig. 5 shows. This gradient, however, does not separate DABS-arginine, DABS-glycine or DABS-threonine, and consequently is used only for the verification of the presence of the GalNAc moiety in synthetic glycopeptides.

Utility of the method

The utility of the strategy outlined above was tested on the amino acid analysis of peptides T5 and RGD and a model tripeptide, and of their glycosylated derivatives. Fig. 6 shows the chromatograms of the analysis of peptide T5 and N-glycopeptide NGlcNAcT5 using gradient 1. The peak at 20.1 min on curve A clearly indicates the presence of the sugar moiety. Fig. 7 shows the chromatograms of the analyses of peptide T5 and O-glycopeptide TGalNAcT5 using gradient 2. The presence of the sugar moiety is shown by the appearance of the peak at 13.8 min on curve A. The N(GlcNAc)PV glycopeptide was prepared and analyzed to verify the baseline separation of DABS-proline, DABS-valine and DABS-glucosamine, not only in the standard but also in a glycopeptide hydro-

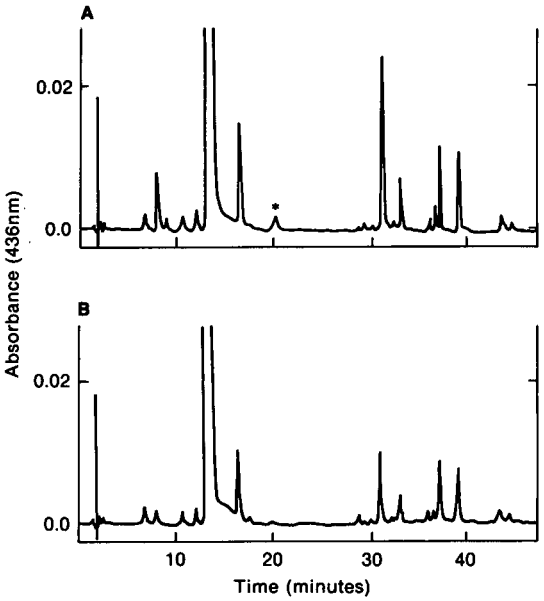

Fig. 6. Chromatograms after HPLC separation of (B) 8% of 1.9 μg of non-glycosylated peptide T5 and (A) 8% of 2.4 μg of N-glycosylated peptide NGlcNAcT5 using gradient 1. The peak marked with asterisk reveals the presence of the sugar moiety.

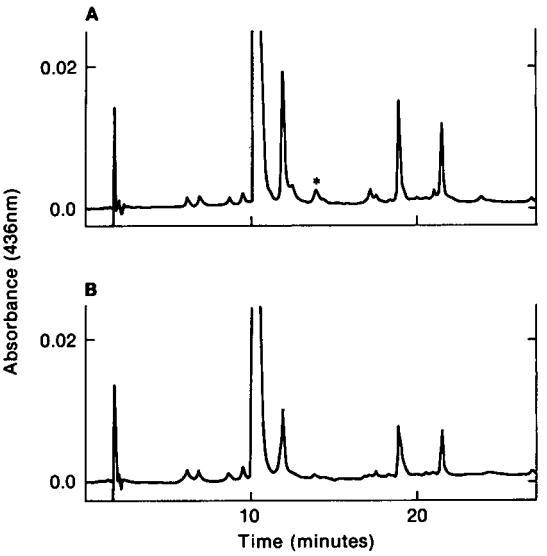

Fig. 7. Chromatograms after the amino acid analysis of (B) 6% of 1.9 μg of non-glycosylated peptide T5 and (A) 6% of 2.2 μg O-glycosylated peptide TGalNAcT5 using gradient 2. The peak marked with an asterisk verifies the presence of the carbohydrate moiety.

lysate that contained all three derivatives in question simultaneously (Figure 8).

Remarkably, both the dabsylated proline and dabsylated sugars could be detected after analysis of the RGD analogs (Table II). Our ability to detect the GlcNAc moiety, even in the O-glycosylated peptide, further justifies the use of this method to analyze glycopeptide structures.

Optimum sugar analysis conditions

During the development of an optimum hydrolysis procedure for the determination of the glycopeptides using amino acid analysis conditions, the following were considered.

The classical methods of protein and peptide hydrolysis feature heating the sample in constant-boiling HCl or 6 *M* HCl for periods of 18–24 h at 110°C to hydrolyze fully all the peptide bonds [31]. Gas-phase hydrolysis has been developed for samples with limited amounts to decrease the background noise caused by contaminants of the 6 *M* HCl [22,32,33]. The effect of raising the temperature on the recovery of amino acids by hydrolysis has also been reported [34–36]. Microwave heating is a viable alternative, and may be a promising method for the hydrolysis of the glycopeptide, but it requires special equipment and consequently its applicability is limited [37,38].

Sugars are less stable than the amino acids to boiling acid, and milder conditions of hydrolysis have to be used for their analysis. This degradation chain gives many intermediate products, and the sugar will be destroyed irrespective of whether the intermediates react with amino acids or whether the degradation proceeds to the final products [24]. It has also been reported that no perfect conditions of hydrolysis by acid can be derived so as to ensure that all glycosidic linkages present in the glycoproteins and glycopep-

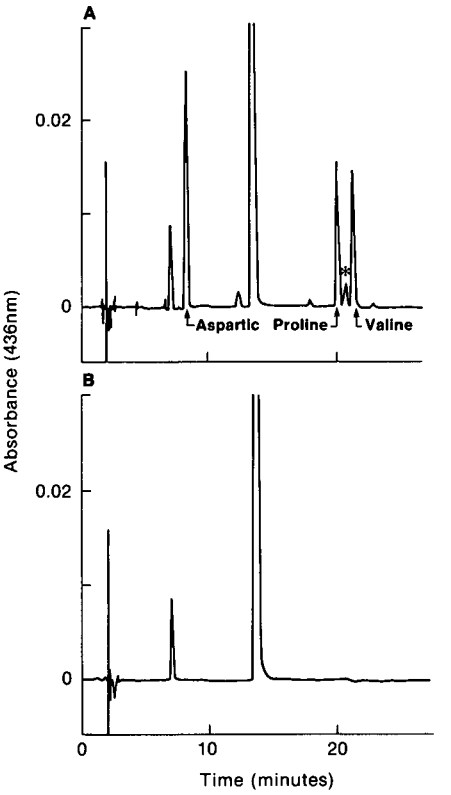

Fig. 8. Chromatogram after hydrolysis and dabsylation of (A) model peptide N(GlcNAc)PV compared with (B) the blank. The peak marked with an asterisk reveals the presence of the sugar.

TABLE II

DETECTION OF THE PRESENCE OF SUGAR IN THE SYNTHETIC RGD PEPTIDE AND OF ITS GLYCOSYLATED ANALOGS USING GRADIENT 1

Sequence	Peak of DABS-proline	Peak of DABS-glucosamine	FAB-MS[a] ($[M+H]^+$, m/z)
Ac-GRGDSPK-NH_2	+	–	758
Ac-N(GlcNAc)GRGDSPK-NH_2	+	+	1075
Ac-N(GlcNAc)GRGDSPKN(GlcNAc)-NH_2	+	+	1392
Ac-GRGDS(GlcNAc)PK-NH_2	+	+	912

[a] Fast atom bombardment mass spectrometry.

tides are cleaved, and at the same time that all monosaccharides are still intact at the end of the acid treatment [39]. Earlier reports of glycopeptide analysis failed to identify and quantify the new peak that was observed after hydrolysis and derivatization by phenyl isothiocyanate [40,41]. We wanted to develop methods to determine the glucosamine and galactosamine as intermediates of acidic hydrolysis of glycopeptides. Preliminary results show that decreasing the degradation of sensitive amino acids by using additives can be successful. A reduction of the degradation products of sensitive amino acids was reported by adding phenol to the hydrolysis mixture during both phenyl isothiocyanate- and DABS-based amino acid analysis [42,43].

Increasing the time of GlcNAc hydrolysis to between 1.5 and 16 h at 110°C or higher temperatures [44] decreased the detected amount of DABS-glucosamine (Table III). On the one hand, it is not recommended to maintain an extended hydrolysis time because the decrease in the detected amount of DABS-glucosamine was not accompanied by higher reproducibility compared with shorter hydrolysis times. On the other hand, it can be expected that the hydrolysis of the acetyl group from GlcNAc takes some time. As Fig. 9 indicates, hydrolysis for 1 h seems to be optimum to obtain the highest amount of DABS-glucosamine. Taken together, the hydrolysis time for the sugar determination should not exceed 1 h. We studied the reproducibility and the determination of DABS-glucosamine in a glucosamine standard and in hydrolyzed and dabsylated GlcNAc using these

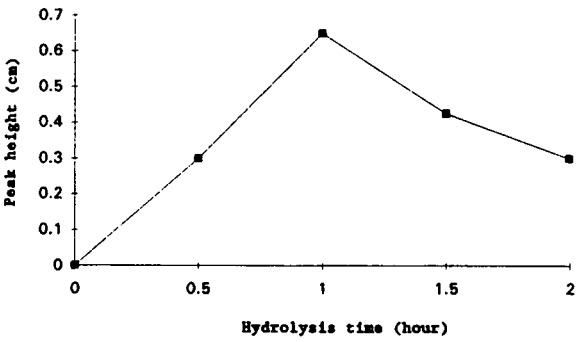

Fig. 9. Amount of dabsylated glucosamine as the function of the hydrolysis time, after acidic hydrolysis of GlcNAc.

conditions. The detected peak area of hydrolyzed and dabsylated GlcNAc equaled that of dabsylated glucosamine (Table IV) in the 2.5–7.5-nmol range (8% of them were injected: 0.2, 0.4 and 0.6 nmol). The detected peak area was directly proportional to the amount of the sugar. The variability of the results was within 10% in the individual experiments. When different sets of experiments were compared, the reproducibility favored the GlcNAc over the glucosamine, and high variability of the detected DABS-glucosamine was found when triplicate samples of glucosamine were subjected to the same hydrolysis conditions. These results show that the underlying events cannot be fully understood when only amino sugar standards are examined. It was also observed that the recovery of the dabsylated glucosamine standard and of the hydrolyzed and dabsylated GlcNAc was 20% of that of the dabsylated asparagine standard. This finding is in strong agreement with our prelimin-

TABLE III

SENSITIVITY OF THE CARBOHYDRATE MOIETY TO ACIDIC HYDROLYSIS

Temperature (°C)	Hydrolysis time (h)	Relative peak height[a]
110	1.5	0.81
	8	0.37
	16	0.22
150	1	0.20

[a] Expressed in 5 nmol GlcNAc / 1 nmol asparagine.

TABLE IV

RECOVERY OF DABSYLATED GLUCOSAMINE AND HYDROLYZED AND DABSYLATED GlcNAc AS A FUNCTION OF THE AMOUNT APPLIED

Injected (units)	One unit area of[a]	
	Dabsylated glucosamine	Hydrolyzed and dabsylated GlcNAc
2.5	0.2208	0.2175
5.0	0.2145	0.1998
7.5	0.2181	0.2175

[a] One unit equals 0.08 nmol of dabsylated sugar.

ary results, which indicate that 8% of 5 nmol of the sugar standards needs to be dabsylated in order to obtain peak heights similar to those for 8% of 1 nmol dabsylated asparagine (8% of the dabsylated amounts were injected). Most of the sugars probably remain undabsylated, as 86 and 81%, respectively, of the radioactivity of GlcNAc was recovered in the flow-through in two replicate experiments. We attempted to improve the efficiency of the dabsylation reaction. An increase in the temperature to 90°C, lengthening of the time of dabsylation from 15 to 25 min or using microwave irradiation were less effective. We also tested whether dabsylation is inferior to the currently partially used phenyl isothiocyanate (PITC) derivatization of glucosamine. The standard derivatization protocol of glucosamine with PITC resulted in 20% of that of phenylthiocarbamyl (PTC)-Aspartic, the same value that was obtained with dabsylation. Moreover, reaction with PITC may lead to the formation of a sugar alcohol [45] and further work-up is required to obtain a single analyzable compound.

Two different possibilities were scrutinized for the determination of sugars in the glycopeptides (using amino acid analysis conditions). First, analysis of the amino sugars cleaved from the glycopeptides was performed. Second, as we demonstrated earlier, a 10–30% loss of the asparagine occurred when peptides containing GlcNAc-conjugated asparagine were subjected to hydrolysis at 150°C for 1 h, followed by PITC amino acid analysis [46]. Different amounts of Asn-GlcNAc and T peptides were hydrolyzed and dabsylated in order to investigate the possibility of obtaining useful information concerning the number of incorporated sugar moieties based on the detected aspartic values. The recovery of dabsylated asparagine from the Asn-GlcNAc standard is reproducibly 57% of that of the asparagine standard, and is constant in the 2.5–5 nmol range. The complete recovery of the sugars remains unsuccessful, as more than 40% variability of the detected carbohydrate was found. Our experiments with the T peptides showed that the detected asparagine is well below the expected amount after hydrolysis at 110°C for 1 h, even when no sugar is attached

TABLE V

RECOVERY OF THE ASPARAGINE RESIDUE AS A FUNCTION OF HYDROLYSIS TIME AND THE PRESENCE AND LOCATION OF THE SUGAR MOIETIES

Peptide	Amount of DABS-ASX[a]		
	Detected after 1 h hydrolysis	Detected after 10 h hydrolysis	Expected
T5	0.66	1.04	1
T5GlcNAc	0.75	0.89	1
GlcNAcNT5	1.71	2.09	2
TGalNAcT5	0.63	0.94	1

[a] The values are normalized to threonines.

(Table V), owing to incomplete hydrolysis of the peptide bonds. Extension of the hydrolysis time to 10 h resulted in the recovery of the correct amount of asparagine for the non-glycosylated peptide T5 and the N-terminally N-glycosylated peptide NGlcNAcT5, but remained low for the N-terminally O-glycosylated peptide TGalNAcT5 and especially the peptide T5GlcNAc, which contains the carbohydrate in a mid-chain position (Table V). Unfortunately, these hydrolysis conditions are not compatible with the analysis of the sugar moieties.

The observed reliable lower detection limit of the sugar moieties in the glycopeptides was estimated to be 0.2 nmol and upper detection limit 0.5 nmol. The DABS-sugar peak is well observed in this range, but increasing the amount of peptide results in an increasing number and heights of unidentified peaks. Although no unidentified peak was observed using 0.2 nmol of peptide, two new peaks were observed at the position of DABS-alanine and DABS-valine when 0.5 nmol of peptide was applied. These new, unidentified peaks may originate from other intermediate products of sugar degradation. Many other unidentified peaks are detected on the chromatogram after derivatization with DABS-Cl [21,22], even when blank samples are analyzed. One of these unidentified peaks appears after several hours of continuous chromatography on any given working day, and is located close to the peaks of DABS-glucosamine and DABS-galactosamine.

We attempted to improve the recovery of sugars by using phenol (as a scavenger of oxidant) with 6 *M* HCl during hydrolysis or, alternatively, with changed reaction conditions [42]. Three kinds of hydrolysis conditions were used: (A) 110°C, 1 h, without phenol; (B) 150°C, 1 h, with addition of 3% phenol; and (C) 100°C, 3 h, with addition of 3% phenol (as was suggested by Muramoto and Kamiya [42]). Although the sugar could be detected at 100°C, the addition of phenol did not improve its recovery from Asn-GlcNAc compared with hydrolysis at 110°C without addition of phenol. A lack of all contaminating peaks was observed at 150°C after addition of phenol. The carbohydrate, however, was also missing from the chromatogram (Table VI). The presence of the sugar was detected in 0.5-nmol amounts of the glycosylated T peptides after applying all three hydrolysis conditions, but the determination of the amino acids was still outside the acceptable range.

In conclusion, we have demonstrated that the presence of GlcNAc and GalNAc (the starting sugar structures of N- and O-glycoproteins, respectively) and, consequently, the integrity of synthetic glycopeptides can be verified by DABS-Cl amino acid analysis. The sugars can be recovered in 15–25% overall yields. The enzymatic cleavage of glycoproteins usually results in peptide fragments bearing glycosylated side chains. The protocol discussed above is a viable alternative for the rapid determination of such glycosylated protein fragments.

TABLE VI

EFFECT OF DIFFERENT HYDROLYSIS CONDITIONS ON THE DETERMINATION OF Asn-GlcNAc

Injected (nmol)	Detected area[a]					
	A		B		C	
	Asn	Sugar	Asn	Sugar	Asn	Sugar
0.2.	1.36	0.15	1.25	–	1.61	0.15
0.4	2.65	0.33	2.89	–	3.03	0.53

[a] The conditions of hydrolysis were (A) 110°C, 1 h, without phenol; (B) 150°C, 1 h, with addition of 3% phenol; and (C) 100°C, 3 h, with addition of 3% phenol. The recovered amounts of asparagine in A, B and C compared with the Asn standard were 57, 62, and 55%, respectively.

ACKNOWLEDGEMENTS

We thank Dr. David W. Speicher for his critical reading of the manuscript. This work was supported by National Institutes of Health grant GM 45011.

REFERENCES

1 R. Kornfeld and S. Kornfeld, *Annu. Rev. Biochem.*, 54 (1985) 631.
2 P.L. Mollison, in C.P. Engelfriet and M. Contreras (Editors), *Blood Transfusion in Clinical Medicine*, Blackwell, Oxford, 1987, p. 269.
3 K. Kakehi, S. Suzuki, S. Honda and Y.C. Lee, *Anal. Biochem.*, 199 (1991) 256.
4 R. Mögele, B. Pabel and R. Galensa, *J. Chromatogr.*, 591 (1992) 165.
5 T. Akiyama, *J. Chromatogr.*, 588 (1991) 53.
6 M.C. Rose, W.A. Voter, H. Sage, C.F. Brown and B. Kaufman, *J. Biol. Chem.*, 259 (1984) 3167.
7 E.A. Kabat, in J.D. Ebert, A.G. Loewy and H.A. Schneiderman (Editors), *Structural Concepts in Immunology and Immunochemistry*, Holt, Rinehart, and Winston, New York, 1987, p. 269.
8 L. Otvos, Jr., J. Thurin, E. Kollat, L. Urge, H.H. Mantsch and M. Hollosi, *Int. J. Pept. Protein Res.*, 38 (1991) 476.
9 A. Kobata, in V. Ginsburg and P. Robbins (Editors), *Biology of Carbohydrates*, Vol. 2, Wiley, New York, 1984, p. 87.
10 C.A. Browne, H.P.J. Bennett and S. Solomon, *Anal. Biochem.*, 124 (1982) 201.
11 L. Otvos, Jr., L. Urge and J. Thurin, *J. Chromatogr.*, 599 (1992) 43.
12 C.B. Pert, J.M. Hill, M.R. Ruff, R.M. Berman, G. Robey, L.O. Arthur, F.W. Ruscetti and W.L. Farrar, *Proc. Natl. Acad. Sci. U.S.A.*, 83 (1986) 9254.
13 L. Urge, L. Gorbics and L. Otvos, Jr., *Biochem. Biophys. Res. Commun.*, 184 (1992) 1125.
14 S. Moore and W.H. Stein, *J. Biol. Chem.*, 211 (1954) 893.
15 D.W. Hill, F.H. Waters, T.D. Wilson and J.D. Stuart, *Anal. Chem.*, 51 (1979) 1338.
16 R.L. Heinrikson and S.C. Meredith, *Anal. Biochem.*, 136 (1984) 65.
17 J.-K. Lin and J.-Y. Chang, *Anal. Chem.*, 7 (1975) 1634.
18 J.-Y. Chang, R. Knecht and D.G. Braun, *Biochem. J.*, 199 (1981) 547.
19 J.-Y. Chang, A. Lehmann and B. Wittmann-Liebold, *Anal. Biochem.*, 102 (1980) 380.
20 C.-Y. Yang and S.J. Wakil, *Anal. Biochem.*, 137 (1984) 54.

21 J.-Y. Chang, R. Knecht and D.G. Braun, *Biochem. J.*, 203 (1982) 803.
22 J.-Y. Chang and R. Knecht, *Anal. Chem.*, 58 (1986) 2375.
23 H. Kunz, H. Waldmann and J. März, *Liebigs Ann. Chem.*, 45 (1989) 45.
24 A. Gottschalk, in A. Gottschalk (Editor), *Glycoproteins, Their Composition, Structure, and Function*, Elsevier, Amsterdam, 1972, p. 96.
25 L. Urge, E. Kollat, M. Hollosi, I. Laczko, K. Wroblewski, J. Thurin and L. Otvos, Jr., *Tetrahedron Lett.*, 32 (1991) 3445.
26 L. Otvos, Jr., L. Urge, M. Hollosi, K. Wroblewski, G. Graczyk, J.D. Fasman and J. Thurin, *Tetrahedron Lett.*, 31 (1990) 5889.
27 F. Altman, *Anal. Biochem.*, 204 (1992) 215.
28 M.J. Spiro and R.G. Spiro, *Anal. Biochem.*, 204 (1992) 152.
29 L. Urge, E. Kollat, M. Hollosi, I. Lacko, K. Wroblewski, J. Thurin and L. Otvos, Jr., *Tetrahedron Lett.*, 32 (1991) 3445.
30 A.B. Foster, *Adv. Carbohydr. Chem.*, 14 (1959) 213.
31 D. Moore and W.H. Stein, *Methods Enzymol.*, 6 (1963) 819.
32 N.M. Meltzer, G.I. Tous, S. Gruber and S. Stein, *Anal. Biochem.*, 160 (1987) 356.
33 D.T. Blankenship, M.A. Krivanek, B.L. Ackermann and A.D. Cardin, *Anal. Biochem.*, 178 (1989) 227.
34 F.C. Westhall and H. Hesser, *Anal. Biochem.*, 61 (1974) 610.
35 D. Roach and C.W. Gehrke, *J. Chromatogr.*, 52 (1970) 393.
36 F.E. Kaiser, C.W. Gehrke, R.W. Zumwalt and K.C. Kuo, *J. Chromatogr.*, 94 (1974) 113.
37 L.B. Gilman and C. Woodward, in J.J. Villafanca (Editor), *Current Research in Protein Chemistry: Techniques, Structure and Function*, Academic Press, New York, 1990, Ch. 3, p. 23.
38 S.-H. Chiou and K.-T. Wang, *J. Chromatogr.*, 491 (1989) 424.
39 A. Neuberger and R.D. Marshall, in A. Gottschalk (Editor), *Glycoproteins, Their Composition, Structure, and Function*, Elsevier, Amsterdam, 1972, p. 190.
40 R. Gupta and N. Jentoft, *J. Chromatogr.*, 474 (1989) 411.
41 D.E.H. Palladino, R.M. House and K.A. Cohen, *J. Chromatogr.*, 599 (1992) 3.
42 K. Muramoto and H. Kamiya, *Anal. Biochem.*, 189 (1990) 223.
43 B.A. Bidlingmeyer, S.A. Cohen and T.L. Tarvin, *J. Chromatogr.*, 336 (1984) 93.
44 G. Allen, in R.H. Burdon and P.H. van Knippenberg (Editors), *Laboratory Techniques in Biochemistry and Molecular Biology: Sequencing of Proteins and Peptides*, Vol. 9, Elsevier, Amsterdam, 1989, p. 40.
45 K.R. Anumula and P.B. Taylor, *Anal. Biochem.*, 197 (1991) 113.
46 L. Otvos, Jr., K. Wroblewski, E. Kollat, A. Perczel, M. Hollosi, J.D. Fasman, H.C.J. Ertl and J. Thurin, *Pept. Res.*, 2 (1989) 362.

Journal of Chromatography, 637 (1993) 55–62
Elsevier Science Publishers B.V., Amsterdam

CHROM. 24 963

Glycosidase digestion, electrophoresis and chromatographic analysis of recombinant human granulocyte colony-stimulating factor glycoforms produced in Chinese hamster ovary cells

Christi L. Clogston, Sylvia Hu, Thomas C. Boone and Hsieng S. Lu*

Amgen Inc., Amgen Center, Thousand Oaks, CA 91320 (USA)

(First received October 19th, 1992; revised manuscript received February 8th, 1993)

ABSTRACT

Recombinant human granulocyte colony stimulating factor (G-CSF) produced in Chinese hamster ovary cells is glycosylated. The carbohydrate compositional analysis indicated that G-CSF molecule contains sialic acid, galactose and galactosamine. By isolation and characterization of the purified glycopeptides obtained from cleavages by *Staphylococcal aureus* V-8 protease and cyanogen bromide, the O-linked glycosylation site was confirmed to be a Thr residue at position 133. Neuraminidase and O-glycanase digestion followed by sodium dodecyl sulfate polyacrylamide and isoelectric focusing gel electrophoreses distinguished two possible carbohydrate structures attached at Thr-133: structure A, NeuNAc-Gal-β(1,3)-GalNAc-O-Thr; and structure B, NeuNAc-Gal-β(1,3)-[NeuNAc]-GalNAc-O-Thr. Different glycoforms, undigested or after glycosidase digestion, can also be separated by ion-exchange or reversed-phase high-performance liquid chromatography. The approach described in this report provides a simple and valuable procedure to characterize glycoprotein structures containing simple carbohydrate moieties.

INTRODUCTION

Granulocyte colony-stimulating factor (G-CSF) is one of the hematopoietic growth factors which play an important role in the stimulation, proliferation, and differentiation of hematopoietic progenitors, and are also required for functional activation of the mature cells [1,2]. G-CSF is capable of supporting neutrophil proliferation *in vivo* and *in vitro* [3–6]. The human G-CSF gene has been cloned and characterized [7,8]. Large quantities of recombinant human G-CSF (rhG-CSF) produced in genetically engineered *E. coli* have been successfully used in human clinical studies to treat neutropenic patients in a variety of clinical situations [9–13].

The natural hG-CSF isolated from tumor cell lines appears to be glycosylated [7] and has equivalent biological activity to the non-glycosylated rhG-CSF derived from *E. coli*. Due to its scarcity, characterization of the carbohydrate structure in hG-CSF isolated from a natural source has been difficult. We have expressed recombinant G-CSF in Chinese hamster ovary (CHO) cells transfected with hG-CSF cDNA to produce sufficient quantities of purified protein. In this mammalian production system, the CHO-rhG-CSF molecule, as isolated, appears to be glycosylated.

Determination of carbohydrate attachment sites and oligosaccharide structures in glycoproteins requires the strategic combination of various analytical techniques including glycosidase digestion, HPLC, isoelectric focusing (IEF)-polyacrylamide gel electrophoresis (PAGE),

* Corresponding author.

0021-9673/93/$06.00

peptide mapping, Edman degradation and amino acid analysis. Detailed analysis of oligosaccharide structures for complex glycoproteins involves the use of sophisticated instrumentation such as mass spectrometry and NMR (for reviews and refs., see refs. 14–19). We report here the analysis of the carbohydrate structures and location of an O-linked glycosylation site in CHO-rhG-CSF by sequence analysis and glycosidase digestion followed by electrophoretic analysis. The structure of oligosaccharides chemically removed from rhG-CSF has been previously determined by NMR analysis [20].

MATERIALS AND METHODS

Materials

E. coli, yeast, and CHO-cell-derived rhG-CSFs were purified by chromatographic procedures similar to those described [7]. Their purified preparations had specific activity of greater than $1 \cdot 10^8$ units/mg when assayed in a granulocyte-macrophage colony-forming unit assay [4]. Neuraminidase (sialidase, E.C. 3.2.1.18) isolated from *Vibrio cholera*, and O-glycanase (endo-α-N-acetyl-D-galactosaminidase, E.C.3.2.1.97) were purchased from CalBiochem and Genzyme, respectively.

Carbohydrate analysis

Acid hydrolysis of samples was carried out according to Hardy *et al.* [21]. Acid in the hydrolysate was then removed by vacuum centrifugation and then the reconstituted hydrolysate subject to composition analysis by high pH anion-exchange chromatography with pulsed amperometric detection (AE–PAD) using a Dionex BioLC system [21]. Sialic acid was quantitated spectrophotometrically according to Jourdian *et al.* [22]. Sialic acid released from neuraminidase digestion of the samples was also analyzed by AE–PAD. The separation of neutral sugars and sialic acid was separately performed on a Dionex Carbopac AS-6 (25×0.46 cm I.D.) pellicular anion-exchange column and eluted with 100 m*M* NaOH and 150 m*M* NaOAc as described previously [21,23].

Protease digestion and HPLC–peptide mapping

Reduction and S-carboxymethylation of G-CSF with dithiothreitol and iodoacetate as well as the HPLC peptide mapping were performed according to a previous procedure [24]. The alkylated derivative in 0.1 *M* ammonium bicarbonate, pH 8.3, was incubated with V-8 protease at an enzyme-to-substrate ratio of 1:30 (w/w) at 37°C for 18 h. The digestion was terminated by injection of the digest onto an HPLC column for peptide separation. Peptides were purified by reversed-phase HPLC using Vydac C-4 widepore columns (300Å: 25×0.46 cm I.D.) and an HP1090 micro liquid chromatographic system equipped with an autosampler and a photodiode array detector. Peptides were monitored at both 215 nm and 280 nm and fractions collected manually.

Amino acid sequence analysis

Polypeptides were sequenced from their amino termini by automated Edman degradation on an Applied Biosystems 477 gas-phase sequencer equipped with an on-line microbore HPLC system to detect PTH-amino acid elucidated at each degradation cycle [25]. The peptides were spotted on TFA-activated glass fiber discs which were treated with Polybrene (120 mg/ml) containing 6.7 mg/ml NaCl and preconditioned with at least two sequencer cycles.

Analytical isoelectric focusing and sodium dodecyl sulfate (SDS)-PAGE

A narrow range IEF gel (pH 5–8; thickness 0.4 mm) was prepared according to the following recipe: 6% acrylamide, 0.16% bis, 3 *M* urea, 0.05% ammonium persulfate, 6.25% servalytes (pH range 5–8). IEF was carried out at a constant power of 10 watt (voltage limit: 1500 V). The gel was prefocused for 30 minutes. Once the samples were spotted, IEF was carried out for 3.5 hours, after which the pH gradient in the gel was measured using a surface electrode (Ingold) connected to an Altex ϕ71 pH meter (Beckman). The proteins in the gel were fixed by soaking the gel in 35% methanol–10% trichloroacetic acid–3.5% sulfosalicyclic acid for 30 minutes; the proteins were stained with a solution of 0.1% Coomassie Blue R-250–35% ethanol–10%

acetic acid (staining solution was filtered through Whatman No. 1 paper before use), and the gel destained with the same solution not containing R-250.

SDS-PAGE was performed using 20 × 20 cm slabs and 15% polyacrylamide according to Laemmli [26].

Endoglycosidase digestion

Purified CHO-rhG-CSF was digested with neuraminidase according to Bhavanandan and Davidson [27] for 2 h at 37°C in a reaction buffer of 0.02 *M* Tris–maleate, 0.001 *M* $CaCl_2$, pH 6.0, and subsequently digested with O-glycanase for 6 h at 37°C [28].

Reversed-phase and cation-exchange HPLC

Reversed-phase HPLC separation was performed using procedures described previously [29]. The HPLC analysis was carried out on a C_4 reversed-phase column (25 × 0.46 cm I.D.; Vydac wide-pore) employing trifluoroacetic acid (TFA)–acetonitrile gradient elution at a flow-rate of 0.8 ml/min at room temperature.

Separation of CHO-rhG-CSF glycoforms was also performed using a TSK SP-5PW cation-exchange column (7.5 × 0.75 cm I.D., Tosoha, Japan). The column was developed with a 85-min gradient of 0 to 75 m*M* sodium sulfate in 20 m*M* sodium acetate, pH 5.4. The flow-rate was 0.7 ml/min and the column effluent was monitored at 230 nm.

RESULTS AND DISCUSSION

Carbohydrate composition

The following compositional analysis confirms that hG-SF expressed in CHO cells is glycosylated. After a desalting step, purified CHO-rhG-CSF was subject to partial acid hydrolysis and carbohydrate analysis. Data shown in Table I is the carbohydrate composition expressed in molar ratio. The results indicate that CHO-rhG-CSF contains a simple carbohydrate composition, *i.e.*, 1–2 mol of sialic acid residues and one residue each of galactose and galactosamine. The content of sialic acid quantitated by the spectrophotometric method is consistent with that determined by HPAE–PAD analysis of the neuraminidase-digested sample. The carbohydrate composition shown above suggests that CHO-rhG-CSF may contain simple Thr/Ser-linked carbohydrate moieties.

TABLE I

CARBOHYDRATE COMPOSITION OF RECOMBINANT HUMAN G-CSF EXPRESSED IN CHO CELLS

Sugar[a]	mol/mol[b]
Gal	1.19
GalNAc	1.00
NeuNAc	1.42[c]
	1.67[d]

[a] Neutral sugars were analyzed by AE–PAD after acid hydrolysis.
[b] Numbers are expressed as mol carbohydrate per mol G-CSF.
[c] Analyzed by spectrophotometric assay.
[d] Analyzed by AE–PAD for neuraminidase-digested sample.

Assignment of a single O-linked sugar attachment site

The location of potential glycosylation sites was assigned by isolation and structural characterization of glycopeptides. In peptide map analysis, purified *E. coli* and CHO-derived G-CSFs were reduced with dithiothreitol to break the disulfide bonds and subsequently alkylated with iodoacetate. These S-carboxymethylated derivatives were digested with *S. aureus* V-8 protease followed by reverse-phase HPLC analyses to isolate peptides. As shown in Fig. 1, the G-CSF digests produced comparable peptide maps between the two samples with only two notable exceptions: (1) the major peptide peak at 49 min in CHO-derived G-CSF had shifted to 50 min in *E. coli* G-CSFs map. These peptides were verified to be the N-terminal peptides of G-CSF. The increase in retention time of *E. coli* G-CSF N-terminal peptide is caused by the additional methionine present in the molecule; and (2) another peptide found at 63 min in the *E. coli*-derived G-CSF map had shifted to earlier retention at 60.5 min in the CHO-rhG-CSF map and elutes as a broader peak. These peptides were confirmed to be the C-terminal peptides of G-CSF. The earlier elution and broadness of the peak shape for the CHO-rhG-CSF C-terminal

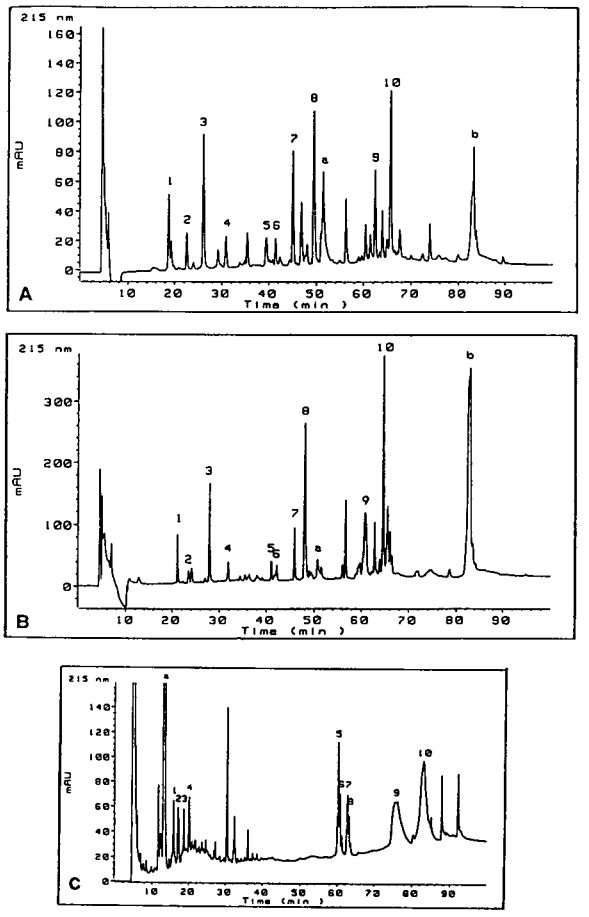

Fig. 1. HPLC peptide maps of different G-CSF preparations derived from digestions using *S. aureus* V–8 protease. (A) Peptide map of carboxymethylated rhG-CSF produced in *E. coli* (75 μg). (B) Peptide map of carboxymethylated CHO-rhG-CSF (75 μg). (C) Peptide map of cyanogen bromide peptides for CHO-rhG-CSF. Solvent A = 0.1% TFA; solvent B = TFA–H_2O–CH_3CN (0.1:9.9:90). The column was initially equilibrated at 97% A–3% B at a flow-rate of 0.7 ml/min. The peptides were separated by a linear gradient from 3% B to 35% B over 10 min followed by 80% B isocratic elution for 20 min. Peptides were numbered arbitrarily according to their elution orders. Peak a is an artifact peak derived from carboxymethylation and peak b is the undigested core protein. Several unnumbered peptides in chromatograms A and B represent those derived from non-specific cleavages.

peptide indicates that this peptide contains heterogeneous carbohydrate moieties.

Amino acid sequence of the C-terminal peptide (t_R 60.5 min) obtained from peptide mapping of the carboxymethylated CHO-rhG-CSF derivative begins with Leu-124 and contains five potential O-linked glycosylation sites, *i.e.*, Thr-133, Ser-142, Ser-155, Ser-159 and Ser-164. Among the first four potential glycosylation sites, only Thr-133 yielded no signal during N-terminal sequence analysis, making it a potential site of glycosylation, however, Ser-164 has yet to be eliminated as a possible site. Table II summarizes the quantitative recovery of PTH-amino acids obtained from automated gas phase Edman degradation of peptide.

CHO-rhG-CSF was further digested with cyanogen bromide to generate larger fragments cleaved at methionine. After separating by HPLC (Fig. 1C), a peak at 60 min was recovered and found to be the C-terminal peptide beginning with Pro-138. This peptide was sequenced through Tyr-165. Recovery of PTH-amino acid can be clearly found at Ser-142, Ser-155, Ser-159 and Ser-164, thus eliminating these serines as potential glycosylation sites. Another peptide with a retention time of 20 min was found to be the Ala-127 to Met-137 peptide. Sequence analysis indicated that Thr-133 is the only amino acid which cannot be detected (Table II). This result corroborates the previous analytical data obtained from a V-8 protease-generated C-terminal peptide described above. These results conclude that the hydroxyl side chain of Thr-133 is the only amino acid linked to carbohydrate moieties in CHO-G-CSF.

Glycosidase digestion and electrophoretic analysis

By taking advantage of the selective specificity of endoglycosidases in hydrolyzing glycosidic bonds of oligosaccharides in glycoproteins, we further studied the carbohydrate structure of CHO-rhG-CSF by neuraminidase and O-glycanase digestion. Neuraminidase catalyzes the hydrolysis of α(2,3)-, α(2,6)-, or α(2,8)-linked sialic acids on oligosaccharides and glycoproteins while O-glycanase catalyzes the hydrolysis of the Gal-β(1,3)-GalNAc core disaccharides attached to serine or threonine residues of glycoproteins or glycopeptides [27,28]. CHO-rhG-CSF was first treated with neuraminidase for 2 hours. A portion of the digest was used to determine concentration of the released sialic acid by HPAE–PAD

TABLE II

SEQUENCE ANALYSIS OF TWO CHO-rhG-CSF GLYCOPEPTIDES AND A C-TERMINAL PEPTIDE

Sequence position	Peptides					
	S-9[a]		CNBr-5[b]		CNBr-4[b]	
	Amino acid	Recovery (pmol)	Amino acid	Recovery (pmol)	Amino acid	Recovery (pmol)
124	Leu	1000				
125	Gly	771				
126	Met	348				
127	Ala	348			Ala	157
128	Pro	171			Pro	62
129	Ala	175			Ala	81
130	Leu	284			Leu	109
131	Gln	128			Gln	52
132	Pro	101			Pro	31
133	( )	ND[c]			( )	ND[c]
134	Gln	66			Gln	26
135	Gly	105			Gly	30
136	Ala	61			Ala	4
137	Met	34				
138	Pro	39	Pro	344		
139	Ala	26	Ala	302		
140	Phe	28	Phe	333		
141	Ala	17	Ala	266		
142	Ser	14	Ser	93		
143	Ala	8	Ala	111		
144	Phe	14	Phe	240		
145	Gln	18	Gln	64		
146	Arg	8	Ala	98		
147	Arg	3	Arg	33		
148	Ala	8	Ala	98		
149	Gly	14	Gly	161		
150	Gly	3	Gly	33		
151	Val	3	Val	107		
152	Leu	4	Leu	142		
153	Val	1	Val	104		
154	Ala	4	Ala	113		
155	Ser	3	Ser	25		
156	His	2	His	4		
157	Leu	4	Leu	67		
158	Gln	3	Gln	28		
159	Ser	1	Ser	11		
160	Phe	1	Phe	53		
161			Leu	27		
162			Glu	8		
163			Val	26		
164			Ser	8		
165			Tyr	9		

[a] Isolated from peptide map from *S. aureus* V-8 protease digest of carboxymethylated CHO-rhG-CSF (see Fig. 1B).
[b] Isolated from peptide map from CNBr cleavage of carboxymethylated CHO-rhG-CSF (see Fig. 1C).
[c] Not detected.

(see Methods). The resulting asialo molecule in another portion of the digest was subsequently digested with O-glycanase for 8 hours to cleave any asialo O-linked sugar. As indicated in Fig. 2, by SDS-PAGE, the neuraminidase-treated G-CSF has M_r 19 200 as opposed to M_r 19 600–20 000 for the untreated sample. Subsequent treatment with O-glycanase further reduced the mass of G-CSF to approximately 18 800. Since neuraminidase and O-glycanase are highly specific glycosidases, the molecular mass reduction of CHO-rhG-CSF by these two hydrolases suggests a possible structure for the carbohydrate component, *i.e.*, NeuNAc-Gal-β(1,3)-GalNAc-O-Thr-133.

The endoglycosidase-treated CHO-rG-CSF was also analyzed by narrow range IEF (Fig. 3). Digestion of samples with neuraminidase results in the disappearance of the diminution for p*I* 5.5 band, a partial decrease for p*I* 5.8 form, and the appearance of a new band at p*I* 6.15. This experiment suggests that the p*I* 5.8 G-CSF band contains one sialic acid and the p*I* 5.5 band two sialic acids, as the removal of sialic acid had generated asialo protein with identical net charges, migrating at a p*I* around 6.15. IEF analysis also shows that the enzyme hydrolyzes the p*I* 5.5 form containing two sialic acids more efficiently than the p*I* 5.8 form containing a single sialic acid. Further treatment of desialylated protein with O-glycanase results in no further change in p*I*, indicating that O-glycanase only removes the expected neutral sugars.

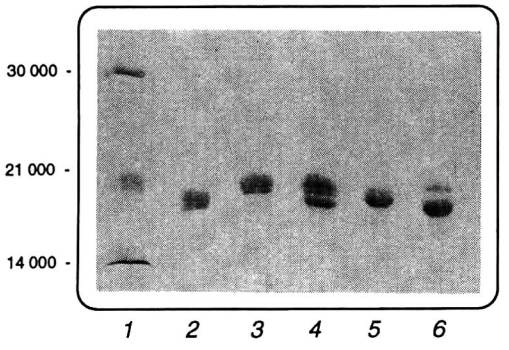

Fig. 2. SDS-polyacrylamide gel electrophoresis. Lanes: 1 = standard protein markers; 2 = rhG-CSF produced in *E. coli*; 3 = CHO-rhG-CSF; 4 = CHO-rhG-CSF and *E. coli*-produced rhG-CSF; 5 = CHO-rhG-CSF treated with neuraminidase; and 6 = CHO-rhG-CSF treated with neuraminidase and O-glycanase (5 μg load on each gel lane).

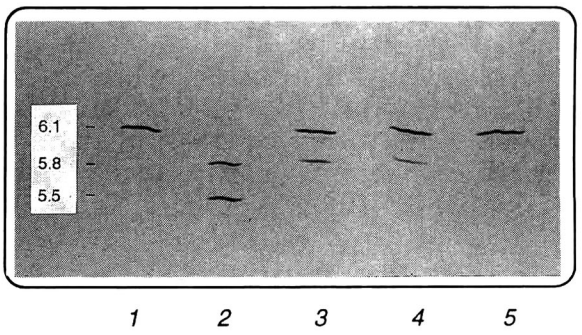

Fig. 3. Narrow-range isoelectric focusing gel electrophoresis. Lanes: 1 and 5 = *E. coli*-produced rhG-CSF; 2 = CHO-rhG-CSF; 3 = CHO-rhG-CSF treated with neuraminidase; and 4 = CHO-rhG-CSF treated with neuraminidase and O-glycanase (2.5 μg loaded on each lane).

Changes in both molecular mass and p*I* for CHO-rhG-CSF after neuraminidase and O-glycanase treatment suggests two possible carbohydrate structures: structure A, NeuNAc-Gal-β(1,3)-GalNAc-O-Thr-133; and structure B, NeuNAc-Gal-β(1,3)-[NeuNAc]-GalNAc-O-Thr-133. The linkage between NeuAc and Gal could be α(2,3) or α(2,6). The α(2,6) linkage is the only possibility connecting the NeuAc to GalNAc in structure B. Under narrow range IEF, CHO-rhG-CSF containing structure A would migrate at p*I* 5.8 and structure B at p*I* 5.5, while non-glycosylated *E. coli*-derived and yeast-derived rhG-CSFs as well as asialo CHO-rhG-CSF containing neutral sugar migrates at p*I* 6.1. This data is consistent with that derived from NMR analysis described previously [20].

Asialo CHO-rhG-CSF and the completely deglycosylated molecule can be clearly differentiated from untreated samples by IEF and SDS-PAGE. These analyses led us to conclude that Thr-133 in CHO-rhG-CSF is fully attached with carbohydrate moieties; the purified material does not contain a non-glycosylated form. Asialo CHO-G-CSF, which still contains neutral sugar, migrates at a p*I* identical to non-glycosylated G-CSF by IEF but is distinguishable by SDS-PAGE. This is supported by data obtained from reversed-phase and cation-exchange HPLC, described below.

Characterization of rhG-CSF glycoforms by chromatographic separation

Shown in Fig. 4A is the reversed-phase HPLC separation of CHO-rhG-CSF, asialo CHO-rhG-CSF obtained from neuraminidase treatment, and deglycosylated CHO-rhG-CSF after O-glycanase treatment. The results show that removal of carbohydrates increases the retention of the deglycosylated molecule in a reversed-phase column, suggesting an increase in hydrophobicity due to deglycosylation. However, CHO-rhG-CSF species varying in content of sialic acids are not separable in reversed-phase HPLC (Fig. 4A, chromatogram 1). Instead, these species can be well separated by ion-exchange HPLC shown in Fig. 4B. Ion-exchange HPLC completely resolves CHO-rhG-CSF into two major species, in approximately equimolar ratio. Peak I was identified as the glycosylated G-CSF containing two sialic acids and peak II as the glycoform with only one sialic acid (data not shown). Both asialo CHO-rhG-CSF and non-glycosylated hG-CSF (derived from yeast expression) coelute, but are also separable from peak II. They elute 4–5 min later than peak II in cation-exchange HPLC (data not shown).

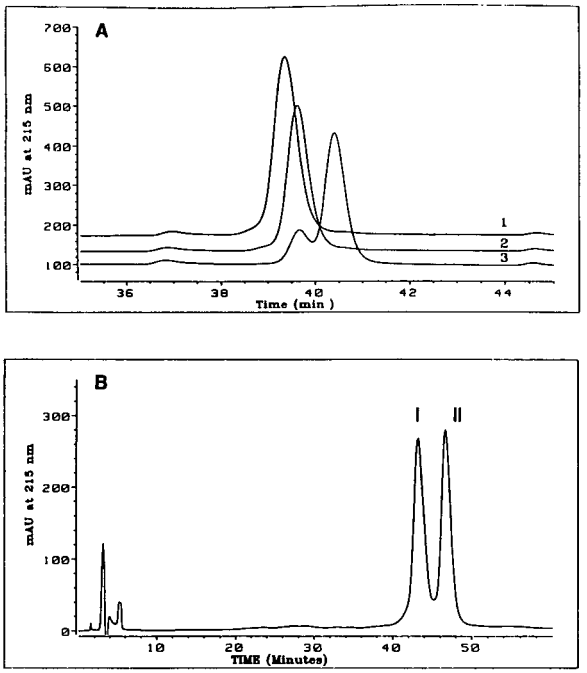

Fig. 4. (A) Reversed-phase HPLC of G-CSF species. Chromatograms 1–3 (25 μg each): CHO-rhG-CSF; asialo CHO-rhG-CSF treated with neuraminidase; and CHO-rhG-CSF treated with neuraminidase and O-glycanase, respectively. (B) Cation-exchange HPLC of CHO-rhG-CSF (50 μg injected).

In contrast to the above data, Nomura *et al.* [30] had reported that human G-CSF produced by a tumor cell line exhibits three distinct p*I* forms (5.5, 5.8 and 6.1). The p*I* 5.5 and 5.8 subforms match the sialylated subforms found in CHO-rhG-CSF, while the 6.1 subform, not detected in CHO-rhG-CSF, may be the asialo or non-glycosylated G-CSF.

CONCLUSION AND DISCUSSION

Experimental approaches using glycosidase digestion in combination with electrophoretic analysis provide useful procedures to study simple carbohydrate structure in glycoproteins. SDS-PAGE can distinguish molecular mass reduction of glycoprotein after deglycosylation, while IEF electrophoresis can identify difference in a single net charge upon removal of sialic acid during neuraminidase digestion. The experimental results yield simple as well as interpretable data and provide further insight on the understanding of carbohydrate structure for small molecular mass glycoproteins. Elucidation of detailed carbohydrate structure is usually not attainable without applying sophisticated techniques such as NMR spectroscopy. However, the NMR analysis requires utilization of the highly expensive equipment and time-consuming preparation of purified oligosaccharides in large quantities. The procedure described here offers an inexpensive and reliable alternative to laboratories which do not have access to the costly equipment. However, this approach may not be applicable to glycoproteins with complex N- and O-linked carbohydrate structures.

The presence of carbohydrate on human G-CSF appears to have little effect on G-CSFs ability to promote the proliferation and differentiation of the granulocyte progenitor lineages *in vitro* or *in vivo* [3,4,7]. One explanation may be that the threonine-linked sugar structure in recombinant human G-CSF is very small and may

not affect the rate of clearance of the molecule *in vivo* so as to alter the biological activity. Moreover, no detectable difference in their stability was observed between glycosylated G-CSF and non-glycosylated G-CSF (our unpublished data).

REFERENCES

1 D. Metcalf, *The Hemopoietic Colony Stimulating Factors*, Elsevier, Amsterdam, 1984.
2 G. Morstyn and A.W. Burgess, *Cancer Res.*, 48 (1988) 5624–5637.
3 K.M. Zsebo, A.M. Cohen, D.C. Murdock, T.C. Boone, H. Inoue, V.R. Chazin, D. Hines and L.M. Souza, *Immunobiol.*, 172 (1986) 175–184.
4 A.M. Cohen, K.M. Zsebo, H. Inoue, D. Hines, T.C. Boone, V.R. Chazin, L. Tsa, T. Ritch and L.M. Souza, *Proc. Natl. Acad. Sci. USA*, 84 (1987) 2484–2488.
5 M. Tamura, K. Hattori, H. Nomura, M. Oheda, N. Kubota, I. Imazeki, M. Ono, Y. Ueyama, S. Nagata, N. Shirafuji and S. Anano, *Biochem. Biophys. Res. Commun.*, 142 (1987) 454–460.
6 K. Welte, M.A. Bonilla, A.P. Gillio, T.C. Boone, G.K. Potter, J.L. Gabrilove, M.A.S. Moore, R.J. O'Reilly and L.M. Souza, *J. Exp. Med.*, 165 (1987) 941–948.
7 L.M. Souza, T.C. Boone, J. Gabrilove, P.H. Lai, K.M. Zsebo, D.C. Murdock, V.R. Chazin, J. Bruszewski, H. Lu, K.K. Chen, J. Barendt, E. Platzer, M.A.S. Moore, R. Mertelsmann and K. Welte, *Science*, 232 (1986) 61–65.
8 S. Nagata, M. Tsuchiya, S. Anano, Y. Kaziro, T. Yamazaki, O. Yamamoto, Y. Hirata, N. Kubota, M. Oheda, H. Normura and M. Oho, *Nature*, 319 (1986) 415–418.
9 M.H. Bronchud, J.H. Scarffe, N. Thatcher, D. Crowther, L.M. Souza, N.K. Alton, N.G. Testa and T.M. Dexter, *Brit. J. Cancer*, 56 (1987) 809–813.
10 G. Morstyn, L.M. Souza, J. Keech, W. Sheridan, L. Campbell, N.K. Alton, M. Green, D. Metcalf and R. Fox, *Lancet*, i (1988) 667–672.
11 J.L. Gabrilove, A. Jakubowski, H. Scher, C. Sternberg, G. Wong, J. Grous, A. Yagoda, K. Fain, M.A.S. Moore, B. Clarkson, H. Oettgen, N.K. Alton, K. Welte and L.M. Souza, *New Engl. J. Med.*, 318 (1988) 1414–1422.
12 M.A. Bonilla, A.P. Gillio, M. Ruggeiro, N.A. Kernan, J.A. Brochstein, M. Abboud, L. Fumagalli, M. Vincent, J.L. Gabrilove, K. Welte, L.M. Souza and R.J. O'Reilly, *N. Engl. J. Med.*, 320 (1989) 1574–1580.
13 W.P. Sheridan, G. Morstyn, M. Wolf, A. Dodds, J. Lusk, D. Maher, J.E. Layton, M.D. Green, L. Souza and R.M. Fox, *Lancet*, ii (1989) 891–895.
14 J. Utsumi, Y. Mizuno, K. Hosoi, K. Okano, R. Sawada, M. Kajitani, I. Sakai, M. Naruto and H. Shimizu, *Eur. J. Biochem.*, 181 (1989) 545–553.
15 R.J. Harris, S.M. Chmow, T.J. Gregory and M.W. Spellman, *Eur. J. Biochem.*, 188 (1990) 291–300.
16 Y.C. Lee, *Anal. Biochem.*, 189 (1990) 151–162.
17 K.G. Rice, N. Takahashi, Y. Namiki, A.D. Tran, P.J. Lisi and Y.C. Lee, *Anal. Biochem.*, 206 (1992) 278–287.
18 R.J. Harris, V.T. Ling and M.W. Spellman, *J. Biol. Chem.*, 267 (1992) 5102–5107.
19 E.G. Berger, E. Buddecke, J.P. Kamerling, A. Kobata, J. Paulson and J.F.G. Vliegenthart, *Experientia*, 38 (1982) 1129–1159.
20 M. Oheda, S. Hase, M. Ono and T. Ikenaka, *J. Biochem. (Tokyo)*, 103 (1988) 544–546.
21 M.R. Hardy, R.R. Townsend and Y.C. Lee, *Anal. Biochem.*, 170 (1988) 54–62.
22 G. Jourdian, L. Dean and S. Roseman, *J. Biol. Chem.*, 246 (1971) 430.
23 D.C. Johnson and T.Z. Polta, *Chromatogr. Forum.*, 1 (1986) 37–44.
24 H.S. Lu, T.C. Boone, L.M. Souza and P.H. Lai, *Arch. Biochem. Biophys.*, 268 (1989) 81–92.
25 *User's Bulletin No. 14*, Applied Biosystems, Foster City, CA, 1985.
26 U.K. Laemmli, *Nature*, 227 (1970) 680–685.
27 V.P. Bhavanandan and E.A. Davidson, *Biochem. Biophys. Res. Commun.*, 70 (1976) 139–145.
28 S. Takasaki and A. Kobata, *J. Biol. Chem.*, 251 (1976) 3603–3609.
29 H.S. Lu, C.L. Clogston, L.O. Narhi, L.A. Merewether, W.R. Pearl and T.C. Boone, *J. Biol. Chem.*, 267 (1992) 8770–8777.
30 H. Nomura, I. Imazeki, M. Omeda, N. Kubota, M. Tamura, M. Ono, Y. Ueyama and S. Asano, *EMBO J.*, 5 (1986) 871–876.

Journal of Chromatography, 637 (1993) 63–70
Elsevier Science Publishers B.V., Amsterdam

CHROM. 24 914

Determination of monovalent and divalent cations and chloride in the carbacephalosporin loracarbef by ion chromatography

James W. Klancke

Lilly Research Laboratories, Eli Lilly and Co., Mail Drop TL12, P.O. Box 685, Lafayette, IN 47902 (USA)

(First received August 7th, 1992; revised manuscript received January 21st, 1993)

ABSTRACT

Sensitive determination of monovalent and divalent cations and chloride in the carbacephalosporin antibiotic loracarbef can be achieved by separation on a high-capacity cation-exchange column followed by chemically suppressed conductivity detection. The methods developed in our laboratory for these determinations are characterized by the absence of matrix interference, rapid separation, ease of sample preparation and good sensitivity. Of these benefits, it is the minimization of matrix interference supplied by micromembrane chemical suppression that has made this technique so powerful for this application. Advantage is taken of the acid–base chemistry of loracarbef, resulting in a drastic reduction in its concentration in the eluent prior to detection of the analytes of interest. Linearities in the presence of the matrix (coefficient of determination > 0.995) and recoveries from the matrix are excellent ($100 \pm 2\%$). However, when the suppression components exhibit decreased efficiency, systems employing eluents composed of both hydrochloric and diaminopropionic acids are susceptible to problems such as poor peak shape, high background conductivity, and noise thus making accurate determinations difficult. Both the suppression system and the eluent are assessed in relation to the sources of high background conductivity and noise.

INTRODUCTION

The determination of sodium, ammonium, potassium, calcium and chloride is of great importance to the pharmaceutical industry. These ions may be introduced with raw materials or as salts of acids or bases, and at times serve as a counterion to the bulk drug. In our laboratories, determination of these cations is required for both environmental monitoring and the research and development of new drugs. The methods used for these assays must be reproducible on a day-to-day basis with respect to accuracy and sensitivity.

In general, ion chromatography has found widespread application in many areas, especially environmental and water analysis [1–7]. Applications of ion chromatography with photometric [8,9] and direct conductivity [10,11] detection to pharmaceutical analysis are numerous, but those utilizing suppressed conductivity detection have received somewhat limited focus. Herbranson *et al.* [12] determined sulfite and sulfate in injectable formulations by this technique. Brown *et al.* [13] utilized a fiber eluent suppressor to alleviate potential interferences from amino acid type matrices. A column-switching technique has also been used to remove matrix interference in pharmaceutical samples containing high levels of sodium and potassium [14]. Potentiometric, titrimetric, and spectroscopic methods have found wide usage for quantitating sodium, potassium, calcium and chloride, but ammonium can be a particularly troublesome analyte because other modes of detection such as colorimetry and voltammetry [15] require derivatization. Here, chemically suppressed ion chromatography has been shown to be an excellent analytical tech-

0021-9673/93/$06.00

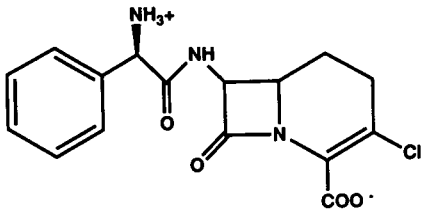

Fig. 1. Loracarbef.

nique for the determination of these common ions in loracarbef, a new carbacephalosporin antibiotic (Fig. 1). The acid–base chemistry of loracarbef, $pK_1 = 2.3$ and $pK_2 = 7$, plays an important role in its analysis.

EXPERIMENTAL

Purified water obtained from a Milli-Q (Millipore, Bedford, MA, USA) water system was used to prepare all solutions. The chromatographic system employed included a Dionex Series 4500i gradient pump and a pulsed electrochemical detector operating in the conductivity mode (Dionex, Sunnyvale, CA, USA). Sample injection was achieved with a Micromeritics 728 autosampler (Norcross, GA, USA) and a 25-μl sample loop. Plastic autosampler vials were used to minimize background signals. All data were collected on a Hewlett-Packard 1000 computer system with custom chromatography software capable of peak integration.

For monovalent cation chromatography, a Dionex IonPac CS2 analytical column (250 mm × 4 mm) was used. For the determination of calcium, the analytical column was an IonPac CS10 (250 mm × 4 mm). Eluents were prepared from ultrapure HCl (99.999%, Aldrich) and 2,3-diaminopropionic acid hydrochloride (DAP) (Dionex). The regenerant was 100 m*M* tetrabutylammonium hydroxide (TBAOH) which was prepared by diluting 65 ml of 40% stock solution (Aldrich, Milwaukee, WI, USA) in 1 l water. Chemical suppression of the eluent was achieved by continuously recycling 100 m*M* TBAOH at a flow of 3–5 ml/min through a CMMS-II micromembrane suppressor and an AutoRegen cartridge (Dionex). This system will be called the "suppression equipment" throughout the paper when referring to cation chromatography. Cation standard solutions were prepared from anhydrous, reagent-grade, chloride salts. All chromatography was performed isocratically at room temperature with an eluent flow-rate of 2.0 ml/min for the monovalent cations and 1.0 ml/min for calcium.

For chloride determinations, a Dionex IonPac AS4 column (250 mm × 4 mm) was used. The eluent was 1.5 m*M* $NaHCO_3$ and 1.2 m*M* Na_2CO_3, prepared from dry, reagent-grade salts (EM Science, Cherry Hill, NJ, USA). The regenerant was 12.5 m*M* sulfuric acid which was prepared by diluting 0.7 ml of the concentrated acid in 1 l water. Chemical suppression of the eluent was achieved with an AMMS-II micromembrane suppressor in the same manner as the cation system. Standard solutions were prepared from reagent-grade KCl. Chromatography was performed isocratically at room temperature with an eluent flow-rate of 1.5 ml/min.

RESULTS AND DISCUSSION

Determination of ions in loracarbef

Determination of Cl^-. Sample solutions were prepared by dissolving 0.6 mg/ml loracarbef in purified water. Under the given experimental conditions, chloride was eluted in 2.9 min (see Fig. 2). Decreasing the concentration of the hydrogencarbonate–carbonate eluent will increase the retention time of Cl^-, giving better selectivity by moving the peak further away from the

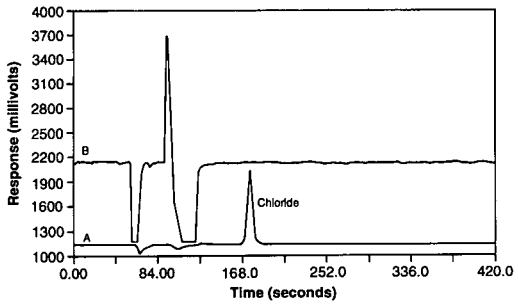

Fig. 2. (A) Chromatogram obtained for Cl^- asay. The absence of the large baseline dip seen when a micromembrane suppressor follows the AS4 analytical column is also shown. Chloride peak represents 4.5 μg chloride/ml. (B) Non-suppressed chromatogram has been baseline offset by −300 μS. Eluent: 1.5 m*M* $NaHCO_3$, 1.2 m*M* Na_2CO_3. 1 mV ≡ 0.01 μS.

void volume and any fluoride ion that may be present. Data relating the retention of Cl^- and other anions on an AS4 column to hydrogencarbonate–carbonate eluent concentrations appear elsewhere [16]. The only other feature in the chromatogram obtained with chemical suppression due to the sample is a second, small baseline dip at 100 s following the water dip. Without chemical suppression, two large dips are seen, the second presumably from loracarbef. Although the size of the second baseline dip is directly proportional to the amount of loracarbef injected (coefficient of determination, COD = 0.987 for injections of 8 to 40 μg), the result of assaying this analytical column effluent fraction by our laboratory's standard HPLC–UV method shows that the dip is not caused by loracarbef directly. Only trace and relatively constant amounts of loracarbef were recovered in the region of the second dip.

Although loracarbef present in the sample solution passes through the analytical column unretained, the suppressor serves to remove a large fraction of it before reaching the detector. Analytical column effluent was collected for three minutes subsequent to sample injection and assayed by HPLC–UV. Quantitative recovery of loracarbef was observed, demonstrating no retention of the matrix on the AS4 column. Assaying suppressor effluent fractions collected over that same time span that first passed through the analytical column yields only a very small concentration of loracarbef and this concentration is also found at later times during the chromatogram. Assaying the regenerant solution shows low levels of loracarbef to be present. Loracarbef enters the suppressor as an anion and subsequently gets protonated to a zwitterion. As a zwitterion, it can be retained in the anion suppressor as the suppressor is essentially a cation exchanger in the H^+ form, similar to a CS2 column on which retention has been demonstrated (see next section). Since loracarbef can both be retained in the micromembrane suppressor and can diffuse across the membrane into the regenerant stream, an interference-free chromatogram is obtained. The displacement of H^+ by loracarbef is likely the cause of the second baseline dip. The association of this displaced H^+ with free HCO_3^- would result in a temporary decrease in the background conductivity and hence a baseline dip.

Linearity in the presence of loracarbef (COD = 0.9999) and recovery (see Table I) of Cl^- from the matrix are excellent from 1 to 20 μg/ml. The within-run R.S.D. (multiple sample preparations, $n = 12$) for Cl^- determined at 4.2 μg/ml in loracarbef is 1.3%. For low-level determinations, it is crucial that sample solutions do not come into contact with low-quality glass such as that found in autosampler vials due to leaching of variable amounts of chloride into solution. The variable background due to this caused the R.S.D. to be 7.9% within the run, or approximately six times worse than when plastic vials were used.

Determination of Na^+, K^+, and NH_4^+. Sample solutions were prepared by dissolving 3 mg/ml loracarbef in purified water for sodium and potassium determination and 8 mg/ml for ammonium determination. These sample loadings do not reflect a significant difference in analyte sensitivity, but are a result of the need to assay appreciably lower levels of ammonium ion. A chromatogram obtained under the given experimental conditions is shown in Fig. 3. An eluent concentration of 7.5 m*M* HCl was found to provide good balance between resolution, analysis time, background conductivity and long-term suppression equipment efficiency. The high resolution of these analytes on the CS2 allows for widely varying amounts of these analytes to be present and still allow for quantitation.

Studies employing ultraviolet detection show that loracarbef, a singly charged cation at the eluent pH, is retained on the analytical column approximately 300 s longer than the most strongly retained analyte, K^+. Analytical column effluent and suppressor effluent (representative of what is measured by the conductivity cell) fractions were collected in 100-s increments beginning 800 s after injection. These fractions were then assayed for loracarbef by HPLC–uv and the results plotted versus time. The results in Fig. 4 indicate that less than 5% of the injected loracarbef eventually makes it to the conductivity detector. Furthermore, the retention time of loracarbef is the same with and without the suppressor

TABLE I

RECOVERY OF IONS IN LORACARBEF

Amount in sample (μg)	Amount added (μg)	Total (μg)	Found (μg)	Recovery (%)
Chloride				
106	25.0	131	125	95
104	125.2	229	231	101
104	250.4	354	353	100
106	375.5	481	483	100
103	500.7	604	614	102
			Average:	100
Sodium				
3.9	128.8	132.7	138	104
3.9	257.5	261.4	258	99
3.9	386.3	390.2	404	104
3.9	515.5	519.4	527	101
			Average:	102
Ammonium				
4.0	10.1	14.1	14.0	99
4.1	50.5	54.6	50.7	93
4.0	100.9	104.9	119	113
4.1	151.4	155.5	156	100
4.1	201.9	206.0	204	99
4.0	252.3	256.3	258	101
			Average:	101
Calcium				
16.9	9.6	26.5	28.2	106
16.9	38.4	55.3	50.9	92
17.0	57.5	74.5	70.7	95
16.7	76.7	93.4	92.4	99
16.9	95.9	112.8	109.3	97
			Average:	98

in-line, showing that it is not retained in the suppressor. Its elution causes a slight, broad baseline depression beginning at approximately

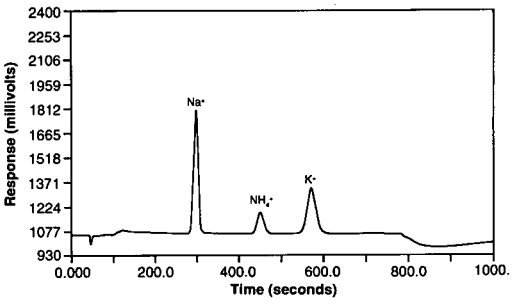

Fig. 3. Separation of monovalent cations. Injected solution: 25 μl of 10 μg Na^+, 7 μg NH_4^+, 9 μg K^+/ml, and 8 mg/ml loracarbef prepared in eluent. Eluent: 7.5 m*M* HCl. 1 mV≡ 0.01 μS.

800 s, returning to baseline at about 1000 s. Any loracarbef that passes through the membrane into the closed-loop TBAOH regenerant stream is quickly decomposed ($t_{1/2} = 8$ min) due to the high alkalinity and cannot affect subsequent injections. Loracarbef enters the suppressor as a singly charged cation and is subsequently deprotonated to its zwitterionic form which, as such, can diffuse across the membrane. Its eventual elution produces minimal response at the conductivity detector due to its drastically reduced concentration and low conductance of the zwitterionic form. The result is an interference-free chromatogram. The CS2 column has retention only for species that are cations at the pH of the eluent, which is about 2. Neutral and negatively charged species that could possibly

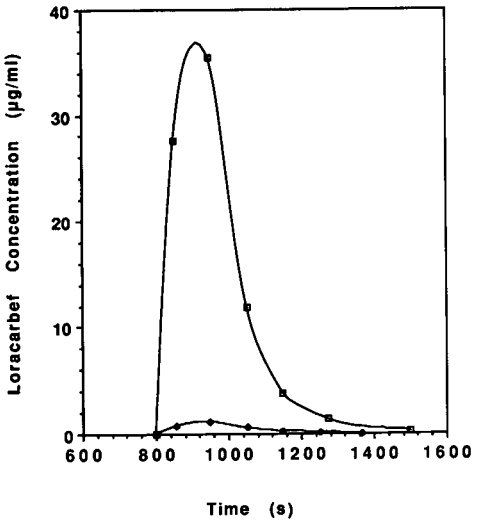

Fig. 4. Concentration of loracarbef in effluent fractions without (□) and with (◆) the micromembrane suppressor following the analytical column. Conditions same as for monovalent cations (see Experimental). Fractions were assayed by HPLC with UV detection.

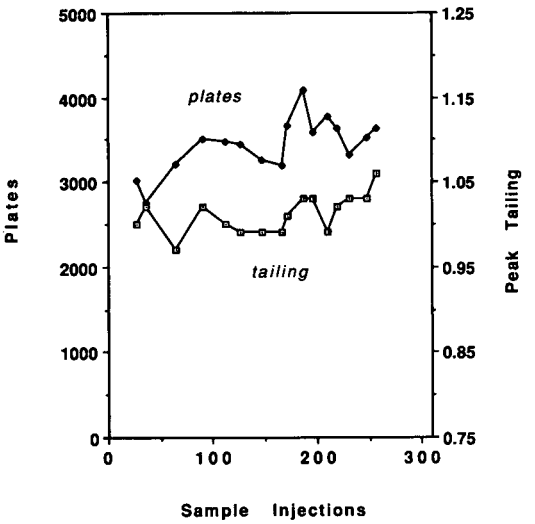

Fig. 5. Column performance over time: plates (◆) and tailing (□) data for ammonium ion on a Dionex CS2 cation-exchange column when assayed for in Loracarbef. Injected: 5 µg NH_4^+/ml.

interfere with these monovalent cations elute in the void volume.

Suitability of the chromatographic system is based upon two criteria: background conductivity and ammonium peak tailing. The system is deemed suitable when both the background conductivity of the system is less than 20 µS and the tailing of the ammonium peak obtained from a 5 µg/ml solution, determined at 10% of the peak height, is between 0.85 and 1.2. Tailing was chosen as a suitability criterion because it is sensitive to the condition of the analytical column and becomes a problem before insufficient resolution of possible interfering analytes does. Additionally, tailing can be indicative of the condition of the micromembrane suppressor (see section *Problems encountered with divalent cation system*). The data shown in Fig. 5 demonstrates the durability of a CS2 cation column used intermittently (for loracarbef exclusively) over the course of a year. Causes and remedies of high background conductivity are addressed in a subsequent section of this article.

Linearity in the matrix (COD = 0.9977) of sample solutions containing from 1.0 to 25 µg/ml NH_4^+ is obtained with excellent recovery (see Table I). The recovery studies for ammonium and sodium ion were performed on loracarbef samples that had low levels of these analytes. The within-run R.S.D. (multiple sample preparations, $n = 12$) for NH_4^+ at 5.6 µg/ml is 5.1%. The detection limit, defined as the ammonium ion level producing a peak amplitude 3× of the noise level, is approximately 0.4 µg/ml (50 ng/mg in the matrix); the limiting factor being the solubility of loracarbef in the mobile phase. (This detection limit is well below the level that our laboratory needs to determine.) Linearity in the matrix (COD = 0.9992) and recovery of Na^+ (at 3 mg/ml loracarbef) and K^+ are also excellent in this working range.

Determination of Ca^{2+}. Sample solutions were prepared by dissolving 4 mg/ml loracarbef in purified water. For the determination of calcium, an added "pusher", DAP, is added to the eluent to elute this species from the CS10 analytical column. Fig. 6B is the chromatogram obtained when determining Ca^{2+} in loracarbef. As with the monovalent cations, linearity in the matrix (COD = 0.9956) and recovery are excellent (see Table I). Rocklin *et al.* [4] have published a general discussion of DAP/HCl eluents and have shown the relation of retention of cations to

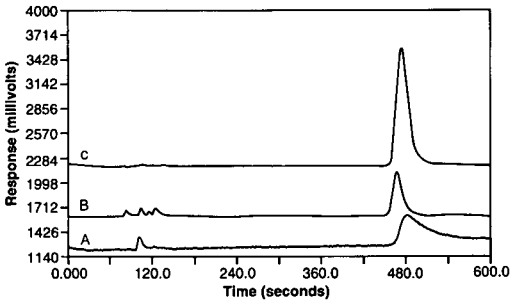

Fig. 6. (A) Chromatographic behavior of Ca^{2+} on a new CS10 separator column and poorly operating suppression equipment and (C) on a new CS10 separator column and new suppression equipment. Injected solution: 25 μl of 23 μg Ca^{2+}/ml, prepared in eluent. (B) Chromatogram with Ca^{2+} present at 9.2 μg/ml and loracarbef present at 4.3 mg/ml. Eluent: 12 m*M* DAP · HCl, 40 m*M* HCl. 1 mV ≡ 0.01 μS.

DAP/HCl eluent concentrations under conditions similar to those described here. Campbell *et al.* [5] give the details of the CS10 column.

Problems encountered with divalent cation system

After relatively short periods of use, the chemically suppressed system for determining divalent cations is susceptible to problems such as poor peak shape and high background conductivity. These problems, as well as system noise, are examined here by assessing the contributions of the analytical column, eluent and suppression system, with focus on the latter.

Poor peak shape. In any chromatographic system, poor peak shape can be attributed to improper chromatographic conditions relating to either the mobile phase or the separator column. When chemical suppression is used, peak shape is also dependent on the condition of the suppressor. Fig. 6A shows the chromatogram obtained by injecting a solution containing 23 μg Ca^{2+}/ml on a system made up of a new IonPac CS10 column and a micromembrane suppressor and AutoRegen cartridge that had been in general service for pharmaceutical assays (loracarbef and other compounds) for approximately 100 h over the course of several months. This amount of use corresponds to slightly less than one-third of the expected lifetime of the AutoRegen cartridge. The peak tails badly, perhaps due to adsorption of Ca^{2+} in the suppressor, and the sensitivity is poor. The poor peak shape can be attributed to poorly functioning suppression equipment rather than the separator column. As shown in Fig. 3, this same "poorly functioning" equipment performed satisfactorily under the monovalent assay conditions. The system employing the DAP/HCl eluent for the determination of a divalent cation such as Ca^{2+} is much more sensitive to the condition of the suppression equipment. This is due to the greater demands put on the suppressor by both the higher [HCl] and the nature of the Ca^{2+} ion. Replacement of all suppression components with new components resulted in satisfactory peak shape for Ca^{2+} (tailing factor = 1.2) and restoration of sensitivity (as shown in Fig. 6C). A sufficient, steady regenerant flow is necessary for efficient chemical suppression. Drug matrices irreversibly bound to the suppressor and iron-containing environmental samples which will precipitate as iron hydroxides in the suppressor may lead to both increased backpressures and analyte adsorption.

High background conductivity. The inability to efficiently suppress the background conductivity

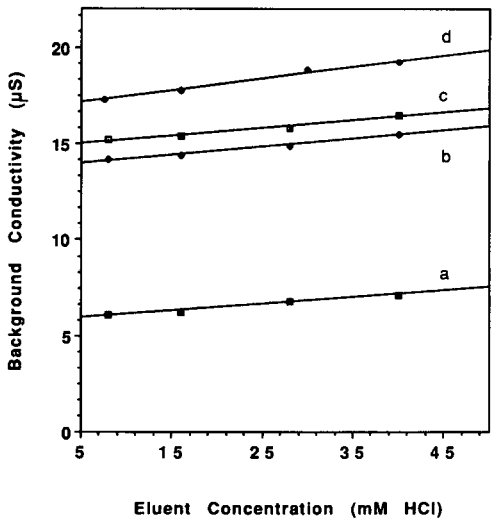

Fig. 7. Dependencies of the background conductivity on the concentration of HCl in the eluent measured on suppression equipment in various stages of use: (a) new, (b) used suppressor after cleaning with 1 *M* HCl, (c) used suppressor before cleaning with 1 *M* HCl, (d) poorly operating suppressor (used in Fig. 6).

leads to decreased sensitivity, non-linearity, and standard calibration curves with negative intercepts [17]. The contributions of HCl, DAP and the suppression equipment as primary sources of high background conductivity were examined.

Plots of [HCl] *versus* background conductivity on suppression equipment that was in various stages of use are shown in Fig. 7. When using poorly functioning suppression equipment, increasing the [HCl] in the eluent caused an increase in the already high background conductivity; the slope of the line corresponding to a 60 nS/m*M* HCl increase (Fig. 7d). On a new micromembrane suppressor and AutoRegen cartridge, the background conductivity decreased significantly, indicating a much higher efficiency (Fig. 7a) and the slope of the line was 35 nS/m*M* HCl, indicating greater capacity. Fig. 7c shows that after receiving fairly light use, the background conductivity displayed a marked increase over when the suppression equipment was new. Despite the increase, Ca^{2+} peak shape was comparable to that obtained when new equipment was part of the system. Cleaning the suppressor per the manufacturer's instructions with 1 *M* HCl did lower the background conductivity slightly, but not to levels seen on new equipment. The capacities to suppress the increase in [HCl] are comparable to new suppressors as the slopes of the lines, Fig. 7b and c, for used and used/cleaned suppressors are 40 and 42 nS/m*M* HCl, respectively.

At constant added [HCl] on poorly functioning suppression equipment, the background conductivity was examined as a function of the [DAP · HCl] in the eluent. At all eluent concentrations studied here, the primary form of DAP is H_3DAP^{2+} ($K_a = 0.047$ [18]). With a [DAP] of 0, 1, 3 and 6 m*M*, the background conductivity was 19.2, 19.5, 18.8 and 18.1 μS, respectively. This constant, even slightly decreasing background conductivity parallels the decrease in the calculated equilibrium $[H^+]$ which is 40, 39, 37 and 31 m*M*, respectively. The same trend was also observed qualitatively on suppression equipment in various conditions, indicating that DAP is converted to an anion and removed from the eluent independent of suppressor condition, and is not contributing to the background conductivity. Since DAP did not contribute to the background conductivity on "poorly operating" suppression equipment, its contribution on a new system was believed to be minimal and therefore not studied.

Noise. Average baseline noise was measured by calculating the average peak-to-peak amplitude of the noise spikes in the region of the chromatogram between 200 and 300 s after injection. For [HCl] between 10 and 40 m*M* (DAP absent) on all suppressor conditions studied here ($n = 16$), the average baseline noise remained under 0.03 μS, still allowing for detection limits stated previously. In general, marked increases in the magnitude of the noise are not related to the condition of the suppression equipment at any eluent concentration of HCl.

CONCLUSIONS

Due to the lack of matrix intereference, ion chromatography with chemical suppression is an excellent technique for determining common ions in a bulk drug such as loracarbef. Advantage is taken of the acid–base chemistry of loracarbef, resulting in a drastic reduction in its concentration in the eluent prior to detection of the analytes of interest. Linearities in the presence of the matrix (COD > 0.995) and recoveries from the matrix are excellent.

Premature exhaustion of suppression efficiency for the divalent cation system can lead to deteriorated peak shapes and high background conductivity. This work provides the analyst with a rationale for system adjustments when the problems studied here are present but not severe.

ACKNOWLEDGEMENTS

I thank Larry Larew, Michael Fogarty and Bernard Olsen for reading the manuscript and providing many useful comments and suggestions.

REFERENCES

1 R.E. Smith, *Ion Chromatography Applications*, CRC Press, Boca Raton, FL, 1988.

2 P.R. Haddad and P.E. Jackson, *Ion Chromatography: Principles and Applications*, Elsevier, Amsterdam, 1990.
3 K. Bachmann, H. Blaskowitz, S. Bukatsch, S. Pohl and U. Sprenger, *J. Chromatogr.*, 382 (1989) 307.
4 R.D. Rocklin, M.A. Rey, J.R. Stillian and D.L. Campbell, *J. Chromatogr. Sci.*, 27 (1989) 474.
5 D.L Campbell, J. Stillian, S. Carson, R. Joyce and S. Heberling, *J. Chromatogr.*, 546 (1991) 229.
6 E.J. Nanni, M.E. Lovette, R.D. Hicks, K.W. Fowler and M.F. Borgerding, *J. Chromatogr. Sci.*, 28 (1990) 432.
7 J.G. Tarter, *Ion Chromatography*, Marcel Dekker, New York, 1987.
8 D.R. Jenke, *J. Chromatogr.*, 437 (1988) 231.
9 D. Jenke and B.P. Downey, *J. Chromatogr. Sci.*, 25 (1987) 519.
10 M. Murayama, M. Suzuki and S. Takitani, *J. Chromatogr.*, 463 (1989) 147.
11 S. Suzuki, H. Tsuchihashi, K. Nakajima, A. Matsushita and T. Nagao, *J. Chromatogr.*, 437 (1988) 322.
12 D.E. Herbranson, M.S. Eliason and N.N. Karnatz, *J. Liq. Chromatogr.*, 10 (1987) 3441.
13 D. Brown, R. Payton and D. Jenke, *Anal. Chem.*, 57 (1985) 2264.
14 D. Jenke, *Anal. Chem.*, 59 (1987) 624.
15 R.M. Ianniello, *J. Assoc. Off. Anal. Chem.*, 71 (1988) 29.
16 J. Weiss, *Handbook of Ion Chromatography*, Dionex Corp., Sunnyvale, CA, 1986.
17 Z.W. Tian, R.Z. Hu, H.S. Lin and W.L. Hu, *J. Chromatogr.*, 439 (1988) 151.
18 A. Martell and R. Smith, *Critical Stability Constants*, Vol. 5, First Supplement, Plenum Press, New York, 1982.

Journal of Chromatography, 637 (1993) 71–80
Elsevier Science Publishers B.V., Amsterdam

CHROM. 24 933

Application of headspace analysis, solvent extraction, thermal desorption and gas chromatography–mass spectrometry to the analysis of chemical warfare samples containing sulphur mustard and related compounds

Robin M. Black*, Raymond J. Clarke, David B. Cooper, Robert W. Read and David Utley

Chemical and Biological Defence Establishment, Porton Down, Salisbury, Wiltshire SP4 0JQ (UK)

(First received November 27th, 1992; revised manuscript received February 2nd, 1993)

ABSTRACT

Samples of soil, munition fragments and wool, associated with a chemical warfare incident involving sulphur mustard, were analysed using headspace, solvent extraction and thermal desorption techniques combined with full scanning gas chromatography–mass spectrometry. Quantitative analysis was undertaken for sulphur mustard, mustard sulphoxide and thiodiglycol, using solvent extraction and gas chromatography–mass spectrometry with selected ion monitoring. In a soil sample contaminated at ppm (w/w) levels all methods gave positive results for mustard and related compounds. Selected ion monitoring and thermal desorption were the more useful techniques at low ppb (w/w) levels. Cyclic decomposition products 1,4-thioxane and 1,4-dithiane appear to be useful indicators of mustard contamination when using thermal desorption analysis. The hydrolysis product thiodiglycol and hydrolysis/elimination product 2-(vinylthio)ethanol appear to be useful indicators of mustard contamination in soil samples when employing extraction methods.

INTRODUCTION

Allegations concerning the use of chemical weapons have increased over the past decade, particularly during the period of the Iraq–Iran war [1]. In August 1988 chemical weapons were reported to have been used against the Kurdish population in the mountainous region of northern Iraq close to the borders of Turkey and Iran. In November of that year an investigative journalist [2] entered the area and collected samples from the hillside site of an impacted bomb. The ruptured, thin-walled metal bomb was embedded in the ground. Samples of soil, bomb casing, and what appeared to be sheep's wool, were collected from the site and brought back to the UK for analysis. Headspace analysis of two of these samples, undertaken in a commercial laboratory, identified three decomposition products of sulphur mustard as 1,4-dithiane, 1,4-thioxane and divinyl sulphide (1,1-thiobis-ethene) [2]. A more extensive analysis for volatile and extractable material was subsequently undertaken at the Chemical and Biological Defence Establishment (CBDE). Headspace sampling, solvent extraction and thermal desorption were applied to the samples, each coupled with analysis by full scanning gas chromatography–mass spectrometry (GC–MS). In addition, samples were

* Corresponding author.

0021-9673/93/$06.00

analysed quantitatively for sulphur mustard and its more stable oxidation and hydrolysis products, mustard sulphoxide and thiodiglycol, using solvent extraction combined with GC–MS-selected ion monitoring. A summary of the results of these analyses has appeared in the literature [2] but with few details of the methods employed. In this paper we report the results of our analyses in full and discuss the relative advantages of the analytical methods employed.

EXPERIMENTAL

Samples

The samples were received in a cold box at CBDE on 9 December 1988 and were stored at −20°C for 5 days prior to analysis. They consisted of the following.

(a) A brown plastic jar, labelled sample 1, containing *ca.* 410 g of soil which had been excavated from beneath the munition.

(b) A similar plastic jar, labelled sample 2, containing some coarse white wool-like material, possibly sheep's wool, plus a few residual soil-like particles at the bottom of the jar.

(c) Two similar samples wrapped in metal foil, each containing a thin, shiny metal fragment *ca.* 5 × 8 cm, together with soil which had been in contact with the fragments; these two samples were numbered 4A and 4B, repectively, at CBDE. Sample 4A contained 34 g of soil, sample 4B contained 17 g of soil.

Headspace analysis (samples 1 and 2)

The headspace in the two plastic containers was sampled immediately on opening by drawing ambient air over the sample at 0.5 l/min for 10 min with the aid of a Cassella pump. Volatiles were adsorbed onto Tenax-GC (50 mg) contained in an ATD50 tube. The trapped volatiles were thermally desorbed and analysed by full scanning GC–MS using a Perkin-Elmer ATD50 thermal desorption system coupled to a Hewlett-Packard 5890 GC/5970B GC–MSD instrument. The thermal desorption system was operated in the two-stage desorption mode with oven temperature 250°C, desorb time 10 min, transfer line 150°C, cold trap low −30°C, cold trap high 300°C, and split flow 13 ml/min. The gas chromatograph was fitted with a Hewlett-Packard Ultra-2 (phenylmethyl silicone) column 25 m × 0.2 mm I.D., film thickness 0.33 μm. Helium at 103 kPa was used as carrier gas. The oven temperature was held at 35°C for 5 min, programmed from 35 to 300°C at 10°C/min, and held at 300°C for 7 min; the GC–MS transfer line was held at 250°C. The mass spectrometer was operated using electron impact ionisation and scanned over the mass range 40–300 u at 1.65 scans/s from 0–10 min, 40–400 u at 1.19 scans/s from 10–20 min, and 40–500 u at 0.93 scans/s from 20–38.5 min.

Extraction with full scanning GC–MS analysis

Aliquots (1–10 g) of soil samples 1, 4A, and 4B were extracted by tumbling in screw-cap vials with dichloromethane (2–10 ml) and dry sodium sulphate (1 g) for 30 min. After filtering, the extracts were concentrated under a stream of nitrogen. Wool sample 2 (0.22 g) was also extracted by tumbling with dichloromethane. GC–MS analysis was performed using a VG 7070EQ instrument coupled to an 11/250 data system. The gas chromatograph was fitted with a DB-5 (J & W) 15 m × 0.25 mm I.D. column, film thickness 0.25 μm; helium at 103 kPa was used as carrier gas. The oven was held at 50°C for 1 min, and then programmed from 50 to 270°C at 15°C/min. On-column injection (0.5 μl) was used. The mass spectrometer was scanned from 45 to 600 u at 1 scan/s with 0.2 s interscan time. Electron impact ionisation at 70 eV or methane chemical ionisation at 150 eV was used. A duplicate analysis was performed using a Hewlett-Packard GC–MSD system employing on column injection and GC–MS conditions as described above.

Thermal desorption analysis

Aliquots of soil from samples 1, 2 (residual soil particles), 4A and 4B, wool sample 2, and metal fragment 4B were heated at 50°C for 30 min, 100°C for 30 min or 250°C for 10 min in ADT50 tubes under a gas flow of 13 ml/min. Volatiles were trapped in a cold trap at −30°C containing Tenax (10 mg) and analysed using a coupled ADT50-GC–MSD system employing GC–MS conditions as described above.

Quantitative trace analysis for mustard and mustard sulphoxide

Aliquots of soil from samples 1, 4A and 4B (*ca.* 0.75 g), and wool sample 2 (0.15 g) were extracted by tumbling for 10 min with dichloromethane (2 ml) and sodium sulphate (0.3 g) in a 3-ml vial. The extract was transferred to a 1-ml vial and concentrated to small volume under a stream of nitrogen at 40°C. The extraction was repeated and the combined extracts concentrated to 100 μl. Remaining dichloromethane was removed by adding ethyl acetate (100 μl), concentrating to 100 μl and repeating the process. Metal fragment 4A was extracted twice with dichloromethane (20 ml then 10 ml) in a beaker. The combined extracts were concentrated on a rotary evaporator and treated as above.

GC–MS analysis was performed using a Finnigan 4600 GC–MS system operated in the selected ion mode. The gas chromatograph was fitted with a 25 m × 0.22 mm I.D. bonded phase column coated with OV1710, film thickness 0.25 μm, inserted directly into the ion source. Helium at 103 kPa was used as carrier gas. The oven was held at 60°C for 2 min, programmed from 60 to 220°C at 10°C/min and held at 220°C for 2 min. Splitless injection (2 μl) was used, 0.5 min delay, injector temp 250°C. The GC–MS interface was held at 240°C. Sulphur mustard was analysed using chemical ionisation with methane as reagent gas [3,4]; electron energy 150 eV, source pressure 80 Pa, source temperature 100°C. Ions monitored were *m/z* 123, 125, 159, and 161, total scan time 1 s. Mustard sulphoxide was analysed similarly but using ammonia as reagent gas, source pressure 80 Pa. Ions monitored were *m/z* 192 and 194. Quantitation was performed against external standards with no allowance for recovery.

Quantitative trace analysis for thiodiglycol

Aliquots of soil samples 1, 4A and 4B (*ca.* 1g), and wool sample 2 (0.1 g), were extracted twice by tumbling for 10 min with ethyl acetate (2 ml) and sodium sulphate (0.3 g) in a 3-ml screw-cap vial. The extracts were concentrated just to dryness under a stream of nitrogen prior to derivatisation. Because of the relatively high concentrations of thiodiglycol present in soil sample 1, the combined extracts were diluted to 5 ml with ethyl acetate and aliquots (100 μl) then concentrated to dryness for derivatisation. Metal fragment 4A was extracted in a beaker with ethyl acetate (20 ml then 10 ml) (the dichloromethane extract used for mustard analysis was also analysed for thiodiglycol).

Thiodiglycol was converted to its bis(*tert.*-butyldimethylsilyl) derivative for GC–MS analysis. The dried residues were treated with pyridine (Regis derivatisation grade, 80 μl) and N-methyl-N-(*tert.*-butyldimethylsilyl)trifluoroacetamide–1% *tert.*-butyldimethylchlorosilane (Regis, 20 μl), and heated at 100°C for 90 min.

GC–MS analysis was performed using a Finnigan 4600 GC–MS system operated in the selected ion mode. The gas chromatograph was fitted with a BP5 25 m × 0.2 mm I.D. column, film thickness 0.25 μm. Helium at 103 kPa was used as carrier gas. The oven was held at 90°C for 0.5 min, programmed from 90 to 280°C at 15°C/min, and held at 280°C for 2 min. Splitless injection (1 μl) was employed (plus toluene needle flush), 0.5 min delay, injector temp. 265°C. The GC–MS interface was held at 260°C. Chemical ionisation was employed with methane as reagent gas, electron energy 100 eV, source pressure 107 Pa, source temperature 120°C. Ions monitored were *m/z* 219, 293, and 335, total scan time 1 s. Quantitation was performed against external standards.

RESULTS

Sample 1

The compounds identified in the headspace, dichloromethane extracts and thermal desorbate from soil sample 1, using full scanning GC–MS, are shown in Table I. Identification in most cases was by comparison with standards [5], with library spectra, or with spectra reported by others [6,7]; tentative identifications based on mass spectral interpretation are indicated in Table I. Partial mass spectra are compiled in Table II.

Headspace GC–MS analysis. Sulphur mustard was readily detected in the headspace above the soil in the plastic jar, along with several related

TABLE I

COMPOUNDS IDENTIFIED OR TENTATIVELY IDENTIFIED IN SOIL SAMPLE 1

Compounds listed in order of retention time.

Compound	Headspace	Extract	Thermal desorbate		
			50°C	100°C	250°C
Ethylene sulphide[a]					+
Divinyl sulphide[b]	+				
2,4-Dimethylthietane[a]	+				
2-Methyl-1,3-thioxalane[a]	+			+	+
1,4-Thioxane[b]	+				+
2-Chloroethyl vinyl sulphide[b]	+		+	+	
2-(Vinylthio)ethanol[b]	+	+	+	+	
1,4-Dithiane[b]	+		+		+
2-(Vinylsulphinyl)ethanol[b]		+	+		
1,4,5-Oxadithiapane[a]			+		+
1,2-Bis(vinylthio)ethane[c]	+				
Sulphur mustard[b]	+	+	+		+
Thiodiglycol[b]		+			
1,2,5-Trithiapane[a]					+
Bis(2-chloroethyl) disulphide[b]	+	+	+		
(2-Chloroethylthio)ethyl vinyl sulphide[c,d]	+				
2-(2-Hydroxyethylthio)ethyl vinyl sulphide[c]			+		
Bis(2-chloroethyl) sulphoxide[b]		+			
Bis[2-(vinylthio)ethyl] ether[c,d]	+	+	+		
Tri-isobutyl phosphate[b]		+			
2-(2-Hydroxyethylthio)ethyl vinyl sulphoxide[c]		+			
1,2-Bis(2-chloroethylthio)ethane[b]		+			
Trinitrotoluene[b]		+			
Tetryl[b]		+			
Bis[2-(2-chloroethylthio)ethyl] sulphide[c,d]		+			

[a] Library search.
[b] Standard.
[c] Tentative.
[d] Ref. 7.

compounds (see Table I). A GC–MS total ion current chromatogram from the headspace of sample 1, and a full spectral scan showing the presence of sulphur mustard, are shown in Fig. 1. Major components in the headspace were the elimination/hydrolysis product 2-(vinylthio)ethanol (2-hydroxyethyl vinyl sulphide) and the elimination product 2-chloroethyl vinyl sulphide, eluting between 10 and 12 min.

Solvent extraction with GC–MS analysis. Sulphur mustard was similarly detected in dichloromethane extracts of soil sample 1, although under the chromatographic conditions employed it was only partially resolved from much larger concentrations of its hydrolysis product thiodiglycol. Thiodiglycol and 2-(vinylthio)ethanol were identified as major components of the extract along with many minor components derived from sulphur mustard. A total ion current chromatogram obtained using the VG 7070EQ instrument is shown in Fig. 2. A similar total ion current chromatogram was obtained using the GC–MSD system. Improved resolution of mustard-related compounds containing an unhydrolysed CH_2CH_2Cl group could be obtained by constructing the mass chromatograms of m/z 63 and 65, ions which are usually relatively intense in compounds containing this

TABLE II

PARTIAL MASS SPECTRA[a] OF COMPOUNDS IDENTIFIED

Compound	m/z (%)
Ethylene sulphide	61 (MH^+, 7), 60 (M^+, 100), 59 (88), 58 (26), 57 (13), 45 (89)
Divinyl sulphide	86 (M^+, 64), 85 (100), 59 (55), 45 (51), 58 (49), 57 (21)
2,4-Dimethylthietane	102 (M^+, 56), 60 (100), 45 (54), 41 (36), 59 (35), 73 (29)
2-Methyl-1,3-thioxalane	104 (M^+, 58), 89 (17), 61 (43), 60 (100), 59 (62), 45 (55)
1,4-Thioxane	104 (M^+, 53), 74 (18), 61 (45), 60 (13), 47 (13), 46 (100)
2-Chloroethyl vinyl sulphide	122 (M^+, 43), 73 (93), 60 (68), 59 (58), 58 (50), 45 (100)
2-(Vinylthio)ethanol	104 (M^+, 36), 73 (51), 60 (52), 59 (33), 58 (27), 45 (100)
1,4-Dithiane	120 (M^+, 100), 61 (61), 60 (32), 59 (23), 46 (71), 45 (47)
2-(Vinylsulphinyl)ethanol	120 (M^+, 26), 74 (55), 61 (25), 47 (25), 46 (100), 45 (41)
1,4,5-Oxadithiapane	136 (M^+, 100), 64 (46), 60 (78), 59 (50), 45 (73), 43 (48)
1,2-Bis(vinylthio)ethane	146 (M^+, 0.2), 118 (33), 87 (64), 85 (47), 59 (67), 58 (49), 45 (100)
Sulphur mustard	158 (M^+, 25), 111 (38), 109 (100), 63 (40), 59 (21), 45 (27)
Thiodiglycol	122 (M^+, 2), 104 (38), 91 (25), 61 (100), 60 (20), 47 (26), 45 (68)
1,2,5-Trithiapane	152 (M^+, 100), 124 (24), 87 (40), 60 (50), 59 (46), 45 (36)
Bis(2-chloroethyl) disulphide	192 (M^+, 51), 190 (M^+,67), 128 (30), 65 (35), 64 (32), 63 (100)
(2-Chloroethylthio)ethyl vinyl sulphide	182 (M^+, 28), 123 (100), 73 (41), 63 (40), 61 (40), 59 (48), 45 (71)
2-(2-Hydroxyethylthio)ethyl vinyl sulphide	164 (M^+, 21), 105 (100), 104 (43), 61 (76), 59 (47), 45 (98), 44 (78)
Bis(2-chloroethyl) sulphoxide	174 (M^+, 15), 76 (26), 65 (28), 63 (100), 47 (21), 45 (32), 44 (55)
Bis[2-(vinylthio)ethyl] ether	190 (M^+, 0.1), 87 (100), 86 (39), 85 (29), 61 (40), 59 (59), 45 (71)
Tri-i-butyl phosphate	155 (20), 139 (9), 112 (10), 99 (100), 57 (18), 41 (17), [266, M^+ absent]
2-(2-Hydroxyethylthio)ethyl vinyl sulphoxide	180 (M^+, 18), 103 (100), 75 (19), 59 (18), 47 (21), 45 (32), 44 (55)
1,2-Bis(2-chloroethylthio)ethane	123 (100), 109 (66), 73 (52), 63 (78), 61 (87), 60 (55), [218, M^+ absent]
Trinitrotoluene	210 (M^+, 100), 89 (43), 76 (17), 63 (36), 62 (17), 51 (18)
Tetryl	242 (61), 194 (100), 77 (48), 76 (35), 75 (35), 51 (30), [287, M^+ absent]
Bis[2-(2-chloroethylthio)ethyl] sulphide	156 (27), 125 (37), 123 (100), 122 (54), 63 (34), 61 (33), 45 (26), [278, M^+ absent]

[a] Six most intense ions m/z 40 and above, plus molecular ion where appropriate; obtained using the GC–MSD system.

fragment; the mass chromatogram of m/z 65 is shown in Fig. 2. Traces of tri-isobutyl phosphate (see below) were also detected in the extract, observed more clearly by constructing a mass chromatogram of the ion m/z 99. This ion is useful for searching for the nerve agents isopropyl, cyclohexyl and pinacolyl methylphosphonofluoridate although none was detected in the extract. Two additional components of the total ion chromatogram, whose partial mass spectra are shown in Table II, were identified as the explosives 2,4,6-trinitrotoluene and tetryl (N-methyl-N,2,4,6-tetranitroaniline), confirmed by comparison with reference samples.

Thermal desorption analysis. Sulphur mustard was again detected as a minor component by thermal desorption of an aliquot of soil sample 1. A total ion current chromatogram obtained at a desorption temperature of 50°C is shown in Fig. 3. Bis(vinylthioethyl) ether was the major component observed using a desorption temperature of 50°C. At higher desorption temperatures cyclic products became more predominant, presumably formed as thermal decomposition products, *e.g.* by cyclisation of 2-(vinylthio)ethanol or via sulphonium intermediates. 2-Methyl-1,3-thioxalane and 2-(vinylthio)ethanol were the major compounds observed at a desorption temperature of 100°C, and 1,4-dithiane and 1,4-thioxane on further heating at 250°C. Other minor cyclic products desorbed at 250°C, identified by data system search, were ethylene sulphide, 1,4,5-oxadithiapane and 1,2,5-trithiapane.

Quantitative analyses for mustard, mustard sulphoxide and thiodiglycol. Quantitative analyses for mustard and its oxidation and hydrolysis products, using GC–MS-selected ion monitoring,

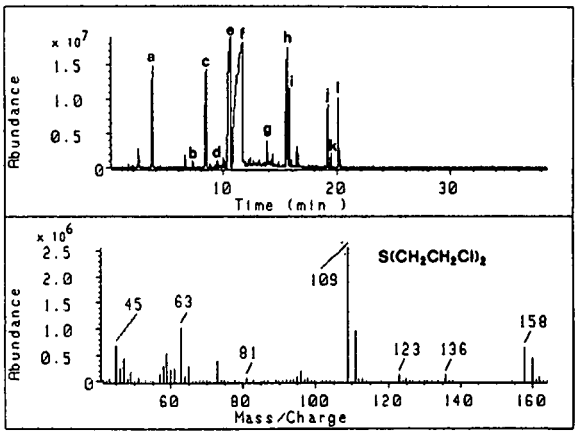

Fig. 1. Headspace of soil sample 1: GC–MSD total ion current chromatogram (upper) and a full spectral scan of peak i (lower) showing the presence of sulphur mustard. Peaks identified were: a = divinyl sulphide, b = 2,4-dimethylthietane, c = 2-methyl-1,3-thioxalane, d = 1,4-thioxane, e = 2-chloroethyl vinyl sulphide, f = 2-(vinylthio)ethanol, g = 1,4-dithiane, h = 1,2-bis(vinylthio)ethane, i = sulphur mustard, j = bis(2-chloroethyl) disulphide, k = (2-chloroethylthio)ethyl vinyl sulphide and l = bis[2-(vinylthio)-ethyl] ether.

are shown in Table III, together with the results for samples 2, 4A and 4B. The values quoted are based on the amount of analyte detected in the extracts and make no allowance for recovery. All control samples (*i.e.* glassware blanks) were negative for the presence of the analytes. Concentrations of sulphur mustard in soil sample 1 were quantitated as *ca.* 10 ppm (10 μg/g). Mustard sulphoxide was quantitated in soil sample 1 at levels *ca.* one fifth those of mustard. As observed by full scanning GC–MS, thiodiglycol was present in very high concentrations, determined as *ca.* 450 ppm.

Sample 2

Headspace, extraction and thermal desorption with GC–MS analysis. No significant compounds were detected in the headspace in the container above sample 2, nor after extraction or thermal desorption of the wool or soil particles using full scanning GC–MS.

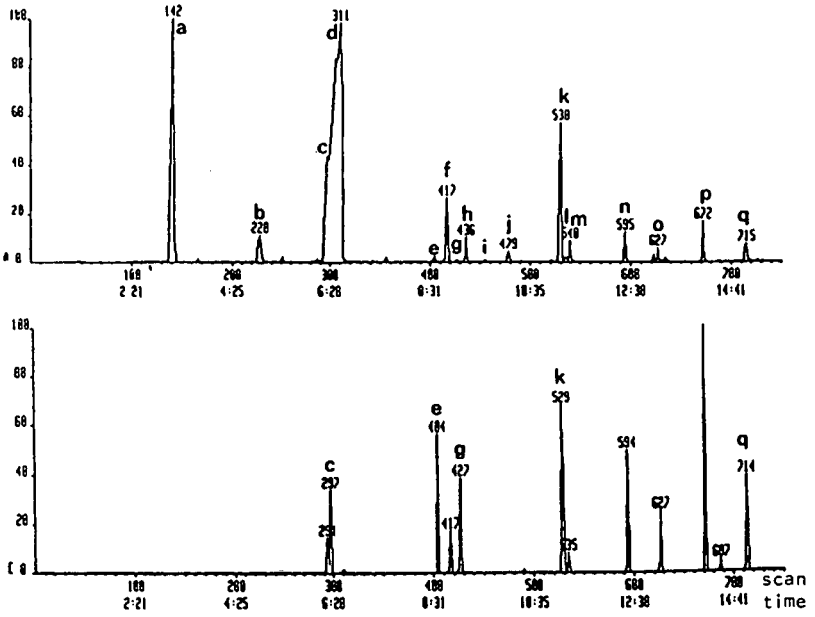

Fig. 2. Dichloromethane extract of soil sample 1: GC–MS (VG 7070EQ) total ion current chromatogram (upper) and mass chromatogram of *m/z* 65 (lower) showing improved resolution of compounds containing the CH_2CH_2Cl fragment. Peaks identified were: a = 2-(vinylthio)ethanol, b = 2-(vinylsulphinyl)ethanol, c = sulphur mustard, d = thiodiglycol, e = bis(2-chloroethyl) disulphide, f = unidentified, g = bis(2-chloroethyl) sulphoxide, h = bis[2-(vinylthio)ethyl] ether, i = tri-isobutyl phosphate, j = 2-(2-hydroxyethylthio)ethyl vinyl sulphoxide, k = 1,2-bis(2-chloroethylthio)ethane, l = trinitrotoluene, m = unidentified, n,o = dibutyl phthalates, p = tetryl and q = bis[2-(2-chloroethylthio)ethyl] sulphide. Time in min:s.

TABLE III

RESULTS OF QUANTITATIVE ANALYSIS FOR MUSTARD, MUSTARD SULPHOXIDE AND THIODIGLYCOL

Analysis	1 soil	2 wool	4A soil	4A fragment	4B soil
Mustard	10.8 ppm 8.2 ppm	7 ppb	4 ppb	18 ng	27 ppb
Mustard sulphoxide	2.1 ppm	[a]	nd[b]	nd	4 ppb
Thiodiglycol	470 ppm 436 ppm	nd	7 ppb	9 ng	26 ppb

[a] detected but not confirmable on ion ratios.
[b] not detected.

Quantitative analyses for mustard, mustard sulphoxide and thiodiglycol. A trace amount of mustard (7 ppb, *ca.* 1 ng) was detected in the dichloromethane extract of wool sample 2. Possible traces of mustard sulphoxide were not confirmable by ion ratios. No thiodiglycol was detected.

Samples 4A and 4B

Extraction with full scanning GC–MS. The total ion current chromatogram from soil sample 4A contained two major peaks of interest, identified as tetryl and a tri-butyl phosphate. Comparison with reference samples showed that the latter was not tri-*n*-butyl phosphate but the isobutyl isomer on the basis of retention time and minor differences in the mass spectra (*e.g.* very low abundance of *m/z* 125). The extract from soil sample 4B contained only one significant volatile component, identified as the explosive tetryl.

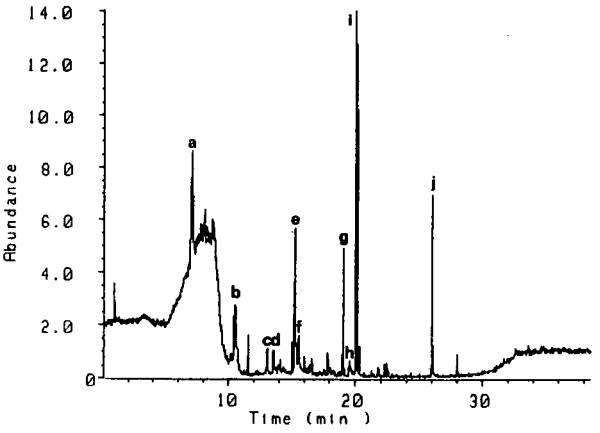

Fig. 3. Thermal desorption (50°C) of soil sample 1: GC–MSD total ion current chromatogram. Peaks identified were: a = 2-chloroethyl vinyl sulphide, b = 2-(vinylthio)ethanol, c = 1,4-dithiane, d = 2-(vinylsulphinyl)ethanol, e = 1,4,5-oxadithiapane, f = sulphur mustard, g = bis(2-chloroethyl) disulphide, h = (2-hydroxyethylthio)ethyl vinyl sulphide, i = bis[2-(vinylthio)ethyl] ether and j = dibutyl phthalate.

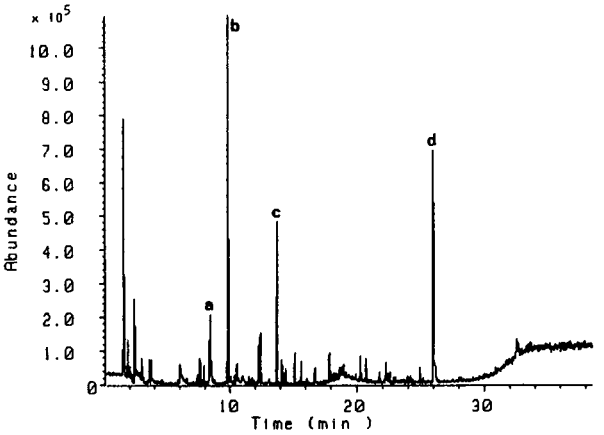

Fig. 4. Thermal desorption (250°C) of metal fragment 4B: GC–MSD total ion current chromatogram. Peaks identified were a = 2-methyl-1,3-thioxalane, b = 1,4-thioxane, c = 1,4-dithiane and d = dibutyl phthalate.

Thermal desorption. Thermal desorption of soil sample 4A at 250°C yielded traces of 1,4-dithiane; soil sample 4B yielded 1,4-dithiane and 1,4-thioxane. The metal fragment in sample 4B also yielded these cyclic products plus a smaller amount of 2-methyl-1,3-thioxalane. The total ion

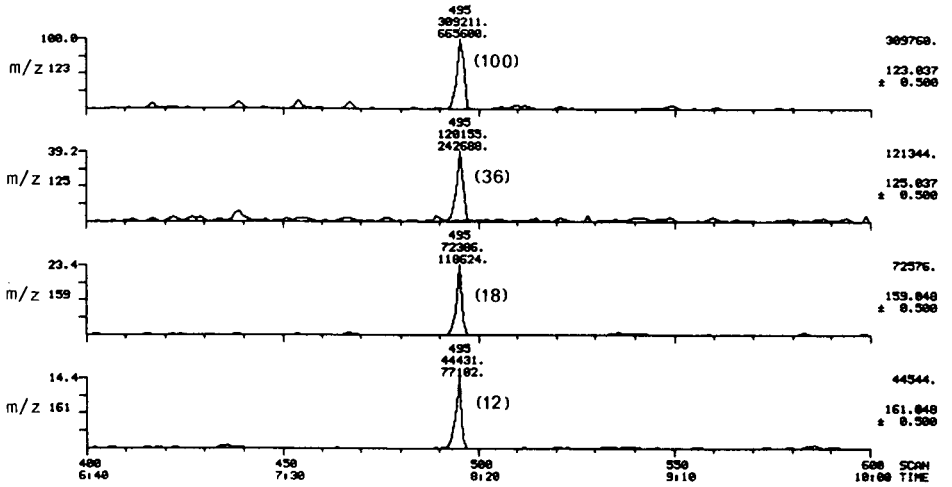

Fig. 5. Dichloromethane extract of metal fragment 4A: selected ion current chromatograms for m/z 123, 125, 159 and 161, showing the detection of sulphur mustard. Ion ratios are shown in parentheses.

current chromatogram obtained from the metal fragment 4B is shown in Fig. 4.

Quantitative analysis for mustard, mustard sulphoxide and thiodiglycol. Low concentrations (up to 27 ppb) of mustard and thiodiglycol were detected in extracts of soil samples 4A and 4B, as shown in Table III, plus a trace of mustard sulphoxide (4 ppb) in sample 4B. Trace levels of mustard and thiodiglycol were also detected in extracts of metal fragment 4A. Selected ion current chromatograms showing the detection of mustard on fragment 4A, and thiodiglycol in soil sample 4B, are shown in Figs. 5 and 6.

DISCUSSION

The results provided unambiguous evidence that the samples were contaminated with sulphur mustard, plus related compounds resulting from hydrolysis, oxidation, elimination reactions, thermal decomposition, or the manufacturing process. Several of these related compounds were detected by D'Agostino and Provost [7] in

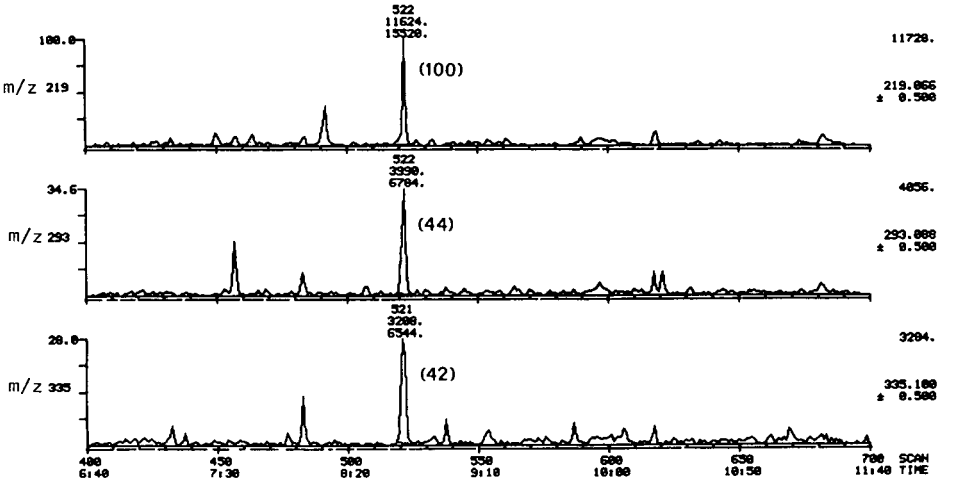

Fig. 6. Ethyl acetate extract of soil sample 4B: selected ion current chromatograms for m/z 219, 293 and 335, showing the detection of thiodiglycol as its bis-TBDMS derivative. Ion ratios are shown in parentheses.

munition residues and hydrolysates of sulphur mustard or in a different soil sample [7,8] obtained from the Iraq–Iran region. The additional detection of two explosives, tetryl and trinitrotoluene, supported the conclusion that the samples originated from a chemical weapon. The samples were also analysed for traces of nerve agents, Lewisite and their hydrolysis products but with negative results.

The bulk soil sample 1 was relatively heavily contaminated with sulphur mustard and related compounds at concentrations in the ppm range. The wool, metal fragments and their associated soil contained trace (nanogram) levels of mustard and thiodiglycol. The different levels of contamination found in the samples allowed a useful comparison of the different methods of analysis employed. With the high levels present in sample 1, all methods of analysis gave positive results for sulphur mustard and related compounds. As would be expected, the more volatile compounds predominated in the headspace and thermal desorption analyses, and these methods provide a very useful means of concentrating these volatiles from high levels of background materials. Cyclic products predominated when soil was thermally desorbed at the higher temperature of 250°C. Headspace and thermal desorption methods did not however detect the major contaminant of the soil which was the hydrolysis product thiodiglycol, although the cyclic products observed at high thermal desorption temperatures may be partly derived from thiodiglycol. Extraction was clearly superior for detecting the less volatile compounds such as thiodiglycol, and these are likely to be particularly important under environmental conditions where hydrolysis is favoured. The method of analysis employed was more crucial for samples where contamination was at low ppb levels. Mustard and thiodiglycol were detected in extracts of all of the samples which were analysed using extraction with GC–MS-selected ion monitoring, where the analysis was directed specifically at these compounds. Thermal desorption, with full scanning GC–MS, also provided a very sensitive method, cyclic decomposition products 1,4-thioxane and/or 1,4-dithiane being detected in all samples analysed with the exception of wool sample 2. Fig. 3 shows the excellent signal-to-noise ratios obtained with this method. Combined with selected ion monitoring thermal desorption would be even more sensitive. The methods employed are therefore complementary, each providing different information, and each with certain advantages depending on the state and amount of the sample, the concentrations of the analytes and the level of background present.

The hydrolysis product thiodiglycol and hydrolysis/elimination product 2-(vinylthio)ethanol appear to be useful indicators of mustard contamination in soil samples when employing extraction methods. The soil in these samples was collected some 10–12 weeks after the incident from an area in cool conditions (0–6°C daytime temperatures) with some rain. Thiodiglycol was present in sample 1 at concentrations approximately 50 times those of sulphur mustard. Cyclic decomposition products, 1,4-thioxane and 1,4-dithiane, appear to be useful indicators of mustard contamination when using thermal desorption analysis. In these particular samples the oxidation product mustard sulphoxide, which reacts with water considerably slower than does sulphur mustard, was present at lower concentrations than mustard.

CONCLUSIONS

Headspace analysis, solvent extraction and thermal desorption methods, in combination with GC–MS, have been successfully applied to the confirmation of sulphur mustard in the residues from a chemical weapon. In addition to the intact agent, 21 compounds related to sulphur mustard were detected plus traces of the explosives TNT and tetryl.

REFERENCES

1 S.J. Lundin, in *SIPRI Yearbook (1989). World Armaments and Disarmament*, Oxford University Press, New York, 1989, Ch. 4.
2 A. Hay and G. Roberts, *JAMA, J. Am. Med. Assoc.*, 263 (1990) 1065.
3 E. Mattila, K. Siivinen, H. Kenttamaa and P. Savolahti, *Int. J. Mass Spectrom. Ion Phys.*, 47 (1983) 371.
4 *Systematic Identification of Chemical Warfare Agents B.3.*

Identification of Non-Phosphorus Warfare Agents, Ministry of Foreign Affairs of Finland, Helsinki (1982).
5 R.M. Black, K. Brewster, J.M. Harrison and N. Stansfield, *Phosphorus, Sulfur Silicon Relat. Elem.*, 71 (1992) 31.
6 E.R.J. Wils and A.G. Hulst, *Fresenius' Z. Anal. Chem.*, 321 (1985) 471.
7 P.A. D'Agostino and L.R. Provost, *Biomed. Environ. Mass Spectrom.*, 15 (1988) 553.
8 P.A. D'Agostino and L.R. Provost, *J. Chromatogr.*, 436 (1988) 399.

Journal of Chromatography, 637 (1993) 81–90
Elsevier Science Publishers B.V., Amsterdam

CHROM. 24 899

(Enantio-)separation of phenoxy acid herbicides using capillary zone electrophoresis

M.W.F. Nielen

Akzo Research Laboratories Arnhem, Corporate Research, Analytical and Environmental Chemistry Department, P.O. Box 9300, 6800 SB Arnhem (Netherlands)

(First received November 24th, 1992; revised manuscript received January 7th, 1993)

ABSTRACT

Capillary zone electrophoretic (CZE) methods were developed for the separation of phenoxy acid herbicides and related impurities (including positional isomers) originating from production processes. In addition, chiral separations of phenoxypropionic acid herbicides were achieved by adding a suitable cyclodextrin-type chiral selector to the electrophoresis buffer. The selectivity of the separation can be controlled and fine-tuned by using different types of cyclodextrins. The presence of specific impurities could be confirmed after comparison of the electropherograms obtained with CZE systems having different selectivities. The CZE method shows good precision, linearity and long-term stability. The methods developed have been successfully applied to the analysis of real production samples and the determination of their enantiopurity. Both the identification and determination of the impurities compare with the results obtained with chromatographic methods. The CZE methods, however, are more flexible and simpler and will be more economical. The methods have potential for automated quality control assays.

INTRODUCTION

Phenoxy acids are widely used in agriculture as selective herbicides. Formulations of these herbicides can be analysed by capillary gas chromatography (GC) [1], but derivatization (esterification) of the carboxyl group will be required prior to the analysis. Liquid chromatography (LC) [1] can be applied directly but might not provide sufficient resolution for the determination of all related impurities. Trace analyses for these herbicides in environmental samples require preconcentration methods in order to meet the stringent requirements of the tolerance levels in, *e.g.*, drinking and ground water [2,3]. Phenoxypropionic acid herbicides are racemic mixtures and only the *d*-isomers are the active ingredient. Chiral separations of these herbicides are required in order to assess the enantiopurity of formulations and to optimize enantioselective production processes. LC using a chiral stationary phase can be applied for these purposes. The main disadvantages of LC approaches using chiral stationary phases are that the columns are relatively expensive, the performance is often much lower than that with regular LC columns and many different types of these LC columns are required in order to cover a relatively narrow range of racemic compounds.

Capillary zone electrophoresis (CZE) offers rapid and efficient separations of ionic and ionizable compounds [4,5]. Initially, CZE was applied mainly in biochemical analyses but in recent years its applicability has been demonstrated in all fields of chemical analysis including the determination of positional isomers in industrial products [6–9]. In addition, CZE has proved to be a very powerful and flexible technique for the separation of stereoisomers [10–15]. It should be noted, however, that CZE with UV absorbance detection lacks sufficient sensitivity for environmental trace analysis [16].

0021-9673/93/$06.00

Therefore, not surprisingly, there are only a few papers on the CZE of pesticides. Cai and El Rassi [17,18] used CZE for the separation of triazine herbicides and paraquat and diquat. Aguilar *et al.* [19] used CZE for the separation of 2,4-dichlorophenoxyacetic acid (2,4-D) and 2,4,5-trichlorophenoxypropionic acid (2,4,5-TP) and their corresponding phenols. Wu *et al.* [20] described the separation of different herbicides by micellar electrokinetic capillary chromatography (MECC). They found free solution electrophoresis (CZE) not to be selective enough for the separation of 2-(2,4-dichlorophenoxy)-propionic acid (2,4-DP) and 2-(2-methyl-4-chlorophenoxy)propionic acid (MCPP). Baseline resolution could only be realized after addition of SDS and Brij-35 to the electrophoresis buffer, thereby changing to a MECC separation mode. Yeo *et al.* [21] described the separation of several plant growth regulators by capillary electrophoresis, including 2,4-D and 2,4,5-trichlorophenoxyacetic acid (2,4,5-T). Again, baseline resolution of these herbicides was only obtained with the help of additives in the electrophoresis buffer: a mixture of α-, β- and γ-cyclodextrins in the CZE buffer increased the selectivity of their system and provided good resolution for the compounds studied. The separations described so far relate to the analysis of aqueous standard solutions in the ppm range. Obviously, the electrophoretic separation of phenoxy acid herbicides without the use of additives, the analysis of real samples from production plants and, moreover, their chiral separation, are still a challenge in capillary electrophoresis.

In this study, we used CZE and cyclodextrin-modified CZE for the separation of structurally related phenoxy acid herbicides and the determination of trace impurities (including positional isomers) in real production samples. In addition, cyclodextrin-modified CZE was successfully applied to the determination of their enantiopurity.

EXPERIMENTAL

Apparatus

A Lauerlabs (Emmen, Netherlands) PRINCE capillary electrophoresis system was used, equipped with an F.u.G. (Rosenheim, Germany) HCN 35-35000 power supply and an Applied Biosystems (San Jose, CA, USA) Model 759 UV absorbance detector operated at 200 nm (1 mAU/mV) and a 0.5-s rise time. CZE was performed in a 79.5 cm (63.1 cm from injector to detector) $\times$ 50 μm I.D. fused-silica capillary (Polymicro Technologies, Phoenix, AZ, USA). The voltage was +30 kV (constant-voltage mode, ramp 6 kV/s), and the oven temperature 30°C. Samples were introduced using the controlled-pressure system (20 mbar for 0.1 min); the instrument injection performance was typically $\pm$0.5% R.S.D. The coefficient of electroosmotic flow (μ_{eo}) was calculated using the migration time of the (negative) system peak. The electrophoretic mobilities (μ_{ep}) and the plate numbers were calculated using the equations in ref. 22. Data were recorded using a Fisons model VG-Multichrom integration system. Peaks were quantified by corrected peak areas (area divided by migration time). As a rule, our integration system did not provide acceptable baselines under the peaks, so the baselines had to be corrected interactively in the reprocess mode followed by recalculation of the peak areas.

Chemicals

Lithium acetate was obtained from Aldrich (Steinheim, Germany), α- and β-cyclodextrins from Fluka (Buchs, Switzerland) and heptakis(2,6-di-O-methyl)-β-cyclodextrin from Sigma (St. Louis, MO, U.S.A.). The following phenoxyacid herbicides and related impurities, kindly provided by Akzo Salt and Basic Chemicals (Hengelo, Netherlands), were investigated (Fig. 1): 2-(2-methyl-4-chlorophenoxy)propionic acid (MCPP), 2-(2-methyl-6-chlorophenoxy)propionic acid (i-MCPP), 2-(2-methyl-4,6-dichlorophenoxy)propionic acid (MD), 2-(2-methylphenoxy)propionic acid (M), 2-(2,4-dichlorophenoxy)propionic acid (DP), 2,4-dichlorophenoxyacetic acid (D) and 2-methyl-4-chlorophenoxyacetic acid (MCPA). All other chemicals were of analytical-grade from J.T. Baker (Deventer, Netherlands). Water was purified in an Alpha-Q apparatus (Millipore, Bedford, MA, USA).

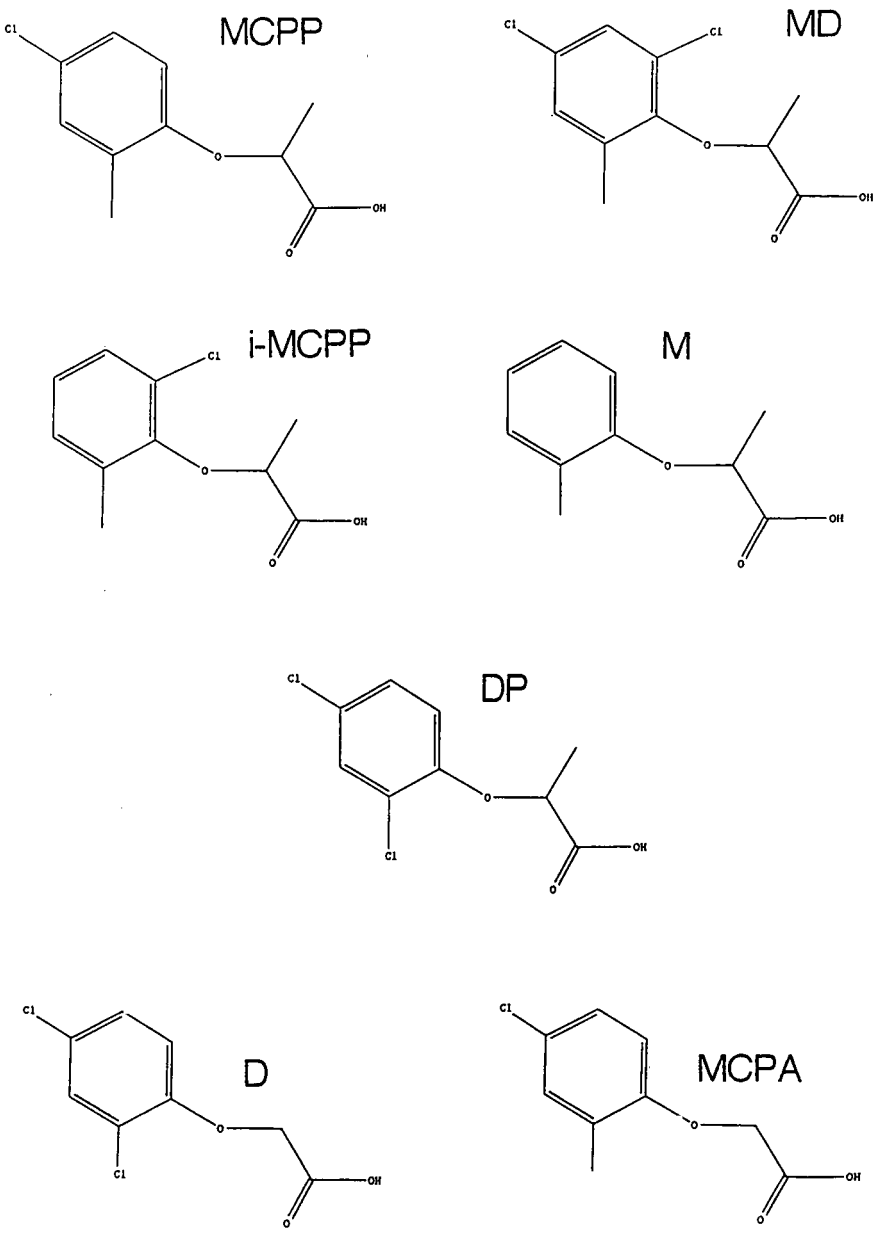

Fig. 1. Structures of the phenoxy acid herbicides and related impurities investigated.

Methods

The detection window in the CZE capillary was prepared by burning off a small part of the protective polyimide layer. Electrophoresis buffers were prepared by dissolving 30 or 50 m*M* lithium acetate in water and adjusting the pH to 4.80 with concentrated acetic acid. Cyclodextrins were dissolved in the lithium acetate buffer. Buffers were filtered through 0.45-μm Spartan 30/B membrane filters (Schleicher & Schüll, Dassel, Germany) prior to use. Stock solutions of the herbicides (0.01 *M*), the production samples (50 mg/ml) and the impurities (1 mg/ml) were prepared in methanol. Sample solutions were prepared by 50–200-fold dilution of the stock solutions with the electrophoresis buffer.

RESULTS AND DISCUSSION

Capillary zone electrophoresis

CZE without any additive (free solution zone electrophoresis) was evaluated for its separation power towards the structurally related herbicides MCPP, DP, MCPA and D. As can be seen in Fig. 1, these compounds differ by one substituent only, so it is not surprising that Wu *et al.* [20] found MCPP and DP difficult to separate. However, according to CZE theory [23], the best resolution would have been obtained at a pH value close to the pK_a values of the analytes, *i.e.*, at an acidic pH. Indeed the resolution increased from almost zero at pH 7.0 towards baseline separation at pH 4.80. Using 50 m*M* lithium acetate buffer (pH 4.80) and +30 kV, all the herbicides could be baseline resolved within 12 min, having plate numbers of 220 000, 240 000, 200 000 and 240 000 for MCPP, DP, MCPA and D, respectively.

The performance of this CZE system in terms of repeatability and linearity (range 0–250 × 10^{-5} *M*) was tested using a mixture of MD, DP, MCPA and D. The results are presented in Table I and it can be concluded that the migration times, the mobilities and the electroosmotic flow are very constant. This separation was found to be reproducible over several months. The relative standard deviations of the area/time data are fairly good and might be even better at higher concentrations, which will be less influenced by integration errors caused by the noisy baseline. Note that quantification was performed without any internal standard throughout this study. These repeatability and linearity data compare favourably with the data in refs. 19 and 20.

It can be seen that at 200 nm, the sensitivity (slope) for MCPA is about 20% less than that for the other compounds. This might be caused by a minor difference in the molar absorptivity at that wavelength. The detection limit of the phenoxy-acid herbicides was $1 \cdot 10^{-5}$ *M* (signal-to-noise ratio = 2). This value could be lowered tenfold while maintaining baseline resolution by using the sample stacking injection technique [24], yielding $1 \cdot 10^{-6}$ *M*. Obviously, this value is much too high for environmental trace analysis. It should be remembered, however, that the objective of this study was product analysis rather than environmental analysis.

Next, the applicability of this CZE system towards the separation and detection of related impurities, as known from chromatographic analyses, was studied. MCPP, DP, MCPA and D were mixed with MD, M and i-MCPP. The electropherogram obtained is shown in Fig. 2A. It can be seen that M and MD do not interfere with the separation. Only the positional isomer i-MCPP showed peak overlap with MCPP. The analysis of a real production sample is shown in Fig. 2B. In addition to the known impurities, an additional compound could be observed at 13

TABLE I

REPEATABILITY AND LINEARITY DATA

CZE system: 50 m*M* lithium acetate buffer (pH 4.80); voltage, +30 kV. The repeatabilities were determined at MD, DP, MCPA and D concentrations of $0.5 \cdot 10^{-4}$, $1.0 \cdot 10^{-4}$, $1.5 \cdot 10^{-4}$ and $2 \cdot 10^{-4}$ *M*, respectively, and are given as the relative standard deviations of the mean values of six replicates. The linearity data range from 0.0, $2.5 \cdot 10^{-5}$, $7.5 \cdot 10^{-5}$, $2.5 \cdot 10^{-4}$ and $7.5 \cdot 10^{-4}$ to $2.5 \cdot 10^{-3}$ *M*. Eof = system peak (electroosmotic flow marker); t_m = migration time; μ_{ep} = electrophoretic mobility. Other conditions as under Experimental.

Component	R.S.D. (%)			Regression (r^2)	Slope (×10^7)	Intercept
	t_m	μ_{ep}	Area/t_m			
MD	0.4	0.2	1.3	0.9998	1.17	195
DP	0.4	0.3	1.1	0.9999	1.25	169
MCPA	0.5	0.3	1.2	0.9998	0.96	177
D	0.5	0.3	1.4	0.9998	1.16	197
Eof	0.3	0.3				

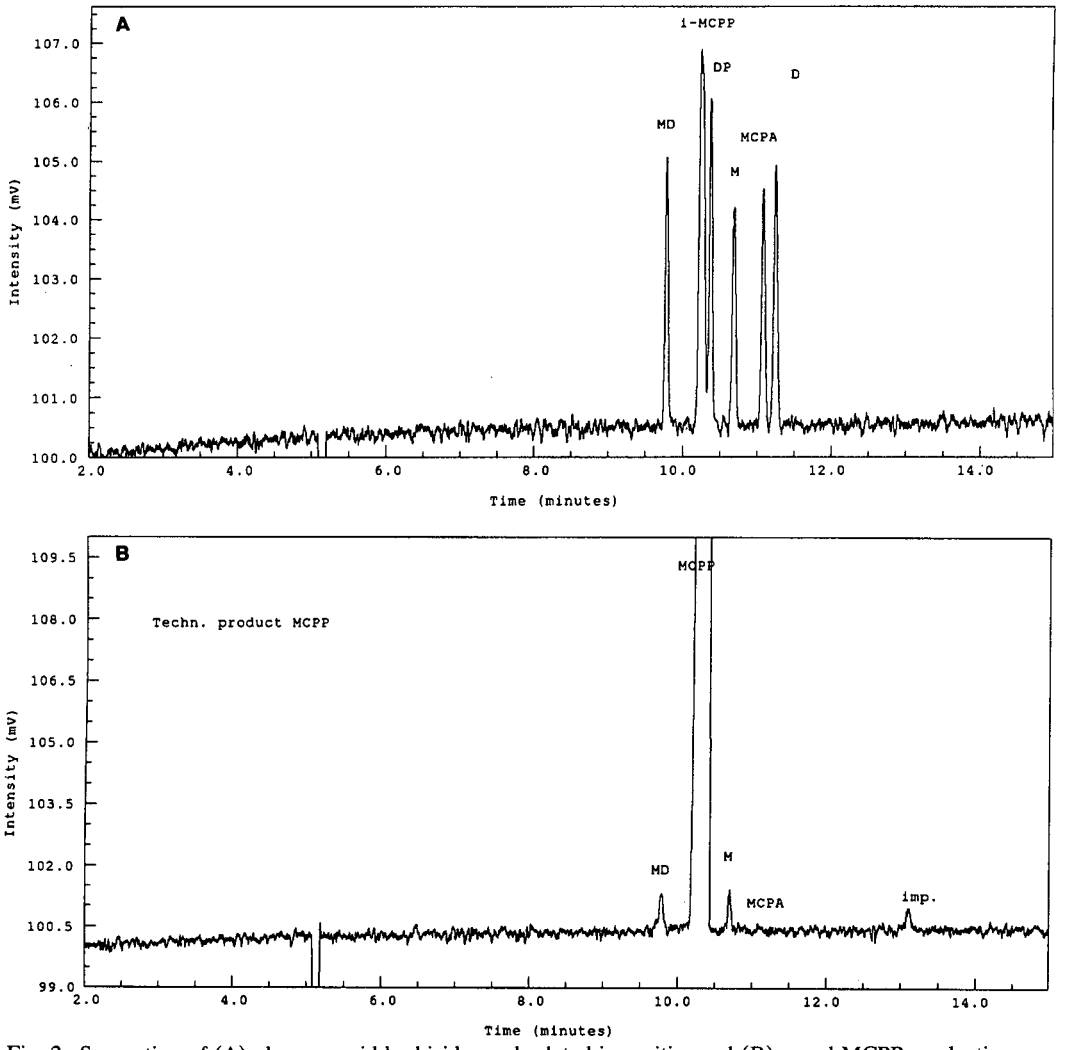

Fig. 2. Separation of (A) phenoxy acid herbicides and related impurities and (B) a real MCPP production sample by CZE using 50 m*M* lithium acetate buffer (pH 4.80) and +30 kV. Detection by UV absorbance at 200 nm (1 mAU/mV). Note that MCPP and i-MCPP co-migrate under these conditions. Other conditions as under Experimental.

min. The excess of MCPP co-migrated with i-MCPP (*cf.*, Fig. 2A) and partly overlapped with DP. The detection limit of DP relative to MCPP was determined experimentally and found to be 20 mg/g.

Cyclodextrin-modified capillary zone electrophoresis

Cyclodextrins (CDs) represent a range of cyclic glucopyranoses having a characteristic conical shape with a hydrophobic cavity and a polar exterior; α-, β- and γ-CDs have increasing diameters of the hydrophobic cavity. Alkylation of CDs induces significant changes in both the shape and the diameter. CDs and their alkylated derivatives are able to form inclusion complexes dynamically, with a variety of compounds. The optimum fit of the compounds studied (Fig. 1) will probably be a combination of inclusion of the aromatic ring and hydrogen bonding at the rim of the CD. Generally, the electrophoretic

mobility of the CD–analyte complex will be less negative than the mobility of the free (uncomplexed) compound. Consequently, the acidic herbicides will migrate closer to the system peak (electroosmotic flow marker), and the analysis time might be shortened considerably.

Initial experiments were carried out with β-CDs added to the electrophoresis buffer. The separation of a test mixture consisting of MD, DP, MCPA and D showed baseline resolution at 7 m*M* β-CD; in addition, partial chiral separation of the MD enantiomers could be obtained. In contrast to the chiral separation of basic compounds [15], the resolution of the enantiomers did not improve at lower field strengths. This was to be expected: from the resolution equation [4]

$$R_s = 0.177(\mu_{ep_1} - \mu_{ep_2})\left(\frac{VL_d}{D(\mu_{epm} + \mu_{osm})L_t}\right)^{1/2}$$

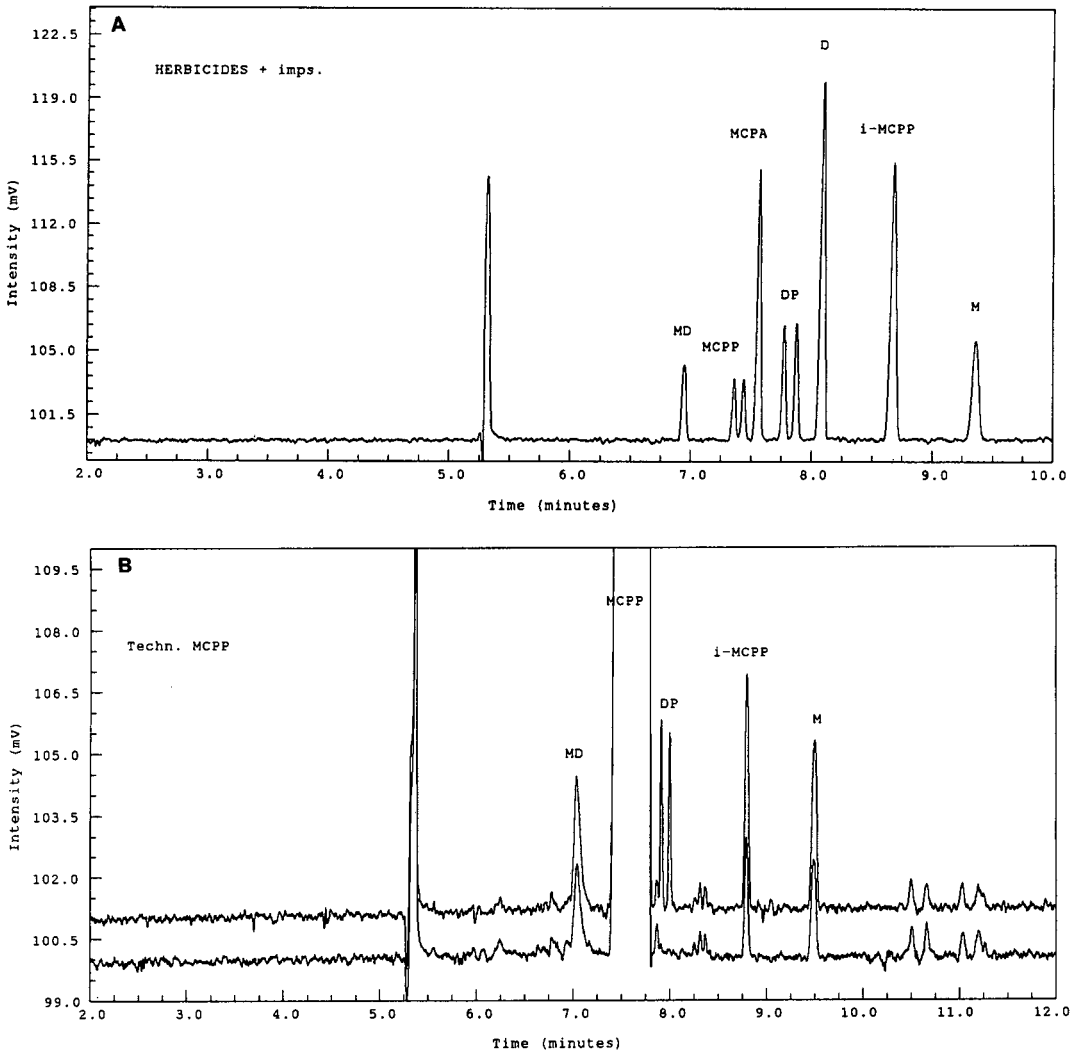

Fig. 3. Separation of (A) phenoxy acid herbicides and related impurities and (B) a real MCPP production sample by CD-modified CZE using 30 m*M* lithium acetate buffer (pH 4.80) with the addition of 20 g/l heptakis(2,6-di-O-methyl)-β-CD. For other conditions, see Fig. 2 and Experimental.

where μ_{ep} is the electrophoretic mobility of the analyte, μ_{epm} the mean of the two electrophoretic mobilities, V the applied voltage, D the diffusion coefficient, L_d and L_t the length of the capillary to the detection window and the total length, respectively, and μ_{osm} the coefficient of electroosmotic flow, it can be seen that small increases in electrophoretic and electroosmotic mobilities (*e.g.*, due to temperature rises at higher field strengths) counterbalance each other if they have opposite signs, as in the present study.

The addition of 20 g/l of heptakis(2,6-di-O-methyl)-β-CD to the electrophoresis buffer was more successful than the β-CD system; all herbicides were baseline resolved and chiral separations of both the MCPP and the DP enantiomers were obtained; in addition, none of the impurities were found to interfere with the separation (Fig. 3A). It should be noted that the selectivity changed dramatically on addition of the alkylated β-CD; compare, for example, Figs. 2A and 3A. The separation of the real production sample before and after addition of potential impurities is shown in Fig. 3B. In contrast to the unmodified CZE system, i-MCPP and DP could be separated from the excess of MCPP. Unidentified impurities can be observed between 10 and 12 min. Traces of MCPA, however, co-migrated with the huge MCPP peak.

The day-to-day reproducibility was studied by comparing duplicate analyses of the production sample on subsequent days. The results are presented in Table II. Except for the area/time reproducibility of MD, the day-to-day reproducibility was fairly good. It should be stressed that the separation of MCPP, i-MCPP, MD and M can also be peformed by LC, using a reversed-phase column and an acidified mobile phase [25]. However, the method requires 35 min and cannot be applied to the determination of the enantiopurity of MCPP and DP (see below).

An entirely different selectivity was obtained after changing to an α-CD-modified CZE system. Too high α-CD concentrations resulted in the co-migration of several peaks close to the system peak (electroosmotic flow marker). Addition of 10 mM α-CD was found to provide baseline resolution of the herbicides, including chiral separation of the DP and MCPP enantiomers. The potential impurities did not interfere with the separation and even the MD enantiomers could be baseline resolved (Fig. 4A). The separation of the production sample is shown in Fig. 4B. Herbicide D co-migrated with the excess of MCPP. Fortunately, the presence of D as an impurity in these MCPP samples is unlikely in practice.

TABLE II

DAY-TO-DAY REPRODUCIBILITY

Separation system and sample as in Fig. 3B. Reproducibilities are given as percentage deviations from the mean values ($n = 2$). For abbreviations, see Table I. Other conditions as under Experimental.

Component	Deviation from mean value (%)		
	t_m	μ_{ep}	Area/t_m
MD	0.8	0.4	6.5
MCPP	0.8	0.6	1.5
i-MCPP	1.0	0.2	2.2
M	1.1	0.2	1.1
Eof	0.7	0.7	

The main advantages of CD-modified CZE as compared with chromatographic approaches are its flexibility and its economy; one can easily and automatically switch to another CD–buffer system, having an entirely different selectivity. The changes in the peak order, the chiral selectivity and the analysis time are all reflected by the impact of the different CZE systems on the electrophoretic mobilities of the phenoxyacid herbicides, and are summarized in Fig. 5. The different selectivities can be utilized as confirmation criteria for impurities that are to be included in product specifications, thereby omitting complicated and expensive hyphenated identification techniques. Following this approach, the impurities in the MCPP production sample (Figs. 2B, 3B and 4B) were identified and determined after standard addition. The results are presented in Table III. The determination of the impurities are in acceptable agreement with each other, except for MD, which also showed the

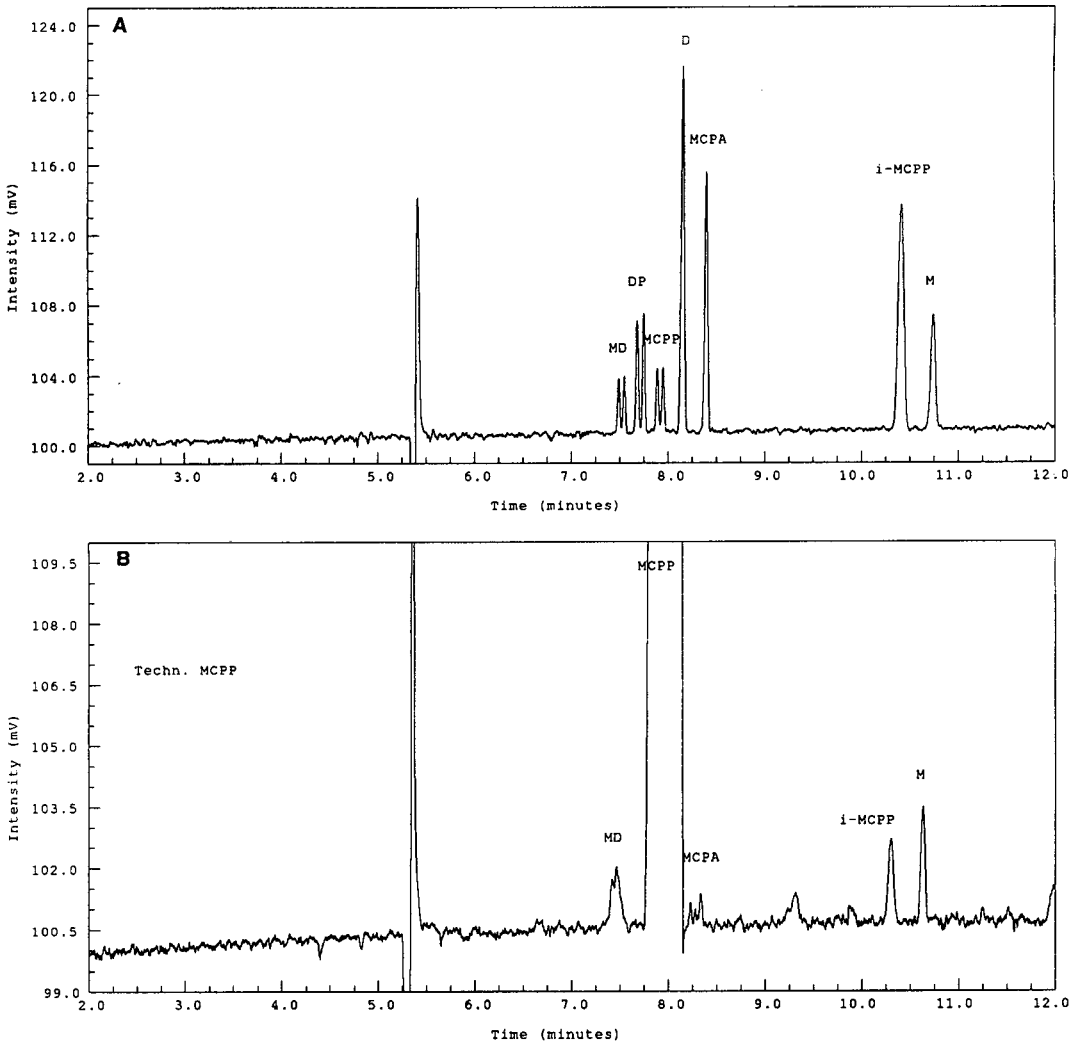

Fig. 4. Separation of (A) phenoxy acid herbicides and related impurities and (B) a real MCPP production sample by CD-modified CZE using 50 m*M* lithium acetate buffer (pH 4.80) with the addition of 10 m*M* α-CD. For other conditions, see Fig. 2 and Experimental.

worst day-to-day reproducibility and peak shapes throughout this study. The determination of the other impurities (*cf.*, Figs. 2B, 3B and 4B) might be carried out in a similar fashion provided that their identities have been assessed previously by, *e.g.*, CZE–MS.

Enantiopurity determination

The feasibility of the determination of the enantiopurity was demonstrated using the heptakis (2,6-di-O-methyl)β-CD-modified CZE system. A *d*-DP production sample was dissolved in methanol and diluted 100-fold with the CD-modified electrophoresis buffer. The electropherogram obtained is shown in Fig. 6A. It can be seen that the *d*-DP sample contained a relatively high amount of *l*-DP. In addition, an unidentified impurity can be observed at 9 min. The enantioimpurity, defined as $[l/(l+d)] \times 100\%$ was determined in duplicate and found to be $13.1 \pm 0.1\%$ ($n = 2$). This value is in good agreement with an LC determination using a CHIRAL-AGP column [25], which gave 12.7%. A *d*-MCPP production sample was analysed after

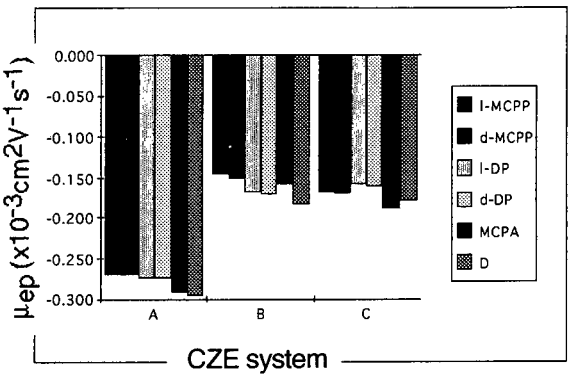

Fig. 5. Electrophoretic mobilities of phenoxy acid herbicides in the CZE systems of (A) Fig. 2, (B) Fig. 3 and (C) Fig. 4.

TABLE III

IMPURITIES IN THE MCPP PRODUCTION SAMPLE

Conditions: A, B and C correspond to Figs. 2B, 3B and 4B, respectively. For other conditions, see Experimental.

Component	Content relative to MCPP (mg/g)		
	A	B	C
MD	6	13	8
MCPA	1	n.d.[a]	1
i-MCPP	n.d.[a]	5	4
M	7	9	8
DP	<20	<1	<1
D	<1	<1	n.d.[a]

[a] Not determined because of peak overlap.

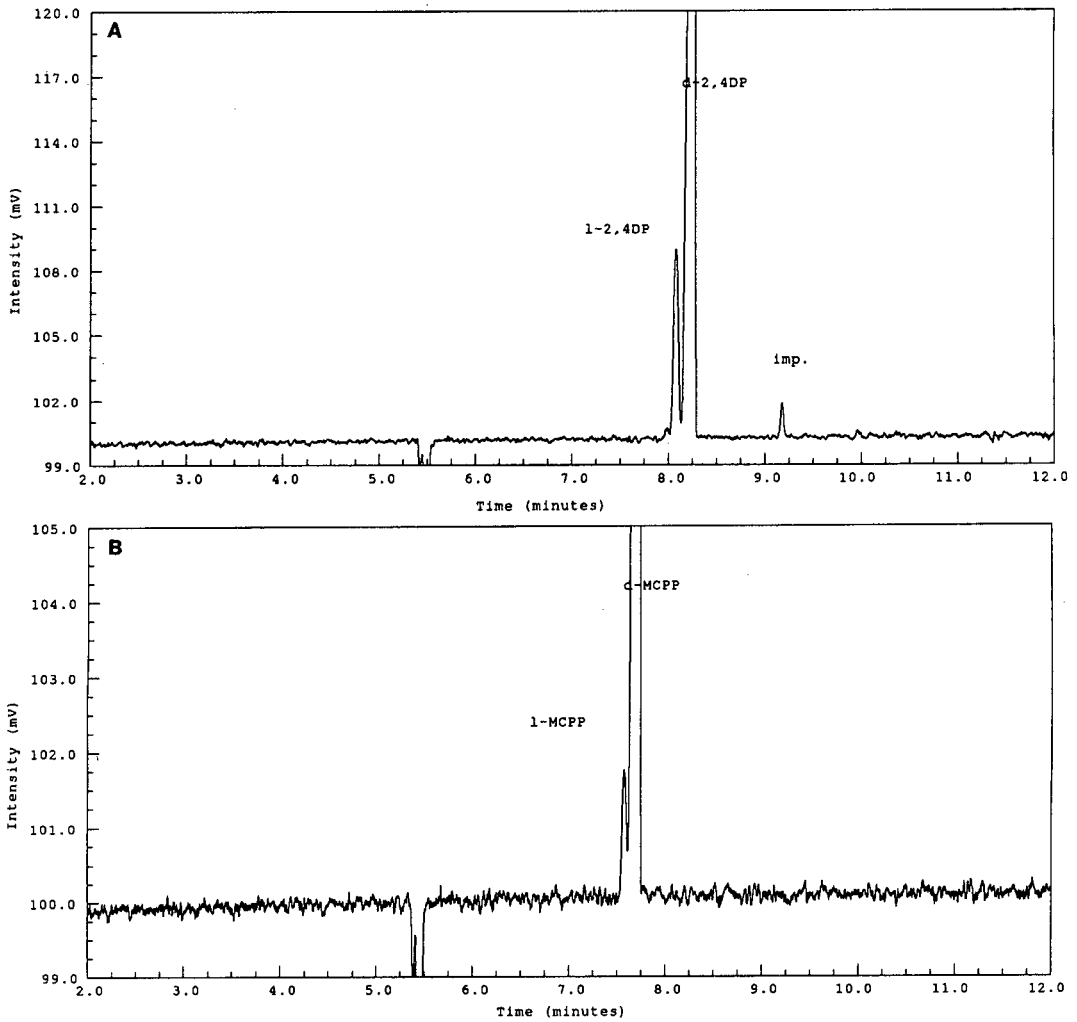

Fig. 6. Chiral separation of (A) *d*-DP and (B) *d*-MCPP samples originating from enantioselective production plants, using the CD-modified CZE system of Fig. 3. For other conditions, see Experimental.

200-fold dilution in a similar fashion. The electropherogram is shown in Fig. 6B. The enantioimpurity of this *d*-MCPP sample was found to be $3.2 \pm 0.1\%$ ($n = 2$), which again is in good agreement with the LC assay, which gave 3.5%. In contrast to the LC method, the enantiopurity of mixed *d*-MCPP–*d*-DP "cocktails" can be determined simultaneously, as the MCPP and DP peaks did not show any overlap. In addition, the same CD-modified CZE system can be used for the determination of related impurities in MCPP samples, as outlined above.

CONCLUSIONS

Phenoxy acid herbicides can be baseline separated by CZE provided that an appropriate buffer pH is selected. The CZE system thus obtained shows good stability, precision and linearity. Addition of CDs to this CZE system allows fine-tuning of the selectivity by using different types of CDs. One might easily and automatically switch to different CD-modified CZE buffers. and utilize the different selectivities to confirm the presence of specific impurities. The impurities could be determined in production samples at a level as low as 1 mg/g relative to the main component. Moreover, the dimethyl-β- and the α-CD systems can be used for chiral separations of phenoxypropionic acid herbicides and the determination of the enantiopurity of samples originating from enantioselective production plants.

REFERENCES

1 C. Sanchez-Brunete, S. Perez and J.L. Tadeo, *J. Chromatogr.*, 522 (1991) 235.
2 D. Barcelo, *Analyst*, 116 (1991) 681.
3 V. Coquart and M.-C. Hennion, *Sci. Total Environ.*, in press.
4 J. Jorgenson and K.D. Lukacs, *Anal. Chem.*, 53 (1981) 1298.
5 S.F.Y. Li, *Capillary Electrophoresis*, Elsevier, Amsterdam, 1992.
6 W.G. Kuhr and C.A. Monnig, *Anal. Chem.*, 64 (1992) 389R–407R.
7 W.G. Kuhr, *Anal. Chem.*, 62 (1990) 403R–414R.
8 M.W.F. Nielen, *J. Chromatogr.*, 625 (1992) 387.
9 M.J.A. Mensink and M.W.F. Nielen, *J. High Resolut. Chromatogr.*, 14 (1991) 417.
10 J. Snopek, I. Jelinek and E. Smolkova-Keulemansova, *J. Chromatogr.*, 452 (1988) 571.
11 J. Snopek, H. Soini, M. Novotny, E. Smolkova-Keulemansova and I. Jelinek, *J. Chromatogr.*, 559 (1991) 215.
12 S. Fanali, *J. Chromatogr.*, 474 (1989) 441.
13 M.J. Sepaniak, R.O. Cole and B.K. Clark, *J. Liq. Chromatogr.*, 15 (1992) 1023.
14 R. Kuhn, F. Stoeckun and F. Erni, *Chromatographia*, 33 (1992) 32.
15 M.W.F. Nielen, *Anal. Chem.*, 65 (1993) 7.
16 M.W.F. Nielen, presented at the *20th International Symposium on Environmental Analytical Chemistry, Strasbourg, 1990.*
17 J. Cai and Z. El Rassi, *J. Liq. Chromatogr.*, 15 (1992) 1179.
18 J. Cai and Z. El Rassi, *J. Liq. Chromatogr.*, 15 (1992) 1193.
19 M. Aguilar, A. Farran and V. Marti, *Sci. Total Environ.*, in press.
20 Q. Wu, H.A. Claessens and C.A. Cramers, *Chromatographia*, 34 (1992) 25.
21 S.K. Yeo, H.K. Lee and S.F.Y. Li, *J. Chromatogr.*, 594 (1992) 335.
22 M.W.F. Nielen, *J. Chromatogr.*, 542 (1991) 173.
23 S. Terabe, T. Yashima, N. Tanaka and M. Araki, *Anal. Chem.*, 60 (1988) 1673.
24 S.E. Moring, J.C. Colburn, P.D. Grossman and H.H. Lauer, *LC · GC Int.*, 3 (1990) 46.
25 B.H. Schel, Akzo Salt and Basic Chemicals, Hengelo, Netherlands, personal communication, 1992.

Journal of Chromatography, 637 (1993) 91–95
Elsevier Science Publishers B.V., Amsterdam

CHROM. 25 003

Short Communication

Determination of the average molecular size of glycosaminoglycans by fast protein liquid chromatography

James Melrose* and Peter Ghosh

The Raymond Purves Bone and Joint Laboratories, University of Sydney, Royal North Shore Hospital, St. Leonards, NSW 2065 (Australia)

(Received January 19th, 1993)

ABSTRACT

The determination of the molecular masses of glycosaminoglycans (GAGs) has in the past been hampered by a lack of readily available standards. In the present study methods were determined for the fractionation of commercially available bovine tracheal chondroitin sulphate A into essentially mono-disperse GAG pools which were shown to be suitable as standards for the calibration of Superose 6 and 12 fast protein liquid chromatograph (FPLC) columns. Superose 6 FPLC was particularly suitable for assessing the size distribution of GAGs of M_r 10 000–40 000 and the relatively high flow-rates possible with this support enabled a considerably faster analysis of samples compared to the soft gels previously used for this purpose.

INTRODUCTION

In 1971 Wasteson [1,2] published details of the fractionation and characterisation of glycosaminoglycans (GAGs) from ox nasal septa using Sephadex G200 gel permeation chromatography [1,2]. Despite the relatively polydisperse nature of the GAGs examined, discrete essentially mono-disperse pools were nevertheless prepared which were shown to be suitable as standards for assigning size distributions to unknown GAG samples. However, the soft gel matrices employed which necessitated slow flow-rates precluded the rapid analysis of samples. In the current study, the original methodology of Wasteson was employed to prepare chondroitin sulphate standards from bovine tracheal chondroitin sulphate A, a commercially available source, and these were subsequently used to calibrate Superose 6 and 12 fast protein liquid chromatography (FPLC) columns. The molecular mass values obtained by FPLC were comparable to those obtained earlier with softer gel matrices [1,2], however a considerably faster analysis of samples was possible (*ca.* 1 h per sample), since a relatively fast flow-rate was possible with these FPLC matrices.

EXPERIMENTAL

Reagents

Sephadex G200, Superose 6 and 12 pre-packed HR 10/30 FPLC columns were obtained from

* Corresponding author.

0021-9673/93/$06.00

Pharmacia Australia (N. Ryde, Australia). Chondroitin sulphate A from bovine trachea was obtained from Calbiochem (Alexandria, Australia). Dimethyl methylene blue was an Aldrich product (Castle Hill, Australia). Four chondroitin sulphate standards (designated II, IV, VI and IX in this manuscript) prepared from bovine nasal cartilage, whose molecular masses had been calculated from intrinsic viscosity measurements [1,3] (see Table I), and human intervertebral disc chondroitin sulphate (CS) and keratan sulphate (KS) [3] were gifts provided by Professor R.H. Pearce, University of British Columbia, Vancouver, Canada). The semi-synthetic polysulphated polysaccharides, glycosaminoglycan polysulphate ester (GPSE, Arteparon) and pentosan polysulphate (PPS, SP-54) were products of Luitpold-Werk and Benechemie respectively, both of Munich, Germany.

Methods

Analysis of chromatographic fractions for glycosaminoglycan. The GAG content of chromatographic fractions from the analytical runs were determined by reaction with the metachromatic dye 1,9-dimethyl methylene blue [4,5]. The carbazole method of Bitter and Muir [6] was used to measure the hexuronic acid contents of fractions from the preparative chromatography runs.

Preparation of the chondroitin sulphate standards. A solution of bovine tracheal CS 2.0 g in 0.2 *M* NaCl (20 ml) was chromatographed on a column of Sephadex G200 (95 × 5.0 cm I.D.) and eluent fractions collected and pooled as described earlier [1,2]. Chondroitin sulphate pools corresponding to the hydrodynamic size-range covered by CS pools 1–6 of Wasteson's methodology [1,2] were collected, concentrated by diafiltration (2000 cut off membrane), dialysed against distilled water and freeze dried. Samples of these CS pools (300 μg GAG) were re-chromatographed on an analytical column of Sephadex G200 (90 × 1.6 cm I.D.) eluting with 0.2% NaCl at a flow-rate of 6 ml/h (Fig. 1).

Superose 6 and 12 FPLC of CS samples.

TABLE I

CHARACTERISTICS OF THE GLYCOSAMINOGLYCAN SAMPLES USED IN THIS STUDY

Sample	K_{av} [a] Sephadex G200	K_{av} [a]		Assigned M_r [b]
		Superose 6	Superose 12	
CS1	0.093	0.456	0.151	36 000
CS2	0.237	0.550	0.210	23 200
CS3	0.300	0.600	0.265	20 000
CS4	0.405	0.673	0.340	14 500
CS5	0.467	0.725	0.437	11 800
CS6	0.533	0.775	0.490	10 700
CS7	0.633	0.900	0.617	7300
II	nd	0.400	0.122	40 000[c]
IV	nd	0.605	0.250	20 000[c]
VI	nd	0.635	0.337	18 000[c]
IX	nd	0.825	0.572	10 000[c]
Disc KS	nd	0.837	0.525	8000–9000
Disc CS	nd	0.675	0.280	17 000–19 000
Arteparon	nd	nd	0.725	5200
SP-54	nd	nd	0.818	4800

[a] K_{av} = Average distribution coefficient described by the formula $K_{av} = (V_e - V_0)/(V_t - V_0)$, where V_e represents the elution volume of the solute of interest and V_0 and V_t represent the void and total volumes of the column, respectively. nd = Not determined.
[b] M_r = Average molecular mass [1,2].
[c] Average molecular mass $M_{[\eta]}$ determined from intrinsic viscosity measurements.

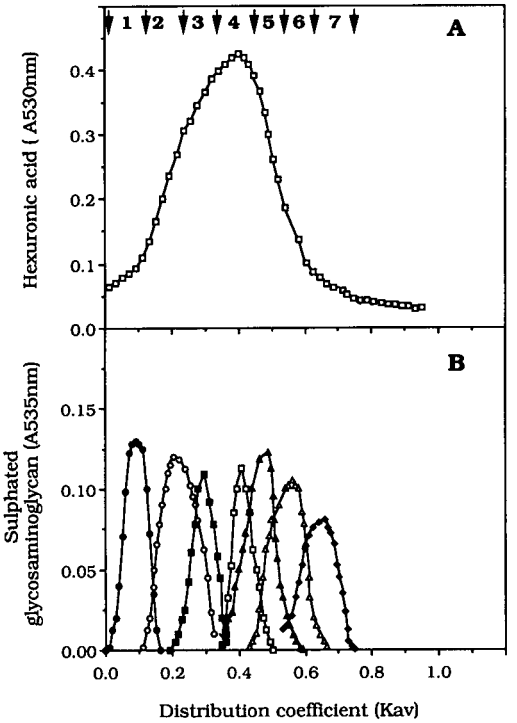

Fig. 1. (A) Preparative chromatography on Sephadex G200 of bovine tracheal CS demonstrating the pooling protocol used for CS pools 1–7 which were subsequently examined by (B) analytical chromatography on the same gel matrix. CS pools 1 = ●; 2 = ○; 3 = ■; 4 = □; 5 = ▲; 6 = △; 7 = ◆. (See Table I for details of the CS pools). In A aliquots of fractions were assayed for hexuronic acid [6] to assess the distribution of GAG species. In B aliquots of fractions were reacted with 1,9-dimethyl methylene blue to assess the distribution of GAG species [4,5].

Samples of CS pools 1–7; CS standards II, IV, VI, IX; Intervertebral disc CS and KS; GPSE and PPS (200–300 μg GAG dry weight) were chromatographed on Superose columns at a flow-rate of 24 ml/h using 0.5 *M* sodium acetate buffer pH 7.0 containing 0.05% (v/v) Tween 20 as eluent (Figs. 2 and 3). Fractions (0.25 ml) were collected directly into 96-well flat bottom microplates using a Gilson Model 201 fraction collector, GAG was determined with 1,9-dimethyl methylene blue [4,5]. The void and total volumes of these columns were determined using ^{35}S-labelled PG aggregate and free ^{35}S, respectively, using liquid scintillation spectrometry.

RESULTS

Re-chromatography of CS samples on Sephadex G200 (Fig. 1), indicated a similar level of polydispersity to that obtained by Wasteson [1,2], and these CS pools were assigned tentative average molecular mass values on the basis of these earlier studies [1,2] (Table I). FPLC of CS pools 1–7 resolved them as well defined peaks and a linear relationship was evident between their average hydrodynamic sizes and assigned molecular masses (Fig. 2). Four CS standards, whose molecular masses had been independently verified by intrinsic viscosity measurements (II, IV, VI, IX, see Table I) were also chromatographed under identical conditions. These samples eluted with hydrodynamic sizes calculated from the elution volume *vs.* assigned molecular mass calibrations (Fig. 2) similar to their sizes by intrinsic viscosity measurements and this was taken as validation of the assigned molecular masses given to the CS pools 1–7 (Table I). Human intervertebral disc KS and CS eluted with assigned average molecular masses of 8000–9000 and 17 000–19 000, respectively, by Superose FPLC which was in close agreement to their literature values [3]. Commercial preparations of the polysulphated polysaccharides GPSE and PPS were also examined by Superose 12 FPLC and were assigned average molecular masses of 5200 and 4800, respectively (Table I), these values however may be under-estimated since they were at the lower limit of the calibration (Fig. 3). Average molecular mass values of 6000–7000 and 5700, respectively, have been reported [7] elsewhere for these polymers.

DISCUSSION

Glycosaminoglycans have a diverse range of functions in connective tissues and consequently are of interest to a wide range of scientists [8]. However until recently no convenient method existed for the characterisation of their molecular masses. This has been the consequence of both an absence of readily available GAG standards of defined molecular mass and of a fast high-resolution chromatographic system for their size separation. In the present study standards

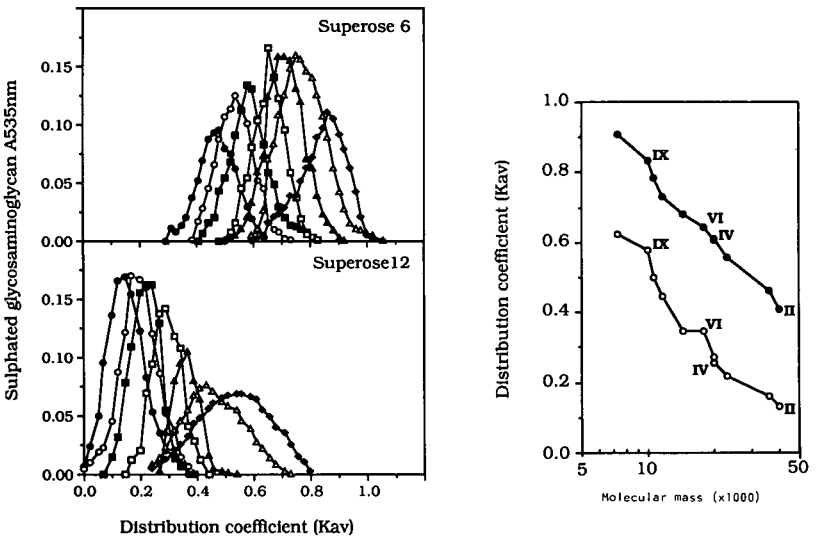

Fig. 2. Superose 6 and 12 FPLC of CS pools 1–7, the symbols used are as depicted in the legend to Fig. 1. Aliquots of fractions were reacted with 1,9-dimethyl methylene blue to assess the distribution of GAG species [4,5]. Linear regression was used to fit the lines of best fit which are indicated at the right-hand side of the figure with the elution positions of CS standards II, IV, VI, IX (see Table I) also indicated. ● = Superose 6: $y = 1.4525 - 0.65400 \log x$ ($R^2 = 0.989$); ○ = Superose 12: $y = 1.2055 - 0.70107 \log x$ ($R^2 = 0.946$).

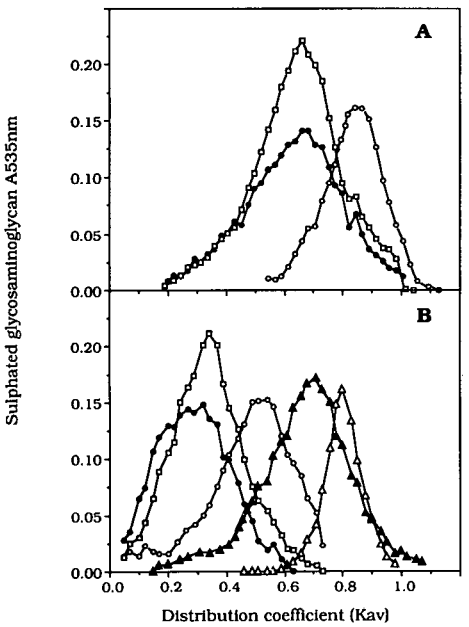

Fig. 3. (A) Superose 6 and (B) Superose 12 FPLC of non-fractionated bovine tracheal CS-A (□) and human intervertebral disc CS (●) and KS (○, 300 μg GAG dry weight each). Arteparon (▲, 300 μg GAG) and SP-54 (△, 300 μg GAG) were also examined by Superose 12 FPLC. Aliquots of fractions were reacted with 1,9-dimethyl methylene blue to assess the distribution of GAG species [4,5].

were prepared using an existing method whereby CS standards of well defined composition and molecular dimensions were obtained [1,2].

Using the methodology described herein, Superose 6 FPLC appeared to be the most suitable means for examination of GAGs of 10 000–40 000 in size. Preparation of smaller CS standards by limited hyaluronidase digestion and fractionation of the products as suggested by Wasteson [2], could however be used to extend the lower end of the calibration for Superose 12 FPLC further increasing the general applicability of FPLC for the examination of the molecular masses of GAGs.

REFERENCES

1 M. Wasteson, *J. Chromatogr.*, 59 (1971) 87–97.
2 M. Wasteson, *Biochem. J.*, 122 (1971) 477–485.
3 R.H. Pearce and B.J. Grimmer, *Biochem. J.*, 157 (1976) 753–763.
4 R.W. Farndale, D.J. Buttle and A.J. Barrett, *Biochim. Biophys. Acta*, 883 (1986) 173–177.
5 J. Melrose and P. Ghosh, *Anal. Biochem.*, 170 (1988) 293–300.
6 T. Bitter and H.M. Muir, *Anal. Biochem.*, 4 (1962) 330–334.

7 P. Ghosh, M. Smith and C. Wells, in J.S. Dixon and D.E. Furst (Editors), *Second Line Agents in the Treatment of Rheumatic Diseases*, Marcel Dekker, NY, 1992, pp. 363–427.

8 J.F. Kennedy, *Proteoglycans —Biological and Chemical Aspects in Human Life*, (*Studies in organic chemistry*, Vol. 2), Elsevier, Amsterdam, 1979.

Journal of Chromatography, 637 (1993) 96–99
Elsevier Science Publishers B.V., Amsterdam

CHROM. 24 955

Short Communication

Immobilized polyethyleneglycol-based stationary phase for the analysis of amines and organic acids by capillary gas chromatography

Marie Horká*, Vladislav Kahle and Miloš Krejčí

Institute of Analytical Chemistry, Czech Academy of Sciences, Veveří 97,,611 42 Brno (Czech Republic)

(First received October 27th, 1992; revised manuscript received February 5th, 1993)

ABSTRACT

A procedure for preparing capillary columns for the analysis of amines and organic acids with a working temperature of 55–300°C was developed for a column coated with immobilized Carbowax 20M/SE-54 stationary phase mixture. The inner wall of the capillary was deactivated with 3-aminopropyl triethoxysilane.

INTRODUCTION

Capillary columns and currently used stationary phases do not enable successful simultaneous analysis of substances of acidic and basic character. In practice, however, such an analysis is required.

The analysis of free fatty acids and other substances —alcohols or phenols containing an active hydroxyl group in their molecule— is limited to the use of capillary columns containing a stationary phase prepared specially for separation of acids. Most frequently polar stationary phases of the polyethyleneglycol type modified with organic acids, such as terephthalic acid or its derivatives, are used [1–3].

Basic heterocyclic nitrogenous compounds and aromatic and aliphatic amines can be separated on various stationary phases, *e.g.* polyethylenimine, polypropylenimine or polyethyleneglycol, with the addition of potassium hydroxide [4], or on some polysiloxane stationary phases [3]. For the analysis of amines, capillary columns with a non-immobilized stationary phase of polyethyleneglycol-type Carbowax 51 have been specially prepared and are commercially available. Recently CP WAX has been used for the analysis of diamines and volatile amines [5]. For the analysis of N-nitroso substances, aromatic and heterocyclic amines and other amino substances, Carbowax Amine capillary columns have been recommended [6].

The requirement for simultaneous analysis of acidic [7] and basic substances could eventually be met by a capillary column containing a mixture of phases.

This work is concentrated on the preparation of capillary columns containing an immobilized film of a mixed stationary phase of poly-

* Corresponding author.

0021-9673/93/$06.00

ethyleneglycol/polysiloxane type with sufficient thermostability suitable for the analysis of acidic and basic solutes. The preparation of the columns was based on knowledge derived from, and modified procedures of, preparation of polyethyleneglycol-type immobilized stationary phase based on polyurethane [8] and polysiloxane-type stationary phase immobilized by a radical mechanism known commercially as SE-54 [9]. Some chromatographic properties of this stationary phase were studied.

EXPERIMENTAL

Chemicals and materials

Simax glass tubes were obtained from Kavalier (Sázava, Czech Republic). Capillary columns containing immobilized and non-immobilized Carbowax 20M (the glass capillary inner surface silanized with a 5% solution of γ-glycidoxypropyltrimethoxysilane [8]) and an immobilized SE-54 silicone stationary phase film (the inner surface silanized with [$^2H_4$]octamethylcyclotetrasiloxane [9]) were prepared in the Institute of Analytical Chemistry, Czech Academy of Sciences, Brno, Czech Republic.

Most of the chemicals were supplied by Lachema (Brno, Czech Republic). The following chemicals were obtained: 3-aminopropyl triethoxysilane (Serva Feinbiochemica, Heidelberg, Germany), [$^2H_4$]octamethylcyclotetrasiloxane (VCHZ Synthesia, Kolín, Czech Republic), Carbowax 20M (Carlo Erba, Milan, Italy), SE-54 silicone stationary phase (W. Günter, Düsseldorf, Germany), azo-*tert.*-butane (Ventron, Karlsruhe, Germany), Desmodur L 75 (Bayer, Dormagen, Germany) and DABCO R-8020 (Air Products Group, Paulsboro, NJ, USA).

Apparatus

The device for drawing glass capillaries was manufactured in the Institute of Analytical Chemistry, Czech Academy of Sciences, Brno, Czech Republic. The capillary columns were thermostated and tested in a Fractovap Model 2300 AC gas chromatograph equipped with a flame ionization detector (Carlo Erba, Milan, Italy).

Preparation of the capillary column containing the mixed stationary phase

Glass capillaries (0.25 mm I.D.) made of Simax glass were drawn by the usual procedure [10]. The inner capillary surface was silylized with 5% 3-aminopropyl triethoxysilane in methanol. Capillaries filled to the 85–90% level with a solution of silane were heated in a thermostat at 80°C for 2 h. Then they were washed with 2 ml of methanol and blown with nitrogen for 30–60 min.

The capillary tubes deactivated by silylation were further coated with the mixed stationary phase from its dichloromethane solution [0.6% (w/v) Carbowax 20M and 0.05% (w/v) SE-54], according to the static method. The solution also contained Desmodur L 75 ($2 \cdot 10^{-3} M$) and DABCO R-8020 catalyst ($5 \cdot 10^{-5} M$).

In the first step Carbowax 20M was cross-linked by heating the sealed column at 145°C for 5 h. Nitrogen was blown through the column. The prepared columns (10–15 m × 0.25 mm I.D., film thickness 0.4 μm) were first tested at 110°C with 2,6-dimethylphenol and 2,6-dimethylaniline to determine efficiency and capacity factor. Nitrogen was used as the carrier gas at the velocity of 10–11 cm/s.

In the second step the column was blown with a stream of nitrogen saturated at 25°C with azo-*tert.*-butane for 1 h (for SE-54 cross-linking) at a flow-rate of 2 cm/s. The sealed column was heated in a thermostat from 40 to 220°C at 10°C/min and then left at 220°C for 1 h. After three cycles, it was washed with 2 ml of chloroform at a rate of 1 cm/s and blown with nitrogen

TABLE I

PROPERTIES OF THE IMMOBILIZED CARBOWAX 20M/SE-54 STATIONARY PHASE MIXTURE

Degree of cross-linking (%)	Column efficiency (theoretical plates/m)	
	2,6-Dimethylphenol	2,6-Dimethylaniline
89.6	5000	4800

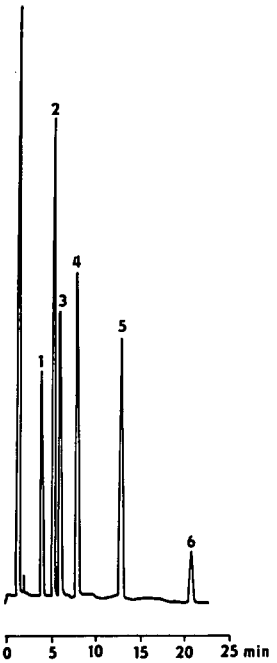

Fig. 1. Chromatogram of volatile free fatty acids. Glass capillary column: 10 m × 0.25 mm I.D.; film thickness: 0.4 μm; stationary phase: immobilized Carbowax 20M/SE-54 mixture; column temperature: 130°C; carrier gas: nitrogen; velocity: 10 cm/s. Peaks: 1 = acetic acid; 2 = propionic acid; 3 = isobutyric acid; 4 = *n*-butyric acid; 5 = valeric acid; 6 = caproic acid.

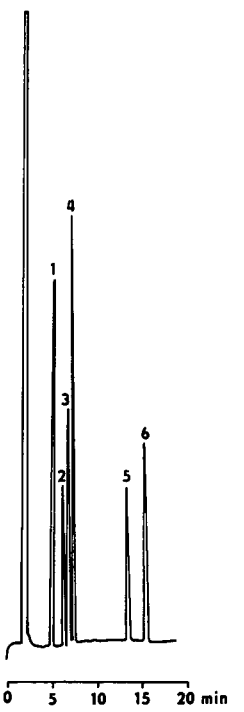

Fig. 2. Chromatogram of heterocyclic and primary amines. Column as in Fig. 1; column temperature programmed from 70 to 100°C at 2°C/min; carrier gas: nitrogen; velocity: 10 cm/s. Peaks: 1 = butylamine; 2 = pyridine; 3 = propylamine; 4 = 4-methylpyridine; 5 = hexylamine; 6 = 4-ethylpyridine.

for 1 h. The procedure was then repeated with 2 ml of methanol and the columns retested.

The degree of stationary phase film immobilization in the treated columns was calculated as the ratio of the capacity factor of 2,6-dimethylphenol after washing the column to that of the same solute before washing, expressed as a percentage.

TABLE II

RETENTION INDEX VALUES OF SELECTED SUBSTANCES MEASURED ON COLUMNS CONTAINING NON-IMMOBILIZED CARBOWAX 20M, IMMOBILIZED CARBOWAX 20M, SE-54 AND CARBOWAX 20M/SE-54 MIXTURE STATIONARY PHASES, AT 60°C

Test substance	I_R			
	Non-immobilized Carbowax 20M	Immobilized Carbowax 20M	SE-54	Carbonwax 20M/ SE-54 mixture
Benzene	955	987	688	902
1-Butanol	961	1228	679	1106
1,4-Dioxane	1073	1173	714	1017
Pyridine	1187	1366	753	1121

RESULTS AND DISCUSSION

Some properties of the capillary columns prepared are summarized in Table I. As an example of application of this stationary phase, a mixture of lower fatty acids (Fig. 1) and a mixture of heterocyclic and primary amines (Fig. 2) are shown.

Influence of immobilization on the polarity of a stationary phase mixture

The influence on polarity of the immobilization procedure used was studied by means of retention indices (I_R) of the test substances determined on columns coated with the non-immobilized and immobilized Carbowax 20M stationary phase films, the immobilized stationary phases mixture film (Carbowax 20M/SE-54) and the immobilized SE-54 stationary phase film. The results in Table II show that the retention indices for all substances on the capillary column coated with the immobilized Carbowax 20M/SE-54 mixture were lower than on the capillary column containing immobilized Carbowax 20M. The retention index values obtained show that the immobilized Carbowax 20M/SE-54 mixed stationary phase is less polar than immobilized Carbowax 20M and that the stationary phase film is mildly acidic.

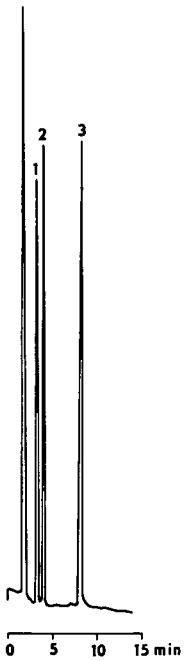

Fig. 3. Chromatogram of solutes mixture. Column as in Fig. 1; column temperature: 270°C; carrier gas: nitrogen; velocity: 10 cm/s. Peaks: 1 = pentachlorphenol; 2 = 2,2-bipyridyl; 3 = acridine.

Temperature stability of the immobilized stationary phase mixture film

The working temperature interval for the immobilized Carbowax 20M/SE-54 stationary phase mixture is in the range 55–300°C. In such a column a mixture of solutes at 270°C was chromatographed (Fig. 3).

REFERENCES

1 M.L. Lee, F.J. Yang and K.D. Bartle, *Open Tubular Column Gas Chromatography*, Wiley, New York, 1984.
2 M. Horká, K. Janák, V. Kahle and K. Tesařík, *Chromatographia*, 23 (1987) 553.
3 *Chromatography Users' Catalog 1992*, Hewlet-Packard, Hoofddorp, Netherlands, 1992.
4 K. Tesařík and K. Komárek, *Kapilární kolony v plynové chromatografii (Capillary Columns in Gas Chromatography)*, SNTL, Prague, 1984.
5 J. van Dalen, J. Buyten, J. Peene and Ph. Mussche, presented at the *7th Danube Symposium on Chromatography and Analytiktreffen 1989*, Leipzig, paper TU 038.
6 *The Supelco Reporter*, Vol. XI, No. 2, Supelco, Bellefonte, PA, 1992, p. 2.
7 J. Sanz, M. de Frutos and I. Martínez-Castro, *Chromatographia*, 33 (1992) 213.
8 M. Horká, V. Kahle, K. Janák and K. Tesařík, *Chromatographia*, 8 (1985) 259.
9 K. Janák, M. Horká and K. Tesařík, *J. Chromatogr.*, 471 (1989) 237
10 D. H. Desty, J. N. Haresnape and B. H. Whyman, *Anal. Chem.*, 32 (1960) 302.

Journal of Chromatography, 637 (1993) 100–103
Elsevier Science Publishers B.V., Amsterdam

CHROM. 25 014

Short Communication

Capillary gas chromatography of partially methylated alditol acetates on a high-polarity, cross-linked, fused-silica BPX70 column

Eva Lau and Antony Bacic*

Plant Cell Biology Research Centre, University of Melbourne, Parkville, Victoria 3052 (Australia)

(First received December 9th, 1992; revised manuscript received February 25th, 1993)

ABSTRACT

A new high-polarity, cross-linked, fused-silica BPX70 capillary column was used to separate complex mixtures of partially methylated alditol acetates derived from the monosaccarides: arabinose, xylose, fucose, rhamnose, galactose, glucose and mannose. These partially methylated alditol acetates are separated by gas chromatography and identified by mass spectrometry by comparison with standard spectra as well as with their retention times relative to *myo*-inositol hexacetate, an internal standard.

INTRODUCTION

Glycosyl linkage positions between monosaccharides in glycoconjugates and polysaccharides are established using methylation analysis [1–6]. A quick and easy method for preparing such partially methylated alditol acetates is described by Doares *et al.* [7]. The separation of the resultant partially methylated alditol acetates can be achieved using capillary gas chromatography (GC) and the derivatives identified by both retention times relative to an internal standard and mass spectrometry (MS).

Partially methylated alditol acetates have been chromatographed on capillary columns coated with high-polarity cyanoalkyl silicone phases. They are CP-Sil88 [8], BP-75 [9], SP-2330 [7] and SP-2340 [10]. The CP-Sil88, SP-2330 and SP-2340 are all non-bonded phase columns whereas the BP-75 is bonded phase. Bonded phase columns are of benefit during GC–MS analysis due to their inherent low bleed characteristics as well as displaying greater stability. The BP-75 column is no longer available. The separation of some partially methylated alditol acetates which would otherwise co-elute can be achieved by chromatography on columns coated with phases of varying polarity. This paper describes the separation of partially methylated alditol acetates using a new, high-polarity, cross-linked, fused-silica BPX70 column with a phase equivalent to 70% cyanopropyl siloxane, recently released by SGE, Melbourne, Australia.

EXPERIMENTAL

Materials

Methyl-α-D-glucopyranoside, methyl-α-D-galactopyranoside, methyl-α-D-mannopyranoside,

* Corresponding author.

0021-9673/93/$06.00

myo-inositol, L-fucose, L-rhamnose and sodium borodeuteride (98 atom% ^2H) were obtained from Sigma (St Louis, MO, USA); methyl-α-D-xylopyranoside was obtained from Pfanstiehl Labs. (Waukegan, IL, USA); L(+)-arabinose was obtained from BDH (Poole, UK). Methanolic HCl (1 *M*) was prepared by diluting 3 *M* methanolic HCl obtained from Supelco (Bellefonte, PA, USA); potassium methylsulphinyl methanide was prepared from potassium hydride (20% in oil) and dimethylsulphoxide as described by Harris *et al.* [11]; *myo*-inositol hexaacetate was prepared as described by Doares *et al.* [7]; methyl iodide and 1-methylimidazole were obtained from Fluka (Buchs, Switzerland). All other reagents were of the highest purity commercially avaliable.

Synthesis of methyl glycosides

The synthesis of methyl glycosides of L-fucose, L-rhamnose and L-arabinose was according to the method by Doares *et al.* [7]

Preparation of partially methylated alditol acetate standards

The methyl glycosides of the sugar were partially methylated, hydrolysed, reduced and acetylated by the procedure outlined by Doares *et al.* [7] using potassium methylsulphinyl methanide carbanion and methyl iodide. The partially methylated alditol acetates were extracted into dichloromethane, dried and reconstituted into an appropriate volume of dichloromethane. *Myo*-inositol hexa-acetate was added as an internal standard.

Gas chromatography–mass spectrometry

Partially methylated alditol acetates were separated and identified by GC–MS on a fully automated Finnigan MAT 1020B GC–MS (Sunnyvale, CA, USA).

A 25 m × 0.22 mm I.D., film thickness 0.25 μm, BPX70 (equivalent to 70% cyanopropyl siloxane), cross-linked, fused-silica capillary column (SGE) was used for GC. The column was interfaced with the ion source via a separator oven held at 260°C. The injector port was held at 240°C. The oven was programmed from 185 to 260°C, ramping at a rate of 3°C/min and held at final temperature for 10 min.

The partially methylated alditol acetates were introduced into the column via a split/splitless injector operating in the split mode. The carrier gas used was helium (ultra-high purity, C.I.G., Melbourne, Australia) at a flow-rate of 0.78 ml/min.

Electron impact ionisation at an ionisation potential of 70 eV was used for MS. Using the reconstructed ion chromatogram (RIC) obtained by scanning from 100 to 350 *m/z* in 0.3 s, derivatives eluting from the gas chromatograph were detected and identified by comparison of their mass spectra with standard spectra.

RESULTS AND DISCUSSION

The retention times of the partially methylated sugars relative to the internal standard, *myo*-inositol hexa-acetate, separated on a high-polarity, bonded phase, fused-silica BPX70 capillary column, are listed in Table I. *myo*-Inositol hexa-acetate eluted at 24.28 min. Peaks were identified by comparison of their mass spectra with standard spectra.

Fig. 1 shows the reconstructed ion chromatogram for partially methylated galactitol acetates separated on a BPX70 capillary column. The peaks which have not been assigned represent contaminants, such as plasticisers, introduced during the preparation of partially methylated alditol acetates. The improved resolution provides easy identification of the derivatives on the basis of both their mass spectra and relative retention times. The BPX70 being a bonded phase column also has the advantage of minimal bleed during chromatography.

Other high-polarity columns such as the CP-Sil88 [8], BP-75 [9], SP-2330 [7] and SP-2340 [10] have also been used to separate partially methylated alditol acetates. The order of polarity for the columns from lowest polarity to highest polarity based on average McReynolds constants [12] is the BPX70, BP-75, SP-2330, CP-Sil88, and SP-2340. The latter two being equivalent in polarity.

The BPX70 exhibited the ability to separate several derivatives which would co-elute on the

TABLE I

RETENTION TIMES OF PARTIALLY METHYLATED ALDITOL ACETATES RELATIVE TO *myo*-INOSITOL ON A BPX70 CAPILLARY COLUMN

Position of O-methyl group[a]	Parent monosaccharide[b]						
	Ara	Xyl	Fuc	Rha	Gal	Glc	Man
None	0.624	0.726	0.512	0.491	0.906	0.949	0.868
2-	0.529	0.586*	0.445	0.430	0.813	0.827	0.779
3-	0.553	0.586*	0.501	0.478	0.897*	0.864	0.855*
4-	0.546	0.586*	0.494	0.455	0.897*	0.909	0.855*
5-	0.440	–	–	–	–	–	–
6-	–	–	–	–	0.699	0.742	0.667
2,3-	0.404*	0.436$^+$	0.384	0.344*	0.742	0.723	0.677
2,4-	0.406*	0.400	0.365	0.344*	0.751	0.701	0.710$^+$
2,5-	0.357	–	–	–	–	–	–
2,6-	–	–	–	–	0.617	0.636	0.595
3,4-	0.413	0.436$^+$	0.395	0.334	0.780	0.727	0.710$^+$
3,5-	0.329	–	–	–	–	–	–
3,6-	–	–	–	–	0.667	0.663	0.654
4,6-	–	–	–	–	0.622	0.648	0.587
2,3,4-	0.270	0.277	0.266	0.219$^+$	0.605	0.533	0.530
2,3,5-	0.228	–	–	0.219$^+$	–	–	–
2,3,6-	–	–	–	–	0.533	0.544	0.501
2,4,6-	–	–	–	–	0.499	0.470	0.478°
2,5,6-	–	–	–	–	–	–	–
3,4,6-	–	–	–	–	0.526	0.482	0.478°
2,3,4,6-	–	–	–	–	0.381	0.342	0.338
2,3,5,6-	–	–	–	–	–	–	–

[a] Denotes 2-O-methyl galactitol = 1,3,4,5-tetra-O-acetyl-2-O-methyl galactitol, etc.

[b] Ara = Arabinitol; Xyl = xylitol; Fuc = fucitol; Rha = rhamnitol; Gal = galactitol; Glc = glucitol and Man = mannitol. *, $^+$ and ° denote co-eluting derivatives.

other columns [7–10]. These derivatives being 4,6-OCH_3/2,6-OCH_3-galactitol which co-eluted on the CP-Sil88 [8], SP-2330 [7] and the SP-2340 [10] and 2,3-OCH_3/4,6-OCH_3-glucitol which co-eluted on the SP-2330 [7] and the SP-2340 [10]. The elution order of fucitol derivatives on all four columns was identical. For derivatives of arabinose, 3,4-OCH_3/5-OCH_3 exhibited a reversed order of elution on the CP-Sil88 [8]. It is also worth noting that while some derivatives were not separated on the BPX70, they were on one or more of the other high-polarity columns. These include: (a) Arabinitol derivatives; 2,3-OCH_3/2,4-OCH_3 which were separated on the BP-75 [9] and CP-Sil88 [8]. (b) Xylitol derivatives; 3-OCH_3 which were separated from 2-OCH_3/4-OCH_3 on both the BP-75 [9] and CP-Sil88 [8] but all three derivatives co-eluted on the BPX70. (c) Rhamnitol derivatives; 2,3,4-OCH_3/2,3,5-OCH_3 which were separated on the BP-75 [9] and 2,3-OCH_3/2,4-OCH_3 were separated on the CP-Sil88 [8]. (d) Mannitol derivatives; 2,4,6-OCH_3/3,4,6-OCH_3-mannitol which were separated on the BP-75 [9] and CP-Sil88 [8]; and 3,4-OCH_3/2,4-OCH_3 which were separated on the SP-2330 [7] and SP-2340 [10].

Although there are some differences in the order of elution of some derivatives on the different high-polarity columns, more significant changes can be achieved by using a capillary column of low polarity such as the SP-2100 [13] and the CP-Sil5 [10]. Both the SP-2100 and CP-Sil5 are dimethyl polysiloxane phase. Thus by using two columns, one of high polarity and one of low polarity, laboratories without access to MS facilities are provided with a greater

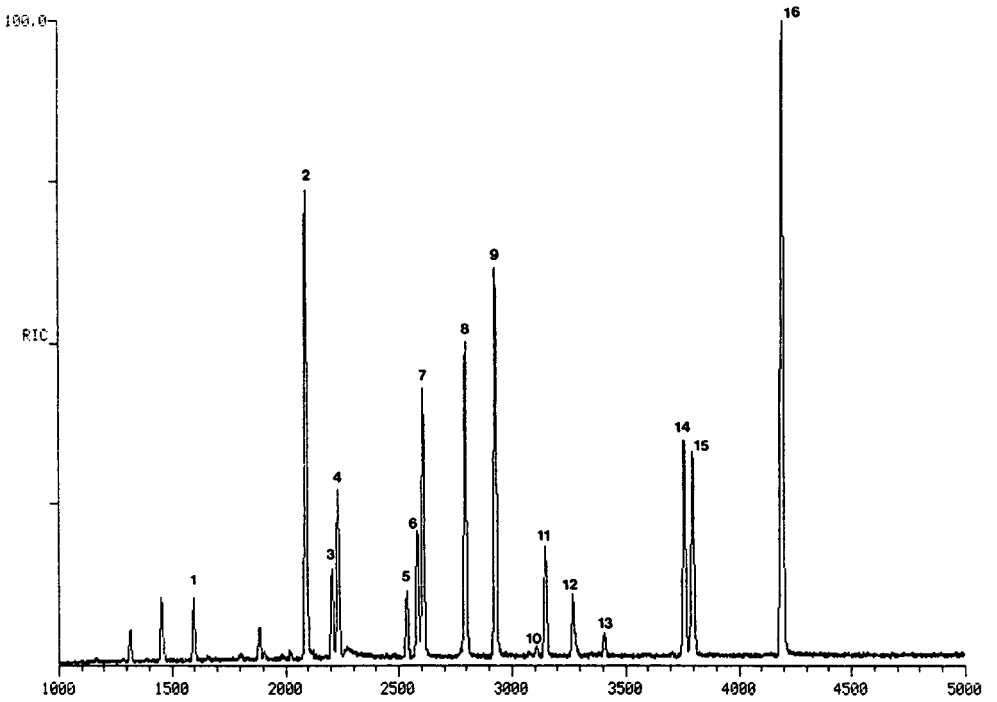

Fig. 1. Reconstructed ion chromatogram of partially methylated galactitol acetates. 1 = 2,3,4,6-OCH_3; 2 = 2,4,6-OCH_3; 3 = 3,4,6-OCH_3; 4 = 2,3,6-OCH_3; 5 = 2,3,4-OCH_3; 6 = 2,6-OCH_3; 7 = 4,6-OCH_3; 8 = 3,6-OCH_3; 9 = 6-OCH_3; 10 = 2,3-OCH_3; 11 = 2,4-OCH_3; 12 = 3,4-OCH_3; 13 = 2-OCH_3; 14 = 3-OCH_3/4-OCH_3; 15 = galactitol hexa-acetate; 16 = *myo*-inositol hexa-acetate (internal standard).

degree of certainty in peak identification based solely on retention times. Routine separation of partially methylated alditol acetates in this manner also provides the added advantage of quantification of the individual components in a mixture.

ACKNOWLEDGEMENT

This work was supported by a Special Research Centre Grant from the Australian Research Council.

REFERENCES

1 H. Bjorndal, C.G. Hellerquist, B. Lindberg and S. Svensson, *Angew. Chem., Int. Ed. Engl.*, 9 (1970) 610.
2 R.G. Spiro, *Methods Enzymol.*, 28 (1972) 3.
3 P.E. Jansson, L. Kenne, H. Liedgren, B. Lindberg and J. Lonngren, *Chem. Commun. Univ. Stockholm*, 8 (1976) 2.
4 J. Montreuil, *Advan. Carbohydr. Chem. Biochem.*, 37 (1980) 157.
5 B.S. Valent, A.G. Darvill, M. McNeill, B.K. Robertson and P. Albersheim, *Carbohydr. Res.*, 79 (1980) 165.
6 B. Lindberg, *Chem. Soc. Rev.*, 10 (1981) 409.
7 S.H. Doares, P. Albersheim and A.G. Darvill, *Carbohydr. Res.*, 210 (1991) 311.
8 J.A. Lomax, A.H. Gordon and A. Chesson, *Carbohydr. Res.*, 138 (1985) 177.
9 A. Bacic, P.J. Harris, E.W. Hak and A.E. Clarke, *J. Chromatogr.*, 315 (1984) 373.
10 A. Bacic, unpublished results.
11 P.J. Harris, R.J. Henry, A.B. Blakeney and B.A. Stone, *Carbohydr. Res.*, 127 (1984) 59.
12 W.O. McReynolds, *J. Chromatogr. Sci.*, 8 (1970) 685.
13 P.J. Harris, A. Bacic and A.E. Clarke, *J. Chromatogr.*, 350 (1985) 304; and references cited therein.

Journal of Chromatography, 637 (1993) 104–108
Elsevier Science Publishers B.V., Amsterdam

CHROM. 25 004

Short Communication

Simple gas chromatographic method for the assay of salts of carboxylic acids as their trimethylsilyl derivatives

Lay-Keow Ng* and Michel Hupé

Laboratory & Scientific Services Directorate, Revenue Canada, Customs & Excise, Ottawa, Ontario K1A 0L5 (Canada)

(First received November 6th, 1992; revised manuscript received February 23rd, 1993)

ABSTRACT

Several potassium and sodium salts of monobasic, dibasic and tribasic organic acids, and sodium and calcium salts of fatty acids were directly silylated by Tri-Sil, a commercially available silylating reagent composed of a mixture of hexamethyldisilazane and trimetylchlorosilane in pyridine. The reaction mixtures were injected directly into a gas chromatograph without any further preparation. Quantitative GC peak area measurements indicated that the yields of trimethylsilyl (TMS) derivatives of the salts and the free acid counterparts were comparable. Identities of the derivatives were confirmed by GC–MS analysis. Carbon chain distributions of the fatty acid salts were determined by GC quantitation of the TMS derivatives formed by direct silylation of the salts and the fatty acids liberated from the salts. The present study indicates that the two results agree with each other favorably.

INTRODUCTION

Salts of carboxylic acids are important chemicals in many facets of industry. For example, potassium sorbate, sodium benzoate and disodium tartrate are often used as food additives; trisodium nitrilotriacetate (NTA) and sodium salts of ethylenediaminetetraacetic acids (EDTA) are sequestering agents; and alkaline salts of fatty acids are used as soaps, as grease thickeners and for other purposes. Their compositions are often determined by gas chromatography (GC) for various purposes. These highly polar chemicals need to be converted to less polar compounds to be amenable for GC analysis. Generally they are acidified to form free acids which are then separated and esterified [1–4] or silylated [5]. It is highly desirable to develop a direct derivatization method which does not require any sample work-up before GC analysis. Such method is particularly useful in cases where the acids are volatile and may be difficult to recover from the extraction solvent.

Direct methylation by BF_3–MeOH has recently been reported for fatty salts of Zn, Mg and Ca [6]. At the end of the reaction, sodium carbonate was added to the reaction mixture which was subsequently injected into the gas chromatograph. Esterification by BF_3 is generally applicable to fatty acids only. Polybasic acids or salts have not been reported to be derivatized by this method. Direct trimethylsilylation of sodium and

* Corresponding author.

0021-9673/93/$06.00

other salts of several short-chain organic acids by reacting the salts with N,O-bis(trimethylsilyl)acetamide and trimethylchlorosilane in pyridine has been mentioned [7,8]. It is not clear, however, if the derivatization reactions are quantitative, and if the method is applicable to silylating fatty acid salts.

This paper describes a simple and fast GC procedure for the assay of several salts of fatty acids, short-chain monobasic and polybasic carboxylic acids as their trimethylsilyl (TMS) derivatives. The salts were directly derivatized quantitatively in a single-step reaction by Tri-Sil, a commercially available silylation cocktail, and the derivatives were analyzed by GC and GC–mass spectrometry (MS) without any further sample pretreatment.

EXPERIMENTAL

Reagents

Tri-Sil and acetonitrile were purchased from Pierce (Rockford, IL, USA). Concentrated hydrochloric acid, methylene chloride, HPLC grade, and calcium disodium salt of EDTA were obtained from J.T. Baker (Toronto, Canada). Sorbic acid, anhydrous and potassium sorbate were purchased from Sigma (St. Louis, MO, USA). Tartaric acid 99%, disodium tartrate dihydrate 99%, nitrilotriacetic acid 99%, trisodium nitrilotriacetate monohydrate 99%, benzoic acid 99%, sodium benzoate 99% were obtained from Aldrich (Milwaukee, WI, USA). Technical-grade calcium stearate, which is a mixture of calcium salts of fatty acids, was purchased from Pfaltz & Bauer (Waterbury, CT, USA). Disodium and tetrasodium dihydrate salts of EDTA, and sodium soap were samples supplied by Canadian customs inspectors.

Derivatization at 70°C

TMS derivatives of potassium sorbate, sodium benzoate, disodium tartrate, trisodium nitrilotriacetate and their acids were prepared by heating a solution of 18 mmol of the salt or acid in 1 ml of Tri-Sil in a Reacti-vial equipped with a PTFE-faced septum at 70°C with stirring. Aliquots of 100 μl of the reaction mixture were withdrawn at 0.5, 3 and 24 h. After cooling to room temperature, 1 μl was injected into a GC–flame ionization detection (FID) with a split ratio of 100:1. GC analysis was done in triplicate for each reaction time. To confirm the identities of the derivatives, 1 μl of each reaction mixture at 0.5 h was injected into the Hewlett-Packard GC–MS system with a split ratio of 100:1 for MS analysis.

Sodium soap and technical-grade calcium stearate were derivatized by stirring a solution of 10 mg of the fatty acid salts in 1 ml of Tri-Sil at 70°C. A 1-μl volume was injected into the GC–FID system and the Finnigan GC–MS system with a split ratio of 100:1 after 1 h of reaction. Fatty acids generated from their salts as described below were silylated in the same manner.

Preparation of fatty acids from sodium soap and technical-grade calcium stearate

Free fatty acids were generated by stirring 0.5 g of the sodium and calcium salts in equal volumes (15 ml) of methylene chloride and 6 *M* HCl at room temperature for 1 h. At the end of the reaction, the organic layer was separated and washed with 2×15 ml water. After drying over anhydrous sodium sulfate, the methylene chloride solution was filtered. The filtrate was evaporated to obtain the free fatty acids.

GC–FID

A Hewlett-Packard Model 5840A gas chromatograph equipped with a flame ionization detector and a Hewlett-Packard Model 5840A integration was employed. The column used was a 15 m $\times$ 0.25 mm I.D., 0.25 μm film thickness DB5 (5% phenyl methylsilicone) fused-silica column. The injector and detector temperature were 250°C and 300°C, respectively. After an initial hold time of 2 min at 100°C, the oven temperature was programmed at 10°C/min until 280°C; helium was used as a carrier gas at a linear velocity of 35 cm/s at 250°C.

GC–MS

The Hewlett-Packard system was composed of a HP 5890 gas chromatograph interfaced to a HP 5970 mass-selective detector via an open-split interface held at 290°C. The mass-selective detector was equipped with an electron impact (EI)

source. The system was controlled by a Pascal series Chemstation. The GC instrument was operated with a 12 m × 0.2 mm I.D., 0.33 μm film thickness HP-1 (methylsilicone) column. Injector temperature was 250°C. The oven temperature was programmed as follows: initial temperature set at 100°C, hold for 2 min then programmed at 10°C/min to a final temperature of 280°C. Helium was the carrier gas at a linear velocity of 41 cm/s at 250°C. EI spectra were obtained at 75 eV with the mass-selective detector scanning at 0.76 scan/s in the range 39–600 u.

The Finnigan system is composed of a Model 1020 OWA mass spectrometer coupled to a Perkin-Elmer Sigma-3B gas chromatograph via a direct interface maintained at a temperature of 300°C. The system is controlled by a Nova 4 data system. The oven temperature program used was the same as for the Hewlett-Packard system. The column was a 15 m × 0.25 mm I.D., 0.25 μm film thickness DB5 (5% phenyl methylsilicone) fused-silica column. Helium was the carrier gas at a linear velocity of 35 cm/s at 250°C. The mass spectrometer was operated in the electron impact mode at 70 eV and a mass range of 39 to 600 u was scanned at a rate of 1 s/scan. The ion source was held at 90°C.

RESULTS AND DISCUSSION

Identification of the formed derivatives

Each salt and its corresponding acid yielded the same derivative based on GC retention time and mass spectral evidence. All derivatives yielded discernible M^+ and $[M-15]^+$ peaks in their EI spectrum. The degree of silylation of each TMS derivative was determined by the molecular mass derived from these ions. As shown in Table I, the monobasic, tribasic and tetrabasic salts yield mono-, tri- and tetrasilylated derivatives, respectively. For the dibasic tartrate, the derivative detected was a tetrasilylated compound in which the two hydroxy groups were also silylated.

Fragmentation patterns of the derivatives were consistent with their structures. All derivatives except trimethylsilyl esters of fatty acids yielded the fragment ions $[M-117]^+$ resulting from loss of COOTMS. For the fatty compounds, the ion at m/z 117 appeared as an intense peak since it is a more stable ion than the $[M-117]^+$ fragments. In general, $[M-59]^+$ fragments formed from loss of CH_3 and CO_2 were observed in the mass spectra of TMS derivatives of monobasic carboxylates which are sorbate, benzoate and the fatty compounds. For carboxylates contain-

TABLE I

AVERAGE GC RESPONSES OF TMS DERIVATIVES AFTER ½-h REACTION

Samples	GC peak area counts[a] (relative standard deviation, %)	Derivatives
Potassium sorbate	14 955 (4.6)	$CH_3CH{=}CHCH{=}CHCOO(TMS)$
Sorbic acid	14 182 (3.1)	
Disodium tartrate	20 737 (6.4)	$[CHO(TMS)COO(TMS)]_2$
Tartaric acid	21 277 (3.5)	
Trisodium nitrilotriacetate	17 853 (4.0)	$N[CH_2COO(TMS)]_3$
Nitrilotriacetic acid	18 197 (2.5)	
Sodium benzoate	18 080 (2.3)	$C_6H_5COO(TMS)$
Benzoic acid	17 406 (0.4)	
Sodium soap and technical-grade Ca stearate; their fatty acids		RCOO(TMS)
Disodium and tetrasodium EDTA		$-[CH_2N(CH_2COOTMS)_2]_2$

[a] Each number presented is the average count of three GC runs of each TMS derivative, which was formed by reacting equal molar amounts (18 mmol) of acids or salts in 1 ml Tri-Sil.

TABLE II

ACID COMPOSITION PROFILES OF CRUDE FATTY ACID SALTS —COMPARISON OF DIRECT TRIMETHYLSILYLATION *VS.* VIA ACIDS

Sample	C_{10}	C_{12}	C_{14}	C_{16}	C_{17}	$C_{18:1}$	$C_{18:2}$	C_{18}
Na soap	1.1	9.5	5.9	23.8		34.7	5.8	19.2
Acids converted from Na soap	1.0	9.3	6.2	23.4		34.9	6.2	19.0
Technical-grade calcium stearate			4.2	51.5	1.4	2.3	2.1	38.5
Acids converted from calcium stearate			3.4	51.7	1.7	2.4	2.2	38.6

ing amino functions such as NTA and EDTA, α-cleavage was a desirable fragmentation pathway yielding ion m/z 290 as the base peak. α-Cleavage also occurred in tartrate which contains hydroxy functions to give the ion at m/z 219.

$[CHO(TMS)COO(TMS)]^+$ m/z 219 $[CH_2N(CH_2COOTMS)_2]^+$ m/z 290

Derivatization conditions and quantitative evaluation

For potassium sorbate, sodium benzoate, disodium tartrate and trisodium nitrilotriacetate, reaction mixtures of the salts and their acids in Tri-Sil at 70°C were analyzed by GC at 0.5, 3 and 24 h. For all the reactions, it was noted that the GC responses remained essentially unchanged over the period of 24 h, indicating that derivatizations were completed in the first half hour of reaction. As shown in Table I, comparable area counts were obtained for the salts and the free acids. It is well known that Tri-Sil is a potent silylating reagent for carboxylic acids [9,10], this study has thus shown that it silylates the salts as quantitatively as their acid counterparts.

Disodium and tetrasodium EDTA were also silylated in a single-step reaction by Tri-Sil. Although the reactions were not monitored quantitatively, the tetrasilyl derivative yielded good response in GC–FID after 2 h stirring at 70°C. Disodium calcium EDTA, however, failed to show any GC peak even after overnight reaction at 70°C.

Unlike the calcium salt of polybasic EDTA, calcium fatty acid salts were readily silylated by Tri-Sil after 1 h of reaction at 70°C. GC chromatograms obtained by direct silylation of the technical-grade calcium stearate were the same as that obtained by silylating the fatty acids liberated from the salts. The responses of the corresponding components in both chromatograms were comparable by visual examination, indicating that the peaks observed in the chromatogram obtained from direct silylation of the calcium salt were not due to the derivatives of the residual free fatty acids only, which could be present in the technical grade fatty salt used in this study. The same observation was also recorded for sodium soap and its acids.

Each homologue distribution presented in Table II is, therefore, the total composition of the acid salt, and residual fatty acids possibly present in the sample. Carbon chain distributions were determined from GC peak areas, assuming equal response factors for all the homologues. The results indicated that the homologue distributions determined by direct silylation of the soaps were in good agreement with those determined by the conventional method which involves conversion of the fatty acid salts into their acids.

ACKNOWLEDGEMENTS

The authors thank Drs. Jan Kovar and A.H. Lawrence for reviewing the manuscript.

REFERENCES

1 S. Tan, T. Tatsuno and T. Okada, *J. Chromatogr.*, 447 (1988) 198.
2 J.V. Wisniewski, *Facts Methods*, 8 (1967) 9.
3 B. Staucher, L. Ceccon and C. Calzolari, *Riv. Ital. Sostanze Grasse*, 59 (1982) 619.
4 T.A. Miller and P. York, *Int. J. Pharm.*, 23 (1985) 55.
5 Y. Tonogai, Y. Ito and M. Iwaida, *Bunseki Kagaku*, 31 (1982) E69.
6 H. Rotzsche, *J. Chromatogr.*, 552 (1991) 281.
7 A.J. Poole, D.I. Slater and D.H. Orrell, *Clin. Chim. Acta*, 73 (1976) 527.
8 G. Petersson, *Tetrahedron*, 26 (1970) 3413.
9 C.A. Burkhard, *J. Org. Chem.*, 22 (1957) 592.
10 R.C. Mehrotra and B.C. Pant, *J. Ind. Chem. Soc.*, 40 (1963) 623.

Journal of Chromatography, 637 (1993) 109–112
Elsevier Science Publishers B.V., Amsterdam

CHROM. 24 907

Short Communication

Gas chromatographic method for the determination of anilophos in soil

Shashi Bala Singh* and Gita Kulshrestha

Division of Agricultural Chemicals, IARI, New Delhi 110012 (India)

(First received September 23rd, 1992; revised manuscript received January 25th, 1993)

ABSTRACT

The gas chromatographic determination of anilophos was studied using four different detectors and it was found that flame photometric and nitrogen–phosphorus detection (NPD) were more sensitive than flame ionization and electron-capture detection. The method was extended to the determination of anilophos residues in soil using NPD. The recoveries of anilophos from soil with ethyl acetate (95–102%) were significantly higher than those with dichloromethane (80–88%) and methanol (44–49%).

INTRODUCTION

Anilophos [(S-4-chlorophenyl-N-isopropylcarbaniloylmethyl) O,O-dimethylphosphorodithioate] (Fig. 1) is a recently introduced herbicide which effectively controls grassy and some broad-leaved weeds in rice (*Oryza sativa*) crops [1,2] either alone [3–5] or as a mixed herbicide [6,7]. There is, however, no information available on the persistence of this herbicide in soil or on methods for its detection.

This paper presents a gas chromatographic (GC) method for the determination of anilophos. The method is simple and sensitive and is conveniently used for the detection of the herbicide at microgram levels. Further, the technique was extended to the determination of residues of the herbicide in soils to evaluate its persistence in the agro-ecosystem.

EXPERIMENTAL

Preparation of standards

Anilophos (90%, technical) obtained from Gharda Chemicals (Bombay, India) was recrystallized from benzene–hexane before use. Distilled analytical-reagent grade acetone, hexane, ethyl acetate, methanol and dichloromethane were used. Anhydrous sodium sulphate was used as a drying agent for soil samples.

Anilophos (25 mg) was dissolved in hexane–acetone (8:2) in a 25-ml volumetric flask and diluted to volume to give a 1000 μg/ml stock solution. A 1-ml volume of this stock solution was diluted to volume in a 100-ml volumetric flask with the same solvent mixture to give a 10 μg/ml stock standard solution of anilophos. Solutions of different concentrations were pre-

* Corresponding author.

0021-9673/93/$06.00

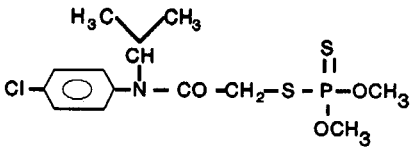

Fig. 1. Anilophos.

pared by diluting this stock standard solution. A 3-μl volume of each sample was injected accurately. The method was quantitatively validated by running solutions of 0.01, 0.02, 0.05, 0.1, 0.2, 0.5, 1.0, 2.0, 5.0 and 10.0 μg/ml of anilophos. Each run was performed in duplicate and the detector response was measured in terms of peak area.

Calibration of instruments

Hewlett-Packard Model 5890A and 5890 Series II, Varian Model 3400 and Nucon Model 5700 gas chromatographs were used. The detectors, columns, packing materials and other chromatographic conditions used were as given in Table I.

Extraction of anilophos from soil

The soil was a sandy loam with a composition of 19% clay, 21% silt, 60% sand and 0.35% organic carbon and had a pH of 7.2. The recovery of anilophos was checked at three different concentrations, each replicated three times. A 10-g amount of dried and sieved soil was fortified with anilophos separately at 1, 5 and 10 μg/g. Three different solvents (methanol, dichloromethane and ethyl acetate) were used separately for the extraction of soil.

The soil was extracted with 50 ml (25 + 15 + 10) of solvent by shaking on a wrist-action shaker for 0.5 h each time, filtered and then passed through anhydrous sodium sulphate (3 g). The extract was evaporated to dryness on a rotary evaporator at 35–40°C. The residue was dissolved in hexane–acetone (8:2) to make a solution of 0.5 ppm. A 3-μl volume of the extract was injected and chromatographed. This was preceded by the injection of a standard solution of known concentration.

The concentration of analyte in the extracted sample of soil was calculated by comparing the peak area of the sample with that of the standard using the equation

$$C = A \cdot RF$$

where C is the concentration of anilophos, A is the area of the peak corresponding to anilophos in the extract and RF (response factor) is the concentration of standard/area of standard.

TABLE I

OPERATING CONDITIONS OF DIFFERENT GC INSTRUMENTS

Model	Detection method	Column	Packing material	Temperature (°C)			Carrier gas (nitrogen) flow-rate (ml/min)
				Oven	Injector	Detector	
Hewlett-Packard 5890A	ECD	Coiled glass, 2 m × 2 mm I.D.	3% OV-25	270	300	300	46
Varian 3400	ECD	As above	As above	270	300	300	46
Hewlett-Packard 5890A	FID	Megabore, 10 m × 0.53 mm I.D.	OV-17	250	250	250	34
Nucon 5700	NPD	Coiled glass, 2 m × 2 mm I.D.	3% OV-25	260	270	280	40
Hewlett-Packard 5890-II	FPD	Megabore, 10 m × 0.53 mm I.D.	HP-1	230	250	250	20

RESULTS AND DISCUSSION

Anilophos could be resolved as a single, sharp peak using a gas chromatograph equipped with detectors for either electron-capture (ECD), nitrogen–phosphorus (NPD), flame photometric (FPD) or flame ionization (FID) detection (Table I). The maximum sensitivity of 0.06 ng of anilophos was obtained by GC–FPD using a megabore column. Next in sensitivity were ECD and NPD, both with detection limits of 0.6 ng of anilophos. Both of these instruments had coiled glass columns. FID exhibited the lowest sensitivity (300 ng). FID was therefore considered suitable for macro analysis of anilophos whereas the other three detection methods were suitable for microanalysis. The better sensitivity of FPD than ECD and NPD could be due to the presence of the more efficient megabore column (HP-1, Table I).

It was observed during bulk analysis of anilophos samples by GC–ECD that the results obtained on the following day were erratic and irreproducible when the same anilophos solutions were injected. It appeared that with continued use anilophos was deposited in the detector, making it unfit for further analysis. This observation was recorded on both the Hewlett-Packard and Varian instruments. ECD was therefore considered unsuitable for the determination of anilophos residues in soil. This erratic behaviour was not observed with NPD or FPD, with which a solution of 0.02 μg/ml anilophos was clearly resolved and a large number of soil extracts could be analysed continuously over several days without losing reproducibility.

The calibration graphs obtained by plotting concentration *versus* average peak area (each sample injected in duplicate) were linear over the range 0.02–10 μg/ml with both FPD and NPD. However, for the simultaneous determination of anilophos and its degradation products, NPD was finally selected and the conditions standardized.

After optimizing the GC conditions (Tables I and II), the method was extended to the determination of anilophos residues in soil. There was no interfering peak in the soil blank (Fig. 2). Of the three solvents used for extraction (methanol, dichloromethane and ethyl acetate), ethyl acetate gave the highest and quantitative recoveries (95–102%) from soil (Table III). The limit of determination of anilophos in soil was 1 μg/g.

TABLE II

RETENTION TIME AND SENSITIVITY OF ANILOPHOS IN GC WITH DIFFERENT DETECTION METHODS

Other conditions are as given in Table I.

Detection	Retention time (min)	Sensitivity (ng)
FID	1.69	300
ECD	3.78	0.6
NPD	6.30	0.6
FPD	2.72	0.06

ACKNOWLEDGEMENT

The authors are grateful to Dr. B.S. Parmar, Head, Division of Agricultural Chemicals, IARI, New Delhi, for providing the facilities for this work.

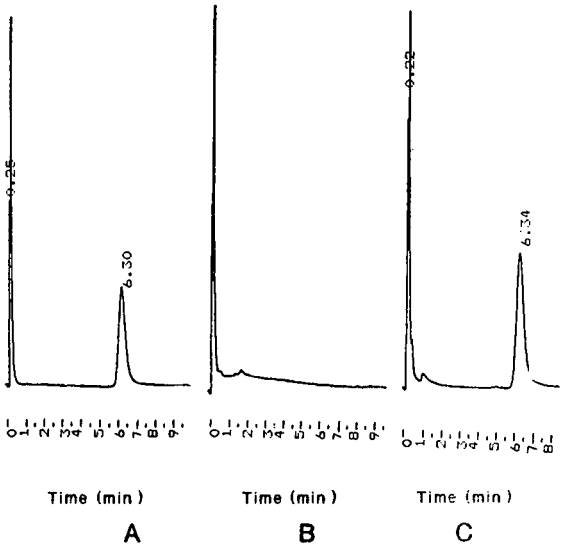

Fig. 2. Gas chromatograms of anilophos: (A) standard solution; (B) blank soil; (C) treated soil.

TABLE III

RECOVERY OF ANILOPHOS FROM SOIL USING DIFFERENT SOLVENTS

Results are averages of three replicates.

Soil sample	Solvent used for extraction	Concentration of anilophos in soil (μg/g)		Retention time (min)	Average recovery (%)
		Added	Found		
Control	Methanol	–	–	–	–
Treated		1	0.485	6.30	48.5 ± 0.8
Treated		5	2.175	6.31	43.5 ± 0.5
Treated		10	4.500	6.30	45.0 ± 1.0
Control	Dichloromethane	–	–	–	–
Treated		1	0.880	6.30	88.0 ± 0.9
Treated		5	4.005	6.29	80.1 ± 0.7
Treated		10	7.990	6.31	79.9 ± 1.1
Control	Ethyl acetate	–	–	–	–
Treated		1	1.018	6.34	101.8 ± 0.5
Treated		5	4.845	6.30	96.9 ± 0.4
Treated		10	9.460	6.31	94.6 ± 1.4

REFERENCES

1 S.S. Tomar, *Int. Rice Res. Newsl.*, 12, No. 3 (1987) 39.
2 J. Kumar and R.C. Gautam, *Indian J. Weed Sci.*, 18 (1986) 54.
3 R.K. Mishra, M.R. Deshmukh, V.K. Paradkar, K.L. Tiwari and R.P. Rajput, *Curr. Res*, 16 (1987) 150.
4 R.K. Mishra and M.R. Deshmukh, *Pesticides*, 22, No. 4 (1988) 10.
5 B.T.S. Moorthy and G.B. Manna, *Sci. Cult.*, 55 (1989) 215.
6 P. Langelueddke and H. Roechling, *Ger. Offen.*, 2 926 636 (1981).
7 H. Bieringer, *Ger. Offen.*, 2 926 668 (1981).

Journal of Chromatography, 637 (1993) 113–114
Elsevier Science Publishers B.V., Amsterdam

CHROM. 24 976

Book Review

The dynamics of electrophoresis, by R.A. Mosher, D.A. Gaville and W. Thormann, VCH, Weinheim, New York, Basle, 1992, XIV + 236 pp., price DM 186.00, £ 70.00, ISBN 3-527-28379-X.

The book is dedicated to our colleague and friend Milan Bier. In the Introduction, numerous pages are used to define history, without giving overwhelming information on references to the past. An overview of the historical research that forms the basis of modern electrophoresis will give especially younger scientists guidelines to finding their way through the literature. Too often it is thought that the leading figures of the past are also the leading figures of today. In this book it is shown that a new generation is taking over the role of those who first created and developed electrophoretic techniques.

In the classification of the electrophoretic methods it is shown that four basic principles (with and without electrophoretic flow) exist. As is well known, these four basic principles can be carried out in any electrophoretic apparatus. In such equipment one can separate small ions, anions, cations, amino acids, even peptides, proteins, DNA and RNA molecules and restriction fragments. In the two-dimensional mode it is important to know that various electrophoretic principles can be combined. It will be clear that such combinations will increase the information output for researchers. In this book it is clearly described which kind of principles should be chosen or which combination. It is therefore important that techniques such as the two-dimensional approach, GC–MS and pulsed-flow and micellar electrokinetic chromatography are described. In the "simplest" forms of electrophoresis such as zone electrophoresis, isotachophoresis, micellar electrokinetic chromatography and liquid chromatography–isoelectric focusing it is fairly easy to write computer programs for both qualitative and quantitative purposes. A very good reader guide to overview this book is given on page 4.

Chapter 2 covers the physical chemical background of electrophoresis. It not only gives attention to electrophoresis, but also to colloid chemistry. A good compromise is found between the well established theory and the current possibilities of using computer programs for evaluation and understanding of the data obtained. This chapter is especially recommended to those scientists who wish to become experts in the field of electrophoresis.

In Chapter 3 sophisticated computer modelling is given, both to understand the programs used and to add the specific requirements of those who are trained in both software and hardware. These programs are checked with experimental data obtained with the so-called CapScan equipment. For most scientists this chapter is difficult, because for one reason or another "wet chemistry" and "colloid chemistry" are no longer taught in standard university education packages. It is therefore a pity that so many beautiful analytical separation techniques seem doomed to disappear. For this reason this book will be extremely useful for physical, analytical and biochemists. Such information must at least be available in the laboratory.

In Chapter 4, moving boundary electrophoresis as introduced by Arne Tiselius is described. Although it does not have great analytical importance, the background of this technique needs to be understood. It is the separation phase of isotachophoresis used especially for injecting samples into gel-filled columns.

Chapter 5 describes zone electrophoresis. This principle is probably the most commonly used

separation technique in, *e.g.*, slab gels, paper, cellulose acetate, capillary tubes, free solutions and gels. In free solutions this principle can be used with and without electroosmotic flow. A clear view of various effects is given. Hybrid forms of capillary zone electrophoresis and isotachophoresis make clear the sharpening effects due to the two techniques and their concentrating effects. Hence it is important to understand the background of these principles.

In Chapter 6 isotachophoresis is described. It is clear that this technique now has great potential because commercial equipment has become available. Again it is important to understand the background of this technique in order to use it effectively for sharpening of the sample before the zone electrophoretic procedure is started. This is comparable to the Ornstein and Davis technique, published in 1964. The computer modelling described has been checked with real experiments in the apparatus.

In Chapter 7 isoelectric focusing is described. Information is given to select the pH gradient needed (wide or narrow). Sometimes just one kind of carrier ampholyte is recommended, sometimes a mixture. The reproducibility of this technique is dependent on reproducible material (ampholytes) being produced batch-to-batch, week-to-week, month-to-month and year-to-year. In my opinion this chapter will be very important for scientists in companies manufacturing these ampholytes. Especially section 7.6 is of extreme importance to students on undergraduate courses, but also for Ph.D. students in fields related to these techniques. More attention could have been paid to immobilized pH gradients (section 7.2.2, pages 217–221), while the focusing of proteins in natural pH gradients is questionable (section 7.8, pages 221–229).

My conclusion is that this book should be available in any laboratory working in this area. The information given is comprehensive and long-lasting. The theory behind the principles of electrophoresis is well established, and needs to be understood by those scientists who wish to develop their own electrolyte systems in order to optimize particular separations.

Eindhoven (Netherlands) Frans M. Everaerts

Journal of Chromatography, 637 (1993) 115
Elsevier Science Publishers B.V., Amsterdam

CHROM. 24 946

Book Review

Capillary electrophoresis, edited by P.D. Grossman and J.C. Colburn, Academic Press, San Diego, CA, 1992, 352 pp., price US$ 69.95, ISBN 0-12-304250-X.

The topic of capillary electrophoresis in this multi-author book is divided into three parts. The first, called Background concepts, offers in three chapters the theoretical background (and to some extent the methodology) of the technique: it deals with factors that affect the performance of capillary electrophoresis, *i.e.*, Joule heating, electroosmosis and zone dispersion (P.D. Grossman), and gives a description of detection methods (T.M. Olefirowicz and A.G. Ewing). Quantitative aspects of capillary electrophoresis (S.E. Moring) complete the first part of the book.

The second part deals with different operational modes of capillary electrophoresis: free solution capillary electrophoresis (P.D. Grossman), capillary gel electrophoresis (R.S. Dubrow), micellar electrokinetic chromatography (M.J. Sepaniak *et al.*), isoelectric focusing in capillaries (S. Hjertén) and capillary electrophoresis in entangled polymer solutions (P.D. Grossman).

In the third part of the book, called Applications of capillary electrophoresis, examples and problems on the separation of peptides (J.C. Colburn), proteins (J.E. Wiktorowicz and J.C. Colburn) and "small molecules" (C.W. Demarest) are described. A two-page appendix devoted to troubleshooting (J.C. Colburn and P.D. Grossman) completes the book.

Like most books, this one also has its advantages and disadvantages. In the reviewer's opinion this volume edited by Grossman and Colburn is remarkably uniform for a multi-author book and the individual chapters are very well presented didactically (see, for instance, the chapter by Hjertén on isoelectric focusing). In particular, the two pages on troubleshooting will be useful for the potential reader using this technique in the laboratory. On the other hand, from the formal point of view, I would have preferred to have had a unified list of symbols used at the beginning of the book, rather than on p. 41, where it is related to the first chapter only, while there are numerous theoretical considerations later in the text. As far as the subject matter is concerned, there are a few items that I missed. The first is chiral separations: I think that this rapidly developing field with numerous applications, particularly in the pharmaceutical field, deserved more than the four pages following p. 333. In general, the part on applications is limited and covers only a fraction of what can be found in the literature today. Some types of compounds are neglected completely, such as carboxylic acids, carbohydrates, phenolics, organic sulphur compounds (glucosinolates) and many more. Practically all types of derivatization of amino acids have been used in capillary electrophoresis, some with excellent results regarding sensitivity. The description of these procedures is limited to a small (and consequently incomplete) paragraph on p. 332. In the technical approaches, I missed the use of pH gradients in electrophoretic separations. Possibly the production of the volume took so long that the authors were technically precluded from keeping up-to-date with the rapidly growing number of applications.

In summary, I would say that the authors have succeeded well in describing the general aspects (theory, equipment and practice) of capillary electrophoretic techniques, but the part on applications certainly does not demonstrate "application of CE to a wide range of molecules supplemented with extensive hands-on illustrations" as declared on the back cover. In spite of this last objection, I liked the book and was pleased to include it in my library.

Prague (Czech Republic) Zdeněk Deyl

Journal of Chromatography, 637 (1993) 116–117
Elsevier Science Publishers B.V., Amsterdam

CHROM. 24 948

Book Review

Trace and ultratrace analysis by HPLC, by S. Ahuja, Wiley, Chichester, New York, 1992, XI + 419 pp., price £ 59.00, ISBN 0-471-51419-5.

This book is the 115th in a series of volumes on chemical analysis dealing with the whole field of analytical chemistry and its applications. The series *Chemical Analysis* was originally edited by I.M. Kolthoff, and now by J.D. Winefordner. The volume discussed here is devoted to trace and ultratrace analysis by HPLC.

In the last decade, high-pressure or high-performance liquid chromatography (HPLC) has proved to be a versatile and robust technique for trace analyses of complex samples. However, the author slightly exaggerates the importance of HPLC by stating that "HPLC is by far the most popular and most commonly used technique" in trace and ultratrace analysis. This statement is immediately followed by a discussion on the need for ultratrace analytical methods for dioxins and polychlorinated biphenyls. In daily practice these analyses are clearly performed by capillary gas chromatography which, in my opinion, competes strongly with HPLC for the qualification most popular and commonly used technique in trace and ultratrace analysis.

The first chapter gives a brief introduction to the potential of HPLC in various application areas that may require trace or ultratrace analysis such as biotechnology, diagnostic studies, pharmacokinetics, foods and beverages. The next chapter, on theoretical considerations, deals with the basic theory of HPLC. Some equations and their derivations are given for plate numbers, peak broadening and detection limits. The last section is entitled "optimum column selection: conventional *vs.* small particle *vs.* microbore columns". Unfortunately, apart from some considerations on N, k' and analysis time, little or no guidance is given on how to select an optimum column for specific problems.

Chapters 3 and 4 deal with the equipment needed for trace and ultratrace analytical work utilizing HPLC. A division is made into detectors, treated in Chapter 4, and other hardware, discussed in Chapter 3. Various kinds of noise and interferences that may adversely affect the detectability are treated. Chapter 4, entitled Sensitive Detectors in HPLC, covers a wide range of detection modes including UV absorbance, (laser-induced) fluorescence, electrochemical, refractive index and mass spectrometric. In addition, some attention is paid to the more exotic luminescence detection schemes based on chemiluminescence or phosphorescence.

A remarkable difference between Chapters 3 and 4 is that the former goes into great detail on the construction of the hardware, *e.g.*, in the section on solvent delivery systems, whereas the latter does not give any detailed information on the construction of detectors. In my view, this is an undervaluation of the great achievements made in detector technology in the last decade.

Adequate sample preparation is the key to effective trace and ultratrace analysis, and in Chapter 5 several aspects of sample preparation are discussed. There is a relatively large section on solid-phase extraction, and other major topics incorporated are liquid–liquid and liquid–solid extraction techniques, clean-up procedures by column chromatography and precolumn switching. Unfortunately, recent developments in coupling with supercritical fluid extraction and electromigration techniques and coupled LC–GC are ignored. Further, sample preparation techniques based on precolumns or solid-phase cartridges packed with selective materials, *e.g.*, immobilized antibodies or metal-loaded phases, should have found a place in this chapter.

Chapter 6 deals with method development for trace and ultratrace analysis, and some basic aspects of mobile phase selection and optimization are discussed. The chapter ends with a discussion on multimodal liquid chromatography, mainly based on references to work published before 1980.

This chapter is followed by two more on specific aspects of method development: Chapter 7 deals with selectivity optimization and Chapter 8 covers detectability optimization. Chapter 7 covers the basic aspects of selectivity enhancement in adsorption/normal-phase chromatography, reversed-phase chromatography and ion-pair chromatography, completed with a review on computer-based optimization. An important part of Chapter 8 is devoted to derivatization techniques.

The last chapter deals with selected applications in different fields. The largest number of examples can be found in the pharmaceutical/biomedical, food and environmental areas. This chapter is completed with 397 references to the literature. However, it must be noted that more than half of these citations refer to work published in 1980 or earlier.

I cannot recommend this book very highly. It could be of some use to scientists starting in the field of HPLC, but I would rather advise them to use readily available text books on HPLC, in combination with monographs on the specific area of interest.

The use of rather dated references is a general drawback to the book; in most chapters the latest literature included relates to 1988, and the major part relates to 1980 or earlier. This book gives the impression that scientific research in HPLC as a trace analytical technique was completed somewhere in 1985.

Bilthoven (Netherlands) Piet van Zoonen

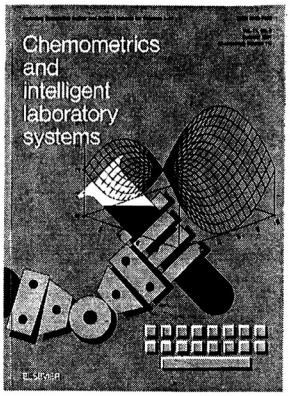

CHEMOMETRICS AND INTELLIGENT LABORATORY SYSTEMS

An International Journal Sponsored by the Chemometrics Society

With the Chemometric Newsletter, official bulletin of the Chemometrics Society and including "Laboratory Information Management"

AIMS AND SCOPE

This international journal publishes articles about new developments on laboratory techniques in chemistry and related disciplines which are characterized by the application of statistical and computer methods. Special attention is given to emerging new technologies and techniques for the building of intelligent laboratory systems, i.e. artificial intelligence and robotics. The journal aims to be interdisciplinary; more particularly it intends to bridge the gap between chemists and scientists from related fields, statisticians, and designers of laboratory systems. In order to promote understanding between scientists from different fields the journal features a special section containing tutorial articles.

The journal deals with the following topics: Chemometrics; Computerized acquisition, processing and evaluation of data; Robotics; Developments in statistical theory and mathematics with application to chemistry; Intelligent laboratory systems; Application (case studies) of statistical and computational methods; New software; Imaging techniques and graphical software applied in chemistry. The research papers and tutorials are complemented by the Monitor Section which contains news, a calendar of forthcoming meetings, reports on meetings, software reviews, book reviews, news on societies and announcements of courses and meetings.

ABSTRACTED/INDEXED IN: ASCA, Analytical Abstracts, BioSciences Information Service, Cambridge Scientific Abstracts, Chemical Abstracts, Chromatography Abstracts, Current Contents, Current Index to Statistics, Excerpta Medica, INSPEC, SCISEARCH.

1993 SUBSCRIPTION INFORMATION

Volumes 18-21 (in 12 issues)
Dfl. 1444.00 / US $ 825.00 (including postage) ISSN 0169-7439

Audience

Chemists and physical and life scientists as well as statisticians and information specialists working in a variety of fields of chemistry, including analytical chemistry, organic chemistry and synthesis, environmental chemistry, food chemistry, industrial chemistry, pharmaceutical chemistry and pharmacy.

I would like ☐ a free sample copy of Chemometrics and Intelligent Laboratory Systems.

☐ Instructions to Authors.

☐ to enter a subscription for 1993. Please send me a Proforma Invoice.

Name _____

Address _____

_____

_____

Elsevier Science Publishers
Attn. Carla G.C. Stokman
P.O. Box 330, 1000 AH Amsterdam
The Netherlands
Fax: (+31-20) 5862 845
In the USA & Canada
Attn. Judy Weislogel
P.O. Box 945, Madison Square Station
New York, NY 10160-0757, USA
Fax: (212) 633 3880

711\414\143\0058

Atmospheric Oxidation and Antioxidants

Volume I

edited by **G. Scott**

Oxidation by molecular oxygen is one of the most practically important of all chemical processes. It is the basis of energy production in animals and, at the same time, a major cause of irreversible deterioration and ultimate death. Man uses oxygen positively in the production of energy by combustion, and many important industrial processes in the petrochemical industry are based on the controlled oxidation of hydrocarbons. At the same time, oxidation is the main cause of deterioration of foodstuffs and of many industrial polymers.

It is clearly of great practical importance that the mechanisms of oxidation and its prevention should be understood in order to utilise the reactions of oxygen more effectively but, equally important, to control the adverse effects of oxygen on man-made products and in biological systems. The three volumes of this work are directed towards these objectives. Although complementary to one another, the three volumes form a single whole and it is hoped that, by frequent cross-reference, the reader will be enabled to utilise ideas and experience from other disciplines to enlighten his own.

Volume I reviews current understanding of autoxidation, largely on the basis of the reactions of oxygen with characterised chemicals. From this flows the modern mechanism of antioxidant actions and their application in stabilisation technology.

Contents:

© 1993 xii + 234 pages
Price: US $ 182.75 / Dfl. 320.00
ISBN 0-444-89615-5

Volumes I, II and III
Set price: US $ 557.00 / Dfl. 975.00
Set ISBN 0-444-89618-X

ORDER INFORMATION

For USA and Canada
ELSEVIER SCIENCE PUBLISHERS
Judy Weislogel, P.O. Box 945
Madison Square Station,
New York, NY 10160-0757
Tel: (212) 989 5800
Fax: (212) 633 3880

In all other countries
ELSEVIER SCIENCE PUBLISHERS
P.O. Box 211, 1000 AE
Amsterdam
The Netherlands
Tel: (+31-20) 5803 753
Fax: (+31-20) 5803 705

US$ prices are valid only for the USA & Canada and are subject to exchange rate fluctuations; in all other countries the Dutch guilder price (Dfl.) is definitive. Customers in the European Community should add the appropriate VAT rate applicable in their country to the price(s). Books are sent postfree if prepaid.

ELSEVIER
SCIENCE PUBLISHERS

PUBLICATION SCHEDULE FOR THE 1993 SUBSCRIPTION

Journal of Chromatography and *Journal of Chromatography, Biomedical Applications*

MONTH	1992	J	F	M	A	M	J	
Journal of Chromatography	623–627	628/1 628/2 629/1 629/2	630/1 + 2 631/1 + 2 632/1 + 2 633/1 + 2	634/1 634/2	635/1 635/2 636/1 636/2	637/1 637/2 638/1 638/2	639/1 639/2 640/1 + 2	The publication schedule for further issues will be published later.
Cumulative Indexes, Vols. 601–650								
Bibliography Section				649/1			649/2	
Biomedical Applications		612/1	612/2	613/1	613/2 614/1	614/2 615/1	615/2 616/1	

INFORMATION FOR AUTHORS

(Detailed *Instructions to Authors* were published in Vol. 609, pp. 437–443. A free reprint can be obtained by application to the publisher, Elsevier Science Publishers B.V., P.O. Box 330, 1000 AH Amsterdam, Netherlands.)

Types of Contributions. The following types of papers are published in the *Journal of Chromatography* and the section on *Biomedical Applications:* Regular research papers (Full-length papers), Review articles, Short Communications and Discussions. Short Communications are usually descriptions of short investigations, or they can report minor technical improvements of previously published procedures; they reflect the same quality of research as Full-length papers, but should preferably not exceed five printed pages. Discussions (one or two pages) should explain, amplify, correct or otherwise comment substantively upon an article recently published in the journal. For Review articles, see inside front cover under Submission of Papers.

Submission. Every paper must be accompanied by a letter from the senior author, stating that he/she is submitting the paper for publication in the *Journal of Chromatography.*

Manuscripts. Manuscripts should be typed in **double spacing** on consecutively numbered pages of uniform size. The manuscript should be preceded by a sheet of manuscript paper carrying the title of the paper and the name and full postal address of the person to whom the proofs are to be sent. As a rule, papers should be divided into sections, headed by a caption (*e.g.*, Abstract, Introduction, Experimental, Results, Discussion, etc.) All illustrations, photographs, tables, etc., should be on separate sheets.

Abstract. All articles should have an abstract of 50–100 words which clearly and briefly indicates what is new, different and significant. No references should be given.

Introduction. Every paper must have a concise introduction mentioning what has been done before on the topic described, and stating clearly what is new in the paper now submitted.

Illustrations. The figures should be submitted in a form suitable for reproduction, drawn in Indian ink on drawing or tracing paper. Each illustration should have a legend, all the *legends* being typed (with double spacing) together on a *separate sheet.* If structures are given in the text, the original drawings should be supplied. Coloured illustrations are reproduced at the author's expense, the cost being determined by the number of pages and by the number of colours needed. The written permission of the author and publisher must be obtained for the use of any figure already published. Its source must be indicated in the legend.

References. References should be numbered in the order in which they are cited in the text, and listed in numerical sequence on a separate sheet at the end of the article. Please check a recent issue for the layout of the reference list. Abbreviations for the titles of journals should follow the system used by *Chemical Abstracts.* Articles not yet published should be given as "in press" (journal should be specified), "submitted for publication" (journal should be specified), "in preparation" or "personal communication".

Dispatch. Before sending the manuscript to the Editor please check that the envelope contains four copies of the paper complete with references, legends and figures. One of the sets of figures must be the originals suitable for direct reproduction. Please also ensure that permission to publish has been obtained from your institute.

Proofs. One set of proofs will be sent to the author to be carefully checked for printer's errors. Corrections must be restricted to instances in which the proof is at variance with the manuscript. "Extra corrections" will be inserted at the author's expense.

Reprints. Fifty reprints will be supplied free of charge. Additional reprints can be ordered by the authors. An order form containing price quotations will be sent to the authors together with the proofs of their article.

Ovomucoid Bonded Column for Direct Chiral Separation

ULTRON ES-OVM

Narrow-Bore Column (2.0 I.D. x 150 mm) for Trace Analyses
Analytical Column (4.6 I.D. , 6.0 I.D. x 150 mm) for Regular Analyses
Semi-Preparative Column (20.0 I.D. x 250 mm) for Preparative Separation

Analysis of Trace FLURBIPROFEN in Metabolite with NARROW-BORE COLUMN

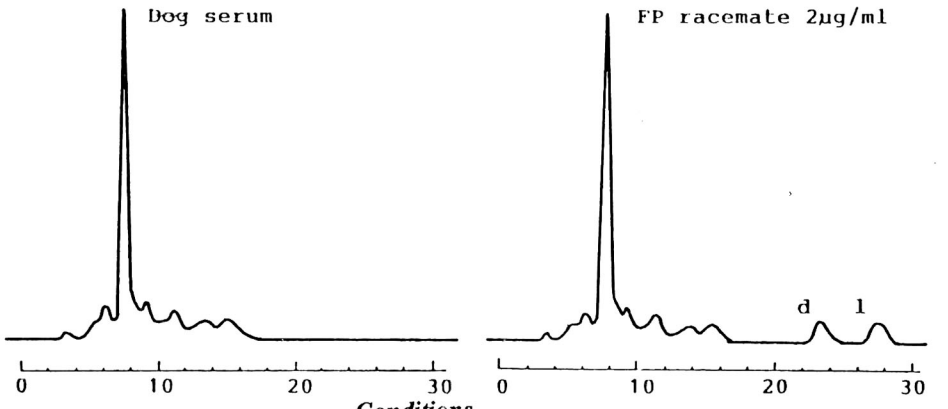

Conditions

Column: ULTRON ES-OVM(2.0I.D. x 150mm)
Mobile Phase: 20mMPhosphate Buffer(pH=3.0)/CH3CN =100/15
Flow Rate: 0.1ml/min
Temperature: 25°C
Injection: 5µl
Detection: UV- 247nm(0.05AUFS)

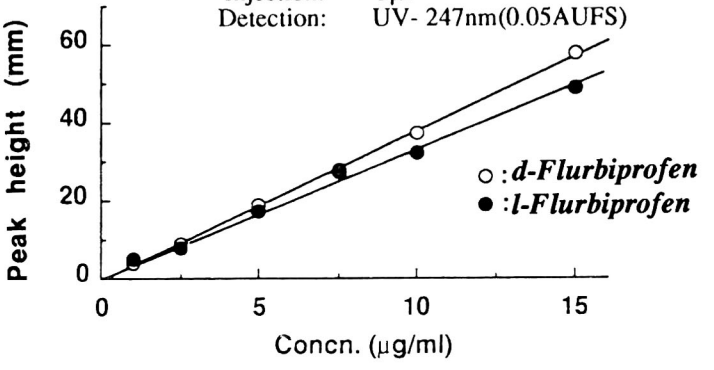

Calibration Curve for Each Enantiomer of Flurbiprofen

SHINWA CHEMICAL INDUSTRIES, LTD.

50 Kagekatsu-cho, Fushimi-ku, Kyoto 612, JAPAN
Phone:+81-75-621-2360 Fax:+81-75-602-2660

In the United States and Europe, please contact:

Rockland Technologies, Inc.

538 First State Boulevard, Newport, DE 19804, U.S.A.
Phone: 302-633-5880 Fax: 302-633-5893

This product is licenced by Eisai Co., Ltd.